

1-1-2012

Dual-Lane Roundabouts Geometric Design for Optimum Design Consistency and Operation

Rana Salah-ud-Din Mujahid
Ryerson University

Follow this and additional works at: <http://digitalcommons.ryerson.ca/dissertations>



Part of the [Civil Engineering Commons](#)

Recommended Citation

Mujahid, Rana Salah-ud-Din, "Dual-Lane Roundabouts Geometric Design for Optimum Design Consistency and Operation" (2012).
Theses and dissertations. Paper 1428.

This Thesis is brought to you for free and open access by Digital Commons @ Ryerson. It has been accepted for inclusion in Theses and dissertations by an authorized administrator of Digital Commons @ Ryerson. For more information, please contact bcameron@ryerson.ca.

**DUAL-LANE ROUNDABOUTS GEOMETRIC DESIGN FOR OPTIMUM
DESIGN CONSISTENCY AND OPERATION**

By

Rana Salah-ud-Din Mujahid

Bachelor of Applied Science in Civil Engineering U.E.T Lahore, Pakistan, 2007

Masters of Applied Science in Civil Engineering U.E.T Lahore, Pakistan, 2009

A thesis

Presented to Ryerson University

in partial fulfillment of the
requirements of the degree of
Master of applied Science
in the Program of
Civil Engineering

Toronto, Ontario, Canada, 2012

© Rana Salah-ud-Din Mujahid 2012

AUTHOR'S DECLARATION

I hereby declare that I am the sole author of this thesis. I authorize Ryerson University to lend this thesis to other Institutions or individuals for the purpose of scholarly research.

I further authorize Ryerson University to reproduce this thesis by photocopying or by other means, in total or in part, at the request of other Institution or individuals for the purpose of scholarly research.

Rana Salah-ud-Din Mujahid
Department of Civil Engineering
Ryerson University

DUAL-LANE ROUNDABOUTS GEOMETRIC DESIGN FOR OPTIMUM DESIGN CONSISTENCY AND OPERATION

By

Rana Salah-ud-Din Mujahid

A Thesis Present to Ryerson University
In partial fulfillment of the
Requirement for the Degree of
Master of Applied Science
In the program of Civil Engineering
Toronto, Ontario, Canada 2012

ABSTRACT

Dual-lane roundabouts successfully controlling traffic because of their slower entry speeds and fewer conflict points compared to conventional intersections. Operational evaluations of dual-lane roundabouts depend on the average delay at each roundabout entry, and the delay of each entry depends on the entry capacity. An optimization model is developed in this thesis for dual-lane right-angle and skewed-angle roundabouts, which determines the design elements of the roundabout based on design consistency and the least average intersection delay. The design element includes vehicle radii for through, left, and right turn traffic paths. The design consistency of an individual path is considered by minimizing the relative speed difference along each vehicle path for all approaches. Operational analysis gives an estimation of the capacity and level of service in terms of queue length and delay. These models use site conditions as inputs and prove the feasibility of the design.

ACKNOWLEDGMENT

I would like to take this opportunity to express my sincere appreciation to my supervisor, Dr. Said Easa for his invaluable advice, guidance, suggestions, patience and encouragement throughout the execution of this research program. His unfailing optimism and constant encouragement always prompted me to overcome the difficulties in completing this research. Dr. Said Easa inspired me with the idea of this research and he kept improving it through very long hours that he dedicated from his valuable time for discussions, guidance and follow up.

I would like to express sincere thanks to Steve van De Keere, Head of Transportation Expansion Program, Region of Waterloo and Philip A. Weber Principal, Project Manager, Ourston Roundabout Engineering for providing data for application of this research. I would also like to thank all other members in the Civil Engineering Department for their assistance in my research work and the completion of my study at Ryerson University.

I would like to thank all of my family members, colleagues, and all friends for their support. They all provided me with endless love, patience and encouragement throughout my study program.

DEDICATION

This thesis is dedicated to my parents, Rana Muhammad Mujahid and Mussarat Mujahid, my brother Rana Haroon Mujahid, my wife Azka Atique, my daughter Mahnoor Mujahid and my sisters who shared with me the sacrifices required to complete it and were always there when I needed them to give me endless love, happiness and hope for better future throughout my studies.

TABLE OF CONTENTS

AUTHOR'S DECLARATION	II
ABSTRACT	III
ACKNOWLEDGMENT	IV
DEDICATION	V
TABLE OF CONTENTS	VI
LIST OF TABLES	X
LIST OF FIGURES	XI
LIST OF APPENDICES	XIV
CHAPTER 1 : INTRODUCTION	1
1.1 Background History	1
1.2 Basic Dual-Lane Roundabout Geometric Features	3
1.3 Modern Roundabouts and Traffic Circles Comparison	5
1.4 Advantages, Disadvantages and Limitations of roundabouts	7
1.4.1 Advantages of Roundabout	7
1.4.2 Disadvantages of Roundabout.....	8
1.4.3 Limitation	8
1.4.4 Common site application.....	9
1.4.5 Safest mechanism for traffic.....	9
1.5 Categories of Roundabouts	10
1.5.1 Mini roundabout	10
1.5.2 Urban compact roundabout	11
1.5.3 Urban single-lane roundabout	11
1.5.4 Urban dual-lane roundabout.....	11
1.5.5 Rural single-lane roundabout	11
1.5.6 Rural dual-lane roundabout	12
1.6 Research Scope and Objective	12
1.7 Thesis Organization	12
CHAPTER 2 : CHARACTERISTICS AND MULTI-MODAL CONSIDERATIONS	15
2.1 Roundabout Characteristics	15
2.1.1 Operation and maintenance cost.....	15
2.1.2 Traffic calming	16
2.1.3 Landscaping.....	16
2.1.4 Environmental factors	19
2.1.5 Other characteristics	19
2.2 Multi-modal Considerations	24
2.2.1 Transit.....	25
2.2.2 Emergency vehicle	25

2.2.3	Large vehicle	26
2.2.4	Pedestrians accommodation	26
2.2.5	Bicycle accommodation	27
CHAPTER 3 : CAPACITY AND DELAY LITERATURE REVIEW.....		29
3.1	Introduction.....	29
3.2	Roundabout Capacity.....	29
3.2.1	Empirical (regression) capacity	31
3.2.2	Gap acceptance capacity	32
3.3	Roundabout Delay	33
3.3.1	Geometric delay	33
3.3.2	Average geometric delay.....	33
3.3.3	Control delay	33
3.4	Review of Entry Capacity and Delay Models.....	34
3.4.1	UK capacity and delay model	34
3.4.2	German capacity and delay model	37
3.4.3	French capacity and delay model	39
3.4.4	Swiss capacity and delay model.....	41
3.4.5	US capacity and delay research.....	44
3.4.6	Australian capacity and delay formula.....	48
3.5	Comparison and Application of Capacity Models.....	52
3.5.1	Gap acceptance method (Vs) Empirical method	52
3.5.2	Comparison of the Australia and US capacity formulas	54
3.5.3	Application	54
3.6	Degree of Saturation	55
3.7	Queue Length	55
CHAPTER 4 : GEOMETRIC DESIGN CONSIDRATIONS		58
4.1	Introduction.....	58
4.2	Approaches Arrangement at Roundabouts.....	58
4.2.1	Right-angle approaches	58
4.2.2	Skewed-angle approaches	59
4.3	Conflicts at a Dual-Lane Roundabout	60
4.3.1	Vehicle-Vehicle and Vehicle-Pedestrian conflicts.....	60
4.3.2	Queuing conflicts	61
4.3.3	Merge and diverge conflicts.....	62
4.3.4	Exit-Circulatory vehicle conflicts	62
4.3.5	Improper lane-use conflicts	63
4.3.6	Improper right and left turn conflicts	63
4.3.7	Bicycle-pedestrian conflicts	64
4.4	Design Principle for a Dual-Lane Roundabout.....	65

4.4.1	Speed management.....	65
4.4.2	Lane number and arrangement.....	68
4.4.3	Design vehicle considerations.....	68
4.4.4	Design vehicle selection.....	68
4.4.5	Entry-Exit separation.....	70
4.4.6	Dual-lane roundabout elements design.....	70
4.4.7	Geometric design at entry and exit.....	76
4.5	Performance Check.....	80
4.5.1	Fastest path.....	80
4.5.2	Speed consistency.....	81
4.5.3	Stopping sight distance.....	82
4.5.4	Intersection sight distance.....	83
CHAPTER 5 : OPTIMIZATION MODEL DEVELOPMENT: DUAL-LANE RIGHT-ANGLE ROUNDABOUTS.....		86
5.1	Introduction.....	86
5.2	Existing Design Methodologies.....	86
5.2.1	Manual method.....	86
5.2.2	Computer aided method.....	87
5.2.3	Optimization modeling technique.....	87
5.3	Feasibility Study for Roundabout Design.....	88
5.4	Required Data for Optimization Model.....	89
5.4.1	Site design parameter ranges.....	89
5.4.2	Traffic data.....	91
5.4.3	Side friction factor.....	92
5.5	Vehicle Path Modeling at Right-angle Roundabouts.....	93
5.5.1	Fastest through path radii.....	93
5.5.2	Fastest right turn path radii.....	100
5.5.3	Fastest left turn path radii.....	105
5.6	Model Development Process.....	111
5.6.1	Define site constraints.....	111
5.6.2	Measurement of speed difference (Consistency measure).....	112
5.6.3	Measurement of average intersection delay (Operational measures).....	114
5.6.4	Define a multi-objective function.....	117
5.7	Summary.....	117
CHAPTER 6 : OPTIMIZATION MODEL DEVELOPMENT: DUAL-LANE SKEWED-ANGLE ROUNDABOUTS.....		119
6.1	Introduction.....	119
6.2	Skewed-angle Roundabouts.....	119

6.3	Sub-Model 1: Vehicle Entering Through An Approach Legs (1, 3)	121
6.3.1	Fastest through path radii	121
6.3.2	Fastest right turn path radii.....	125
6.3.3	Fastest left turn path radii	129
6.4	Sub-Model 2: A Vehicle Entering Through Approach Legs (2, 4)	132
6.4.1	Fastest through path radii	132
6.4.2	Fastest right turn path radii.....	136
6.4.3	Fastest left turn path radii	139
6.5	Model Development Process	142
CHAPTER 7 : APPLICATION OF MODEL TO ACTUAL ROUNDABOUT		143
7.1	Introduction	143
7.2	Data Preparation	143
7.3	Sensitive Analysis	147
7.3.1	Right-angle roundabout sensitive analysis	148
7.3.2	Skewed-angle roundabout sensitive analysis	154
7.4	Results Comparison for Skewed & Right-angle Roundabouts	157
CHAPTER 8 : CONCLUSIONS AND FUTURE RESEARCH		160
8.1	Summary	160
8.2	Conclusions	164
8.3	Future Research Directions	166
APPENDIX-A		168
APPENDIX-B		174
APPENDIX-C		180
APPENDIX-D		194
REFERENCE		199

LIST OF TABLES

Table 1.1	Basic dual-lane roundabout geometric features	4
Table 1.2	Modern roundabouts and traffic circles comparison	6
Table 2.1	Cost comparison between traffic signal and roundabout	16
Table 2.2	Crash at roundabout in several countries (NCHRP Report 672, 2010).....	24
Table 3.1	Maximum dual-lane roundabout capacity	30
Table 3.2	Conversion factors for traffic to passenger cars equivalent (FHWA, 2000)	30
Table 3.3	Regression parameters (Brilon, Werner, Ning Wu, and Lothar Bondzio, 1997)	37
Table 3.4	Critical gap and follow up time in (Highway Capacity Manual, 2000).....	44
Table 3.5	Parameters used in HCM 2010 roundabout capacity model (HCM, 2010).....	46
Table 3.6	Level-of-service thresholds for roundabouts (NCHRP Report 572, 2007)	48
Table 3.7	Critical gap (s), follow-up time (s) and minimum headway ranges	49
Table 3.8	Comparison of dominant and subdominant traffic entry lane	50
Table 3.9	Comparison between Gap acceptance and Empirical technique (Taekratok, 1998) ..	53
Table 3.10	Comparison of Australia and US capacity formulas (Taekratok, 1998).....	54
Table 4.1	Basic intersection traffic conflicts control (Glauz, W., and Migletz, D, 1980).....	64
Table 4.2	Recommended maximum entry design speeds (Zong Z. Tian, 2007)	66
Table 4.3	Design vehicle-turning radius (AASHTO, 2004)	69
Table 4.4	Comparison of inscribed circle diameter ranges.....	70
Table 4.5	Minimum circulatory lane width for dual-lane roundabouts (FHWA, 2000).....	72
Table 4.6	Design element for the non-motorized roundabout users	79
Table 4.7	Intersection site distance and stopping site distance (FHWA, 2000)	85
Table 7.1	Input geometric parameter range for proposed site roundabout.	146
Table 7.2	Input traffic data for proposed site roundabout.....	147
Table 7.3	Comparison of the sensitive analyses for a right-angle roundabout.	148
Table 7.4	Comparison of the sensitive analyses for a skewed-angle roundabout.....	154
Table 7.5	Comparison of model results	157

LIST OF FIGURES

Figure 1.1	Dual-lane roundabout geometric elements (NCHRP Report 672, 2010)	3
Figure 1.2	Thesis research structure and its organization	14
Figure 2.1	Central island landscaping profile	18
Figure 2.2	Example of Central Island landscaping at Avon, Colorado.....	18
Figure 2.3	Landscaping encroaching on sight lines at San Diego, California	19
Figure 2.4	Graphical depiction of crash types (Bared, J. G. and K. Kennedy, 1999).....	23
Figure 2.5	Bicycle treatment at entry and exit ramp (WisDOT, 2011).....	28
Figure 2.6	Bicycle design treatments (FHWA, 2000).....	28
Figure 3.1	Single-lane and dual-lane roundabouts capacity comparison (FHWA, 2000).	32
Figure 3.2	Roundabout capacity (Brilon, Werner, Ning Wu, and Lothar Bondzio, 1997)	38
Figure 3.3	German Gap acceptance capacity formula behavior	39
Figure 3.4	Capacity Flow diagram for Swiss Roundabout (Swiss Roundabout Guid, 1991)...	42
Figure 3.5	Entry capacity reduction factors due to pedestrian (Brilon, 1991)	43
Figure 3.6	Capacity curves for single-lane and dual-lane roundabout scenarios (HCM, 2010)	45
Figure 3.7	95 th percentile queue length estimation Figure (Wu, 1994).....	56
Figure 4.1	Conventional intersection conflicts (FHWA, 2000)	60
Figure 4.2	Single-lane roundabout (NCHRP Report 672, 2010)	61
Figure 4.3	Dual-lane roundabout (NCHRP Report 672, 2010).....	61
Figure 4.4	Exit-circulating conflicts.....	62
Figure 4.5	Resolve exit-circulating conflicts	62
Figure 4.6	Improper lane use conflicts	63
Figure 4.7	Improper right and left conflicts	63
Figure 4.8	Bicyclists, vehicular and pedestrian conflicts (Google)	65
Figure 4.9	Measurement of entry angle when ($\Phi = 2\Phi/2$) (WisDOT, 2011).....	73
Figure 4.10	Measurement of entry angle when ($\Phi = \Phi$) (WisDOT, 2011).....	73
Figure 4.11	Min. Splitter Island dimensions (NCHRP Report 672, 2010)	74
Figure 4.12	Minimum splitter island nose radii and offsets (NCHRP Report 672, 2010).....	74
Figure 4.13	Roundabout approach alignment (FHWA, 2000).....	75
Figure 4.14	Vehicle natural path	77

Figure 4.15	Vehicle path overlap	77
Figure 4.16	Technique to avoid path overlap at entry (KDOT, 2003; WisDOT, 2011)	77
Figure 4.17	Technique to increase entry deflection (NCHRP Report 672, 2010)	78
Figure 4.18	Vehicle fastest through, right and left turn path curves radius	80
Figure 4.19	Approach sight distance (FHWA, 2000)	82
Figure 4.20	SD on circulatory roadway	83
Figure 4.21	SD to crosswalk on exit	83
Figure 4.22	Intersection sight distance triangle (FHWA, 2000)	83
Figure 5.1	Possible LINGO model outcomes	88
Figure 5.2	Roundabout geometry for traffic flow	91
Figure 5.3	Fastest paths curve at right-angle roundabout intersections	93
Figure 5.4	Vehicle fastest through path curve at entry, exit and around central island	94
Figure 5.5	Fastest through path curve around Central Island at right-angle roundabout	95
Figure 5.6	Fastest through entry paths curve at right-angle roundabout	97
Figure 5.7	Fastest through exit paths curve at right-angle roundabout	98
Figure 5.8	Vehicle fastest through path curve at entry, exit and around central island	100
Figure 5.9	Vehicle fastest right turn path curve at inside inscribed circle diameter	101
Figure 5.10	Vehicle fastest right turn entry path curve at right-angle roundabout	102
Figure 5.11	Vehicle fastest right turn exit path curve at right-angle roundabout	104
Figure 5.12	Vehicle fastest left turn path curve at right-angle roundabout	105
Figure 5.13	Left turn path curve around Central Island at right-angle roundabout	106
Figure 5.14	Left turn entry path curve at right-angle roundabout	107
Figure 5.15	Left turn exit path curve at right-angle roundabout	109
Figure 5.16	Conflicting points at right-angle dual-lane roundabout	113
Figure 6.1	Vehicle fastest paths at skewed-angle roundabouts	120
Figure 6.2	Fastest through path modeling at skewed-angle roundabouts (Sub-model 1)	122
Figure 6.3	Through path around central island at skewed-angle roundabout (Sub-model 1)	123
Figure 6.4	Right turn fastest path at skewed-angle roundabouts (sub-model 1)	125
Figure 6.5	Right turn fastest path in ICD at skewed-angle roundabouts (sub-model 1)	126
Figure 6.6	Right turn exit path at skewed-angle roundabouts (sub-model 1)	128
Figure 6.7	Fastest left turn path at skewed-angle roundabout (sub-model 1)	129

Figure 6.8	Fastest left turn exit path at skewed-angle roundabouts (sub-model 1).....	131
Figure 6.9	Fastest through path modeling at a skewed-angle roundabout (sub-model 2).....	132
Figure 6.10	Through path around central island at a skewed-angle roundabout (sub-model 2)	133
Figure 6.11	Fastest through entry path at a skewed-angle roundabout (Sub-model 2).....	134
Figure 6.12	Fastest through exit path at a skewed-angle roundabout (sub-model 2).....	135
Figure 6.13	Fastest right turn path modeling at skewed-angle roundabout (sub-model 2).....	136
Figure 6.14	Fastest right turn entry path at skewed-angle roundabouts (sub-model 2)	137
Figure 6.15	Fastest left turn path at a skewed-angle roundabout (sub-model 2)	140
Figure 6.16	Fastest left turn entry path at a skewed-angle roundabout (sub-model 2)	141
Figure 7.1	The intersection at Warden Avenue @ 14 th avenue (Google image).	144
Figure 7.2	Ira Needles Boulevard @ Erb Street intersection (Google image).....	144
Figure 7.3	Graphical comparison of the sensitive analyses for a right-angle roundabout.	149
Figure 7.4	Drawing of a right-angle dual-lane roundabout.....	150
Figure 7.5	Effect of weighted factor α on multi-objective optimization model analysis.....	152
Figure 7.6	Graphical representation of multi-objective optimization function.....	153
Figure 7.7	Graphical comparison of the sensitive analyses for a skewed-angle roundabout..	155
Figure 7.8	Drawing of a skewed-angle dual-lane roundabout	156
Figure 7.9	Graphical comparison of right-angle and skewed-angle roundabouts.....	158

LIST OF APPENDICES

- Appendix-A** Optimization model for right-angle dual-lane roundabouts
- Appendix-B** Optimization model for skewed-angle dual-lane roundabouts
- Appendix-C** Lingo-13 software coding for dual-lane right-angle and skewed- angle roundabouts
- Appendix-D** Glossary of Terms

CHAPTER 1 : INTRODUCTION

Roundabouts have been used productively in many cities around the world. The safe and efficient manner in which roundabouts accommodate traffic, in addition to their improved aesthetics, has focused strong attention on roundabouts as an important element in the design of state and local roadways in Canada. Roundabouts perform better than traffic lights at intersections with roughly similar traffic flows in each direction and a high proportion of left turning traffic. As compared with conventional ways for channeling traffic, roundabouts can improve safety by simplifying potential vehicle conflicts, reducing vehicle speeds, and providing a clearer indication of the driver's right-of-way. Several transportation authority's worldwide (UK, US, Australia, Canada) are now considering constructing roundabouts to advance vehicle safety, boost roadway capacity and effectiveness, reduce vehicular delay and emissions, and identify opportunities for the community (Bill Baranowski, 2005).

1.1 BACKGROUND HISTORY

In 1903 the rotating operation of intersecting traffic concept was introduced, when Eugene Henard proposed a revolving operation system for traffic control at intersecting streets (Henard, 1903). In New York City, 1905, the initial convenient use of a revolving-traffic intersection in the USA was Columbus Circle, inaugurated by William Phelps Eno (Todd, 1988).

In the early 1900s traffic circles, or rotaries, were used in the United States, but there was great difficulty in regulating traffic. Local ordinances were unenforceable and there were no regular rules of the road in the country. The first spiraling intersection in Britain was constructed in 1909. A common effort between the Ministry of Transport and the Town Planning Institute in Britain issued MOT Circular in 1929, which appears to have been the earliest use of the term "Roundabout" (Brown, 1995).

Several studies performed in Britain have shown that a drop in traffic speed at roundabouts is due to deflecting of traffic at an entry. In 1975 a modified design indicated that a curved vehicle path or "deflection" can be achieved by providing angled deflection islands usually raised at entry, and a correctly sized and positioned central island to stop vehicles from taking too straight a path through the intersection (Brown, 1995).

In the 1970s the first roundabouts in France were installed experimentally; these showed definite advantages in safety, fluidity and simplicity. Several modifications in actual design and in design strategy were made in France in the mid-1980s, and none of the circular roundabouts designed and built earlier than this is a modern one. In September 1983, the rule of priority for traffic on the roundabout was introduced into the Highway Code in France, and since then, the number of roundabouts has grown rapidly throughout the country (Thai Van, et al, 2000).

In Britain in 1984, a design standard was issued, which launched “entry path curvature” requirements and the roundabout perception. Thus, the concept of the “modern roundabout” was created in 1984 with introduction of the three principal features of yielding to traffic in the circle, deflection at entry, and low design speed (controlled by the amount of deflection or entry path curvature). In the early stages of the roundabout era, designers gave precedence to entering vehicles, thereby facilitating high-speed entry, high-crash experience, and congestion. International experiences with roundabouts were negative, with Britain and others experiencing circles that locked up as traffic volumes increased. Although many of these old traffic circles in Europe and the USA were removed, many remain today, for example, in Washington D.C. Subsequent research in Britain led to the idea of yield at entry (FHWA, 2000). Modern roundabouts are ring-shaped intersections through which traffic runs in a counter-clockwise direction wherever vehicles drive on the left-hand side of the road, as in Britain, and clockwise wherever vehicles drive on the right; vehicles going through the roundabout must yield to those already inside. The first modern roundabout was built after 1990 in Summerlin, Nevada, the United States, and any circular intersection designed and built before 1990 is not a modern roundabout in the US. In June 2002, the *Seattle Times* reported that at least 600 roundabouts had been built in the United States since 1990. There were, however, about 2000 roundabouts there in 2010, and the number is growing rapidly (Keh Andreh, 2010).

In 2000 Alberta Transportation took control of all highways in the province to advance operations and maintenance. After researching various types of intersection, engineers and Alberta Transportation decided to construct a modern roundabout at the end of a straight overpass of Highway 63, King Street, in Fort McMurray. This interchange was opened to traffic on July 4, 2003, and is believed to have been the first modern roundabout interchange in Canada. Many municipalities in Ontario – including the Region of Waterloo, City of Ottawa, and the City of Hamilton – have constructed roundabouts on municipal roads with great success. Although

roundabouts are a relatively new method of traffic control at intersections in Ontario, they have been implemented successfully on provincial highways in other Canadian provinces. Modern roundabouts are common in Australia, China, France, Germany, New Zealand, Netherlands, Qatar, Spain, United Arab Emirates, United Kingdom, and the United States, among other countries (B.Guichet's 2008).

1.2 BASIC DUAL-LANE ROUNDABOUT GEOMETRIC FEATURES

As shown in Figure 1.1, dual-lane roundabouts can offer numerous advantages over traditional signalized and stop-controlled substitutes, including enhanced overall safety performance and management of speeds, with inferior delays and shorter queues during off-peak periods. The safe operational design and analysis of a dual-lane roundabout require an understanding of all elements and properties of a roundabout. It is helpful, therefore, to define here all the elements of a roundabout. A roundabout is a circular intersection with the following specific geometric and traffic control features, as discussed in Table 1.1.

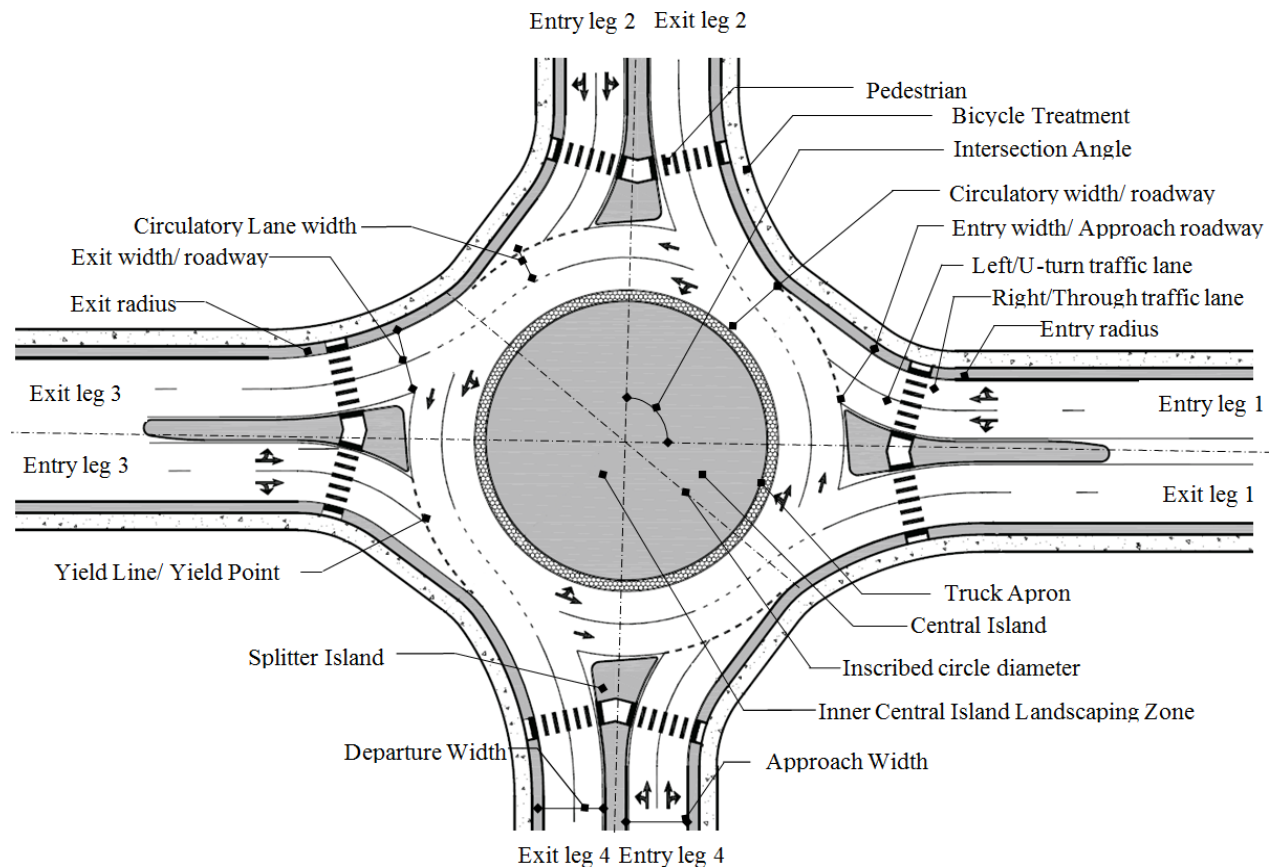


Figure 1.1 Dual-lane roundabout geometric elements (NCHRP Report 672, 2010)

Table 1.1 Basic dual-lane roundabout geometric features

Features	Description
Central island	The raised central area of the roundabout around which traffic circulates. Roundabout can have a raised central island with a mountable apron surrounding it.
Splitter island	A raised or painted area on an approach used to divide; entering traffic from exiting traffic, deflect and slow entering traffic, and offer storage space for pedestrians crossing the road in two stages.
Circulatory roadway	The curved path used by vehicles to travel around the central island in one direction.
Circulating roadway width	The total width of the circulating lanes measured from inscribed circle to the central island.
Approach width	One way width of roadway approaching the roundabout.
Departure width	One way width of roadway used by departing vehicle from the roundabout. It is typically equal to the approach width.
Truck apron	A truck apron is the mountable portion of the central island adjacent to the circulatory roadway which accommodates the wheel tracking of large vehicles. Truck aprons are not necessary at all roundabouts.
Yield-line	A pavement marking used to mark the point of entry from an approach into the circulatory roadway and is generally marked along the inscribed circle. Entering vehicles must yield to any circulating traffic coming from the left before crossing this line into the circulatory roadway.
Yield-point	The point at which entering traffic must yield to circulating traffic before entering the circulating roadway.
Accessible pedestrian crossings	It should be considered at all roundabouts. The crossing location is set back from the entrance line, and the splitter island is cut to allow pedestrians, wheelchairs, strollers, and bicycles to pass through. Striped crossings may be omitted at rural roundabouts where pedestrian activity is nonexistent and not expected.

Bicycle treatments	Roundabouts provide bicyclists the option of traveling through the roundabout either as a vehicle or as a pedestrian, depending on the bicyclist's level of comfort.
Entry width	The width of an entrance leg at the inscribed circle measured perpendicular to travel.
Exit width	Perpendicular distance measured from right to left between edge of the exit to intersection at yield line and edge of inscribed circle.
Entry radius	The minimum radius of curvature of the right side curb at the entry.
Exit radius	The minimum radius of curvature of the right side curb at the exit.
Inscribed circle diameter	This parameter is used to define the roundabout size. It is the diameter of the outer curb line of the circulatory roadway.
Entry angle	The angle between the entry roadway and the circulating roadway measured at the yield point.
Deflection	The change in the path of a vehicle imposed by the geometric features of a roundabout resulting in a slowing of vehicles.
Entry curve	The curve of the left edge of the roadway that leads into the circulating Roadway.
Flare	The widening of the approach to the roundabout to increase capacity and facilitate natural vehicle paths.
Natural vehicle path	The natural path that a driver navigates a vehicle given the layout of the intersection and the ultimate destination.
Turning radius	The radius that the front wheel of the design vehicle on the outside of the curve travels while making a turn.

1.3 MODERN ROUNDABOUTS AND TRAFFIC CIRCLES COMPARISON

A roundabout is a circular intersection similar to the traffic circle used in the past in several countries. Traffic circles are found in many places in the United States, including Washington DC, New Jersey, and Pennsylvania. Although modern roundabouts are relatively new to the United States, they are common in the United Kingdom and Australia and are becoming popular in many European countries. Based on their travel experiences, travellers are likely to agree that nonconforming traffic circles do not work well. The major differences

between a traffic circle and a roundabout are yield at entry, deflection, and flare. Table 1.2 presents a comparison of modern roundabouts with traffic circles.

Table 1.2 Modern roundabouts and traffic circles comparison

MODERN ROUNDABOUT	TRAFFIC CIRCLE
<p>Yield-at-Entry;</p> <ul style="list-style-type: none"> • Entering traffic yields to circulating traffic, which always keeps moving • Very efficient with heavy traffic • No weaving distance is needed, so roundabouts are small and fit in compact spaces 	<p>Entering traffic may interfere with circulating traffic;</p> <ul style="list-style-type: none"> • Circulating traffic can not clear when entering traffic fills circle • Motorists entering early traffic circles had right-of-way, thereby locking up traffic • Heavy traffic causes gridlock • Circles must be large to provide long weaving distances
<p>Entering traffic is deflected slowly around the central island;</p> <ul style="list-style-type: none"> • Deflection controls speed without enforcement, thereby reducing accidents • Deflection forms gaps in traffic so other vehicles can enter • Entry flare adds lanes 	<p>Inconsistent entry design may allow traffic to enter at high speed;</p> <ul style="list-style-type: none"> • Serious accidents can result on high speed streets • Fast entries impede gap acceptance and defeat the yielding process • parking was permitted within the circle
<ul style="list-style-type: none"> • Flare increases capacity at the intersection, where capacity is needed most • Flare promotes narrow streets between roundabouts, saving cost and neighborhood impacts 	<ul style="list-style-type: none"> • Poor entry conditions may not benefit from flare • Poor intersection capacity even with large traffic circles • Higher capacity requires wide streets between circles, wasting money and land

1.4 ADVANTAGES, DISADVANTAGES AND LIMITATIONS OF ROUNDABOUTS

A roundabout helps in improve the efficiency of traffic flow; it also reduces vehicle emissions and conserves fuel. Varhelyi (2002) found that the installation of a roundabout in place of an intersection with signals reduces carbon monoxide emissions by 29% and nitrous oxide emissions by 21%. In addition, replacing traffic signals and stop signs with roundabouts reduces carbon monoxide emissions by 32%, nitrous oxide emissions by 34%, carbon dioxide emissions by 37%, and hydrocarbon emissions by 42%. Constructing roundabouts in place of traffic signals can reduce fuel consumption by about 30% (Nitymaki, J. and Hoglund P.G. 1999). While the initial construction cost of a roundabout varies and depends upon location, its maintenance is cheaper than that of an intersection with signals.

1.4.1 Advantages of Roundabout

- Fewer overall conflict points and no left turn conflicts
- Motorists experience fewer and shorter delays at the intersection
- Attractive and calming entrance into the city
- Lower maintenance because no signal equipment to be installed and repaired
- Traffic is required to slow down when it is approaching a roundabout
- Improvement in environment due to reduction in pollution, fuel use and noise
- Emissions are reduced because of fewer cars in the backup
- In areas with high traffic volume, roundabouts reduce fatal accidents by 75%
- Low vehicle speed because drivers cannot travel at a fast speed in a roundabout
- More feasibility to accommodate parking, wider sidewalks, planter strips, and wider bicycle lanes on the approaches
- Reduced crash severity for all users; safer merges into circulating traffic; more time for all users to detect and correct for their mistakes or the mistakes of others, given the lower vehicle speeds
- Roundabouts offer more safety, because when cars enter a roundabout, the driver needs look only one way. Vehicles slow down, so decision making is simplified.

1.4.2 Disadvantages of Roundabout

- Often requires more space at the intersection itself than do other intersection designs
- Intersection traffic flows are severely unbalanced. Many roundabouts require landscape maintenance
- Equal priority for all approaches can reduce the progression for high-volume approaches
- Space required for an acceptable outside diameter is not available or is too expensive to acquire
- May create a safety hazard if hard objects are placed in the central island directly facing an entrance
- Multilane roundabouts present more difficulties for individuals with poor vision, due to challenges in detecting gaps and determining that vehicles have yielded at crosswalks
- Cannot provide explicit priority to specific users (e.g., trains, emergency vehicles, transit, pedestrians) unless supplemental traffic control devices are provided
- Construction staging for retrofits is expensive and complex. Typically, a four-lane roadway with constrained right-of-way requires temporary traffic signals. The key to minimizing traffic impact of construction staging is to make the intersection operate as a roundabout as soon into its construction as possible. This slows vehicle speeds and switches left turns to right turns, reducing the potential for crash

1.4.3 Limitation

Roundabouts have certain limitations, as follows:

- Two way stop control (TWSC) and all way stop control (AWSC) intersections are easier and less expensive to implement for low-volume applications
- Roundabouts offer the least positive form of control. Each vehicle entering the intersection must yield to all traffic that has already entered
- Steady-state entry headways are shorter at traffic signals because of the positive assignment of right-of-way. By using long cycle times to minimize the effects of start-up lost time, it is possible under most conditions to achieve higher approach capacities
- Since roundabout operation is not periodic, it is not feasible to coordinate the operation of roundabouts on an arterial route to provide smooth progression for arterial flows

1.4.4 Common site application

Roundabouts may be appropriate at intersections in the following situations:

- When future traffic growth is expected to be high, with uncertain or changeable patterns
- Roundabouts can operate efficiently, if major roads intersect at Y- or T-junctions with high volumes of left turning vehicles, unlike most other intersection designs. It helps in reducing left turn-opposed type of accidents and overall delays
- When traffic signals result in greater delays than a roundabout. It should be noted that in many situations, roundabouts provide a similar capacity to signals, but many operate with lower delays and better safety, particularly in off-peak periods
- At T- or cross intersections where the major traffic is routed through a right-angle. This often occurs on highways in country towns. In these situations the major movements within the intersection are turning movements, which are accommodated effectively and safely at roundabouts

1.4.5 Safest mechanism for traffic

Studies performed in the United States, Europe, and Australia have found that roundabouts have superior safety performance to other intersections. In 2000 the Insurance Institute for Highway Safety published a Study of Crash Reductions Following Installation of Roundabouts in the United States, illustrating a reduction in frequency of crashes after the installation of a roundabout. The increased safety levels in roundabouts can be attributed to:

- Yield at entry operation
- Pedestrians have to cross in only one direction of traffic at a time
- Central and splitter islands decrease the number of conflict points
- Fewer conflicting points than standard four-way intersections
- Vehicles travel in the one direction, virtually eliminating the right-angle or head-on collision
- Lower absolute speeds, allowing more time for drivers to react, reducing crash severity

In 2001, an institute research study of 23 intersections in the United States found that changing intersections from traffic signals or stop signs to roundabouts decreased injury crashes by 80%, and all crashes by 40% (Persaud, B.N, Retting, R.A, Garder, P.E, and Lord, D.

2001). Similar results were reported by Eisenman et al., that is, 75% decrease in injury crashes and 37% decrease in total crashes at 35 intersections that were converted from traffic signals to roundabouts (Eisenman, S.; Josselyn, J.; List, G.; Persaud, B.; Lyon, C.; Robinson, B.; Blogg, M.; Waltman, E.; and Troutbeck, R. 2004). A research study on 17 rural intersections on roads with 40 mph and higher speed limits reported that the average injury crash rate per million entering vehicles was reduced by 84%, and that fatal crashes were eliminated when the intersections were converted to roundabouts (Isebrands, H. 2009). Studies of intersections in Europe and Australia that were converted to roundabouts have reported 41%-61% reductions in injury crashes and 45%-75% reductions in severe injury crashes (FHWA, 2000). Following are reasons to construct a roundabout rather than a traffic signal:

- Solve special problems, such as 5-legged intersections
- Provide LOS A during the night and LOS A&B in off-peak hours
- Reduce the severity of injuries sustained in crashes
- Provide storm-proof intersections that continue to operate after hurricanes and tornados
- Drop of 90% in fatalities, 76% in injury crashes, and 30%-40% in pedestrian injuries (FHWA)
- Traffic is always on the move, meaning less delay and 20%-30% increase in capacity during peak hours

1.5 CATEGORIES OF ROUNDABOUTS

Roundabouts have been classified with respect to size and environment to differentiate their design and operational characteristics within different perspectives. There are six types, based on site location, number of lanes, and size as described in following section.

1.5.1 Mini roundabout

The mini roundabouts are used in built-up urban environments, in low-speed (25 mph or less) areas. Due to their small size, the central island is completely mountable. These roundabouts are relatively inexpensive due to minimal additional pavement at the intersecting roads – for example, minor widening at the corner curbs. Capacity for this type of roundabout is expected to be similar to that of the compact urban roundabout.

1.5.2 Urban compact roundabout

Urban compact roundabouts are characterized by their reasonably small inscribed circle diameter (30 to 37 m), a non-mountable central island, and almost right-angle entry geometry. These roundabouts are proposed to be pedestrian and bicycle friendly because they are at a 90° degree angle approach and legs require very low vehicle speeds to make a right turn into and out of the circulatory roadway. All legs have single-lane entries. Generally, aprons encircle the non-mountable part of the central island to accommodate large vehicles.

1.5.3 Urban single-lane roundabout

Urban single-lane roundabouts have a single-lane entry at all legs and a single circulatory lane. They are differentiated from urban compact roundabouts by having larger inscribed circle diameters (37 to 45 m) and more tangential entries and exits, resulting in higher capacities. The design of single-lane allows slightly higher speeds at the entry, on the circulatory roadway, and at the exit. The roundabout design is focused on getting consistent entering and circulating vehicle speeds. The geometric design includes raised splitter islands, a non-mountable central island and sometimes an apron.

1.5.4 Urban dual-lane roundabout

Urban dual-lane roundabouts incorporate all roundabouts that have at least one entry with two lanes in urban areas. These types require wider circulatory roadways to accommodate more vehicles journeying alongside. The speeds at the roundabout entry and exit, and on the circulatory roadway, are slightly higher than those for the urban single-lane roundabouts. It is important that the vehicular speeds be consistent throughout the roundabout. The geometric design includes raised splitter islands, a non-mountable central island, and sometimes an apron.

1.5.5 Rural single-lane roundabout

Rural single-lane roundabouts have bigger diameters than urban roundabouts to permit slightly higher speeds at the entries and exits, and on the circulatory roadway. This is possible if currently, and in the future, few pedestrians are expected at these intersections. The larger

diameters should accommodate larger vehicles, avoiding the need for an apron. Supplemental geometric design elements include extended and raised splitter islands, a non-mountable central island, and adequate horizontal deflection. Because they are often located in high-speed environments, roundabouts may require supplementary geometric and traffic control device management systems on approaches to warn drivers to slow to an appropriate speed before entering the roundabout.

1.5.6 Rural dual-lane roundabout

The main design differences between rural and urban dual-lane roundabouts are designs with vaguely upper entry speeds, larger diameters, and supplementary approach arrangements. Rural roundabouts should be designed with geometric features that permit effortless transfer to an urban roundabout, with slower speeds and design facts that fully provide for pedestrians and bicyclists. At rural roundabouts, where installation of pedestrian crossings is adjourned, an adequate splitter island width should be allowed, to accommodate the simple addition of a pedestrian refuge in combination with installing the pedestrian crossings.

1.6 RESEARCH SCOPE AND OBJECTIVE

The main objective of this research study is to develop an optimization model for the dual-lane right-angle and skewed-angle roundabouts, which will be supportive in determining the optimum geometric design parameters of dual-lane roundabouts and will satisfy the design consistency, capacity and operational performance. It also eradicates the present iterative time consuming design process. Future conservatory or research of this model may be in multi-lane, magic roundabouts. This model will operate as comprehensive software for the optimum design of dual-lane right-angle and skewed-angle roundabouts.

1.7 THESIS ORGANIZATION

Optimization models are developed in this thesis for dual-lane right-angle and skewed-angle roundabouts having intersecting lags angle range from 70 to 110 degrees. These optimization models determine the design elements of the roundabouts based on design consistency and the least average intersection delay. These models will also offer vehicle path

radii for through, left, and right turning traffic at all roundabout approaches. It forecasts the operating speeds along each vehicle path. These models have site conditions as input and prove to the utmost design consistency and the least average intersection delay for given traffic and geometric circumstances. Figure 1.2 represents the whole thesis structure.

Chapter 1 covers the history, basic geometric features, advantages, disadvantages and limitations of roundabouts. It also deals with the category of roundabout and its site application.

Chapter 2 presents roundabout characteristics and multi-modal consideration. The roundabout characteristics include the costs of operation and maintenance, traffic calming, landscaping, signing and lighting, aesthetics, spatial requirements, environmental factors, signal progression, vehicle delay, queue storage, delay of major movements, design for older drivers and safety characteristics and its aspects, while multi-model considerations include the study of transit, emergency vehicles, large vehicles and pedestrian and cyclist accommodation.

Chapter 3 presents the literature review on capacity and operational performance of roundabouts, capacity analysis of roundabouts, delay and queues at roundabouts, entry and exit capacity, and review of capacity, delay and queue models relating to different countries.

Chapter 4 covers the literature and other details on geometric design considerations for dual-lane roundabouts, conflicts at dual-lane roundabouts, design principal and objectives, performance checks and safety aspects for pedestrians, bicycles, large vehicles and old drivers, among others.

Chapter 5 presents the procedure for development of an optimization model for right-angle dual-lane roundabouts, which gives optimum design consistency and operational performance.

Chapter 6 presents the procedure for development of an optimization model for skewed-angle dual-lane roundabouts, providing optimum design consistency and operational performance. This chapter also includes the two sub-models.

Chapter 7 presents the application of both dual-lane right-angle and skewed-angle roundabout's models in the field, a sensitive analysis of them, and a comparison of both models.

Chapter 8 presents the conclusions and summary of thesis, and provides recommendations for additional research on this model.

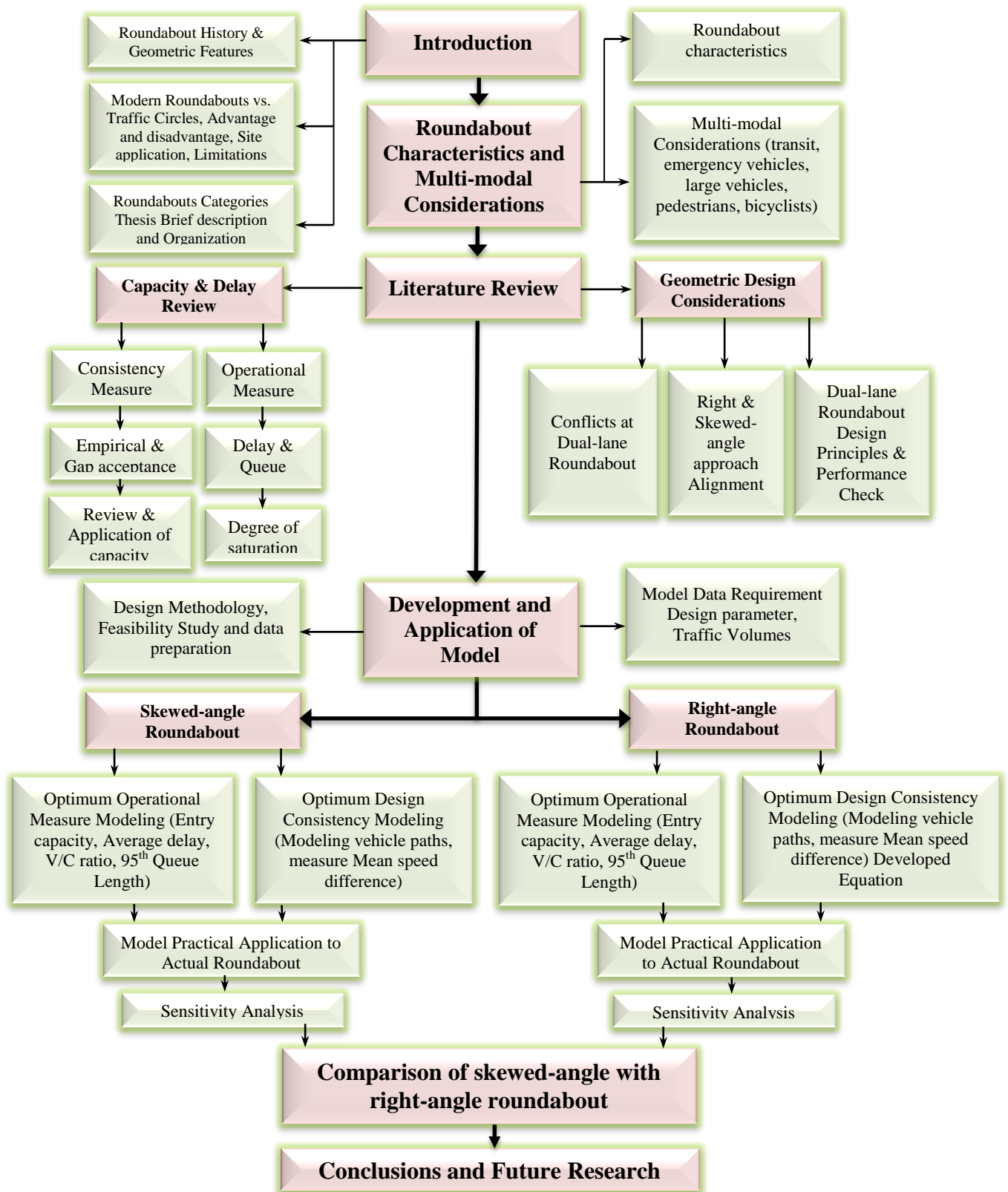


Figure 1.2 Thesis research structure and its organization

CHAPTER 2 : CHARACTERISTICS AND MULTI-MODAL CONSIDERATIONS

2.1 ROUNDABOUT CHARACTERISTICS

As the population increases the traffic density also increases, increasing the probability of fatal accidents at intersections. Several authorities are looking for unconventional intersection control techniques to advance safety and transmit additional traffic lacking wide roadways. Due to numerous benefits that promote safety, operations, and aesthetics, roundabouts are becoming more acceptable.

2.1.1 Operation and maintenance cost

The roundabout installation cost depends on several factors including pavement area, road work, land cost, and relocation of utilities. Traffic signals are normally less expensive to install than roundabouts; traffic signals can often be installed with slight or no change to the accessible pavement and curb lines, while this is hardly ever possible for a roundabout. When completing a cost and benefit ratios for a roundabout, the life cycle costs for the predicted duration of the development are extensive. Roundabout maintenance costs include pavements, drainage systems, traffic signs, and pavement markings, street lighting and landscaping maintenance costs. The road pavement is usually damaged by the scrubbing action of heavy vehicles turning through a roundabout. It is necessary therefore to think cautiously about the nature of surface treatment, because it may influence the frequency of resurfacing. Overall, there is little difference between the cost of maintenance for these items at roundabouts and that of other forms of channeling of the same pavement area.

In 2008, during an intersection control study in the Region of Waterloo, a life cycle cost estimate included the implementation cost and 20-year present value of injury collision, operating, and maintenance costs. This study showed that multi-lane roundabouts are more beneficial than traffic signals. Often a roundabout is estimated to cost more to construct than a signal system, but to cost less over a 20-year life cycle due to societal savings from fewer collisions. Table 2.1 presents a cost comparison of traffic signals and roundabouts.

In general roundabouts are a less expensive alternative to signalized intersections based on operations and maintenance costs, even though they have high landscaping costs for

maintaining the central island and splitter islands. In addition, the signalized intersections incur high energy and equipment maintenance costs that are not required by roundabouts.

Table 2.1 Cost comparison between traffic signal and roundabout

Item	Traffic signal	Roundabout
Total construction cost	\$1095000	\$1262000
Property acquisition	\$140000	\$320000
Injury crash cost	\$905000	\$316000
Traffic signal maintenance and replacement per year	\$184000	-
Additional street lighting and annual maintenance	-	\$33000
Total cost	\$2324000	\$1931000

Source; (Steve van de Keere and Phil Weber, 2008)

2.1.2 Traffic calming

There can be a traffic calming effect at a street through reducing vehicle speeds by means of modifying the geometric design elements instead of installing traffic control devices or reducing traffic volume at roundabouts. Consequently, speed reduction can be realized at all times and on streets of any traffic volume. It is difficult to drive a vehicle at a fast speed through a correctly designed roundabout, due to elevated channelization that forces vehicles to change track. A roundabout at the transition from a high-speed rural environment to a low-speed urban environment is a best example of traffic calming. Roundabouts have also been used effectively as doorway treatments at the interface between rural and urban areas where speed limits change.

2.1.3 Landscaping

Roundabouts offer the prospect to deliver attractive entrances to population centers, because landscaping is an attractive aesthetic feature. Landscaping can be installed on the central island and splitter islands satisfying all the sight distance requirements. Without any significant safety hazard to errant vehicles, designers can place monuments and art in some portions of the central island. The visual appearance of roundabouts can be improved with different pavement textures and colors for truck aprons or other elements. Landscaping should be designed to allow

drivers to see the signage and outline of the roundabout as they approach and have sufficient visibility to make decisions within the roundabout. Clear distances and offsets should be carefully considered during the installation of landscaping or other artistic features in the central island, to make sure that objects facing the entries do not generate a safety hazard.

To ensure acceptable sight distances in the critical visibility areas, landscaping must be limited to a height of 0.6 m. The acceptable types and location of landscape features are dependent on the operating environment. There is usually more flexibility with low speed urban (~55 km/h) traffic than with high speed suburban and rural environments (~65 km/h), where drivers are traveling at higher speeds upstream of the roundabout (NCHRP Report 672, 2010).

The safety of the intersection can improve with central island landscaping by making the intersection a pivotal point, by encouraging lower speeds, and by interrupting the approaching vehicles' headlight glare. It is necessary to build a vaulted or mounded central island to upsurge the perceptibility of the intersection on the approach. The elevation of the rounded area on the central island ranges from 1 to 1.8 m as recommended by Wisconsin Department of Transportation Facilities Development Manual. The central island slope should not exceed a 6:1 (H: V), in order to allow erratic vehicles to recover. The dimensions of the roundabout can impact the nature and locality of landscaping. Landscaping within the central island should disappoint pedestrian traffic to and through the central island (AASHTO, 2006).

According to Kansas Roundabout Guide, trees, shrubs, statues and other items can be placed on the inner central island to benefit the line of sight straight through the roundabout, to deliver a sign for drivers that they cannot precede straight through the intersection. This landscaping zone makes the roundabout more noticeable at night, with the vehicle front lights illuminating the central island (Kittelson & Associates, 2003). Figure 2.1 and Figure 2.2 represent the inner central landscaping zone within the roundabout

The typical landscaping zones within roundabouts are;

- Inner central island landscaping zone
- Perimeter central island landscaping zone
- Approach and corner radii landscaping zone

The main point to consider with the landscaping design for splitter islands and along the outside approach edges is, to avoid obstructing the sight distance, because the splitter islands are commonly situated within the critical site triangle.

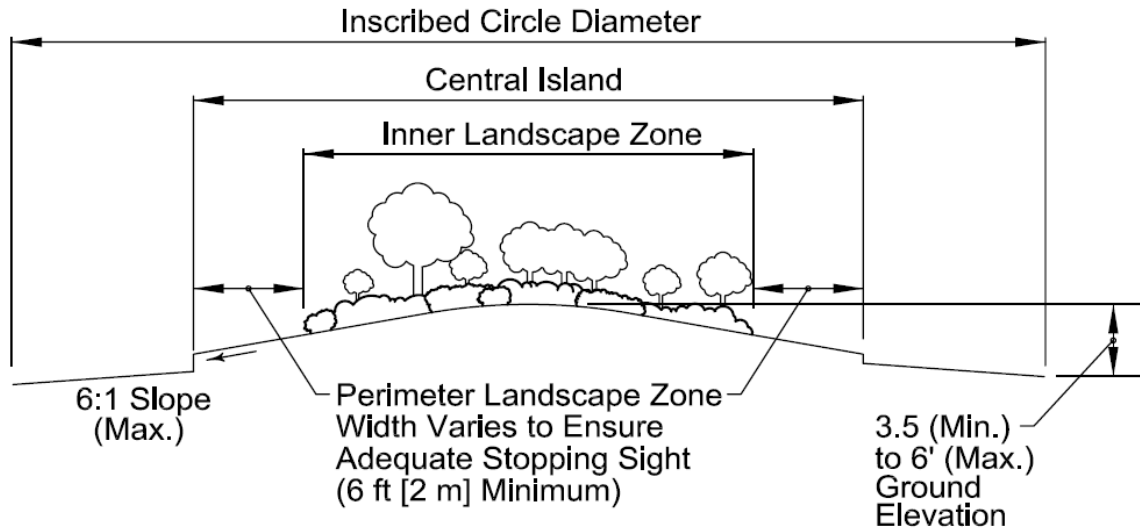


Figure 2.1 Central island landscaping profile

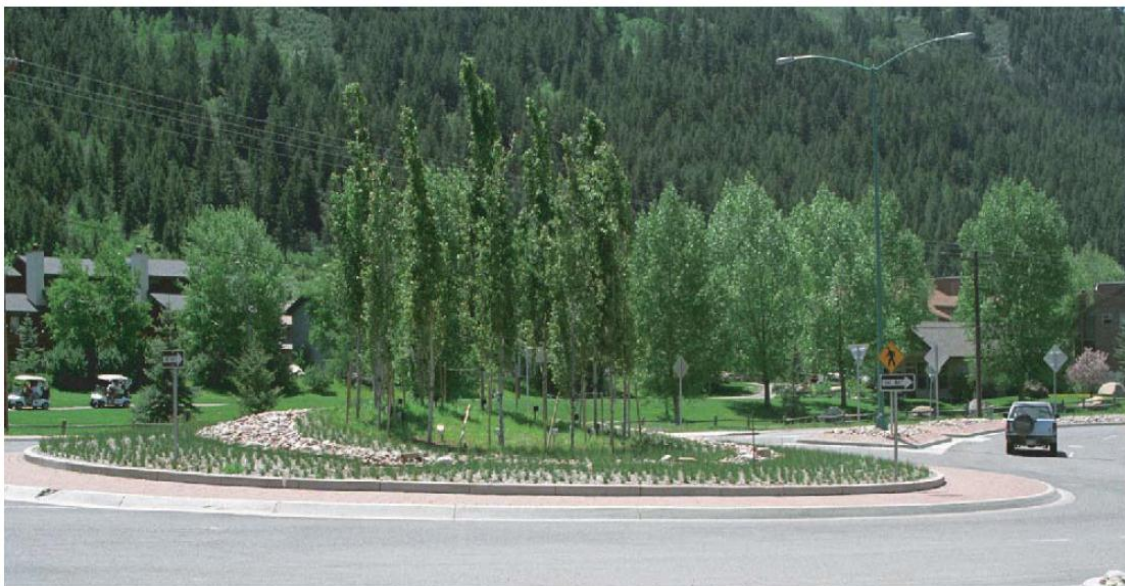


Figure 2.2 Example of Central Island landscaping at Avon, Colorado

Figure 2.3 is taken from (Facilities Development Manual, 2009) Wisconsin Department of Transportation data representing an example where the landscaping in the splitter island is commencing to infringe driver sight lines. There are two determining factors when evaluating whether to arrange for landscaping inside the splitter islands (WisDOT, 2011): one is splitter island size, and the other is roundabout location.



Figure 2.3 Landscaping encroaching on sight lines at San Diego, California

2.1.4 Environmental factors

Roundabouts can have environmental advantages if they decrease vehicle delay, the number of stops, and duration of stops at an intersection compared with a substitute arrangement for the intersection. The substitute involves heavy traffic volumes and traffic vehicles that progress gradually in moving queues rather than coming to a complete stop. In this scenario, the number of acceleration/deceleration cycles and the waiting time decrease, resulting in reduction of noise and gas emission and fuel consumption.

2.1.5 Other characteristics

Spatial requirements

Roundabouts frequently involve a larger space than signalized intersections. They reduce delay; therefore shorter queues result, including on the approach legs. It may also be possible to space roundabouts closer together than traffic signals because of the shorter queue lengths. If a signalized intersection needs multiple turn lanes to accommodate sufficient capacity, then a roundabout with the same capacity may need a shorter space on the approaches. Signalized intersections function most effectively when they accommodate groups of traffic, permitting the greatest number of vehicles to pass during green without stopping, resulting in the shorter

headways. Conversely, the lanes between signals are required to maintain these volumes of traffic through a sequence of signals. Roundabouts generate effectiveness through a gap acceptance process, although through-traffic capacity is limited by conflicting circulatory flow. Drivers can accept gaps as they appear instead of waiting for their time in the cycle; therefore, more random flow ensues and makes more resourceful use of the links involving intersections.

Signal progression

Roundabouts offer equivalent importance to all traffic movements; major street traffic movements may be delayed too long. The delay for through traffic on major roads can be minimized by coordinating operation of traffic signals on arterial roads. Roundabouts cannot deal with using a traffic management system to assist extraordinary events such as averted traffic volumes. The other prospect for roundabouts is that they help to make more efficient use of the existing traffic signals in the area. In many cases, the least cycle length required for a whole system is governed by the highest volume intersection in the system. We can reduce the delay by distributing the signal system into subsystems separated by roundabouts and allocating all subsystems a cycle length that may be shorter than earlier. In this way, the overall total delay and queues may be reduced.

Vehicle delay

Roundabouts normally function with shorter vehicle delays than other intersection configurations, when the operation is contained by capacity. It is pointless for traffic to come to a complete stop at roundabouts when no conflicts exist. When queues are present on one or more approaches, traffic within the queues usually continues to move, and this is normally more appealing to drivers than a stopped queue. The existing roundabout may be evaluated by the designer to determine its performance and whether modifications to its design are required. Designers can perform a qualitative evaluation of the roundabout performance during designing a roundabout. The main concern is to reduce the traffic delay at following locations;

- Meeting of more than two roadways
- Where Pedestrian crossing volumes are minimal
- Where approach volumes are similar, and the left turning traffic volumes are high at intersecting roads

Aesthetics

The central and splitter islands offer the opportunities to provide attractive entries or centerpieces to communities through use of landscaping, monuments and art, provided they are appropriate for the speed environment in which the roundabout is located (FHWA, 2000).

Queue storage

Roundabouts are better than traffic signals in terms of shorter queues, and they involve smaller amounts of queue storage space on the approach legs. For a similar traffic capacity, roundabouts may require less space on the approaches than signalized intersections, which require elongated or several turn lanes to supply adequate capacity. Therefore, roundabouts eliminate the requirement of extra right-of-way on links between intersections.

Delay of major movements

Roundabouts are likely to involve all movements at an intersection in the same way without any preference for major movements above minor movements. Every approach is required to yield to circulating traffic in a roundabout at yield line, whether the approach is a local street or a major arterial, resulting in larger delays to the major movements. This problem is most critical at the intersection of high-volume major streets supporting low to medium volume minor streets. The delay of each approach should be calculated individually because it depends on the volume of turning movement of that approach.

Design for older drivers

In North America, especially in the United States, the tendency is for people to keep driving at old age. The capability of older drivers and pedestrians to safely move through intersections is of utmost concern during dual-lane roundabouts design. Movement is more challenging for older drivers and pedestrians than for younger during such driving conditions, which relates speed and distance decisions under time constraints. Older drivers are upset at the curved alignment, and most likely they are engaged in crashes where the driver is driving at too high a speed at the curve.

The loss-of-control crashes result from an inability to maintain lateral position through the curve because of excessive speed, with inadequate deceleration in the approach zone. These

problems in turn stem from a combination of factors, including poor anticipation of vehicle control requirements, induced by the driver's prior speed, and inadequate perception of the demands of the curve. Older drivers have difficulty in paying attention to all necessary aspects in different driving circumstances. The response time of older drivers to events is greater than for average drivers (FHWA, 2000).

Safety

Compared with signalized and un-signalized intersections, roundabouts enhance the operation and safety of a vehicle if they are designed according to operational and safety requirements. Roundabout installation results in reduction of vehicle delays and queues, collision frequency, and severity due to lower traffic speeds, vehicle emissions with fewer starts and stops, operation and maintenance costs. When we look at the drawbacks associated with roundabouts in a developed city like the City of Toronto, and then we can find that roundabouts are

- Not friendly to cyclists and pedestrians, particularly children, elderly, those who are disabled, blind, and visually impaired
- Likely to require land acquisition
- Expensive and disruptive to implement

The latest study represented overall reductions of 35% in total crashes and 76% in injury crashes (Rodegerdts & D. Carter, 2007). Cunningham states that there is 100% reduction in fatalities at roundabouts (Cunningham, March 2007). Persaud evaluated changes in motor vehicle crashes at 24 intersections that had been converted from stop signs and traffic signals control to modern roundabouts. These intersections were located in eight states and in a mix of urban, suburban, and rural environments. A before-and-after study was conducted using the empirical Bayes approach, which accounts for regression to the mean. Overall, results showed reductions of 39% for all crash types combined, 76% for all injury crashes, and 90% for fatal, severe and incapacitating injury crashes. The results are consistent with those of many international studies and suggest that roundabout installation should be strongly promoted as an effective safety treatment for intersections (Persaud, B. N.; R. A. Retting; P. E. Garder; and D. Lord, March 2000).

Conflicting traffic at roundabout

Maryland Insurance Institute for Highway safety is responsible for a summary of crash types at 29 single-lane roundabouts and 9 multilane roundabouts with at least two years of crash data. This research shows 149 and 134 crashes at the single-lane and multilane roundabout locations. Six of the single-lane roundabouts accounted for 59% of total crashes at the single-lane roundabouts studied, and two roundabouts represent greater than 80% of total crashes at the multi-lane roundabouts. Crash type results from the Insurance Institute for Highway safety study are presented in Figure 2.4 and Table 2.2, along with international data for comparison. The numbering in Figure 2.4 corresponds to that in Table 2.2, which shows that a variety of distinctive crash types can take place at roundabouts. A designer should consider these crash types when making decisions about alignment and location of fixed objects. These crash types are suggested as conflict types for reporting crashes at roundabouts and conducting traffic conflict analyses (Mandavilli, S., A. McCartt, and R. Retting, May, 2008).

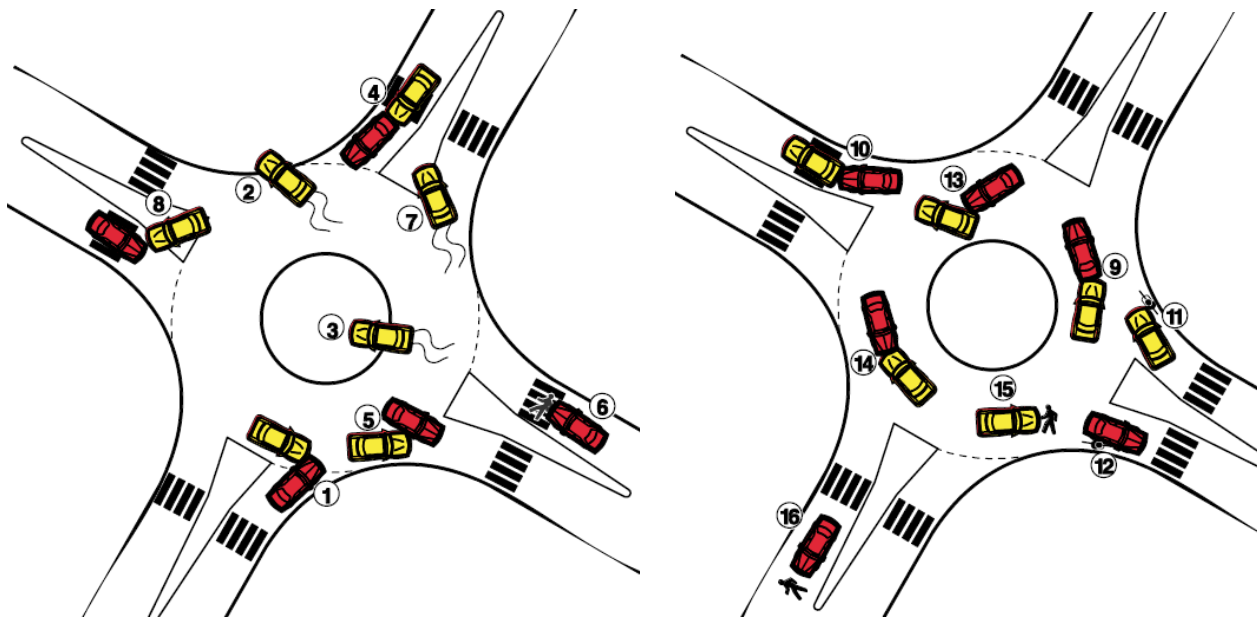


Figure 2.4 Graphical depiction of crash types (Bared, J. G. and K. Kennedy, 1999)

Table 2.2 Crush at roundabout in several countries (NCHRP Report 672, 2010)

Crash type	France	Queensland, Australia	United Kingdom ¹	United States	
				Single-Lane	Double-Lane
1. Failure to yield at entry (entering-circulating)	36.6%	50.8%	71.1%	13%	17%
2. Single-vehicle run off the circulatory roadway	16.3%	10.4%	8.2% ²	50% ²	28% ²
3. Single vehicle loss of control at entry	11.4%	5.2%	2	2	2
4. Rear-end at entry	7.4%	16.9%	7.0% ³	34%	19%
5. Circulating-exiting	5.9%	6.5%			4%
6. Pedestrian on crosswalk	5.9%		3.5% ⁴		4% ⁵
7. Single vehicle loss of control at exit	2.5%	2.6%	2		
8. Exiting-entering	2.5%			1%	
9. Rear-end in circulatory roadway	0.5%	1.2%			
10. Rear-end at exit	1.0%	0.2%			
11. Passing a bicycle at entry	1.0%				
12. Passing a bicycle at exit	1.0%				
13. Weaving in circulatory roadway	2.5%	2.0%			
14. Wrong direction in circulatory roadway	1.0%				
15. Pedestrian on circulatory roadway	3.5%		4		
16. Pedestrian at approach outside crosswalk	1.0%		4		
Other collision types		2.4%	10.2%	2%	3%
Other sideswipe crashes		1.6%			24% ⁶

Notes:

1. Data are for “small” roundabouts [curbed central islands >13ft (4 m) diameter, relatively large ratio of inscribed circle diameter to central island size.
2. Reported findings do not distinguish among single-vehicle crashes.
3. Reported findings do not distinguish among approaching crashes.
4. Reported findings do not distinguish among pedestrian crashes.
5. Reported findings combine pedestrian and bicycle crashes.
6. Reported findings do not distinguish among sideswipe crashes.

2.2 MULTI-MODAL CONSIDERATIONS

The intersection design required consideration of all transportation kinds such as transit, emergency vehicles, large vehicles, pedestrians, cyclists and motorcyclists, with full information on approaching or being already present at that intersection. Each transportation mode has its own safety and operational requirements to be satisfied during design of roundabouts. The general issues associated with each mode are described as follows.

2.2.1 Transit

Roundabouts and conventional intersection configurations have similar transit considerations. Appropriately designed roundabouts will smoothly accommodate buses. There is a chance of traffic backing up downstream of buses, therefore the bus stops should be installed sufficiently far away downstream of the roundabout, to take care of traffic backing up into the roundabout (FHWA, 2000). Bus stops should be located suitable to minimize the probability of vehicle queues spilling back into the circulatory roadway.

Accessibility routes of pedestrian towards transit should be well designed for safety, ease and suitability. Pedestrian crossing capacity should also be accounted for. Roundabouts may offer prospects for benevolent right-of-way to transit and emergency vehicles – with geometry or use of signals as at signalized intersections. These aspects could be done by a separate right turn bypass lane, or signals controlling entering traffic while the transit vehicle enters its own right-of-way.

2.2.2 Emergency vehicle

Emergency vehicles at the roundabout may require the use of a traversable truck apron and aspects akin to large vehicles. One objective in roundabout design is to reduce vehicle speed at entry, providing additional safety and benefits for emergency vehicles at roundabouts compared with conventional intersections.

According to Wisconsin department, drivers must yield the right-of-way for emergency vehicles using a siren, air horn, or a red or blue flashing light. The driver in the circulatory roadway should exit the roundabout before pulling over if it is safe to do so. Emergency vehicles typically find the safest and clearest path through an intersection. This may include driving the emergency vehicle with caution and with lights and siren on, in the opposing lanes, or however the operator sees as the most desirable alternative path (WisDOT, 2011). Drivers should be instructed not to enter a roundabout when an emergency vehicle is approaching on another leg. After the vehicle has entered, the circulatory roadway should be clear if possible, and there should be queue clearance in front of the emergency vehicle. In case of roundabouts, emergency vehicle drivers are not encountered with through vehicles suddenly in succession as in case of conventional intersections.

2.2.3 Large vehicle

Single-lane or dual-lane roundabouts are designed with consideration of the largest vehicles that can consistently be anticipated (WisDOT, 2011). The truck apron is designed to avoid the wheel off-tracking of larger vehicles when travelling in a circulatory roadway through roundabouts. Single-lane roundabouts may require the use of a mountable apron to provide the additional width needed for tracking the trailer wheels while on double lane roundabouts, and large vehicles may track across the whole width of the circulatory roadway to negotiate the roundabout (FHWA, 2000). Dual or multi lanes roundabouts can be designed in two ways to avoid wheel off-tracking of larger vehicles:

1. To assume a truck will use two lanes by encroaching into the adjacent lane at entry, circulatory, and exit of the roundabout.
2. Trucks can stay in lane at entry by providing a separation or gore area between lanes.

According to Wisconsin department of transportation, an elegant roundabout addresses load-shifting problems with larger vehicles. Inadequate entry deflection leading to high entry speeds, long tangents leading into tight curves, sharp turns at exits, excessive cross slopes, and adverse cross slopes – these have been the principal causes of load shifting. Right turns are also problematic for trucks, as trucks tend to run over sidewalks and splitter islands when making a turn. A few roundabouts are designed to allow a large vehicle to stay in the lane at entry and in the circulating roadway, which results in the possibility of a larger diameter, wide entries, and bigger right-of-way requirements – possibly leading to increases in certain types of crashes or other unique design problems.

2.2.4 Pedestrians accommodation

The roundabout should be designed to discourage pedestrians from crossing to the central island. Pedestrian safety is normally improved with a roundabout design better than with other intersection types, due to relatively low operating speeds (FHWA, 2000). Roundabouts have the following benefits and detriments for pedestrians:

- Fewer pedestrian conflict points, and slow vehicle speed
- Due to fewer conflicting points, pedestrians more easily judge their crossing opportunities.

- Separate vehicle-vehicle and vehicle-pedestrian conflict points
- Depending on age, mobility, visual impairments, and ability to judge gaps in traffic, the design may be disturbing to the pedestrian
- Pedestrians may be undecided on crossing at first because traffic does not necessarily come to a full stop – due to yield control.

The crossing location for pedestrians should be appropriate because it maintains a balance between their safety, suitability, and operation of the roundabout. Both crossing location and crossing distance are important in design. Generally, locate the pedestrian crossing at one car length, or approximately 20 ft, upstream of the yield point; this results in reduction of decision making problems for drivers and avoids creating a queue of vehicles waiting to enter the roundabout (FHWA, 2000). Dutch guidelines also recommend that crossing position be improved with handicapped ramps or colored concrete or both (CROW, 1993).

2.2.5 Bicycle accommodation

The Insurance Institute for Highway Safety states that roundabouts in the United States offer a 10% drop in bicycle crashes at signalized intersection after being converted to roundabouts. Operation of a bicycle through a roundabout presents challenges: experienced cyclists may have no trouble steering through a roundabout whereas less skilled cyclists may have struggle and uneasiness mixing with vehicles. Cyclist speeds are generally 25 km/h (15 mph), so entering a roundabout designed for circulating traffic to flow at comparable speeds should be harmless compared with larger and faster roundabout designs. Generally, designers treat a bicycle as a vehicle. However when entering traffic volumes are larger than 12000 AADT, we should then consider the other options such as shared-use paths, which offer a physical separation from vehicles around the periphery of the roundabout (FHWA, 2000). The Figure 2.5 and Figure 2.6 show the guidance for shared-use paths at roundabouts.

- Start and finish this path about (50 – 150 ft) upstream and downstream of the yield point.
- Avoid right turn free flow lanes for vehicles in high bicycle volume areas, because they may be awkward for cyclists.
- To manage the cyclists who do not like to travel through roundabouts, construct a wide path around the exterior of a roundabout.

- Provide a ramp between the sidewalk and the bike lane. The entry and exit ramp generally has an angle range of $25^{\circ} - 35^{\circ}$ toward and from the roadway, respectively, as shown in Figure 2.5. Generally, the width is 8 ft, but 6 ft is acceptable if pedestrian use is minimal.

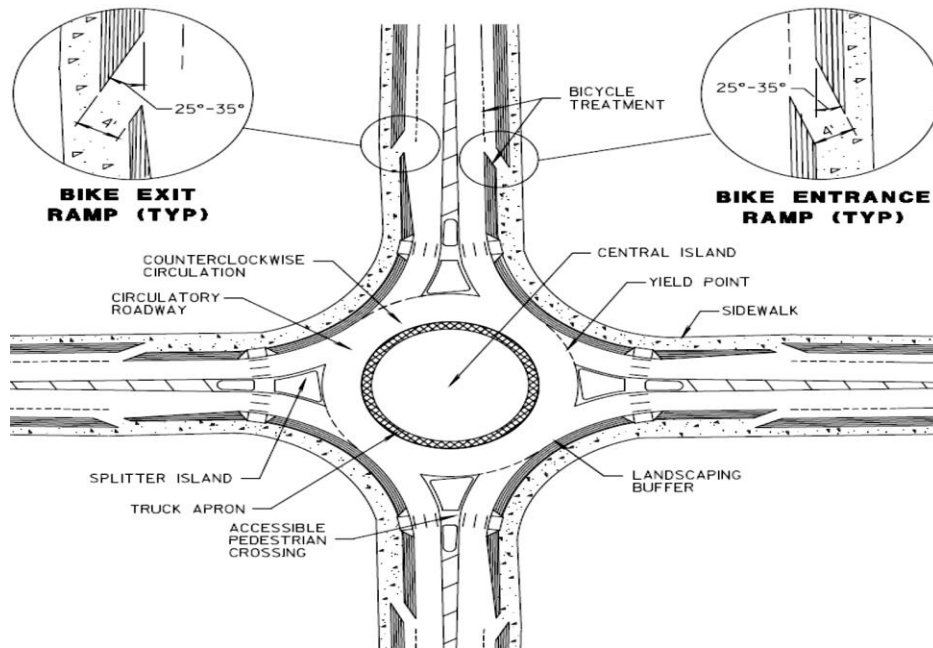


Figure 2.5 Bicycle treatment at entry and exit ramp (WisDOT, 2011)

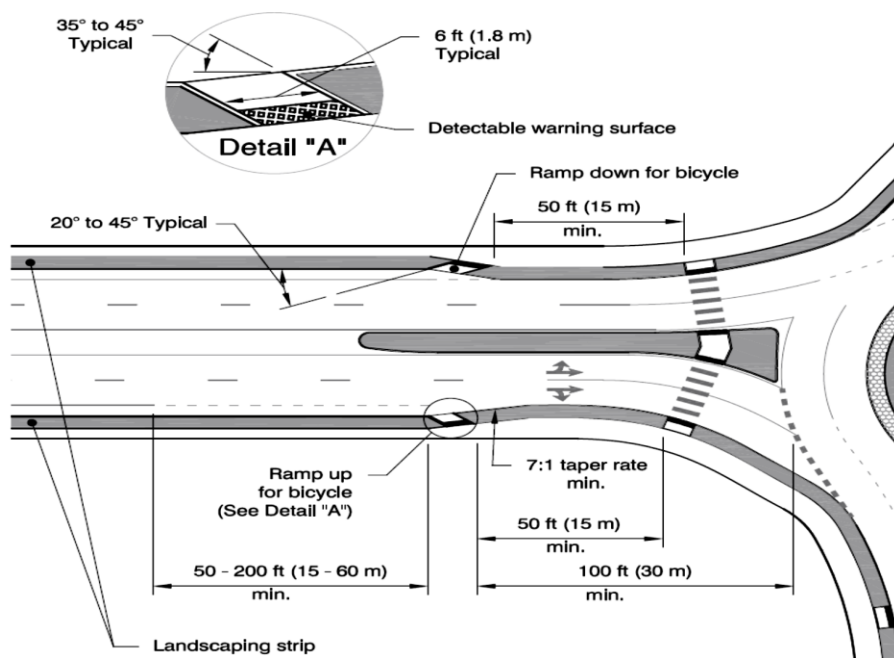


Figure 2.6 Bicycle design treatments (FHWA, 2000)

CHAPTER 3 : CAPACITY AND DELAY LITERATURE REVIEW

3.1 INTRODUCTION

Given the significance increase in construction of roundabouts worldwide, several capacity models have been developed and applied (Kittelson and Associates, 2002; FHWA, 2000). Roundabouts are superior to conventional intersections because they enhance capacity, reduce delay, and promote safety and operational benefits. An operational analysis of roundabouts has been performed based upon capacity and level of performance. The highway capacity manual defines capacity as “the maximum hourly rate at which person or vehicles can realistically be anticipated to pass through a point or roadway during a given time period under prevailing roadway, traffic and control conditions.” Queue length and delay at intersections represent the level of service of performance. The capacity not only manages the traffic streams but also affects delay and queue of vehicles. Empirical and gap acceptance techniques were used in the past, and also now in the present, for calculating entry capacity of a roundabout at approaches. The empirical technique based upon empirical formulas, which were developed based on field measurements at roundabouts, were based primarily on several geometric characteristics of the roundabout in addition to the circulating volume. The gap acceptance technique is theoretical based on the behavior of drivers waiting for a gap large enough to enter the circulating roadway. This chapter explores most of the approaches taken to determine roundabout performance. The literature review of capacity, delay, and queue at roundabout entries looks at the different theories, published articles, and design guides upon which these formulations are based, and the various equations that have used a myriad of variables and parameters to estimate capacity, delay, and queue.

3.2 ROUNDABOUT CAPACITY

The objective of capacity analysis is to evaluate the operational performance of roundabouts. Nowadays the entry capacity concept is used for operational analysis. The entry capacity is the maximum numbers of vehicles per hour that can enter a roundabout at given traffic and roadway conditions. The circulating traffic has a priority in roundabout design; subsequently, entry capacity decreases with increase in circulating traffic due to fewer

appropriate gaps available for entry to a circulating portion. Entry capacity depends on geometric design. Dual-lane roundabouts can likely handle AADTs between 25,000 and 55,000 vpd and peak-hour flows between 2,500 vph and 5,500 vph.

Capacity at a roundabout is maximum when all the entry approach traffic volumes are relatively balanced and pedestrian volumes are low. A dual-lane roundabout has almost twice the capacity of a single-lane roundabout; however, various standards agree that roundabout geometry can affect capacity (Carl C., Chuan K., Brice S, 2004). Table 3.1 shows the maximum capacities at dual-lane roundabout relating to different countries' guidelines.

Table 3.1 Maximum dual-lane roundabout capacity

Guidelines	Max. dual-lane roundabout capacity (AADT)
Continental Europe	35,000 – 40,000
Australia	35,000 – 50,000
United Kingdom	40,000 – 60,000
United States	40,000 – 60,000

For capacity analysis, empirical and gap acceptance techniques require geometric and 15-minute period conflicting circulating traffic flow data at each entry of each lane. Todd in 1979 described that US roundabouts capacity would be less than in other countries due to larger vehicle sizes. In 1997 Akcelik recommended that when percentage of heavy vehicles surpasses 5%, pce/hour be used in place of vehicles/hour (Rahmi Akcelik, 1997), and several authors agreed with Akcelik's recommendation. Traffic flow volumes are normally expressed in passenger cars equivalent per hour (pce/hr), while the analysis period is AM or PM peak hours. If any other type of vehicle is present, then it should be converted to a passenger car equivalent by using the conversion factors given in Table 3.2 (FHWA, 2000).

Table 3.2 Conversion factors for traffic to passenger cars equivalent (FHWA, 2000)

Vehicle Category	Passenger cars equivalent (pce)
Bicycle or Motorcycle	0.5
Car	1.0
Truck or Bus	1.5
Truck with trailer	2.0

Once the flows of each movement at each entry are known, we can find the conflicting circulating flow for each entry. Entry flow is the sum of the left, right, through and U-turn flow at each entry. Exit flow calculations are based on the observed data to authenticate the establishment of single, dual-lane or multi-lane roundabouts (Robinson, B. et al, 2000).

3.2.1 Empirical (regression) capacity

In the United Kingdom, several research studies on entry capacity analysis were performed during 1973 -1985. Based on these studies, TRL developed their capacity equations that exposed a robust relationship between geometry, safety, capacity, and delay (Seiberlich, 2001). However, Akcelik states that the UK linear regression model underestimates the capacity for low circulating flows and overrates the capacity for high circulating flows. The UK model appears to have been derived with a relatively small number of data points with low circulating flows, and it reflects strange effects of the geometric designs of UK roundabouts included in the database used for its development. Another factor is lack of sensitivity to demand flow patterns in the UK linear regression and other models. The UK linear regression model was developed through surveys conducted at both large conventional design systems and smaller offside-priority design roundabouts in the UK. The model uses the total circulating flow rate to determine the total entry capacity at each approach. Individual-lane details are not accounted for (Akçelik, 2003). WisDOT recognizes during the analysis of roundabout capacity and delay that the British Empirical Method is successful in modeling real world conditions for roundabout operation and prescribes its use in the design of roundabouts (WisDOT, 2011). The problem of unbalanced flows is quite common, and the signalized roundabout solution has been used extensively in the UK, as well (Huddart, K.W, 1983).

The graphical representation in the Figure 3.1 shows the single-lane and double lane roundabouts capacity comparison forecast based on British regression relationships. It shows that the number of lanes, size of the entry, and circulating roadways have a major influence on the entry capacity. Larger inscribed diameter roundabouts are expected to have slightly higher capacities at moderate to high circulating flows (FHWA, 2000). Although important, roundabout geometry alone is not sufficient for modeling the capacity of roundabouts; the model must also include driver behaviour parameters, as in the Australian method (Rahmi Akcelik, 2011).

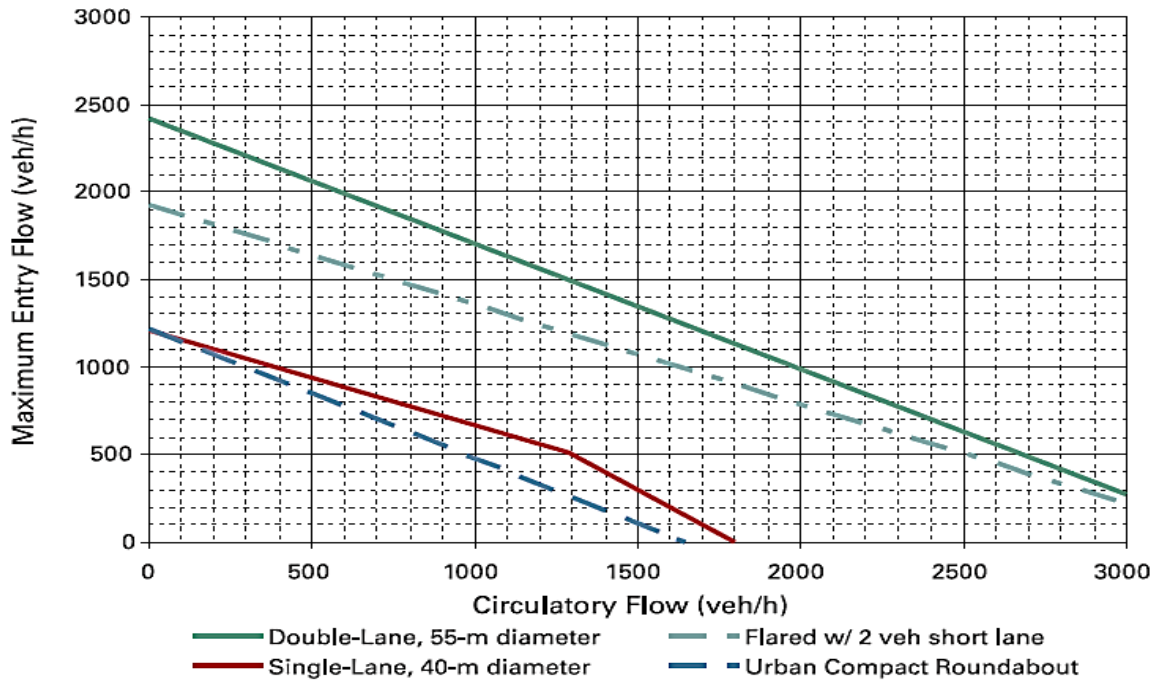


Figure 3.1 Single-lane and dual-lane roundabouts capacity comparison (FHWA, 2000).

3.2.2 Gap acceptance capacity

The gap acceptance model assumes that the capacity of a roundabout depends on the circulating traffic flow and driver behaviors described by key microscopic parameters, namely, critical headway and follow-up headway (Xu, 2007). The gap acceptance model reflects driver behavior and circulating traffic conditions, even though a simple gap acceptance model may not annex all driver behaviors information and a more complex gap acceptance model is difficult to calibrate, but it is still the preferred analytical model at un-signalized intersections including roundabouts.

The approach capacity at roundabouts is affected by the entering, circulating and the exiting flow. The main conflicting flow is the circulating flow that passes directly in front of the subject entry. At entry point, drivers yield to the circulating traffic flow and look for adequately large gap to make the gap acceptance decision without being intrusive with the circulating traffic. The approach capacity decreases with the increase of circulating flow. Drivers entering the flow are assumed to take gap acceptance action consistently, which means that a driver with a specific critical headway will accept every headway larger than his or her critical headway and will never accept the headway that is smaller than his or her critical headway.

3.3 ROUNDABOUT DELAY

Roundabouts are rated as the most competitive alternative for heavy traffic intersections with dual-lane approaches in terms of capacity and delay. For intersections with single-lane approaches, the performance of roundabouts is similar to that of signalized intersections, as the flare effect is maximized. Although roundabouts with three-lane approaches provide higher capacities than do three lane signalized intersections, they show inferior performance in terms of delay (Virginia P. Sisiopiku and Heung-Un Oh, 2001).

3.3.1 Geometric delay

The delay experienced by a vehicle negotiating an intersection in the absence of any other vehicle is called geometric delay. Geometric delay results in a collective effect due to decrease in approach speed to safe cooperation speed, passing through at that speed, acceleration to an exit negotiation speed, and then exit acceleration to the cruise speed of vehicle. The estimation by analytical models, as gap acceptance and queuing theory model in the case of roundabouts, requires a clarification of whether the model includes acceleration and deceleration delays. The AUSTROADS 1993 method assumes that the analytical model does not include any acceleration and deceleration delay. It calculates a separate geometric delay value for queued and un-queued vehicles (Rahmi Akcelik, 2002).

3.3.2 Average geometric delay

Average geometric delay varies with the roundabout size; it decreases with an increase in inscribed circle diameter at constant cruise speed, and it increases with an increase in cruise speed at the constant inscribed circle diameter (Rahmi Akcelik, 2002)..

3.3.3 Control delay

Control delay is the delay of a vehicle that results in slowdown from approach cruise speed to the complete-stop condition due to such cause as a red signal, queue ahead, or insufficient gap; it waits, and then accelerates to exit cruise speed (Rahmi Akcelik, 2002). There are numerous forms of delay; however, control delay is the delay experienced due to the

existence of a traffic control device, and this is the major measure in the highway capacity manual for calculating the level of service at intersections. Control delay includes a delay associated with vehicles slowing in advance of an intersection, the time spent stopped on an intersection approach, the time spent as vehicles move ahead in the queue, and the time needed for vehicles to accelerate to their desired speed (HCM, 2010).

3.4 REVIEW OF ENTRY CAPACITY AND DELAY MODELS

The empirical technique based upon empirical formulas which were developed based on field measurements at roundabouts are based primarily on several geometric characteristics of the roundabout in addition to the circulating traffic volume. The theoretical gap acceptance technique is based on the behavior of drivers waiting for a gap large enough to enter the circulating roadway. There has been some controversy about capacity estimations from the gap-acceptance based Australian and Highway Capacity Manual methods and the linear-regression-based UK (empirical) method. As the use of roundabouts became more common in the US, the softwares based on US Highway Capacity Manual, Australian (aaSIDRA, AUSTROADS, NAASRA), and the UK Linear Regression (empirical) models give differences in results from the analysis.

As described in NCHRP report 572, the largest variable affecting roundabout performance is driver behavior, and "the fine details of geometric design (lane width, for example)" appears to be secondary and less significant than variations in driver behavior at a given site and between sites (NCHRP Report 572, 2007). Still, research is being performed on development of new models for entry capacity calculation in several countries. A brief introduction is as given below.

3.4.1 UK capacity and delay model

Capacity model

The UK capacity model is based on the regression capacity formula developed in the 1980s through Kimber's research. According to Kimber, there is a small effect on capacity when an inscribed circle diameter is less than or equal to 50 m. According to Kimber's research, capacity at the roundabout can be calculated with Equation [3.1].

$$Q_e = k(F - f_c Q_c) \quad [f_c Q_c \leq F] \quad [3.1]$$

$$Q_e = 0 \quad [f_c Q_c > F] \quad [3.2]$$

$$k = 1 - 0.00347[\phi - 30] - 0.978 \left[\frac{1}{r} - 0.05 \right] \quad [3.3]$$

$$t_D = 1 + \left[\frac{0.5}{1 + \exp\left(\frac{D - 60}{10}\right)} \right] \quad [3.4]$$

$$f_c = 0.21 t_D [1 + 0.2 x_2] \quad [3.5]$$

$$x_2 = v + \left[\frac{e - v}{1 + 2S} \right] \quad [3.6]$$

$$S = \frac{1.6[e - v]}{l'} \quad [3.7]$$

$$F = 303[x_2] \quad [3.8]$$

where

- Q_e = Entry capacity, pce/hr.
- Q_c = Circulating flow, pce/hr.
- e = Entry width, m
- v = Approach half width, m
- l' = Effective flare length, m
- S = Sharpness of flare, m/m
- D = Inscribed circle diameter, m
- ϕ = Entry angle, degrees
- r = Entry radius, m
- x_2 = Effective entry width, m
- F = Capacity equation intercept
- f_c = Slope of capacity equation

The capacity equation intercept is calculated using linear regression of F as a function of x_2 . Kimber's research concludes that x_2 depends on e , v and S . Kimber studied the effect of an increase in inscribed circle diameter on entry capacity and slope of capacity equation; Kimber concluded that there is an increase in the entry capacity but a decrease in the slope of capacity

equation, while entry flow and roundabout geometry characteristics remain same. According to Kimber, 30° is the best entry angle. It is a conflict angle between entering and circulating streams of traffic. The entry angle and radius have little effect on capacity; therefore, he modified the entry capacity equation by multiplying with a correction factor k . He concluded that a linear approximation is the superlative for roundabout entry capacity analysis. Equation [3.1] with other sporting equations from [3.2] to [3.8] is adopted as the UK capacity formula for urban and rural roundabouts (Kimber R. , 1980).

Delay model

Roundabout negotiation speeds and distances are estimated and geometric delays are calculated as functions of approach, exit and negotiation speeds and distances, thus allowing for speed variations of vehicles negotiating roundabouts. Kimber developed a delay and queue calculation formula that can be used for both under and over-saturated conditions (Kimber, RM & Hollis EM, 1979), as described in Equations [3.9] and [3.10].

$$d = 0.5 \sqrt{\left[t_i \frac{\left(1 - \frac{q}{\mu}\right)}{2} - \frac{L_o + 1}{\mu} \right]^2 + 2 \frac{t_i}{\mu} - 2 \frac{t_i}{\mu}} \quad [3.9]$$

$$L = 0.5 \sqrt{\left[\left(1 - \frac{q}{\mu}\right) \mu t_i + 1 - L_o \right]^2 + 4 \left(L_o + \frac{q}{\mu} \mu t_i \right) - \left[\left(1 - \frac{q}{\mu}\right) \mu t_i + 1 - L_o \right]} \quad [3.10]$$

where

- d = Delay in (sec/hr.)
- L_o = Initial queue length (veh.)
- t_i = Time interval (sec)
- q = Arriving flow (veh/sec)
- μ = Capacity rate (veh/sec)
- L = Average queue length (veh.)

The UK design guide follows this formula, which is based on the probabilistic theory, for delay analysis of roundabouts. It first determines the probability distribution of different queue length as a function of time, and then calculates the average queue length which will be used later in the calculation of average queuing delay.

3.4.2 German capacity and delay model

Regression capacity model

In 1980, German researchers developed a gap acceptance based capacity formula, but due to unfavorable results, it did not seem reliable (Kimber R. , 1980). The German capacity results were found to be 70 – 80 % of British values. Brilon explains that this difference is due to driver behavior. The drivers in England are more familiar with roundabout type intersections than those in Germany (Brilon, 1991). Next, empirical regression models were established, leading to an exponential regression curve. During the period 1993 – 1996, more capacity measurements were performed by the German government federal department of transportation, which concerned a revised linear formula with consideration only of the circulating flow and the number of entering and circulating lanes. Research shows that linear regression instead of an exponential function has an enhanced convention of variance data (Brilon, Werner, Ning Wu, and Lothar Bondzio, 1997). The new modified capacity formula is shown in Equation [3.11].

$$C_e = A + BQ_c \quad [3.11]$$

C_e and Q_c are entry capacity and circulating flow, respectively, and where parameters A and B are based on the number of entry and circulatory lanes and determined from empirical data. Thus, in Table 3.3, values of A and B are recommended for practical application in Equation [3.11], and the capacity estimated by this equation is also illustrated in Figure 3.2.

Table 3.3 Regression parameters (Brilon, Werner, Ning Wu, and Lothar Bondzio, 1997)

No. of entry/Circle lane	A	B	N (sample size) No. of observed during 1 minute interval
1/1	1218	0.74	1504
1/2 or 3	1250	0.53	879
2/2	1380	0.50	4574
2/3	1409	0.42	295

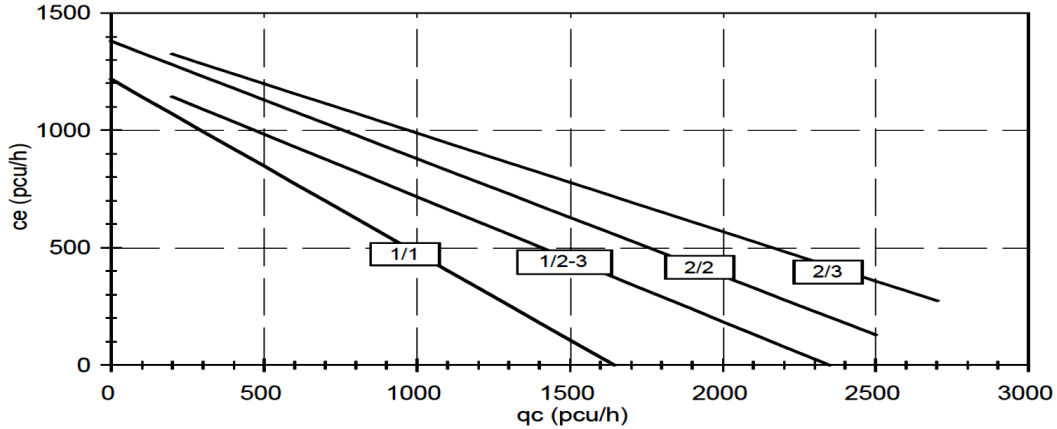


Figure 3.2 Roundabout capacity (Brilon, Werner, Ning Wu, and Lothar Bondzio, 1997)

Gap acceptance capacity model

Brilon, Werner, Ning Wu, and Bondzio suggested the following formula for estimation of entry capacity of roundabouts after modification of the Tanner basic idea of entry capacity. According to them, the capacity estimating empirical regression approach at roundabouts is somewhat reasonable. On one side, it does not make use of theories for un-signalized intersections, while on the other side one cannot be sure that these linear functions also apply in areas of the C_e diagram where only a few measurement points have been observed (Brilon, Werner, Ning Wu, and Lothar Bondzio, 1997).

$$C_e = \left(1 - \frac{\Delta q_c}{n_c}\right)^{n_c} * \frac{n_e}{t_f} * \exp \left[-q_c * \left(t_o - \frac{\Delta}{n_c}\right)\right] \quad [3.12]$$

where

- q_c = Circulating flow in front of the entry (pcu/h)
- C_e = Maximum entry capacity
- n_e = Number of entry lanes
- n_c = Number of circle lanes
- t_o = $t_c - (t_f/2)$
- t_c = Critical gap(s)
- t_f = Follow-up time(s)
- Δ = Minimum head-way time between vehicles traveling in the circle(s)

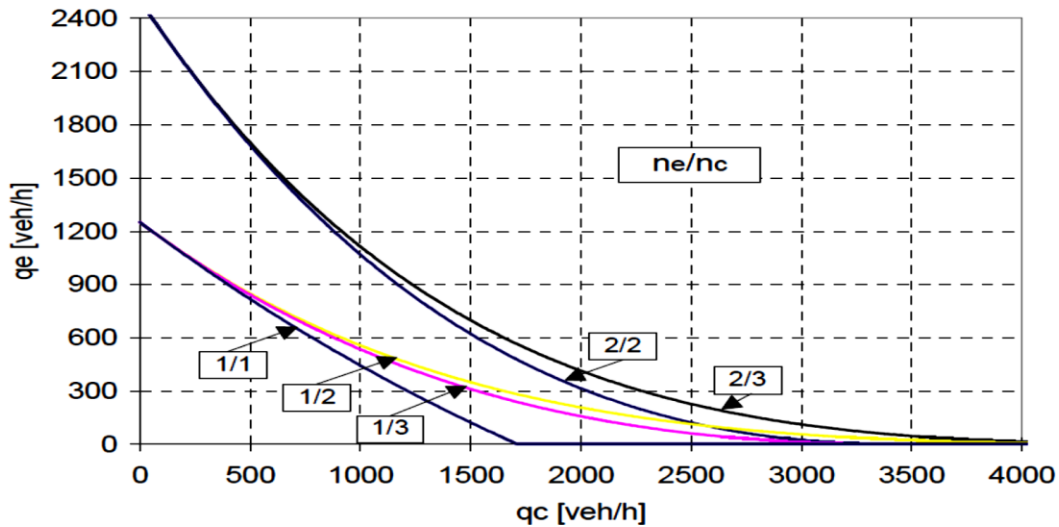


Figure 3.3 German Gap acceptance capacity formula behavior

Figure 3.3 represents the behavior of the German gap acceptance capacity formula when using the parameters $t_c = 4.12$ sec, $t_f = 2.88$ sec, and $\Delta = 2.10$ sec, which represent driver behavior at roundabouts in Germany.

Delay model

Mostly in Germany, the delay at roundabout entries is calculated from (Kimber, R.M., E.M. Hollis, 1978) universal delay formula, which also considers the effects of time dependencies.

3.4.3 French capacity and delay model

Capacity model for urban roundabouts

A government body known as (CERTU), liable for transportation urban guiding principles nationwide, developed the French formula for roundabout capacities in urban areas (CETUR, 1988). The CETUR formula considers the impeding flow instead of circulating flow for entry capacity analysis. Like the United States method for un-signalized intersections, the impeding flow is a sum of circulating flow and a proportion of the exiting flow at the same branch as described in Equation [3.13], where Q_g , Q_c and Q_s are impeding, circulating, and exiting flow, respectively, and α is the variable, the function of the width of the splitter island. The average value of α is 0.2.

$$Q_g = Q_c + \alpha Q_s \quad [3.13]$$

The main idea delivered by this theory is that the entering traffic is confused by the exiting traffic due to doubt over whether these vehicles really exit. When the circulating roadway is a minimum of 8 m wide, Q_g should be adjusted to equivalent Q_g . The entry capacity C as defined in Equations [3.14] & [3.15] represents the straight line, and its mean entry capacity is the function of impeded flow. With two entry lanes, entry capacity upturns by 40%.

$$C = 1500 - \left[\frac{5}{6}\right] Q_g \quad \text{for}[Q_g < 1800] \quad [3.14]$$

$$C = 0 \quad \text{for}[Q_g > 1800] \quad [3.15]$$

Capacity model for ruler roundabout

In 1987, the French national design service for rural highways, SETRA, developed an original entry capacity calculation method for rural roundabouts, as described in Equation [3.16] (SETRA, 1988,1997). SETRA is analogous to the CETUR formula with slight deviations. It is applicable to roundabouts with central islands having a diameter greater than or equal to 30 m. The SETRA entry capacity formula is described in Equation [3.16].

$$C = (1330 - 0.7Q_g)[1 + 0.1(l_e - 3.5)] \quad [3.16]$$

$$Q_g = \left[Q_c + \frac{2}{3}Q'_s\right][1 - 0.085[l_a - 8]] \quad [3.17]$$

$$Q'_s = Q_s \left[\frac{15 - l_i}{15}\right] \quad \text{for}[l_i < 15\text{m}] \quad [3.18]$$

$$Q'_s = 0 \quad \text{for}[l_i > 15\text{m}] \quad [3.19]$$

$$Q_g = C - Q_e \quad \text{The reserve capacity} \quad [3.20]$$

$$Q_g = \frac{C - Q_e}{Q_g \%} \quad \text{Percentage of reserve capacity} \quad [3.21]$$

where l_e , l_a , and l_i are the entry, circulatory road, and splitter island width in meters, respectively.

Delay Model

CETUR proposed Equation [3.22] for delay per arriving vehicle (CETUR, 1988). While Harder is proposed more complex, Equation [3.23] is proposed for calculating delay (Harder, J, 1989).

$$d = \frac{[2000 + 2Q_g]}{Q_c - Q_e} \quad [3.22]$$

$$d = \frac{3600 \left[1 - e^{-\left[\frac{[Q_g t_{gn} - Q_d t_f]}{3600} \right]} \right]}{Q_e - Q_d} \quad [3.23]$$

where

- Q_e = Entry flow (pcu/hr.)
- C = Entry Capacity (pcu/hr.)
- Q_c = Circulating flow (pcu/hr.)
- Q_g = Impeding flow (pcu/hr.)
- d = Delay per arriving vehicle (sec)
- t_g = Critical gap (sec)
- t_f = Move up time (sec)

3.4.4 Swiss capacity and delay model

In Switzerland, roundabouts have become more common because of concern for traffic safety at a high level of capacity. But the capacity of a one-lane roundabout is limited and therefore, dual- lane and multi-lanes roundabouts are built.

Capacity model

Federal Polytechnic School of Lausanne under the direction of Professor Bovy and under contract with the Swiss Fund prepared “The Swiss Roundabout Guide for Roadway Safety.” This guide presents a linear empirical formula, which expresses the entry capacity Q_e in Equation [3.23] as a function of the impeding flow Q_g , and it is analogous to the CETUR formula with a different slope (Swiss Roundabout Guid, 1991).

$$Q_e = \frac{[1500 - \frac{8}{9}(Q_g)]}{\gamma} \quad [3.23]$$

$$Q_g = (\beta Q_c + \alpha Q_u) \quad [3.24]$$

where

- Q_e = Entry capacity (pcu/h)
- Q_c = Circulating flow (pcu/h)
- Q_u = Exiting flow (pcu/h)
- Q_g = Impeding flow (pcu/h)
- α = Influence of pseudo conflict depend upon distance “ l ” between conflict points
- β = Influence of the number of lanes of the circulatory
(β , ranges (0.9-1), (0.6-0.8) and (0.5-0.6) for Single, Dual and three lane roundabouts respectively)
- γ = Influence of the number of lanes of the entry
(γ , ranges (1), (0.6-0.7) and (0.5) for Single, Dual and three lane roundabouts respectively)

The capacity model in Equation [3.23] can be applied for single-lane or dual-lane roundabouts. The model considers both the influence of the number of lanes at entry and the circulatory roadway.

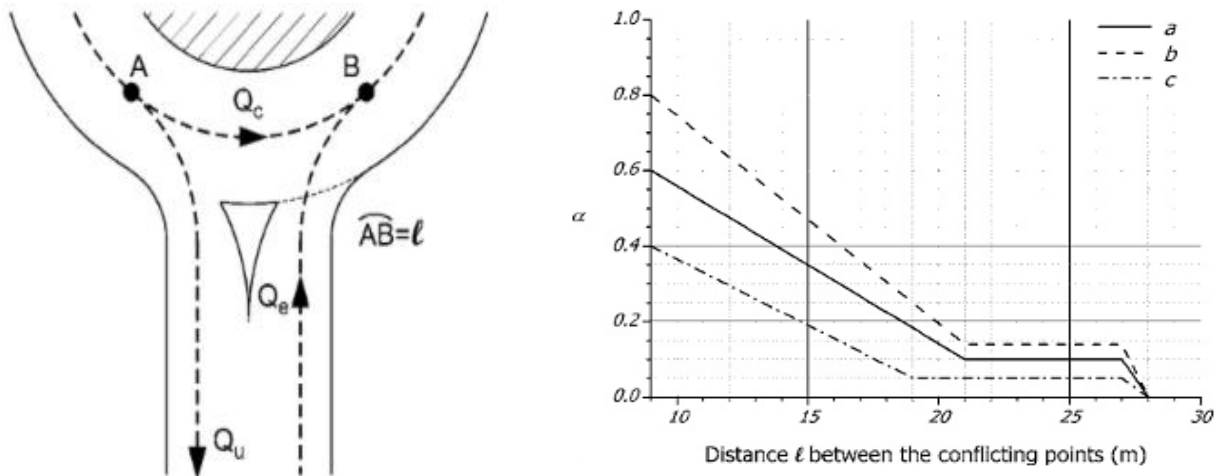


Figure 3.4 Capacity Flow diagram for Swiss Roundabout (Swiss Roundabout Guid, 1991)

The model assumes an entry capacity of 1,500 pcu/hr. The capacity model in Equation [3.23] is recommended for roundabouts (urban and suburban environments) with flared entries, a

non-mountable central island, having internal diameter D_{in} ranging from 18 to 20 m and external diameter D_{ext} ranging from 24 to 34 m (Raffaele Mauro, 2010). The value of α can be calculated with the help of Figure 3.4.

Pseudo Conflict; Sometimes at entry yield point, drivers observe a quantity of the exiting flow as conflicting therefore some drivers wait for vehicles that in fact exit the circulatory roadway, and this is called the pseudo conflict. Consequently, the effectiveness of conflicting flow consists of the actual conflicting flow and a part of the exiting flow. Therefore Bovy considers this part of the exiting flow as the product of the exiting flow and the coefficient α . For high capacity of exiting flow the effect of the pseudo conflict on capacity is greater. α coefficient is most greatly affected by the roundabout geometric design. Designers decide the distance in the middle of the entry and the ultimate point where leaving the roundabout becomes obvious. In Bovy's model, this distance is measured between the points *A* and *B* as described in Figure 3.4.

Capacity Reduction Factors Due to Pedestrians; Crossings can have a substantial influence on entry capacity at intersections; with high volumes of pedestrians in this condition, the vehicular capacity decreases by factor M , as shown in Figure 3.5 (Brilon, 1991). Pedestrian impedance decreases with an increase of circulatory flow rate in front of the subject approach (Raffaele Mauro, 2010).

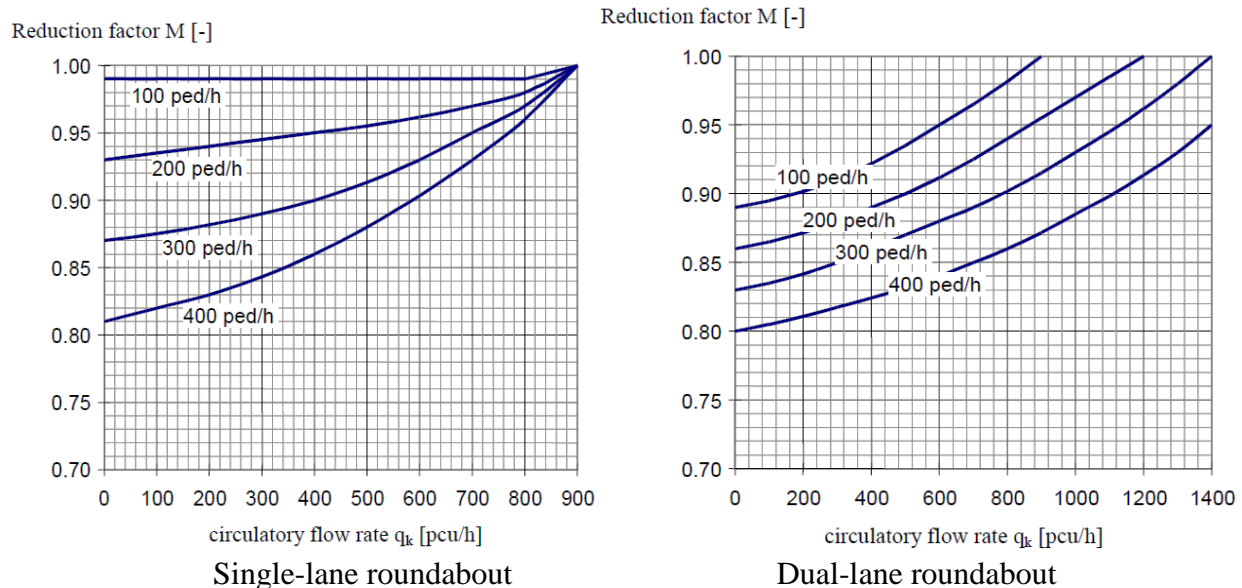


Figure 3.5 Entry capacity reduction factors due to pedestrian (Brilon, 1991)

3.4.5 US capacity and delay research

Florida recommends using the Australian SIDRA program to analyze roundabout performance, while Maryland follows the AUSTROAD capacity and delay formula. A California design guideline makes no recommendation for capacity calculation (Taekratok, 1998).

HCM 2000 roundabout capacity model

Highway capacity manual 2000 is limited to arrangements with one lane in the circle and at the entries, and with circulating flow Q_c less than 1200 pcu/hr. (Kottegoda, N., Rosso, R, 1997). Equation [3.25] is used for evaluation of entry capacity C .

$$C = \frac{Q_c e^{-Q_c T_c / 3600}}{1 - e^{-Q_c T_f / 3600}} \quad [3.25]$$

Q_c = Circulating flow in front of the entry (pcu/hr)

T_c = Critical gap (sec)

T_f = Follow-up time (sec)

The gap acceptance characteristics of drivers are expected to be similar to those of drivers making right turns at two way stop control (TWSC) intersections and at roundabouts (Kyte, 1997).

Table 3.4 Critical gap and follow up time in (Highway Capacity Manual, 2000)

	$T_c = \text{Critical gap (s)}$	$T_f = \text{Follow up time (s)}$
Upper bond solution	4.1	2.6
Lower bond solution	4.6	3.1

HCM 2010 roundabout capacity model

An exponential capacity estimation model for single or dual-lane roundabouts is defined in Highway Capacity Manual 2010. The model can be viewed both as an empirical (exponential regression) model and a gap acceptance model. Highway Capacity Manual 2010 states that this is a "combination of simple, lane-based regression and gap-acceptance models." The capacity of each entry lane is calculated based on the conflict traffic flow in the circulatory roadway in front of subject entry (HCM, 2010). In Figure 3.6, the lower curve can be used to calculate the

capacity of a one-lane entry to a single-lane roundabout, or either lane of a dual-lane entry conflicted by one circulating lane. For a dual-lane roundabout with two circulatory lanes, the two curves representing the left and right entry lanes should be used.

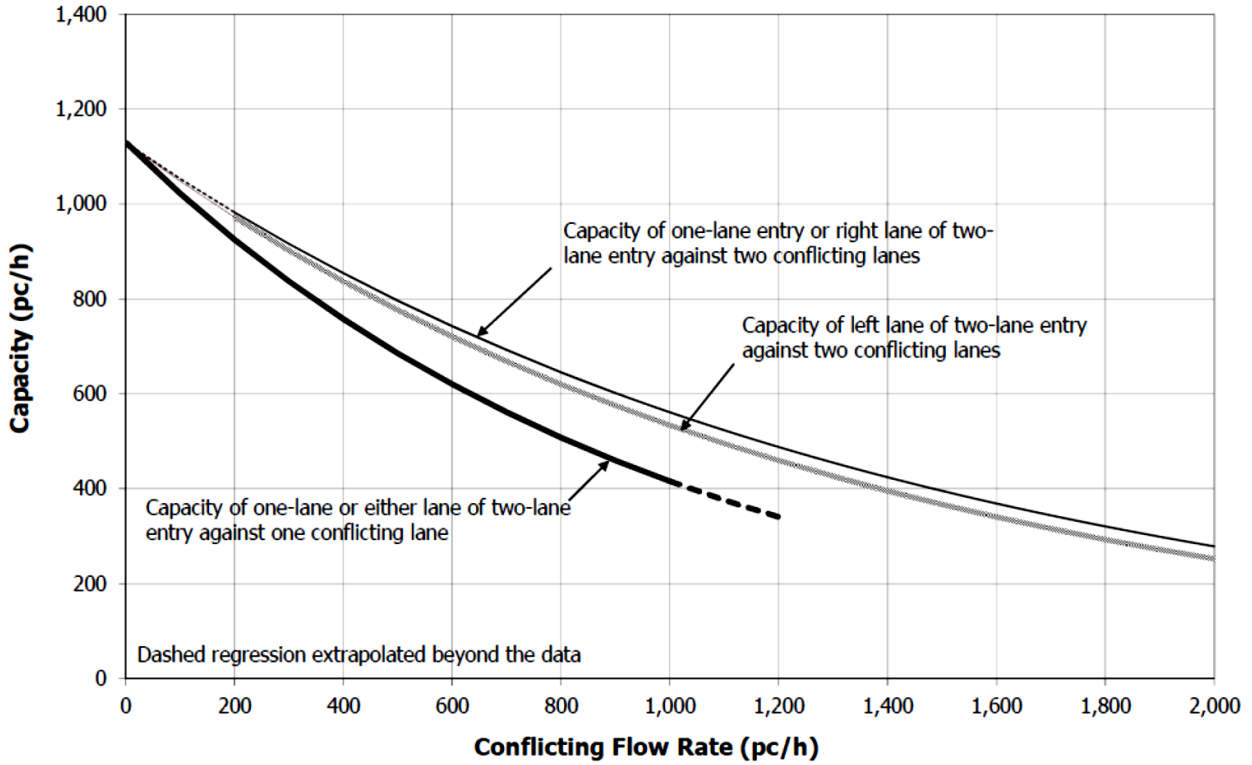


Figure 3.6 Capacity curves for single-lane and dual-lane roundabout scenarios (HCM, 2010)

The HCM 2010 roundabout capacity model for an entry lane consists of Equations [3.26] to [3.30].

$$Q_g = F_{HVe} F_p F_A \left(\frac{3600}{T_f} \right) e^{-\left(\frac{B}{F_B}\right)_{qm}} \quad [3.26]$$

$$B = \frac{T_o}{3600} = \frac{[T_c - 0.5T_f]}{3600} \quad [3.27]$$

$$T_c = 3600B + 0.5T_f \quad [3.28]$$

$$F_{HVe} = \frac{1}{[1 + (e_{HV} - 1)p_{HVe}]} \quad \text{subjected to } (e_{HV} > 1) \quad [3.29]$$

$$F_A = F_B = \frac{Q'}{Q} \quad [3.30]$$

- F_{HVe} = Heavy vehicle factor for entry lane capacity
 e_{HV} = Passenger car equivalent of a heavy vehicle for gap-acceptance purposes (pcu/veh.),
 (the default value of $e_{HV} = 2.0$)
 Q'/Q = Ratio of the measured capacity to the estimated capacity
 $F_A = F_B$ = Ratios of follow-up headway to critical gap (T_F / T_C) are kept unchanged
 p_{HVe} = Proportion of heavy vehicles in the entry lane traffic stream
 F_P = Pedestrian factor for the effect of pedestrians crossing in front of entry lanes
 F_A = Adjustment factor for parameter A
 F_B = Adjustment factor for parameter B
 q_m = Opposing (conflicting) flow rate in pcu/hr. (adjusted for heavy vehicles)
 T_F = Follow-up headway (sec)
 T_C = Critical gap (sec)
 T_O = A parameter that relates critical gap and follow-up headway parameters (sec).
 n_e = Number of entry lanes
 n_c = Number of circulating lanes

The opposing (conflicting) flow rate, q_m , is normally the circulating flow rate in front of the subject lane, but may include a percentage of exiting flow rate depending on user specifications. A , and B are related to the follow-up headway and critical gap parameters. The HCM 2010 model is sensitive only to the number of entry and circulating lanes. The parameters used in the Highway Capacity Manual 2010 roundabout capacity model are described in Table 3.5.

Table 3.5 Parameters used in HCM 2010 roundabout capacity model (HCM, 2010)

	A	B	t_f	t_c	t_o	t_f / t_c
Single-lane circulating stream ($n_c = 1$)						
Single-lane entry ($n_e = 1, n_c = 1$)	1130	0.00100	3.19	5.19	3.60	0.615
Multi-lane entry ($n_e > 1, n_c = 1$): apply to all lanes	1130	0.00100	3.19	5.19	3.60	0.615
Multi-lane circulating stream ($n_c > 1$)						
Single-lane entry ($n_e = 1, n_c > 1$) *	1130	0.00070	3.19	4.11	2.52	0.776
Multi-lane entry ($n_e > 1, n_c > 1$)						
Dominant lane (Right lane for US driving)	1130	0.00070	3.19	4.11	2.52	0.776
Subdominant lane (Left lane for US driving)	1130	0.00075	3.19	4.29	2.70	0.744

Delay formula

The Highway Capacity Manual 2000 suggests the formula in Equation [3.31] for delay calculation at each entry of roundabouts, and Equation [3.32] for total average delay calculation at roundabouts. These formulas are based on the Akcelic and Troutbeck (1991).

$$W_{s,i} = \frac{3600}{C_i} + 900T * \left[\left(\frac{Q_{ei}}{C_i} - 1 \right) + \sqrt{\left(\frac{Q_{ei}}{C_i} - 1 \right)^2 + \frac{3600 Q_{ei}}{450T C_i}} \right] \quad [3.31]$$

$$\left(W_s = \frac{\sum_{i=1}^4 (W_{s,i} Q_{ei})}{\sum_{i=1}^4 Q_{ei}} \right) \quad [3.32]$$

where

- $W_{s,i}$ = Control delay for leg i (sec/veh)
- T = Duration of analysis period h , normally $0.25hr$.
- Q_{ei} = Flow rate for leg i (pcu/hr.)
- C_i = Overall capacity for leg i (pcu/hr.)
- W_s = Weighted mean control delay for all legs (sec/veh)

For one lane entry there are no difficulties but for dual-lanes entries, equation is applied under the assumption that the entry has only a single-lane and has the same capacity and flow rate as the dual-lane entry. The delay obtained in this way is thus intended as the mean delay of every vehicle at the entry.

Level-of-service criteria for stop-controlled intersections and signalized intersections differ because the intersection types create different user perceptions. To determine the intersection LOS at a signalized intersection, the average control delay for the entire intersection is commonly used. LOS criteria for roundabouts are given in Table 3.6 are the same as the LOS criteria for stop-controlled intersections in HCM 2000. The LOS for a roundabout is determined by the computed or measured control delay for each lane. Defining the LOS for the intersection as a whole is not recommended because doing so may mask an entry that is operating with much higher delay than the others (NCHRP Report 572, 2007).

LOS	Signalized Intersection	Stop control / Un-signalized Intersection
A	≤10 sec	≤10 sec
B	10-20 sec	10-15 sec
C	20-35 sec	15-25 sec
D	35-55 sec	25-35 sec
E	55-80 sec	35-50 sec
F	≥80 sec	≥50 sec

Table 3.6 Level-of-service thresholds for roundabouts (NCHRP Report 572, 2007)

3.4.6 Australian capacity and delay formula

“Jacquemart” found that the Australian guidelines were followed in two-thirds of cases. For one-third of the cases, the British method was used. However, one-quarter of the respondents checked both the Australian and British methods as sources for design and analysis (Jacquemart, 1998). The Australian capacity model is based on the gap acceptance technique. The Gap acceptance capacity model concerns the analysis of minor movements at intersection controlled by a two-way stop and yield signs, entry streams at roundabouts. The same modeling principle applies to all cases with different model parameters representing the intersection geometry, control, and driver behaviour. Lane-by-Lane technique is used for capacity and performance modeling; thus the arrival headway distribution in a single-lane of the approach road is considered. However, in entry stream capacity modeling, the headway distribution of the entire traffic demand in all lanes of a major traffic stream is accepted with different values of minimum headway and bunching parameters for single or dual-lane cases (Rahmi Akcelik, 2007).

Capacity model

In 1962, Tanner analyzed the delays at an intersection where major traffic had priority. He assumed traffic arrivals were random at both major and minor approaches, but a major traffic vehicle could not enter the intersection sooner than Δ seconds after the preceding major traffic vehicle. The minor traffic vehicle then entered when any available Gap was greater than T seconds. If the chosen gap was large enough, several minor traffic vehicles then followed each other through the intersection at intervals of T_o seconds (Taekratok, 1998). Equation [3.33] is the Tanner’s capacity equation.

$$q_e = \frac{q_c [1 - \Delta q_c] e^{q_c[T-\Delta]}}{1 - e^{-q_c T_o}} \quad [3.33]$$

where q_e, q_c, T, T_o and Δ are entering capacity (veh/sec), circulating flow (veh/sec), critical gap (s), follow-up time (s) and minimum headway respectively as shown in (Table 3.7).

Table 3.7 Critical gap (s), follow-up time (s) and minimum headway ranges

Researches	T	T _o	Δ	Remarks
Horman and Turnbull's	3 to 4	2	1 or 2	According to (Troutbeck, 1984)
Avent and Taylor	4	2	0	For dual-lane circulating flow
	3.5	2-2.7	0	Studied 3 Brisbane roundabout multilane circulation flow
	2.5	2.1	2.2	For single-lane roadway
	2.5	2.1	1.1	For dual-lane roadway (Avent, 1979)

Tanner's assumptions that T & T_o are constants and that headway distribution of priority traffic was random were not realistic. In 1991, Troutbeck modified Tanner's capacity Equation [3.33] to the new form of Equation [3.34] (Troutbeck, R.J., 1991). He also questioned real drivers' interactions at roundabouts. He assumed that both traffic streams would have some influence on each other (Taekratok, 1998).

$$Q_e = \frac{3600 [1 - \theta] q_c e^{-\beta[T-\Delta]}}{1 - e^{-\beta T_o}} \quad [3.34]$$

$$\beta = \frac{(1 - \theta)q_c}{1 - \Delta q_c} \quad [3.35]$$

where

- Q_e = Entry capacity (veh/hr)
- q_c = Circulating flow (veh/hr)
- θ = Proportion of bunched vehicles
- Δ = Minimum headway in circulating traffic. For (Multi-lane=1, Single-lane =2)
- T = The critical gap (sec)

T_o = The follow up time (sec)

β = Decay parameters

The idea of dominant and subdominant traffic entry lanes was presented in Troutbeck's study, as described in Table 3.8, which is used to take into account the difference in each lane. If there is only one entry stream, it will be a dominant stream. Troutbeck established equations for critical gap and follow-up time calculations in each lane, which are used in the AUSTROAD design guideline.

Table 3.8 Comparison of dominant and subdominant traffic entry lane

Dominant traffic entry lane	Subdominant traffic entry lane
<ul style="list-style-type: none"> • Greatest entry flow traffic with lower critical gap parameters and higher entry lane capacity • Only one dominant stream at each entry 	<ul style="list-style-type: none"> • At the same leg have larger critical gap with inferior capacity • May be many subdominant streams

Dominant traffic follow-up time;

$$T_{\text{odom}} = 3.37 - 0.000394Q_c - 0.0208D_i + 0.0000889D_i^2 - 0.395n_e + 0.388n_c \quad [3.36]$$

Subdominant traffic follow-up time;

$$T_{\text{osub}} = 2.149 - 0.5135T_{\text{odom}} \frac{Q_{\text{dom}}}{Q_{\text{sub}}} - 0.8735 \frac{Q_{\text{dom}}}{Q_{\text{sub}}} \quad [3.37]$$

The critical gap relies on the follow-up time, circulating flow, No. of circulating lanes, and the average entry lane width. It was found that the critical gap to follow-up time ratio is inversely proportional to circulating flow, number of circulating lanes, and average entry lane width. Equation [3.38] was applied to the conditions in all entry lanes.

$$\frac{T}{T_o} = 3.6135 - 0.0003137Q_c - 0.3390e_e - 0.2775n_c \quad [3.38]$$

where

Q_c = Circulating flow (veh/hr)

D_i = largest Inscribed diameter that can be drawn inside a roundabout

- n_e = Number of entry lanes
- n_c = Number of circulating lanes
- T_{odom} = Dominant traffic follow-up time
- T_{osub} = Subdominant traffic follow-up time
- Q_{dom} = Dominant traffic entry flow
- Q_{sub} = Subdominant traffic entry flow
- T = Critical gap
- T_o = Follow-up time
- e_e = Average entry lane width

The dominant traffic follow-up time is directly proportional to subdominant traffic follow-up time. The dominant traffic follow-up time also increases with larger variations in the lane entry flows (Taekratok, 1998).

Delay model

Dunne and Buckley rearranged Tanner's delay equation, which was adopted earlier as a delay equation with gap parameters from Table 3.7, defined by (Avent, 1979) into the easier form of Equation [3.39].

$$D = \frac{D_{min} + \delta x}{1 - x} \quad [3.39]$$

$$D_{min} = e^{Q_c [T-\Delta]} - T - \frac{1}{Q_c} - \frac{\Delta^2 Q_c}{2} \quad [3.40]$$

$$\delta = \frac{e^{Q_c T_o} - Q_c T_o - 1}{Q_c [e^{Q_c T_o} - 1]} \quad [3.41]$$

$$D_{min} = \frac{e^{\beta [T-\Delta]}}{Q_c \alpha} - T - \frac{1}{\beta} - \frac{\beta \Delta^2 - 2\Delta + 2\Delta \alpha}{2[\Delta \alpha + \alpha]} \quad [3.42]$$

$$D = D_{min} + \frac{3600kx}{Q_e [1 - x]} \quad [3.43]$$

$$k = \frac{D_{min} Q_e}{3600} \quad [3.44]$$

The new capacity formula in Equation [3.34] is based upon dichotomized headway distribution; therefore, Troutbeck redefined Adam's delay with dichotomized headway distribution as shown in Equation [3.42] (Troutbeck, R.J., 1989). Queue length at arrival of vehicles is assumed to be zero in Tanner's and Troutbeck's equations. Therefore, Troutbeck also revised his formula by considering the delay due to the queue presence at the entry lanes. The average delay is then calculated by Equation [3.43].

Later, Akcelik and Troutbeck reset the model with a time-dependent model because all previous models represented the steady state delay models. This new delay model was adopted in the AUSTROAD design guideline (1993) with the substitution of $8k = m$, as described in Equation [3.45].

$$D = D_{\min} + 900 \left[Z + \sqrt{Z^2 + \frac{8kx}{Q_e H}} \right] \quad [3.45]$$

$$Z = x - 1 \quad [3.46]$$

where

- x = Degree of saturation in the specified flow period, entry flow/entry capacity
- D_{\min} = Adam's delay
- H = Flow period in hours
- Q_e = Entry lane capacity (veh/hr)
- k = Delay parameter

3.5 COMPARISON AND APPLICATION OF CAPACITY MODELS

3.5.1 Gap acceptance method (Vs.) Empirical method

Kimber, Maycock, G, and Hall, RD, conducted extensive research in England from 1979 to 1985; their findings support the empirical formula method of roundabout analysis over the gap acceptance method of analysis (Kimber, RM & Hollis EM, 1979; Kimber R. , 1980; Kimber R. ; Maycock, 1984). Taekratok differentiates between Gap acceptance and the empirical technique based on methodology, data acquisition to develop the models, reliability of prediction, and simplicity criteria, as explained in Table 3.9 (Taekratok, 1998).

Table 3.9 Comparison between Gap acceptance and Empirical technique (Taekratok, 1998)

Criteria	Gap Acceptance	Empirical
Methodology	<ul style="list-style-type: none"> • Theoretical basis • Based on vehicle-vehicle interaction it represents driver behavior. • The use of single estimators of critical gap and follow-up time is questionable for the accuracy of capacity prediction. 	<ul style="list-style-type: none"> • Statistical regression basis • Suggest driver behavior by the relationship between geometric elements and road performances. • Some geometric parameters may prove to be statistically significant, but cannot be explained logically.
Data Acquisition to Develop the Models	<ul style="list-style-type: none"> • Fewer amounts of data are required due to under the simplified assumption of gap acceptance theory. • When model gets complicated, method to obtain and verify data seems to get complicated as well. 	<ul style="list-style-type: none"> • Requires an extensive amount of data with the sufficient variation of each parameter.
Reliability of Prediction	<ul style="list-style-type: none"> • Depends on the developed model and assumptions. 	<ul style="list-style-type: none"> • Depends on the methods of sampling and sample sizes.
Simplicity	<ul style="list-style-type: none"> • Easy for planning purposes 	<ul style="list-style-type: none"> • Easy for geometric design purposes.

When we perform entry capacity analysis with the empirical regression technique, the required geometric data for analysis includes entry width, entry angles, approach half width, entry radius, inscribed circle diameter, and average effective flare length. For the Gap acceptance technique, the required geometric data is only the number of entry and circulating lanes and inscribed circle diameter (Mehmood, 2003).

3.5.2 Comparison of the Australia and US capacity formulas

A comparison between Australian and United State methods was done by (Taekratok, 1998), as explain in Table 3.10.

Table 3.10 Comparison of Australia and US capacity formulas (Taekratok, 1998)

Category	Australia	United State
Methodology	Gap acceptance	Gap acceptance
Parameters	Critical Gap, follow-up time	Critical Gap, follow-up time
Parameters determination	Equation developed by the study of Troutbeck	Upper and Lower values from the study in the US
The relationship between parameters and geometries	Inscribed circle diameter, Number of lanes	N/A
Traffic flow distribution	Cowan M3 distribution	Exponential distribution
Application for multi-lane	Apply in terms of subdominant and dominant flows	Not recommended

3.5.3 Application

The Highway Capacity Manual 2000 states that the sites where driver behavior characteristics are incomplete, the designer can use the empirical models. The Gap acceptance model is recommended in HCM 2000 for single-lane roundabouts, and the regression model is recommended for multilane or dual-lane roundabouts (Highway Capacity Manual, 2000). The capacity analysis models suggested in the FHWA roundabout guide depend on comprehensive worldwide research. These models are either based directly on international models for similar roundabout types or adopted by adapting international models with assumed parameters. The models for single-lane and dual-lane roundabouts are based on a simplified British relationship with assumed geometric parameters (Rodegerdtz, L, 2005). The Gap acceptance model is generally accepted by most engineers in the United States due to an absence of United States

data to calibrate the regression model proposed by international research studies, since driver behavior is the largest variable disturbing capacity performance. Due to local driver behavior and variations in driving skill over time, it is essential that models be calibrated for accurate capacity estimate calculation (Kittelson & Associates, Inc. NCHRP 3-65, 2006).

3.6 DEGREE OF SATURATION

The degree of saturation is represented by the volume-to-capacity ratio. According to the Australian guide, it should be in the range 0.8 to 0.9 for satisfactory operation, although this value may not always be attainable. The Highway Capacity Manual 2010 suggested that degree of saturation range from 0.85 to 0.90 represents an approximate threshold for satisfactory operation (HCM, 2010). For a given lane, the volume to capacity ratio x , is calculated by dividing the lane's calculated capacity (veh/hr) by demand flow rate (veh/hr) as shown in Equation [3.51].

$$x = \frac{v}{c} \quad [3.51]$$

If the degree of saturation exceeds this range, the operation of the roundabout enters a more unstable range in which conditions could deteriorate rapidly, particularly over short periods (NCHRP Report 572, 2007).

3.7 QUEUE LENGTH

When evaluating the suitability of the geometric design of the roundabout approaches, queue length plays a significant role. In 1994, Wu proposed the Equation [3.47] for percentile of queue length, whereas (CETUR, 1988) and (Harder. J, 1989) proposed Equation [3.48] for queue length calculations.

$$Q_\alpha \approx \frac{QT}{4} \left[x - 1 + \sqrt{[1 - x]^2 + \frac{8x}{QT} [-\ln(\alpha)]} \right] \quad [3.47]$$

where

Q_α = (1- α)% percentile of queue lengths

x = Saturation degree during the dimensioning period "T"

Q = Capacity during the dimensioning period “T”
 n_e = Number of lanes in the subject entry

$$L = d \frac{Q_e}{3600} \quad [3.48]$$

where

Q_e = Entry capacity (pcu/hr)
 d = Average delay (sec)
 L = Average queue length (vehicle)

Average queue length is useful information when comparing roundabout performance with that of other intersections. For designing purposes, 95th percentile queue length is used, and it varies with the degree of saturation of an approach (Heidemann, 1991).

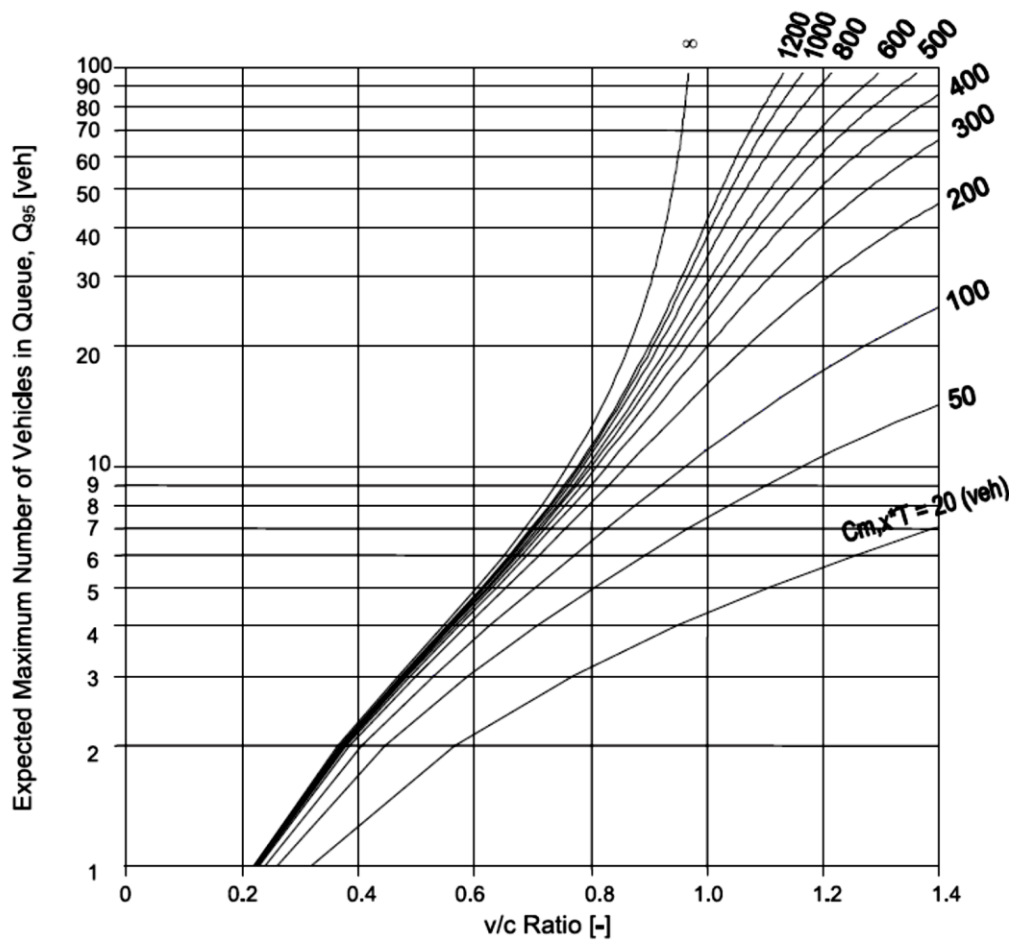


Figure 3.7 95th percentile queue length estimation Figure (Wu, 1994)

Equation [3.49] and Figure 3.7 can be used to approximate the 95th percentile queue. These are operational only where the degree of saturation immediately before and immediately after the study period is no greater than 0.85 or where the residual queues are negligible (Wu, 1994).

$$Q_{95} \approx 900T \left[\frac{V_x}{C_{m,x}} - 1 + \sqrt{\left[1 - \frac{V_x}{C_{m,x}}\right]^2 + \frac{\left(\frac{3600}{C_{m,x}}\right)\left(\frac{V_x}{C_{m,x}}\right)}{450T}} \right] \frac{C_{m,x}}{3600} \quad [3.49]$$

where

- Q_{95} = 95th percentile queue, (veh)
- V_x = Flow rate for movement x, (veh/hr.)
- $C_{m,x}$ = Capacity of movement x, (veh/hr.)
- T = Analysis time period, h (0.25 for 15 minute period).

CHAPTER 4 : GEOMETRIC DESIGN CONSIDRATIONS

4.1 INTRODUCTION

Safety and operational performance of a roundabout is particularly sensitive to the geometric design of elements. The design problem is principally the defining of a design that will manage the traffic demand while minimizing some combination of delays, crashes, and cost to all users – motor vehicles, pedestrians, and cyclists. How well a design reaches each of these goals is dependent on evaluation procedures that are suggested. Over-design and less safety can result from uncertainty regarding evaluation procedures (FHWA, 2000).

Besides capacity and safety, the geometric element is also governed by the requirement of design vehicle; therefore, the design process should be an optimum balance between safety, operational performance, and large vehicle accommodation. The design techniques are different depending on the site and speed environment, but the basic features of roundabouts are uniform for all locations. This chapter represents the design procedure and literature review of design guidelines.

4.2 APPROACHES ARRANGEMENT AT ROUNDABOUTS

Generally, consecutive approaches at roundabout intersect at a right-angle or at skewed-angle. It is generally preferred for the approaches to intersect at perpendicular or near-perpendicular intersection angles. If two approach legs intersect at an angle significantly less than or greater than 90° , it often results in excessive speeds for one or more right turn movements. At the same time, left turn movements from all approaches are relatively low, resulting in a higher speed differential than desired. Designing the approaches at perpendicular or near-perpendicular angles generally results in relatively slow and consistent speeds for all movements. Highly skewed-angle intersection can often require significantly larger inscribed circle diameters to achieve the speed objectives (KDOT, 2003).

4.2.1 Right-angle approaches

Highways approaching roundabouts should intersect at right angles, and intersections placed at acute angles are undesirable (Bureau of Local Roads & Streets, 2007). In many places,

site conditions impose definite alignment and grade limitations on intersection roads. However, it is often possible to modify the alignment and grade to better suit traffic conditions and reduces hazards. For safety and economic reasons, it is desirable that consecutive intersecting approaches meet at or nearly a 90° angle.

4.2.2 Skewed-angle approaches

The intersection angle of two roadways encourages the operation and safety of an intersection. Larger skewed-angles increase the pavement area and thus the area of possible conflict. Operationally, the skewed-angles are undesirable because:

- Pedestrians and crossing vehicles are exposed for longer periods;
- Driver's sight angle is more constrained and more difficulties arise during gap perception
- Large trucks require more space, therefore vehicular movements are more difficult
- It becomes more difficult to defining vehicle paths by channelization

The angle of intersection within 15° of perpendicular can often be tolerated because the impact on sight lines and turning movements is not significant. Under a restricted situation and because of right-of-way constraint, an intersection angle up to 30° from the perpendicular may be used.

For new intersections, the crossing angle should preferably be in the range of 75° to 120°. Particularly trucks with closed cabs have difficulty at such a skewed-angle in seeing vehicles approaching from the left (Bureau of Local Roads & Streets, 2007). According to TAC, some experience has shown that the practice of realignment of a road with increased intersection angle has proven beneficial. The acceptable range is between 70° and 110°, to produce only a small reduction in visibility. Therefore, if the condition as indicated below is not satisfied at a particular location, it is appropriate to realign the roadway or approaches to the roundabout (TAC , 2007).

$$[70^\circ < \textit{Intersection Angle} < 110^\circ]$$

Generally, approaches that intersect at angles greater than approximately 105° should be realigned by introducing curvature in advance of the roundabout to produce a more perpendicular intersection (KDOT, 2003). AASHTO recommends avoiding intersection angles of less than 60° (AASHTO, 2004). The Caltrans Highway Design Manual recommends intersection angles of no less than 75° for at-grade intersections (CDOT, 2006), and FHWA's

design handbook for older drivers and pedestrians also recommends using 75° as the minimum intersection angle.

4.3 CONFLICTS AT A DUAL-LANE ROUNDABOUT

Similar conflicts occur at dual-lane roundabouts, and additional unique conflicts with dual-lane roundabouts are generally low-speed sideswipe conflicts that typically have low severity. Therefore, although the number of conflict points increases at multilane roundabouts when compared with a single-lane roundabout, the overall severity of conflicts is generally less than with alternative intersection control.

Conflict points occur, where one vehicle path crosses, merges with, diverges from, or queues behind, the path of another vehicle, a pedestrian, or a bicycle. Conflicts can arise from both legal and illegal maneuvers; many of the most serious crashes are caused by failure to observe traffic control devices (FHWA, 2000). These are the following conflicts normally observed at dual-lane roundabouts.

4.3.1 Vehicle-Vehicle and Vehicle-Pedestrian conflicts

There are a total of 32 potential conflicts (16 pedestrian-vehicle and 16 vehicle-vehicle conflicts) at conventional intersections with four single-lane approaches, as illustrated in Figure 4.1.

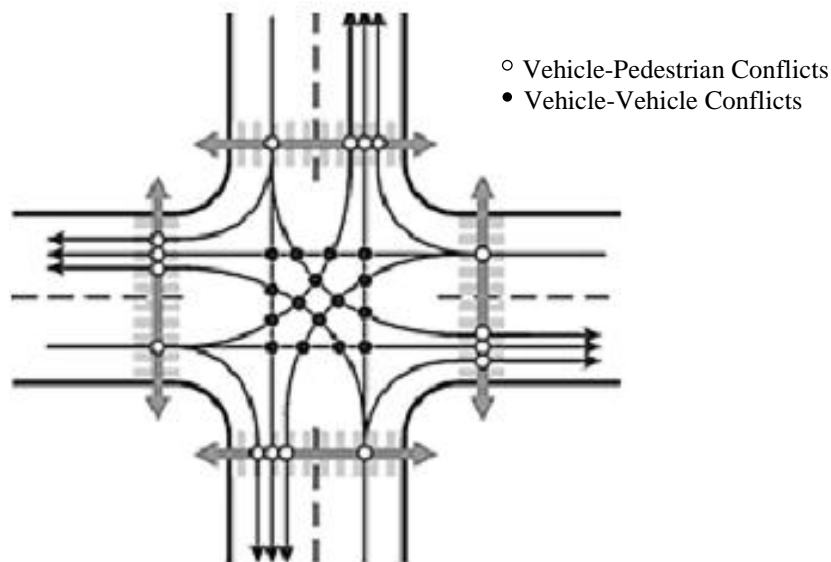


Figure 4.1 Conventional intersection conflicts (FHWA, 2000)

While the single-lane roundabouts face a total of 16 potential conflicts (8 pedestrian-vehicle and 8 vehicle-vehicle conflicts). Each approach of a single-lane roundabout faces two (1 pedestrian-vehicle and 1 vehicle-vehicle) conflicting vehicular movements, as illustrated in Figure 4.2.

At conventional intersections and roundabouts, the numbers of vehicular and pedestrian conflict points increases considerably with the additional approach lanes and increase in pedestrian crossing distances. There are more potential conflicts in case of dual-lane intersections with four dual-lane approaches – a total of 40 conflicts (16 pedestrian-vehicle and 24 vehicle-vehicle conflicts) as illustrated in Figure 4.3 – but overall, the severity of conflicts is generally less than for alternative intersection control (FHWA, 2000).

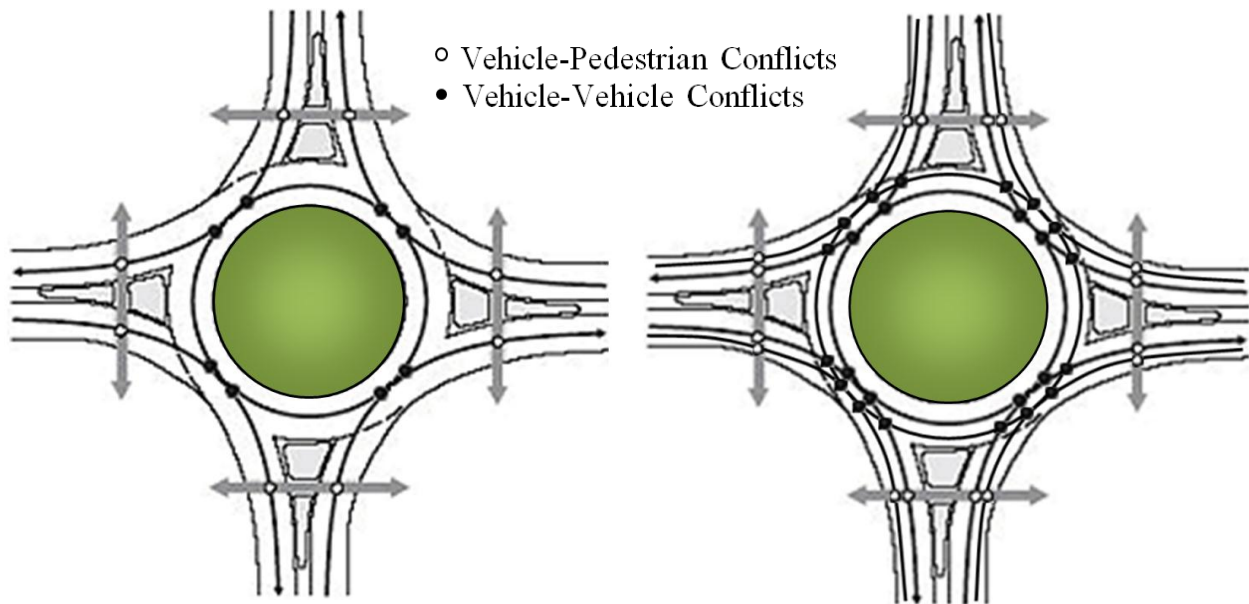


Figure 4.2 Single-lane roundabout (NCHRP Report 672, 2010)

Figure 4.3 Dual-lane roundabout (NCHRP Report 672, 2010)

4.3.2 Queuing conflicts

Queue conflicts are caused by a vehicle running into the back of a vehicle queue on an approach. These types of conflict can occur at the back of a through-movement queue or where left turning vehicles are queued, waiting for gaps. These conflicts are typically the least severe of all conflicts because the collisions involve the most protected parts of the vehicle and the relative speed difference between vehicles is less than in other conflicts (FHWA, 2000).

4.3.3 Merge and diverge conflicts

Merge and diverge conflicts are due to the joining or separating of two traffic streams. The most common types of crashes due to merge conflicts are sideswipes and rear-enders. Merge conflicts can be more severe than diverge conflicts due to the greater probability of collisions to the side of the vehicle, which is typically less protected than the front and rear (FHWA, 2000).

4.3.4 Exit-Circulatory vehicle conflicts

A large separation angle between approach legs causes entering vehicles to join adjacent to circulating traffic that may be intending to exit at the next leg, rather than crossing the path of the exiting vehicles as illustrate in Figure 4.4. This results in conflicts at the exit point between exiting and circulating vehicles (KDOT, 2003)

A variety of solutions are possible to mitigate this problem, including changes to lane configurations, changes to inscribed circle diameter, and realignment of the approaches. Figure 4.5 shows the possible solution, which involves realignment of the approach legs to have the paths of entering vehicles cross the paths of the circulating traffic (rather than merge), to diminish the conflict.

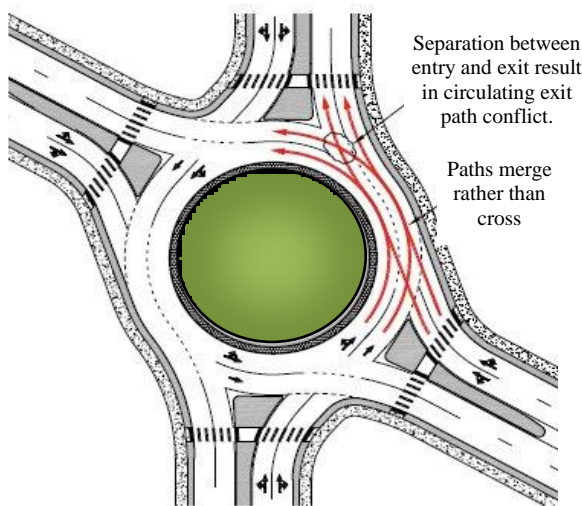


Figure 4.4 Exit-circulating conflicts

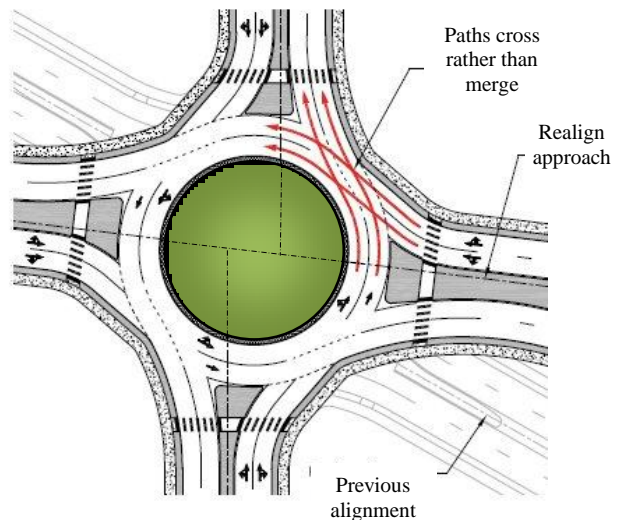


Figure 4.5 Resolve exit-circulating conflicts

(NCHRP Report 672, 2010)

4.3.5 Improper lane-use conflicts

The conflicts illustrated in Figure 4.6, present in multilane roundabouts that do not exist in single-lane roundabouts, occur when drivers use the incorrect lane or make an improper turn. These conflicts can be prevalent with drivers who are unfamiliar with roundabout operation. Crashes resulting from both types of conflict can also be reduced through proper driver education (Bared, J.G., and K. Kennedy., 2000).

4.3.6 Improper right and left turn conflicts

The conflicts shown in Figure 4.7 in particular can be created by not providing proper design geometry to allow vehicles to travel side-by-side through the entire roundabout (Bared, J.G., and K. Kennedy., 2000). Thirteen basic intersection traffic conflicts are defined in NCHRP report number 219 arising from the 32-vehicle/vehicle intersection conflict points as shown in Table 4.1. This table shows that by using a roundabout at an intersection, all but four of the 13 basic intersection conflicts are alleviated (Glauz, W., and Migletz, D, 1980).

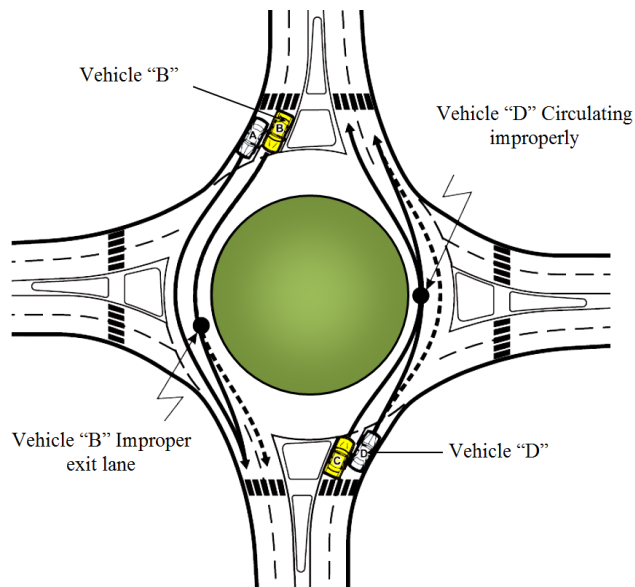


Figure 4.6 Improper lane use conflicts

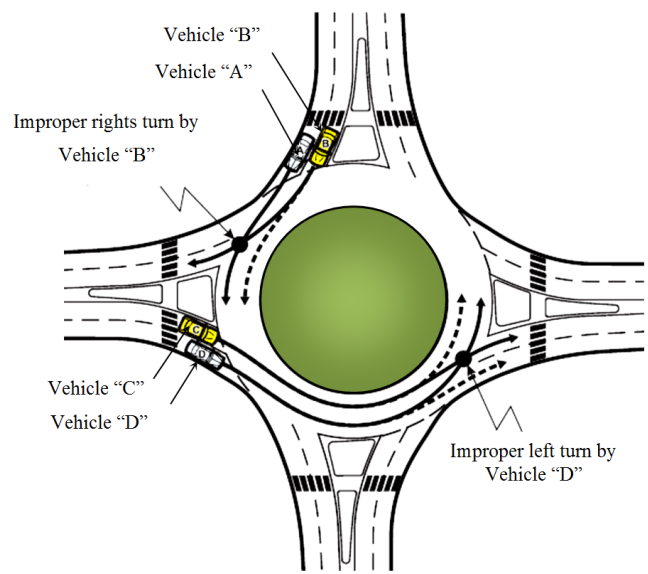


Figure 4.7 Improper right and left conflicts

(Bared, J.G., and K. Kennedy., 2000)

Table 4.1 Basic intersection traffic conflicts control (Glauz, W., and Migletz, D, 1980)

Conflict Type	Standard Intersection*	Roundabout
Left turn, same direction	Yes	No
Right turn, same direction	Yes	Yes
Slow vehicle, same direction	Yes	Yes
Lane change	No	No
Opposing left turn	Yes	No
Right turn cross traffic, from right	Yes	Yes
Left turn cross traffic, from right	Yes	No
Through cross traffic, from right	Yes	No
Right turn cross traffic, from	Yes	No
Left turn cross traffic, from left	Yes	No
Through cross traffic, from left	Yes	No
Opposing right turn on red (during protected left turn phase)	Yes	No
Pedestrian	Yes	Yes
Total	12	4

*Standard intersections include YIELD, STOP and signal control

4.3.7 Bicycle-pedestrian conflicts

Cyclists can negotiate a roundabout as either a vehicle or a pedestrian; they can continue into the roundabout using the same path as vehicles. According to Maryland roundabout design guide, “cyclists use roundabouts in a similar manner to motor vehicles.” The design of roundabouts for pedestrians follows a design philosophy similar to that of standard intersections (Maryland DOT, 1995). “In respect to geometric design, the provision for pedestrians does not differ greatly to that required for other intersection treatments, however, certain roundabout designs, particularly large roundabouts, can result in greater walking distances and thus inconvenience of pedestrians” (AUSTROADS, 1993). Pedestrian crosswalks should be located one vehicle length back from the entrances and exits of the roundabout (Maryland DOT, 1995; Wallwork, 1996). When crossing volumes of pedestrians are high, it may be desirable to move the crosswalk location farther back from the entrance and exit to allow both the motorist and the pedestrian a chance to see each other away a safe distance from the activities in the roundabout (Wallwork, 1996).

Figure 4.8 shows that at double-lane roundabouts, bicycles are typically traveling on the outside part of the circulatory roadway, and cyclists face a potential conflict with exiting vehicles where the cyclist is continuing to circulate the roundabout (FHWA, 2000).

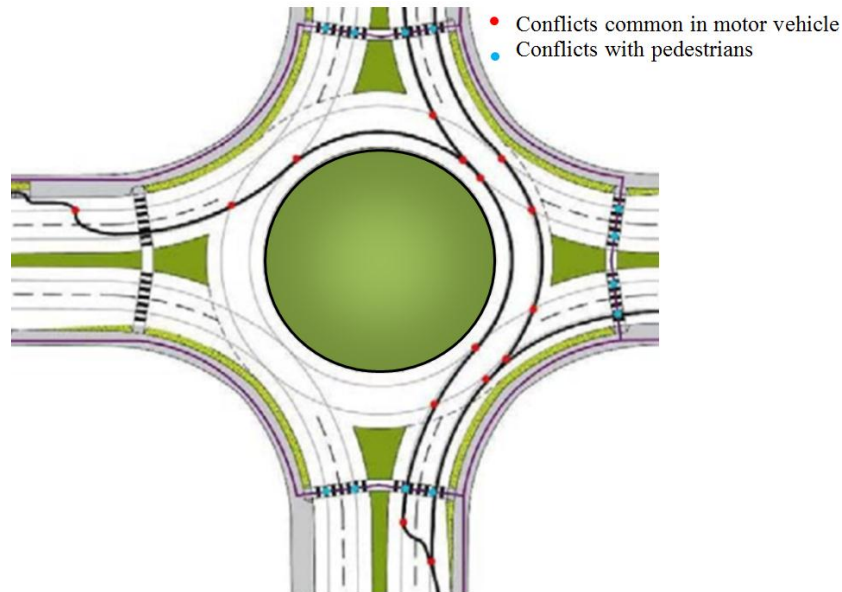


Figure 4.8 Bicyclists, vehicular and pedestrian conflicts (Google)

4.4 DESIGN PRINCIPLE FOR A DUAL-LANE ROUNDABOUT

The determination of design speed for the fastest vehicle paths acceptable in roundabout design features that safely accommodate design vehicle and speed consistency is the same for all roundabouts, but there is little difference in the design of dual and multi-lane roundabouts.

4.4.1 Speed management

The speeds at roundabouts are influenced by a variety of factors, including the geometry of the roundabout and the operating speeds of the approaching roadways. Therefore, speed management is often a combination of managing speeds at the roundabout itself and managing speeds on the approaching roadways (NCHRP Report 672, 2010).

Design speed

“It is the theoretical speed that drivers could achieve through the roundabout, if drivers taking the fastest path through the roundabout regardless to lane line striping” (FHWA, 2000).

For dual-lane roundabouts, typical maximum theoretical entering speeds between 25 to 30 mph are recommended for right-angle roundabouts (FHWA, 2000). Roundabout design speed is the most important attribute in terms of safety performance, because although the frequency of crashes is most directly tied to volume, collision severity is more directly correlated with speed. Therefore, the design speed of a roundabout needs attention to achieve good safety performance. Kansas and Arizona have slightly modified the entry design speeds at roundabouts, both states recommending a 5 mph higher entry speed for mini-roundabouts, urban compact roundabouts, and urban single-lane roundabouts (Kittelson & Associates, 2003; Lee Engineering and Kittelson & Associates, 2003). Roundabouts are categorized based on the size of the inscribed circle diameter, the number of circulating lanes, and urban/rural environment. Table 4.2 represents comparison of the recommended maximum entry design speeds.

Table 4.2 Recommended maximum entry design speeds (Zong Z. Tian, 2007)

Roundabout Category	Recommended Maximum Entry Design Speed (mph)	
	FHWA	Kansas/Arizona
Mini Roundabout	15	20
Urban Compact	15	20
Urban Single-lane	20	25
Urban Double Lane	25	25
Rural Single-lane	25	25
Rural Multilane	30	30

Approach design speeds calculated at the two points of 50 ft and 150 ft prior to the yield line are critical to the safe operation of the roundabout. The design should meet the maximum entry speed of single-lane at 20 mph, and of dual-lane at 25 mph at 50 ft, and 5 mph faster than entry speed at the 150 ft point (Roundabout Design Standards, 2005). Due to conflicting interaction between the various geometric parameters, it can be difficult to achieve a reasonably low design speed at dual-lane roundabouts while avoiding vehicle path overlap. Provision of small entry radii less than 65 ft can produce low entry speeds, but this often leads to path overlap at the entry because vehicles cut across lanes to avoid running into the central island. Similarly, the provision of small exit radii can aid in keeping circulating speeds low, but may result in path

overlap at the exits. Therefore, exits radii should be more in number than entry radii to avoid entry and exit path overlaps (FHWA, 2000). Maximum entry design speed of 25 mph to 30 mph (40 to 48 km/h) is recommended for 90° approaches at dual-lane roundabout intersections (NCHRP Report 672, 2010).

Safe negotiation speed

The safe negotiation speed is the maximum operating speed of a vehicle at a roundabout. Safe negotiation speed is the functions of turn radius, side friction factor, super elevation, and vehicle mass. Vehicle path radii are used to calculate the safe negotiation speed (operating speed) at each radius (AUSTROADS, 1993; Robinson, B. et al, 2000). According to (AUSTROADS 1993, section 4.2.6, and FHWA 2000, section 6.2.1.4), the safe negotiation speed V_n determined with the help of Equation [4.1] is

$$V_n = 3.6 \sqrt{(9.81(f_s + e)R_n)} \quad (V_{nmin} \leq V_n \leq V_{nmax}) \quad [4.1]$$

where

- V_n = Negotiation speed (km/hr)
- f_s = Side friction factor
- e = Super elevation (m/m)
- R_n = Negotiation radius (m)

The values of super elevation for entry and exit curves are +0.2, while for circulatory curves the value is -0.2 as recommended by (FHWA, 2000). It is observed that negotiation speed V_n is the function of turning radius. The minimum negotiation speed $V_{nmin} \geq 5$ km/h and minimum negotiation speed V_{nmax} is the minimum of exit cruise speed and 50 km/h (AUSTROADS, 1993).

Negotiation radius and angle

Negotiation radius and speed are given for through, left turn, and right turn movements as a function of roundabout size. Negotiation radius depends on central island diameter, circulatory exit, and entry roadway width. Negotiation angles for through and right turn a function of radius (Rahmi Akcelik, 2002).

4.4.2 Lane number and arrangement

The number of entering, circulating, and exiting lanes at a roundabout is the most important factor in determining the capacity of a roundabout. The number of lanes has a direct effect on the safety of the roundabout (CDOT, 2006). Dual-lane roundabouts generally have larger inscribed circle diameters than single-lane roundabouts to accommodate a greater number of lanes. A large inscribed circle diameter at dual-lane roundabouts can create entry-exit separation problems (Zong Z. Tian, 2007). Lane widths at the yield line must be not less than 3 m or more than 4.5 m, with the 4.5 m value appropriate at single-lane entries and values of 3 m to 3.5 m appropriate at dual-lane entries. If flaring is provided, tapered lanes should have a minimum width of 2.5 m (TD 16/93 DMRB 6.2.3, 2007).

4.4.3 Design vehicle considerations

At dual-lane or multilane roundabouts, the choice of design vehicle is more complex than for single-lane cases. In most cases, it is not feasible and not necessary to accommodate two semi-trailers side-by-side through the roundabout. Semi-trailers are usually allowed to track over lane markings within the roundabout entries, circulatory roadway, and exits. Commonly, WB-50 (WB-15) vehicles are the largest vehicles along collectors and arterials. Larger trucks, such as WB-67, may need to be accommodated at intersections on interstate freeways or state highway systems. The standard design vehicle for the state highway system in Wisconsin is the WB-65 (Facilities Development Manual, 2009).

4.4.4 Design vehicle selection

A dual-lane roundabout should be designed in such a way that its geometry accommodates the swept path of the vehicle's tires and body. Accommodation of vehicles plays a key role in dual-lane roundabout design. Designing for large semi-trailers usually has adverse effects on the ability to manage speeds; wider lanes and larger radii for trucks result in faster speeds for passenger cars. This can also have some influence on multilane roundabouts, depending on how trucks are expected to circulate within the roundabout – particularly true for single-lane roundabouts, where the design vehicle has the most direct influence on ICD (Zong Z. Tian, 2007). Selection of a design vehicle will vary depending upon the approaching roadway

types and the surrounding land use characteristics. The design vehicle affects the radius returns, left turn radii, lane widths, median openings, turning roadways, and sight distances at an intersection. (FHWA, 2000). AASHTO defines the minimum turning, centerline turning, and minimum inside radius for each type of design vehicle as shown in Table 4.3.

Table 4.3 Design vehicle-turning radius (AASHTO, 2004)

Design Vehicle Type	Passenger Car	Single-Unit Truck	Intercity Bus (Motor Coach)		City Transit Bus	Conventional School Bus (65 pass.)	Large ² School Bus (84 pass.)	Articulated Bus	Intermediate Semi-trailer	Intermediate Semi-trailer
			BUS-12	BUS-14						
Symbol	P	SU	BUS-12	BUS-14	CITY-BUS	S-BUS11	S-BUS12	A-BUS	WB-12	WB-15
Minimum Design Turning Radius (m)	7.3	12.8	13.7	13.7	12.8	11.9	12.0	12.1	12.2	13.7
Center-line ¹ Turning Radius (CTR) (m)	6.4	11.6	12.4	12.4	11.5	10.6	10.8	10.8	11.0	12.5
Minimum Inside Radius (m)	4.4	8.6	8.4	7.8	7.5	7.3	7.7	6.5	5.9	5.2
Design Vehicle Type	Interstate Semitrailer		"Double Bottom" Combination	Triple Semi-trailer/trailers	Turnpike Double Semi-trailer/trailer	Motor Home	Car and Camper Trailer	Car and Boat Trailer	Motor Home and Boat Trailer	Farm Tractor w/One Wagon
	WB-19*	WB-20**								
Symbol	WB-19*	WB-20**	WB-20D	WB-30T	WB-33D*	MH	P/T	P/B	MH/B	TR/W
Minimum Design Turning Radius (m)	13.7	13.7	13.7	13.7	18.3	12.2	10.1	7.3	15.2	5.5
Center-line ¹ Turning Radius (CTR) (m)	12.5	12.5	12.5	12.5	17.1	11.0	9.1	6.4	14.0	4.3
Minimum Inside Radius (m)	2.4	1.3	5.9	3.0	4.5	7.9	5.3	2.4	10.7	3.2

- Note: Numbers in table have been rounded to the nearest tenth of a meter.
- * = Design vehicle with 14.63-m trailer as adopted in 1982 Surface Transportation Assistance Act (STAA).
 - ** = Design vehicle with 16.16-m trailer as grandfathered in with 1982 Surface Transportation Assistance Act (STAA).
 - ¹ = The turning radius assumed by a designer when investigating possible turning paths and is set at the centerline of the front axle of a vehicle. If the minimum turning path is assumed, the CTR approximately equals the minimum design turning radius minus one-half the front width of the vehicle.
 - ² = School buses are manufactured from 42-passenger to 84-passenger sizes. This corresponds to wheelbase lengths of 3.35 m to 6.1 m, respectively. For these different sizes, the minimum design turning radii vary from 8.78 m to 12.01 m and the minimum inside radii vary from 4.27 m to 7.74 m.
 - ³ = Turning radius is for 150–200 hp tractor with one 5.64 m long wagon attached to hitch point. Front wheel drive is disengaged and without brakes being applied.

4.4.5 Entry-Exit separation

That problem can occur at dual-lane roundabouts when vehicular paths from the entry merge with the vehicular paths in the circulatory roadway and then diverge at the next exit, as illustrated in Figure 4.4. This is a consequence of profligate separation between the entry and exit of adjacent legs. Realigning one or more approaches to reduce the separation between legs would be a general solution option, as illustrated in Figure 4.5. Realigning the approaches creates a more perpendicular intersection angle and results in entry circulating paths that cross rather than merge (Zong Z. Tian, 2007). The spacing between entry and exit approaches is particularly important at dual-lane, multilane, skewed roundabouts, and roundabouts with more than four legs.

4.4.6 Dual-lane roundabout elements design

Inscribed circle diameter

One of the major dimensions in roundabout design is the inscribed circle diameter. It represents the overall size of a roundabout and helps in the selection of design speed, design vehicle, number of lanes, and natural path alignment. An iterative process is usually required to determine the optimal inscribed circle diameter.

Table 4.4 Comparison of inscribed circle diameter ranges

Roundabout category	Inscribed circle diameter ranges				Design vehicle (KDOT, 2003)
	FHWA*	Kansas /Arizona	Wisconsin	British Columbia*	
Mini Roundabout	13-25	15-28	N/A	N/A	Single unit Truck
Urban compact	25-30	28-37	N/A	N/A	Single unit Truck/Bus
Urban single-lane	30-40	37-45	35-45	37-46	WB-50(WB-15m)
Urban dual-lane	45-55	45-67	50-65	46-67	WB-50(WB-15m)
Urban multilane (3-4 entry lane)	N/A	N/A	65-80	N/A	
Rural single-lane	35-40	40-60	40-45	40-61	WB-67(WB-20m)
Rural dual-lane	55-60	53-77	50-65	53-76	WB-67(WB-20m)
Rural Multilane (3 lane entry)	N/A	N/A	65-90	N/A	

(FHWA, 2000; Kansas Roundabout Guide, 2005; BC MOT, 2007; TAC, 2007; WisDOT, 2011)

Note; * Assume 90 degree angle between entries and no more than 4 approach legs.

Table 4.4 summarizes the FHWA Guide, Kansas /Arizona guide, Wisconsin guide and Ministry of transportation British Columbia recommendations. In practice, it is not unusual for the real value to fall outside these typical ranges. Roundabouts with consecutive leg angles smaller than 90° require a larger inscribed circle diameter to facilitate turning movements at approaches. Furthermore, a larger inscribed circle diameter may be used as a method to provide adequate speed control for right turn movements between approaches greater than 90° apart (Zong Z. Tian, 2007).

Entry width

The entry width E_w , is the width of carriageway at point of entry, and is a key factor affecting capacity, in conjunction with length and sharpness of flare. On a single carriageway approach to a normal roundabout, the entry width must not exceed 10.5 m. On a dual carriageway approach to a normal roundabout, the entry width must not exceed 15 m (TD 16/93 DMRB 6.2.3, 2007).

Entry width is the largest determinant of a roundabout's capacity and should be kept to a minimum to maximize safety while achieving capacity and performance objectives. Increasing the effective flare length L' or entry width results in upsurge capacity. The increase of both elements may produce a dramatic enhancement in roundabout capacity (FHWA, 2000). To maximize the roundabout's safety, entry widths should be kept to a minimum. In addition, the turning requirements of the design vehicle may require that the entry be wider still. However, larger entry and circulatory widths increase crash frequency (KDOT, 2003).

Circulatory roadway width

Circulatory roadway width is the distance between the outer edge of outer flow lane in a circulatory roadway and the central island, excluding the width of any apron. It is a function of the swept path of the design vehicle and layout of the exit and entry approaches, and generally should be always at least as wide as the maximum entry width (up to 120 percent of the maximum entry width). At dual-lane roundabouts, the design vehicle is usually not a constraint unless the designer chooses to allow side-by-side passage of a car and a truck (Facilities Development Manual, 2009). Table 4.5 represents the minimum circulatory lane width for dual-lane roundabouts as described by FHWA. This width should be constant throughout the circle. (FHWA, 2000).

Table 4.5 Minimum circulatory lane width for dual-lane roundabouts (FHWA, 2000)

Inscribed Circle Diameter (m)	Min. Circulatory Lane width (m)	Central Island Diameter (m)
45	9.8	25.4
50	9.3	31.4
55	9.1	36.8
60	9.1	41.8
65	8.7	47.6
70	8.7	52.6

Central Island

The center or highest portion of the central island ground surface elevation should be raised a minimum of approximately 3.5 feet and a maximum of approximately 6 feet from the circulatory roadway surface (FHWA, 2000). The ground slope in the central island shall not exceed 6:1 (AASHTO, 1994). AASHTO calculates the central island diameter with respect to an inscribed circle diameter as shown in Table 4.5.

Entry angle (Phi)

The entry angle will not be a controlling design measure but is important for both capacity and safety at roundabout intersections. The typical range of Phi angle is between 20° and 40°, 30° being the optimal. The following are the two situations or design conditions in which Phi can be measured (Facilities Development Manual, 2009):

Condition 1: Condition 1 means the distance between the left sides of an entry and the next exit is less than approximately 100 ft. Phi is measured by dividing the entry and exit radii into three segments, as illustrated in Figure 4.9. Assume we draw the lines \overline{ab} and \overline{cd} at the intersection of the best-fit arc and face of curb of the splitter island extended. Line \overline{ab} and \overline{cd} are then projected tangential from the best-fit arc towards the circulating roadway, and the angle formed by the intersection of the two lines is twice the value of Phi. The acute angle is denoted as 2Phi, to obtain Phi must divide the actual value by 2.

Condition 2: Condition 2 exists if the distance between the left sides of an entry and the next exit is greater than 100 ft, as shown in Figure 4.10. By dividing the entry radii into three segments, the midpoint of the lane for each segment is the best fit with a curve that extends to the face of curb of the splitter island extended. Begin line \overline{ab} at the intersection of the best-fit arc

and face of curb of the splitter island extended. Line \overline{ab} is then projected tangential from the best-fit arc towards the circulating roadway. Begin line \overline{cd} at the intersection of line \overline{ab} and the arc located at the center of the circulating roadway. Line \overline{cd} is then projected tangential from the arc located in the center of the circulating roadway. Phi is the angle formed by the intersection lines \overline{ab} and \overline{cd} .

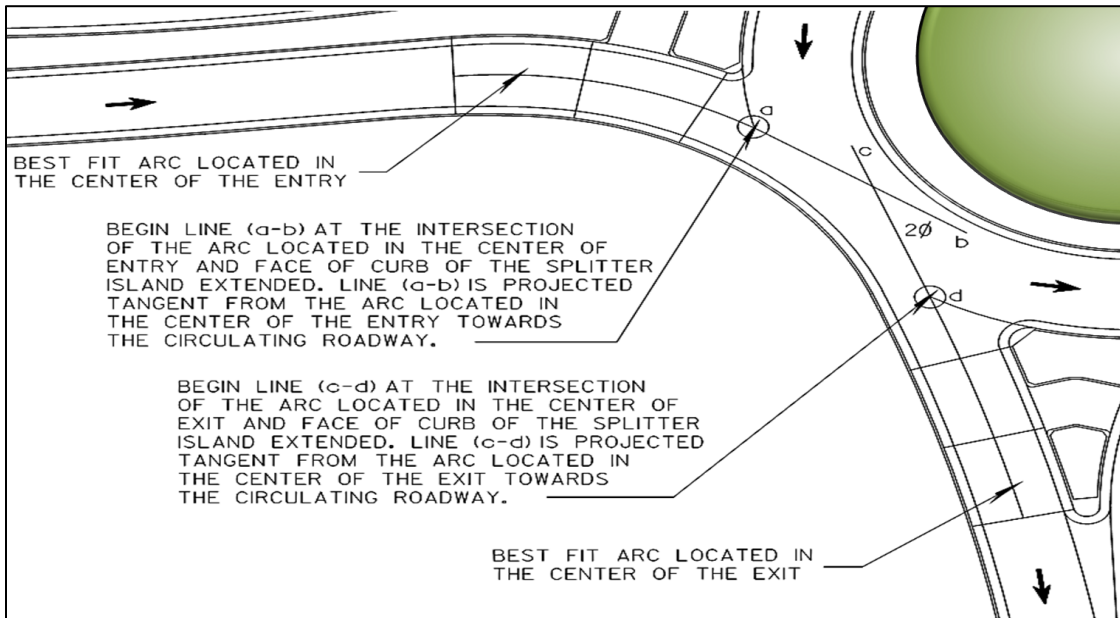


Figure 4.9 Measurement of entry angle when ($\Phi = 2\Phi/2$) (WisDOT, 2011)

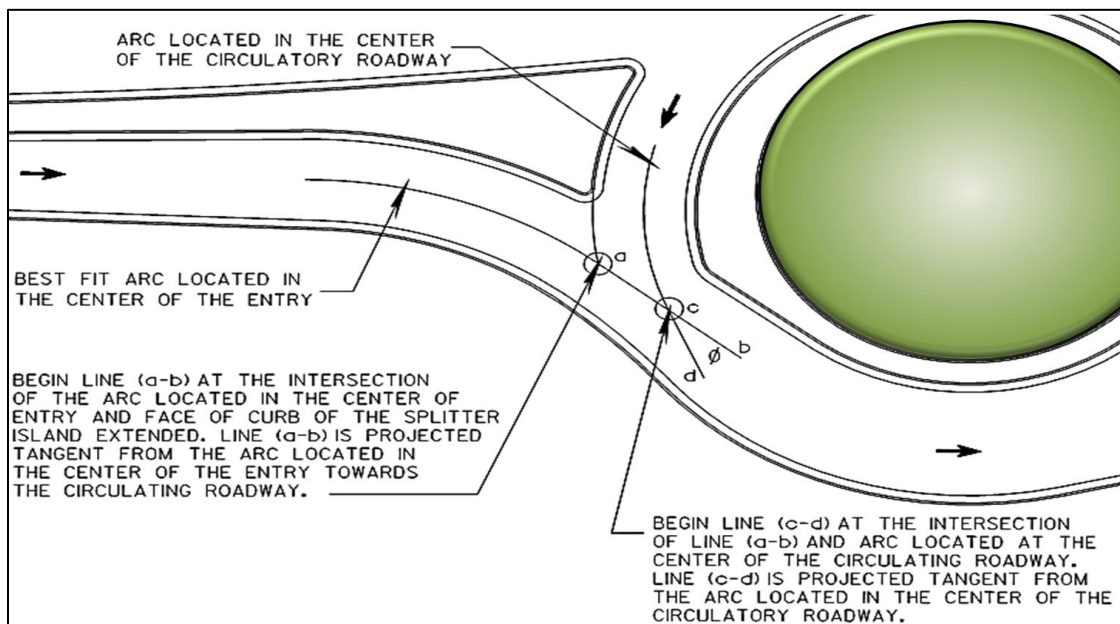


Figure 4.10 Measurement of entry angle when ($\Phi = \Phi$) (WisDOT, 2011)

Effective flare length

Greater than 25 m effective flare length may result in improvement in geometric layout but may have little effect in increasing capacity. If the effective flare length exceeds 100 m, the design becomes one of link widening. Where the design speed is high, entry widening should be developed gradually with no sudden changes in direction (TD 16/93 DMRB 6.2.3, 2007). The effective flare length may be as short as 15 ft or as long as 330 ft (Facilities Development Manual, 2009). According to FHWA, the flare lengths should be at least 25 m in urban areas and 40 m in rural areas. However, if right-of-way is constrained, shorter lengths can be used with noticeable effects on capacity (FHWA, 2000).

Splitter Island

Splitter islands perform multiple functions, so they should be provided. The recommended minimum length for a splitter island that will provide adequate visibility and refuge is 50 ft, as shown in Figure 4.11 and Figure 4.12.

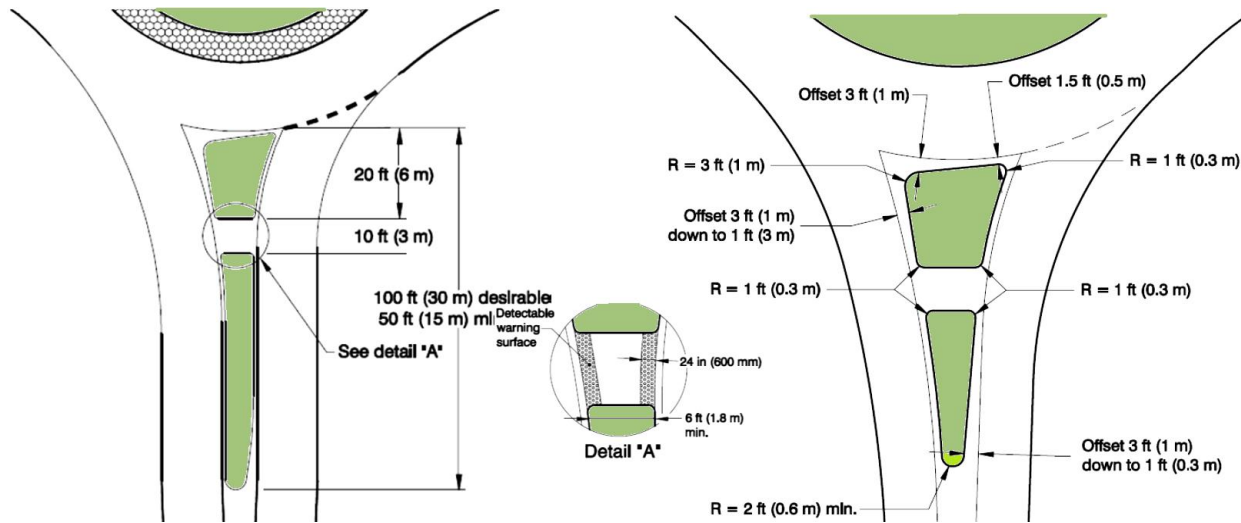


Figure 4.11 Min. Splitter Island dimensions (NCHRP Report 672, 2010)

Figure 4.12 Minimum splitter island nose radii and offsets (NCHRP Report 672, 2010)

A distance of 100 ft (30 m) is desirable to provide sufficient protection for pedestrians and to alert approaching drivers about the roundabouts. On higher speed roadways, splitter island lengths of 150 ft (45 m) or more are often beneficial (NCHRP Report 672, 2010). Splitter islands provide proper deflection of vehicular traffic for speed control and pedestrian refuge areas. The

splitter island minimum width is 6 ft (face of curb to face of curb), while 8 ft is the desirable width within the pedestrian refuge area. The minimum crosswalk width in the splitter island outside of the white edge line is 7 ft, while the desirable is 10 ft (FHWA, 2000). A splitter island should be a minimum 50 ft long (measured from the outside edge of the circulator road) if a pedestrian crossing is used. Splitter islands shall have a minimum 6'x6' pedestrian refuge (an 8'x8' refuge is preferable) where crosswalks exist or are projected. Crosswalks should be at 25 ft from the yield line for single-lane roundabouts, and 45 ft – 50 ft for dual-lane roundabouts. On dual-lane approaches, the crosswalks should be radial to the traveled section, to improve visibility for pedestrians (Colorado DOT, 2005).

Approach alignment

The desirable alignment of a roundabout is at the centerline passing to the left of the center of the circle, as described in Figure 4.13. This alignment provides aids to entry deflection and angle on the approaches, and aligns entering vehicles into the circulating roadway, but it also reduces an entry speed, which is a safety key. An approach alignment offset to the right of the roundabout's center point is undesirable because it makes it more difficult to achieve adequate deflection and allows vehicles to enter with higher speed, usually resulting in a reduction in safety (FHWA, 2000).

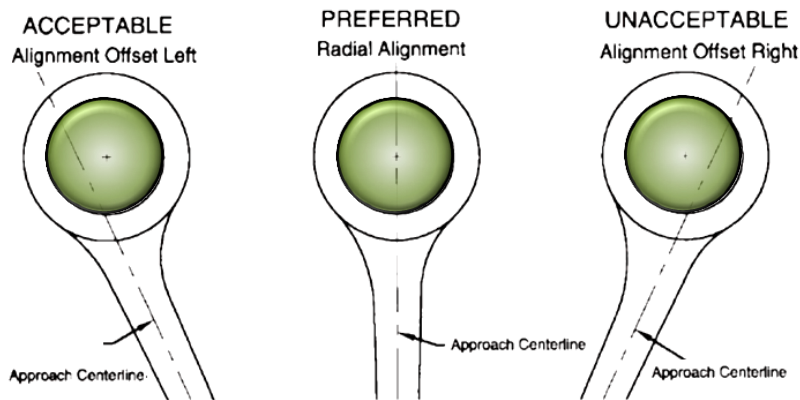


Figure 4.13 Roundabout approach alignment (FHWA, 2000)

Truck apron

Truck aprons generally provide a lower level of operation than regular paths, but may be needed to provide adequate deflection while still accommodating the design vehicle (FHWA, 2000).

4.4.7 Geometric design at entry and exit

Entry geometric design

Entry is the critical element in dual-lane roundabout design, as the geometric features of the entry are governing factors to control vehicle speeds. At dual-lane roundabouts, the speeds are not the only consideration at the entry – the design must also provide appropriate alignment of vehicles at the entrance line to prevent sideswipes and angle collisions accompanying the overlapping of natural vehicle paths. The design of entry curves is more complicated due to attention given to side-by-side traffic streams entering the dual-lane roundabout (KDOT, 2003). The entry radius has little effect on capacity provided that it is 65 ft. Using entry radiuses significantly lower than 45 ft reduces capacity with increasing severity for lower radii. The optimum value for the entry radius is between 50 ft to 65 ft. A small entry radius tends to produce large entry angles, and the converse is also true (WisDOT, 2011). Equation [4.2] represents the relation of entry radius with entry angle.

$$\text{Entry Radius} \propto \frac{1}{\text{Entry Angle}} \quad [4.2]$$

Vehicle natural path: The path will naturally follow based on the speed and orientation imposed by the geometry. The main design objective at single-lane roundabouts is to make sure the fastest vehicular paths are adequately slow and consistent in speed. With dual-lane roundabouts, the designer must also consider the natural paths of vehicles. The natural path is drawn by assuming the vehicle stays within the center of the lane up to the entrance line. At the yield point, the vehicle will continue its natural path into the circulatory roadway and exit with no sudden changes in curvature or speed, as illustrate in Figure 4.14.

Entry and exit vehicle path overlap: If roundabout geometry tends to lead vehicles into the wrong lane, it will result in path overlap with operational or safety deficiencies. Most commonly, it occurs at entry of dual-lane roundabouts, where the geometry of the right hand lane tends to lead vehicles into the left hand circulatory lane. At the entrance line, vehicles in the right-hand lane are oriented toward the inside lane of the circulatory roadway. If vehicles follow this natural path, they will cut off vehicles in the left lane, as illustrated in Figure 4.15. A potential method to check for exit overlap is to draw (on a scaled plan) the smoothest continuous connection between the centerline of the circulatory roadway and the centerline of the exiting lanes. If the radius of

this connection is less than the radius of the centerline of the circulatory roadway, vehicle path overlap may result (Arndt, O., 1998).

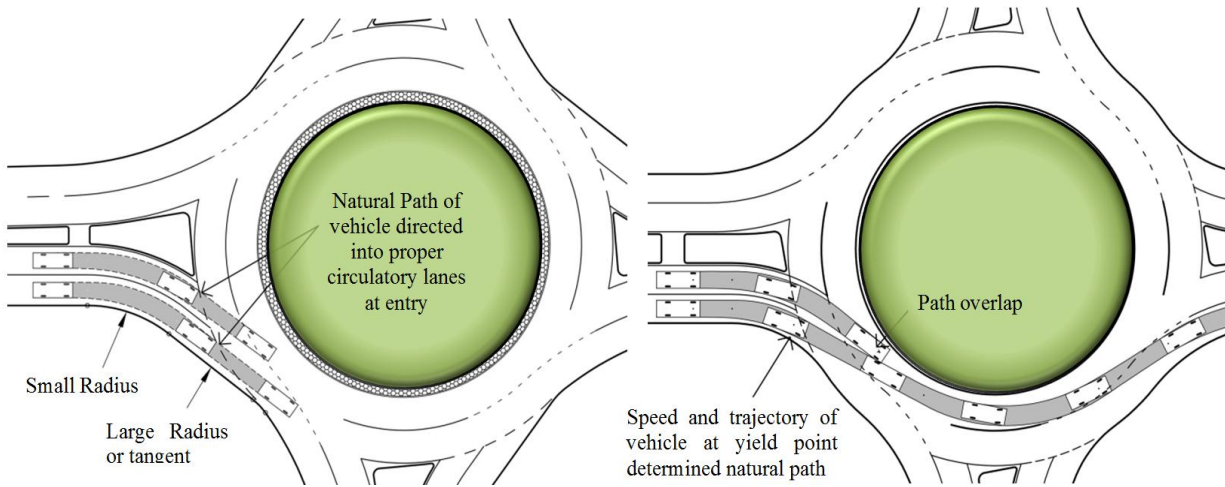


Figure 4.14 Vehicle natural path

Figure 4.15 Vehicle path overlap

(NCHRP Report 672, 2010)

Technique to avoid path overlap at entry: The design consists of a small radius entry curve of approximately 50 ft to 100 ft (15 to 30 m) and set back approximately 10 ft to 20 ft (3 to 6 m) from the edge of the circulatory roadway.

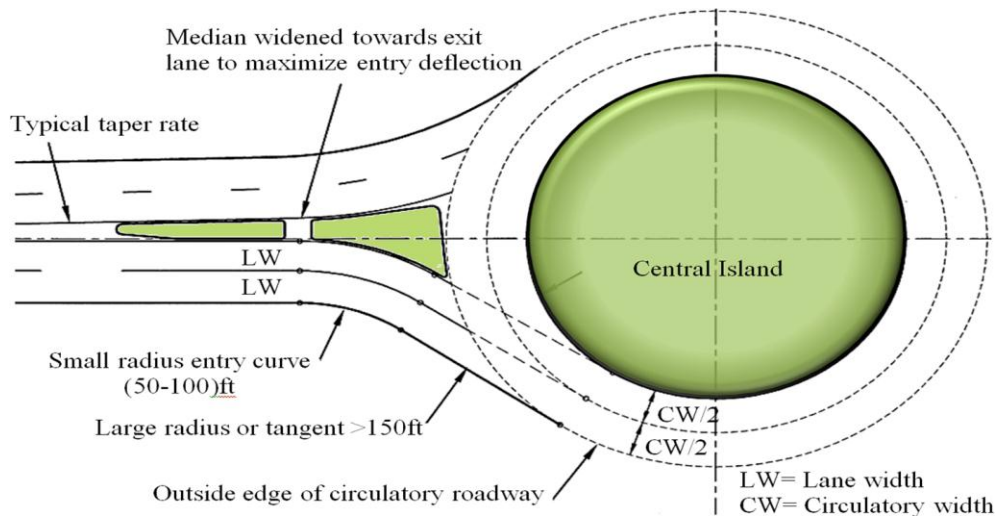


Figure 4.16 Technique to avoid path overlap at entry (KDOT, 2003; WisDOT, 2011)

A short section of tangent or large radius greater than a 150 ft (45 m) curve is provided between the entry curve and the circulatory roadway edge to ensure vehicles are directed into the proper

circulatory lane at the entrance line, as illustrated in Figure 4.16 (KDOT, 2003; WisDOT, 2011). The main objective of this technique is to locate the entry curve at the optimal placement. If it is located too close to the circulatory roadway, it can result in path overlap issues. However, if it is located too far away from the circulatory roadway, it can result in inadequate deflection and fast entry speeds.

Techniques to increase entry deflection: Control entry speeds can be difficult during designing of dual-lane roundabouts, while reaching satisfactory deflection without path overlap problems. The actions that reduce the path overlap problem usually result in greater than previously fastest path speeds. When the entry speed of a dual-lane roundabout is too fast, the inscribed circle diameter should be increased, if the right-of-way has no problem. That increase in inscribed circle diameter results in reducing the entry speed without creating path overlap, and slightly increases circulatory speeds. Dual-lane roundabout must be 175 ft to 200 ft (53 to 60 m) in diameter, or more, to achieve a satisfactory entry design (KDOT, 2003). At the location where right-of-way is constrained in that situation, the entry deflection can be improved by offsetting the approach alignment left of the roundabout center; on the other hand, it also reduces the deflection of the exit on the same leg. Therefore, the distance of the approach offset from the roundabout center should generally be kept to a minimum to maximize safety for pedestrians, as demonstrated in Figure 4.17 (KDOT, 2003).

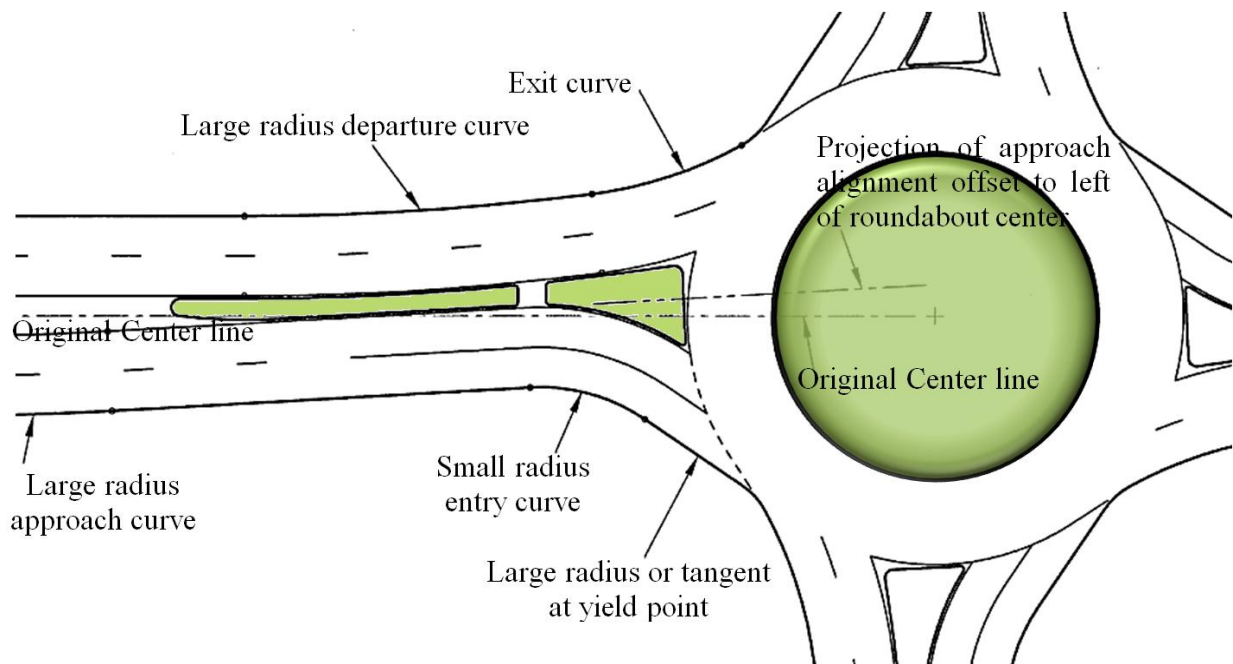


Figure 4.17 Technique to increase entry deflection (NCHRP Report 672, 2010)

Exit geometric design

The exit radius at a dual-lane roundabout should not be too small to avoid path overlap on the exit. If the exit radius is too small, traffic on the inside of the circulatory roadway will tend to exit into the outside exit lane with more contented turning radius. Larger exit curve radii are also typically used to promote good vehicle path alignment (NCHRP Report 672, 2010). The principle for maximizing pedestrian safety at dual-lane roundabouts in urban environments is to reduce aforementioned vehicle speeds to the yield and uphold alike or slightly lower speeds within the circulatory roadway (FHWA, 2000). The exit curve should produce an exit path radius greater than the circulating path radius to minimize the likelihood of congestion at the exits. If the exit path radius is smaller than the circulating path radius, vehicles will be traveling too fast to negotiate the exit geometry and may crash into the splitter island or into oncoming traffic in the adjacent approach lane (KDOT, 2003).

Non-motorized users design

The design element for the non-motorized roundabout users should be designed. Table 4.6 defines the basic design dimensions for various non-motorized roundabout users.

Table 4.6 Design element for the non-motorized roundabout users

Non-Motorized user	Dimension (m)	Affected roundabout features
Bicycles		
Length	1.8	Splitter island width at crosswalk
Minimum operating width	1.5	Bike lane width
Lateral clearance on each side	0.6, (1.0 to obstructions)	Shared bicycle-pedestrian path width
Pedestrian (walking)		
Width	0.5	Sidewalk width, crosswalk width
Wheelchair		
Minimum width	0.75	Sidewalk width, crosswalk width
Operating width	0.90	Sidewalk width, crosswalk width
Person pushing stroller		
Length	1.7	Splitter island width at crosswalk
Skaters		
Operating width	1.8	Sidewalk width

4.5 PERFORMANCE CHECK

4.5.1 Fastest path

The fastest path is the likely path taken by a single vehicle in the absence of other traffic, and pays no attention to lane line markings, or navigating through the entry, around the central island, and then out the exit. Generally, through movement is the critical fastest path, but in some circumstances it may be a right turn movement (WisDOT, 2011). The fastest speed path is a basic principle of roundabout's design to restrict operating speed by deflecting the paths of entering and circulating vehicles (FHWA, 2000). There are three vehicle paths (right, through and left turn), which are analyzed while determining the speed of a roundabout.

When a standard vehicle 2 m wide starts traversing a roundabout, the centerline of the vehicle is at distance of 1.5 m from edge of curb and at 1m from the painted line in case of a single-lane roundabout. During traversing, the vehicle maintains a 0.5 m clearance distance from concrete curb and keeps flush with painted edge line. However in a dual-lane roundabout, the centerline of the traversing vehicle is at a distance of 1 m from the centerline at the start; when it approaches to entry yield line it maintains a 1.5 m clearance from the edge of the outer curb. During traversing through a circulatory area, it again maintains a 1.5 m clear distance from the edge of inner curb and exits from the outer lane by crossing the exit yield line with a clearance distance of 1.5 m from the outer curb, as shown in Figure 4.18.

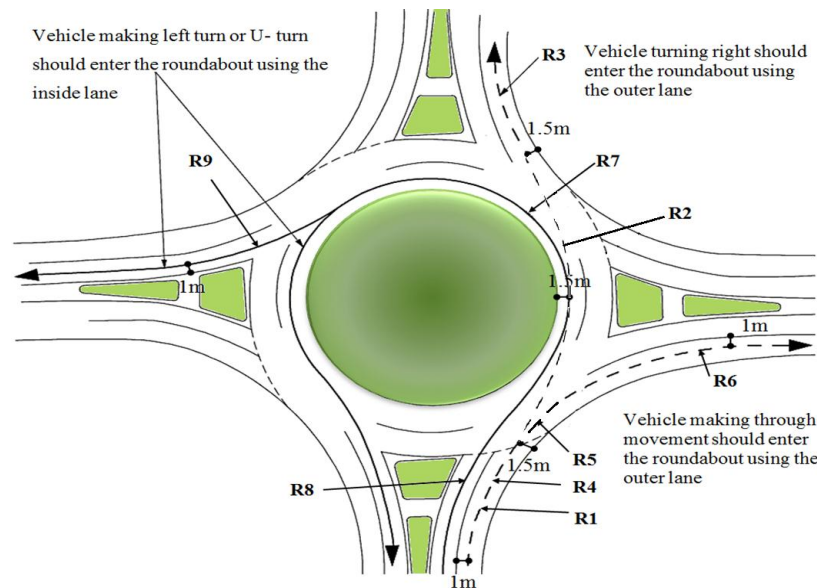


Figure 4.18 Vehicle fastest through, right and left turn path curves radius

where

R_1 = The minimum entry radius on the fastest through path prior to the yield line. This is not the same as entry radius.

R_2 = The minimum radius on the fastest through path around the central island.

R_3 = The minimum exit Path radius on the fastest through path into the exit.

R_4 = The minimum right turn entry radius on the fastest right turn path prior to the yield line.

R_5 = The minimum radius on the fastest right turn path inside circulatory roadway.

R_6 = The minimum right turn exit path radius on the fastest right turn path into the exit.

R_7 = The minimum radius on the path of the conflicting left turn movement.

R_8 = The minimum left turn entry radius on the fastest left turn path prior to the yield line.

R_9 = The minimum left turn exit Path radius on the fastest left turn path into the exit.

Similarly, the fastest path should be drawn for all approaches for design consistency. The design speed of a roundabout is determined from smallest radius along the fastest path, which usually occurs on circulatory roadways. At dual-lane roundabouts during off-peak time, the fastest-path exit speed not only depends on the exit path radius but also depends on the following:

- The circulatory radius
- The distance from the end of the R_2 radius to the exit crosswalk
- The acceleration from the end of R_2 to the exit crosswalk (BC MOT, 2007)

4.5.2 Speed consistency

The relative speeds between consecutive geometric elements and between conflicting traffic streams should be minimized for achieving the appropriate design speed for the fastest movements. The relative differences between all speeds within the roundabout will be less than or equal to 6 mph. However, it is difficult to achieve this objective at dual-lane roundabouts that must accommodate large trucks. In such a case, the maximum speed differential between movements should be less than or equal to 12 mph, ideally for 90° approach legs (FHWA, 2000; WisDOT, 2011). The overall speed limitation for operation is the maximum speed differential between any two parts of the traveled path, generally less than or equal to 12 mph, to reduce the potential for rear-end accidents for vehicles turning left or exiting (Colorado DOT, 2005).

4.5.3 Stopping Sight Distance

Stopping Sight Distance SSD is the distance between the hazard and the approaching driver, measured along the vehicle path (AASHTO, 2004). SSD for the approach at the roundabout is based on AASHTO standards for urban roadways, Section 9 of the 2001 geometric design manual. According to US federal highway authority, “Stopping sight distance is the distance along a roadway required for a driver to perceive and react to an object in the roadway and to brake to a complete stop before reaching that object” (FHWA, 2000). National Cooperative Highway Research Program (NCHRP) Report 400, “Determination of Stopping Sight Distances,” recommends application of Equation [4.3] for stopping sight distance calculation. SSD should be measured using an assumed height of driver’s eye of 1.08 m and an assumed height of object of 0.6 m, in accordance with the recommendations to be adopted in the next AASHTO “Green Book” (Fambro, D.B., et al., 1997).

$$d = 0.278(tV) + \frac{V^2}{a} \quad [4.3]$$

where

- d = Stopping sight distance, m
- t = Perception brake reaction time, assumed to be 2.5 s
- V = Initial speed, km/hr
- a = Driver deceleration, assumed to be 3.4 m/s²

At least three critical types of locations should be checked for stopping sight distance:

1. Approach sight distance as illustrated in Figure 4.19.
2. Sight distance (SD) on circulatory roadway as illustrated in Figure 4.20
3. Sight distance (SD) to crosswalk on exit as illustrated in Figure 4.21

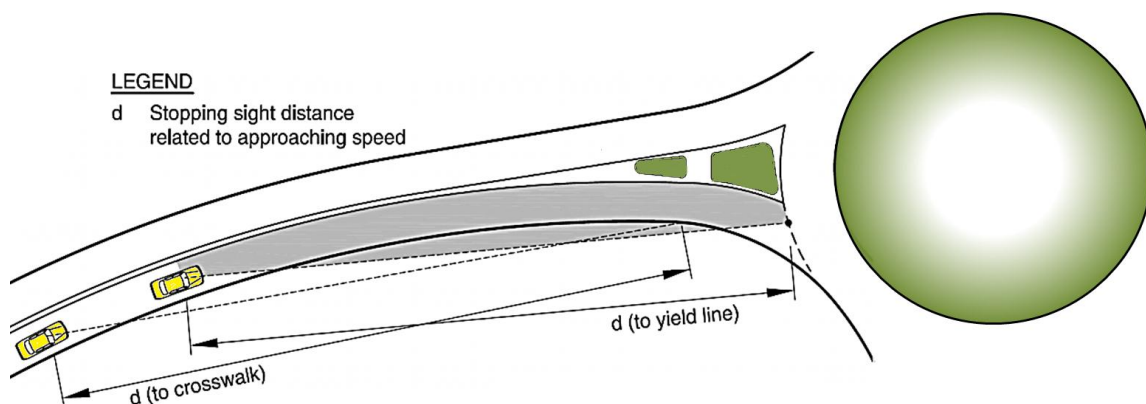


Figure 4.19 Approach sight distance (FHWA, 2000)

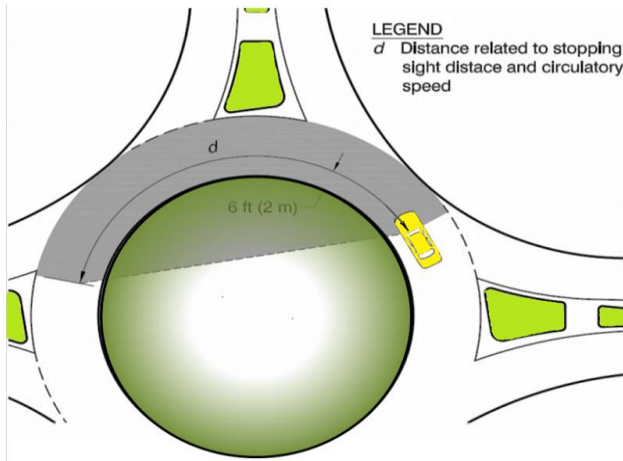


Figure 4.20 SD on circulatory roadway

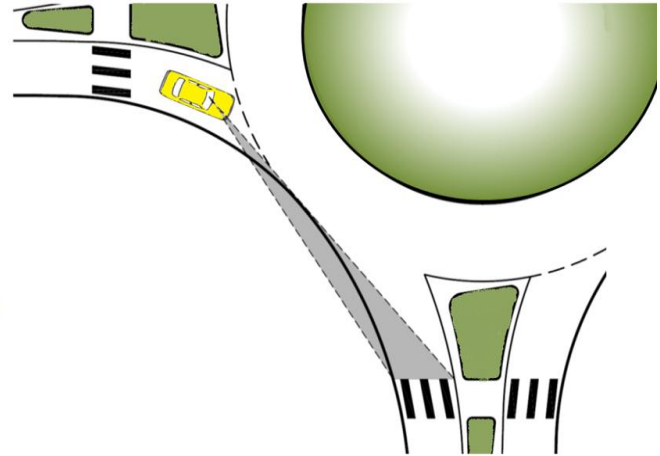


Figure 4.21 SD to crosswalk on exit

(FHWA, 2000)

4.5.4 Intersection sight distance

Intersection sight distance is the distance required for a driver without the right-of-way to perceive and react to the presence of conflicting vehicles. It is measured through the determination of a sight triangle, as shown in Figure 4.22, which is bounded by a length of roadway defining a limit away from the intersection on each of the two conflicting approaches and by a line connecting those two limits. We required adequate intersection sight distance evaluation at entries in the case of roundabout intersections (FHWA, 2000).

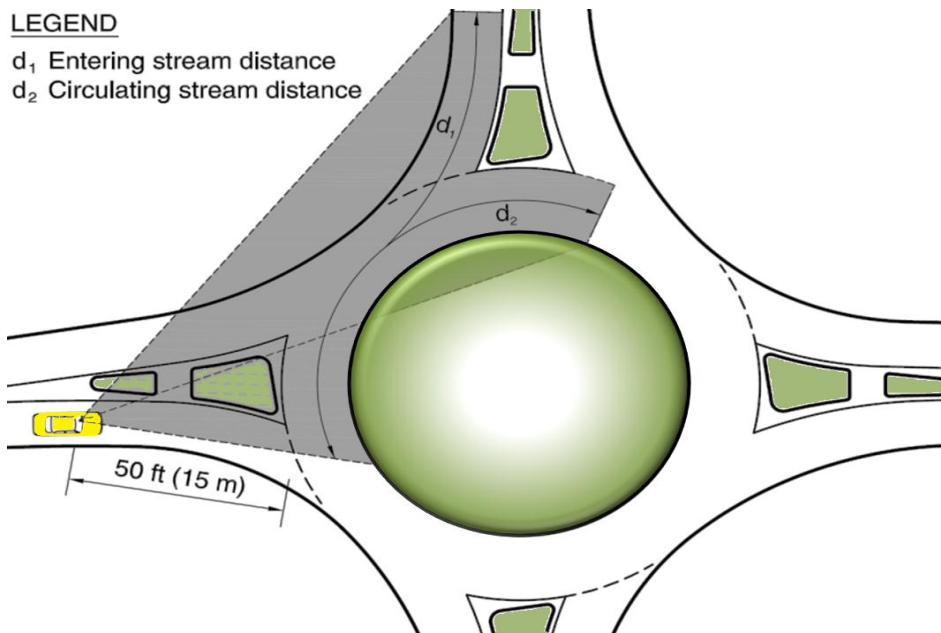


Figure 4.22 Intersection sight distance triangle (FHWA, 2000)

According to Colorado DOT, the intersection sight distance, also known as approach decision sight distance (DSD), is the distance at which the driver is aware of the change in alignment caused specifically by the roundabout. If the required *DSD* is not available due to topographic limitations, advance warning signs will be required (Colorado DOT, 2005). DSD should be measured using an assumed height of the driver's eye and object of 1.08 m, in accordance with (AASHTO, 1994).

Length of approach leg of sight triangle

British research on sight distance limited this length to 15 m; according to their research, excessive intersection sight distance results in a higher frequency of crashes, as illustrated in Figure 4.22. If the approach leg of the sight triangle is greater than 15 m, it may be advisable to add landscaping to limit sight distance to the minimum requirement (FHWA, 2000).

Length of conflicting leg of sight triangle

The length of the conflicting leg is calculated using the Equation [4.4].

$$b = 0.278(V_{major})(t_c) \quad [4.4]$$

where

- b = Length of conflicting leg of sight triangle, m
- V_{major} = Design speed of conflicting movement, km/hr.
- t_c = Critical gap for entering the major road, equal to 6.5 (sec)

Two conflicting traffic streams should be checked at each entry:

- 1) Entering stream – the vehicles from the immediate upstream entry. The speed of entering stream movement can be approximated by taking the average of the entry path speed along radii R_1 , R_4 , and the circulating path speed along radius R_2 , as illustrated in Figure 4.18.
- 2) Circulating stream-comprising vehicles that entered the roundabout prior to the immediate upstream entry. This speed can be approximated by taking the speed of left turning vehicles with radius R_7 , as illustrated in Figure 4.18.

Table 4.7 Intersection site distance and stopping site distance (FHWA, 2000)

Speed (mph)	Stopping Sight Distance (SSD) (m)		Intersection sight distance (DSD) (m)	Conflicting Approach Speed (mph)	Computed Distance (m)
	AASHTO	FHWA	Colorado DOT		FHWA
10	-	15	-	10	30
15	25	24	-	15	44
20	35	35	-	20	58
25	48	47	115	25	73
30	61	61	138	30	88
35	77	76	160	35	102
40	93	93	183	40	117
45	110	111	206	45	131

Table 4.7 represents the intersection site distance and stopping site distance based on AASHTO, FHWA and Colorado design guideline. It also illustrates the length of conflicting approach by using Equation [4.4] relating to conflicting approach speed.

CHAPTER 5 : OPTIMIZATION MODEL DEVELOPMENT: DUAL-LANE RIGHT-ANGLE ROUNDABOUTS

5.1 INTRODUCTION

In the early past, the design process of roundabouts was difficult to develop because design, analysis, drawing and evaluation were performed by an iterative process which required great effort in time and calculation. However, in today's fast paced environment, designer requirements (less time, effort and data storage) are fulfilled by enhancements in computerized technology, which provides an opportunity for the designer or researcher to develop better techniques and software for roundabout design and analysis instead of using an iterative process. The optimization technique is one of the modern programming methods used to determine decision variables (entry width, inscribed circle diameter, central island diameter, circulatory width, entry and exit radii), subject to certain constraints (site and geometric design standards) for a given objective function, which includes design consistency and average intersection delay to satisfy the design requirements of roundabouts. The object function deals with safety and operational performance in terms of average intersection delay, which depends on entry and exit capacity or flow at roundabouts approaches. The application of a given developed model is limited to dual-lane roundabouts with four legs, where entry and consecutive exit legs are separated at a right-angle. This chapter describes the design modeling process of right-angle dual-lane roundabouts.

5.2 EXISTING DESIGN METHODOLOGIES

Roundabout designing is difficult because it involves several elements of design which are interrelated. Two methods which involve the iterative process to achieve the best design are used for roundabouts are as follows:

5.2.1 Manual method

This method includes the drawing of a preliminary, proposed geometric design of a roundabout for a particular situation, and then checking its safety, capacity and operational

performance benefits pertaining to one of the approved geometric guidelines for the roundabout's design.

5.2.2 Computer aided method

Different transportation agencies use different design guidelines and software. A designer selects the geometric parameters that may achieve the best design on the basis of experience or reference to current design guidelines as discussed in Chapter 3 and 4. The computer aided method involves the use of proposed geometric design parameters data (entry width, inscribed circle diameter, central island diameter, circulatory width, and entry and exit radii) and expected traffic data in one of the available roundabout design softwares, and then checking its safety, capacity and operational performance benefits with respect to one of the approved geometric guidelines for the roundabouts design. These parameters will be modified many times as needed, and the design process will be repeated until the acceptable design is achieved, but still, this may not be the optimum design solution for a particular site with given site constraints.

5.2.3 Optimization modeling technique

An optimization model has been developed for only single-lane roundabouts. Dual-lane roundabouts design requires a large number of calculations as compared to single-lane roundabouts; therefore, the design is best performed by an optimization computer program. An optimization technique is one of the modern programming techniques for geometric design of roundabouts, which is used to determine decision variables (entry width, inscribed circle diameter, central island diameter, circulatory width, entry and exit radii), subject to certain constraints (site and geometric design standards) for a given objective function which includes design consistency and average intersection delay to satisfy the design requirements of roundabouts. The object function deals with safety and operational performance in terms of average intersection delay, which depends on entry and exit capacity or flow at roundabout approaches. LINGO is the optimization software which permits a designer to input a rapidly model formulation with the available range of geometric data, with site and geometric constraints and traffic data, solve it, evaluate the accuracy or suitability of the design based on the model

outcomes as shown in Figure 5.1. The global optimum solution is the best solution for given constraints and objective of design.

Feasible solution; satisfies all geometric or non-geometric constraints simultaneously, but does not necessarily maximize the objective function. It depends solely on the constraints, not on objective function.

Non-Feasible Solution; Two or more constraints that cannot be simultaneously satisfied.

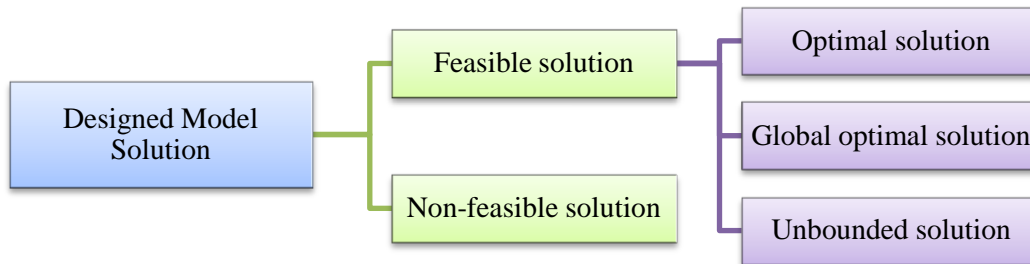


Figure 5.1 Possible LINGO model outcomes

If a feasible solution has been found, then the procedure attempts to find an optimal or global optimal solution. If the unbounded solution has been found, then a termination occurs. A more realistic conclusion is that an important constraint has been omitted or the formulation contains a critical typographical error. Lingo-13 extended software is used in this thesis for dual-lane roundabout geometric design modeling solutions.

5.3 FEASIBILITY STUDY FOR ROUNDABOUT DESIGN

A feasibility study should be arranged for all roundabouts. The main task is to decide in the assessment whether or not a roundabout is the most suitable intersection regulatory form for a particular intersection. It can be organized as follows;

Site conditions: This includes descriptive details on the corridor, and a sketch of existing conditions (land-use, access, existing right-of-way and constraints) in the vicinity of the intersection which may affect the location and design of a roundabout.

Safety assessment: Safety assessment includes an analysis of a crash for which data is available and a comparison of statewide averages. It is recommended that a crash diagram be prepared which shows the crash types and the travelling direction of each car.

Alternate sketches: This includes sketches of all design alternatives being considered.

Operational analyses: This includes peak hour traffic operational analyses (volume-to-capacity ratio, average control delay, level of service, and 95th percentile queue) for each design substitute, for current and design years. Evaluate the performance of each alternate and identify adequate performance intersection type.

Cost comparison: Cost comparisons should be prepared with consideration of aids relating to safety, operational, and environmental factors, and significant costs relating to construction, required right-of-way, operations and maintenance for multiple alternates, which provide adequate operational performance.

Alternative selection: The alternative selection includes a brief summary of the findings, followed by recommendation of the most favorable alternative.

Conceptual roundabout design with layout: This design should include the size and location of the roundabout with alignment and arrangement of approaches. Geometric and performance checks are required with chief geometric elements including circulatory roadway, Center Island, Splitter Island and truck aprons should be include.

5.4 REQUIRED DATA FOR OPTIMIZATION MODEL

Based on a feasibility study, expected traffic flow, and available site space, the categories of roundabout are determined. For the development of an optimization model, three kinds of data are required.

5.4.1 Site design parameter ranges

The range of design parameters can be defined from an Arial photograph using GIS software such as ArcView. We can measure from the site the ranges of approximate decision variables (entry width, inscribed circle diameter, central island diameter, approach half width and flare length) with the help of Google satellite images. These ranges include the minimum and maximum measurement values for that specific element. If the intersection is between the populated areas where right-of-way is constrained, the maximum inscribed circle diameter $D_{c_{max}}$ is calculated between the available spaces of road curb, as illustrated in Figure 7.1. On other locations where right-of-way is not a constrained, the designer selects the $D_{c_{max}}$ value based on experience, as illustrated in Figure 7.2. The minimum inscribed circle diameter $D_{c_{min}}$ depends on

the design vehicle. Therefore, inscribed circle diameter D_c should be constrained, as shown in Equation [5.1], to lie between both minimum and maximum values for the best design.

$$D_{cmin} \leq D_c \leq D_{cmax} \quad [5.1]$$

Similarly, maximum entry $E_{wi_{max}}$ and exit $E_{xwi_{max}}$ widths can be calculated from the centerline, as illustrated in Figure 7.2. The minimum entry width $E_{wi_{min}}$ and exit width $E_{xwi_{min}}$ are dependent on the minimum two-lane width of a dual-lane roundabout. During the modeling process, it was assumed that entry width at leg-1 was equal to the exit width at leg-3, and therefore, entry and exit constraints are displayed in Equations [5.2] and [5.3], respectively.

$$E_{wi_{min}} \leq E_{wi} \leq E_{wi_{max}} \quad [5.2]$$

$$E_{xwi_{min}} \leq E_{xwi} \leq E_{xwi_{max}} \quad [5.3]$$

If needed, provide flare length range based on site condition should be provided. Flaring the approach from one lane to two lanes can result in double the approach capacity without requiring a dual-lane roadway prior to the roundabout. Increasing the effective flare length F_i or entry width E_{wi} will increase the capacity but decrease the path definition and increase the speed variance. Equations [5.5] and [5.4] represent the entry width with and without flare length, respectively, at approach leg i . The approach half width for leg i represents with W_i , in meters.

$$E_i = W_i \quad [5.4]$$

$$E_i > W_i \quad [5.5]$$

Equation [5.6] indicates the effective flare length constraint. The circulatory width is the function of maximum entry width at roundabout approaches, and therefore, it needs to constrain, as shown in Equation [5.8].

$$F_{imin} \leq F_i \leq F_{imax} \quad [5.6]$$

$$E_{max} = Max[E_i] \quad [5.7]$$

$$E_{wmin} < C_w < [1.2E_{wmax}] \quad [5.8]$$

The central island radius R_{ic} is the function of inscribed circle diameter and circulatory width; therefore Equation [5.9] constrains the central island radius. In some cases, maximum queue length can be used as a constraint so that the queue length of each approach at inner and

outer lanes $Q_{i[i,o]}$ should be less than the maximum queue length Q_{max_i} , at that approach as indicated in Equation [5.10].

$$R_{ic} = \frac{[D_c - 2 * C_w]}{2} \quad [5.9]$$

$$Q_{i[i,o]} \leq Q_{max_i} \quad [5.10]$$

5.4.2 Traffic data

For operational performance, we need to collect the AM and PM peak hour traffic data of all the traffic movements at selected intersections. Operational performance ensures that the proposed design model has the best level of performance in terms of minimum delay and queue. It also ensures that volume capacity ratio VC for inner lane VC_{I_i} and outer lane VC_{O_i} at each approach does not exceed the limited value of 0.85 defined by FHWA. At each approach of a roundabout in each lane, it is necessary to calculate the entry flow separately with respect to arrangement of that approach traffic's movements. It is assumed that at each approach, the inner lane deals with left turn traffic QL_i and U-turn traffic QU_i volumes, while the outer lane in a dual-lane roundabout entry approach deals with through Qt_i and right turn Qr_i traffic volumes. Therefore, the entry flow for the inner lane is the sum of U-turn and left turn traffic movements at approach, as indicated in Equation [5.11], whereas Equation [5.12] represents the outer lane flow.

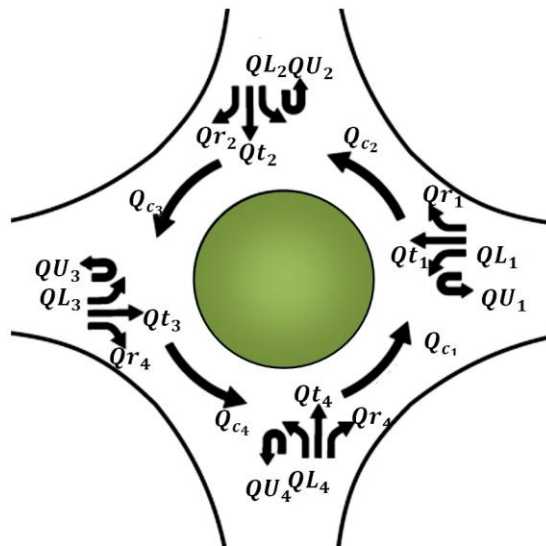


Figure 5.2 Roundabout geometry for traffic flow

$$Qe_{I_i} = QU_i + QL_i \quad [5.11]$$

$$Qe_{O_i} = Qr_i + Qt_i \quad [5.12]$$

$$Q_{C_i} = QU_{i+1} + QU_{i+2} + QL_{i+2} + QU_{i+3} + QL_{i+3} + Qt_{i+3} \quad [5.13]$$

The conflicting flow at the front of each approach is required for capacity analysis as described in

Figure 5.2. Right turn traffic is not included in the circulating volume because vehicles exit before next approach entrance. Therefore, the entry flow rate at the roundabout entrance in an outer and inner lane is affected by circulating flow rate Q_{C_i} as indicated in Equation [5.13]. Equations [5.11], [5.12] and [5.13] are the general forms of entry flow rate at inner and outer lanes and circulatory flow rate at front of that entry approach leg at roundabout, where [i = 1,2,3,4] represents the roundabout approach legs. Traffic data are collected from the site and used in the model. All types of counted site traffic data need multiplication with a peak hour factor, and then must be converted into passenger car equivalent (pec/hr) using conversion factors. Qe_{I_i} , Qe_{O_i} and Q_{C_i} should be in passenger car equivalent (pec/hr).

5.4.3 Side friction factor

(Rahmi Akcelik, 2002); (Akçelik, 2003) use the following formula for estimating operating speed:

$$f_{SLV} = 0.3 - 0.00084\sqrt{M_{vLV}} \quad [5.14]$$

$$f_{SHV} = 0.3 - 0.00084\sqrt{M_{vHV}} \quad [5.15]$$

$$f_s = (1 - P_{HV})f_{SLV} + (P_{HV})f_{SHV} \quad [5.16]$$

Equations [5.14], [5.15] and [5.16] are used to calculate the side friction factor of light vehicles, heavy vehicles, and combined vehicles, where $M_{vLV}=1400$ and $M_{vHV}=11000$ are the average vehicle masses for light and heavy vehicles in kilograms. f_s represent the average side friction factor, and P_{HV} is the percentage of heavy vehicles at a roundabout (in decimals).

5.5 VEHICLE PATH MODELING AT RIGHT-ANGLE ROUNDABOUTS

As discussed in Chapter 4, there are three vehicle paths in a roundabout (right, through and left turn), as illustrated in Figure 5.3, which need analysis while determining vehicle speed. The critical element in roundabout design is the fastest speed path. The fastest speed path is a basic principle of roundabout design to restrict operating speed by deflecting the paths of entering and circulating vehicles. Generally, through movement is the critical fastest path, but in some circumstances it may be a right turn movement. The design speed of a roundabout is determined from the smallest radius along the fastest path which usually occurs on a circulatory roadway. That is the general case and the desirable alignment for dual-lane roundabouts.

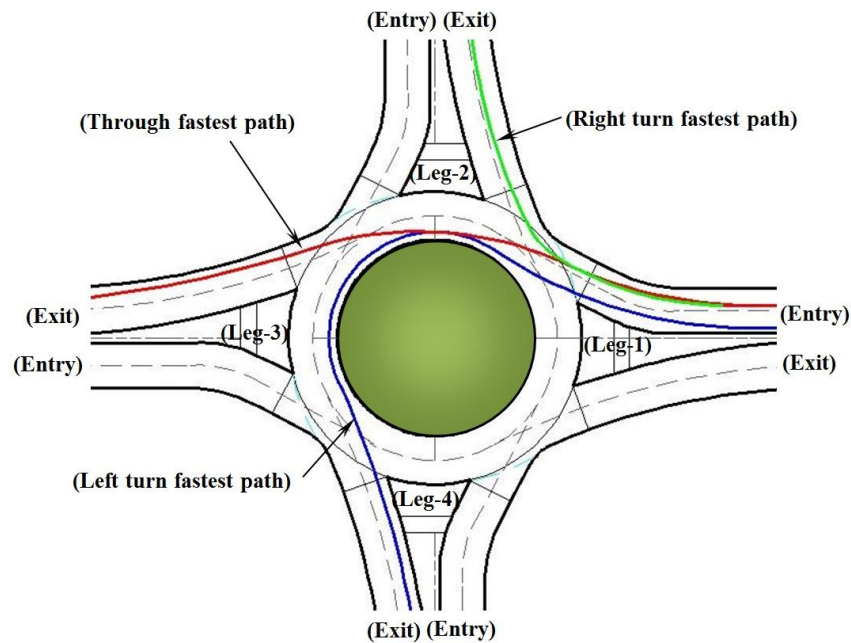


Figure 5.3 Fastest paths curve at right-angle roundabout intersections

5.5.1 Fastest through path radii

The fastest vehicle path through the roundabout is the combination of three reversal curves through entry curve, through circular curve around the central island, and through the exit curve with radii of R_1 , R_2 and R_3 , respectively, as illustrated in Figure 5.4. The central island radius R_{iC} is the function of inscribed circle diameter and circulatory width, as described in Equation [5.9]. The circulatory width is dependent on maximum entry width amongst all the entries at the roundabout, as Equation [5.8] indicates.

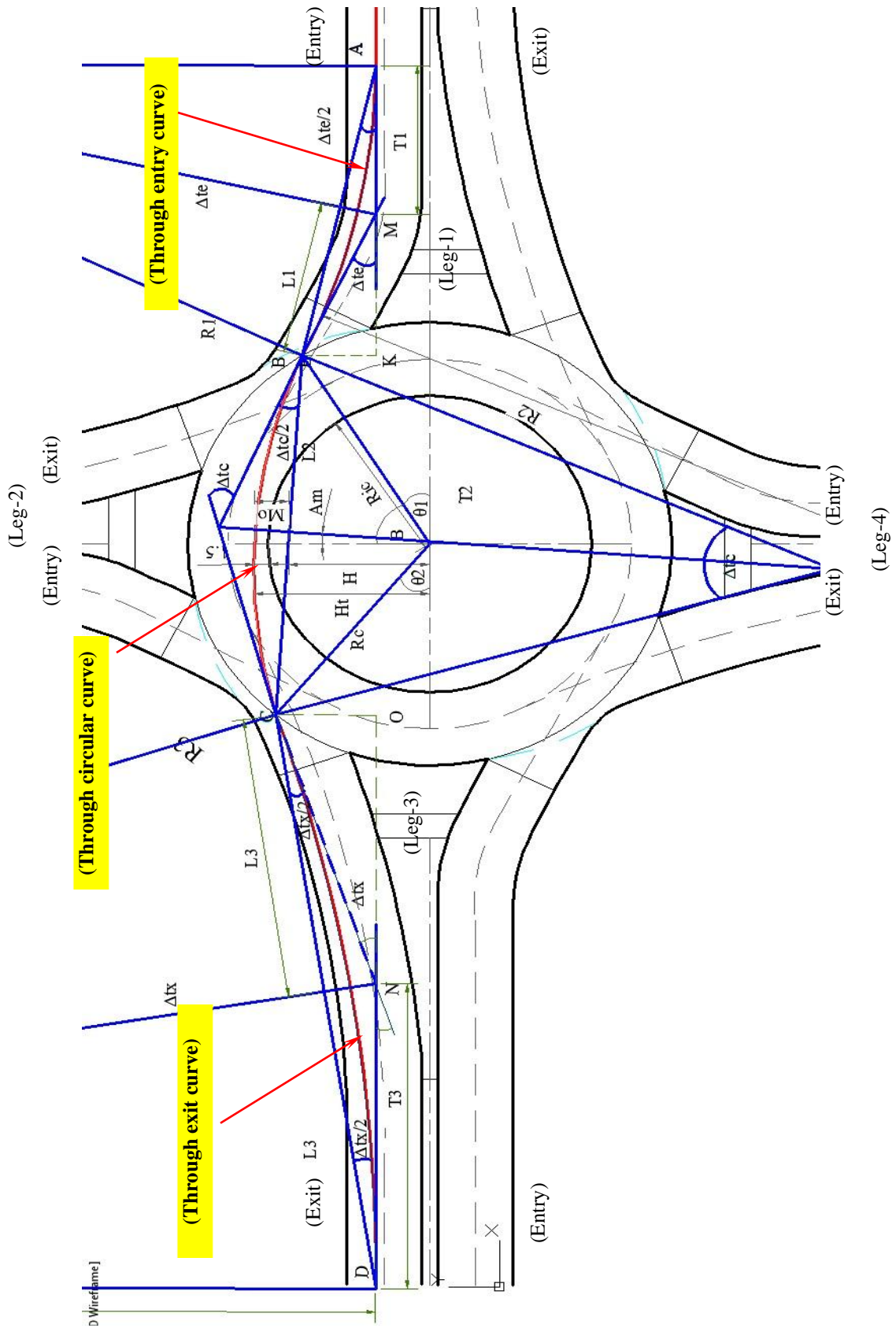


Figure 5.4 Vehicle fastest through path curve at entry, exit and around central island

Therefore, radii of fastest through path are governed by an inscribed circle diameter D_c , circulatory width C_w and central island radius R_{ic} . It was observed during drawing sketches of through entry, circular, and exit fastest paths against different values of inscribed circle diameter, manually as well as by the aid of computerized software AutoCAD, that entry and exit points are not at the same angle as the center of inscribed circle diameter at the yield line, due to different entry and exit geometries at a dual-lane roundabout. The following explanation is provided for through fastest path curve in detail with the help of modeling drawings and equations of each through entry, exit, and around central island path curve separately:

Through path curve around central island

The radius R_2 is calculated with the help of the deflection angle between both ends of through circulatory fastest path arc joining yield line at a distance of 1.5 m from the edge of the curve, whereas the midpoint of an arc maintains the space of 1.5 m from the edge of the central island and length of cord, as demonstrated in Figure 5.5.

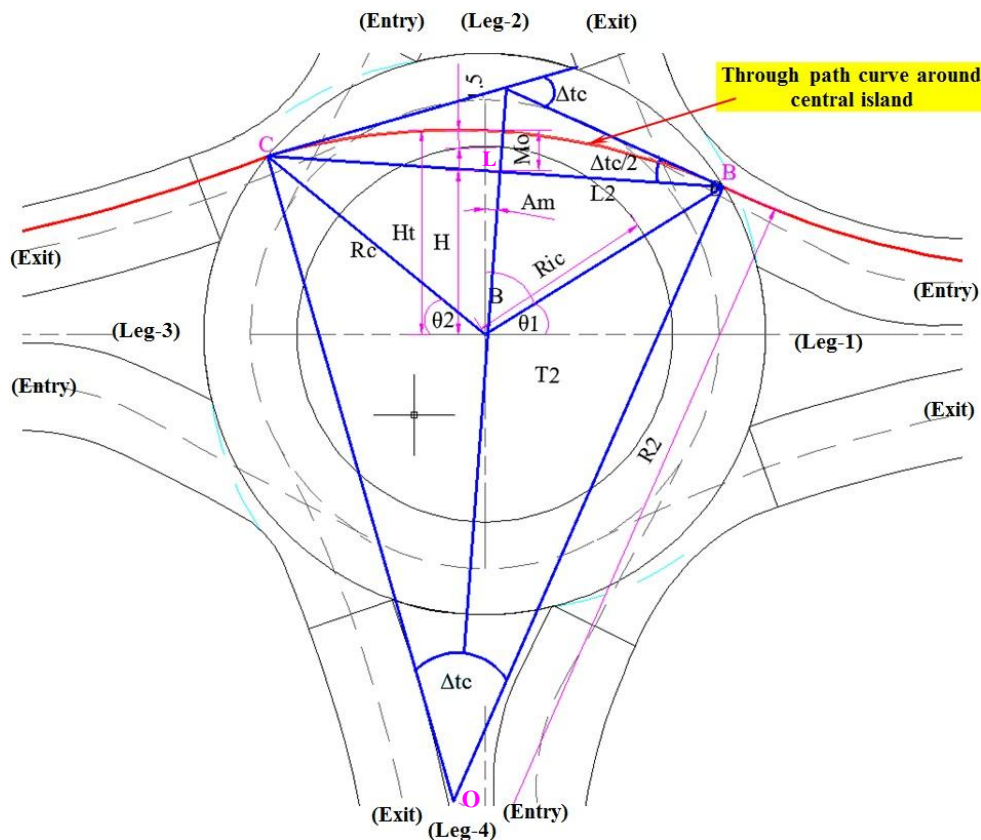


Figure 5.5 Fastest through path curve around Central Island at right-angle roundabout

\bar{H}_t is dependent on the central island radius, whereas \bar{H} depends on the inscribed circle diameter. X_{ai} is the optimization factor used in the modeling with minimum and maximum values. The \bar{M}_o in Equation [5.19] is the mid ordinate; it is the difference between \bar{H}_t and \bar{H} , and these depend on the D_c and R_{ic} . The constraint in Equation [5.20] ensures that the mid-ordinate is in proper position.

$$H = 0.19D_c + X_{ai} \quad [5.17]$$

$$H_t = R_{ic} + 1.52 \quad [5.18]$$

$$M_o = H_t - H \quad [5.19]$$

$$R_{ic} \geq H \quad [5.20]$$

The half cord length \bar{L}_2 and \bar{M}_o can be determined by solving the geometry of the right-angle triangle ΔBOL in

Figure 5.5. The deflection angle of through curve around Central Island Δ_{tc} is calculated by dividing the half cord length by the mid-ordinate, as shown in Equation [5.21].

$$\frac{L_2}{M_o} = \frac{R_2 \left[\sin \left[\frac{\Delta_{tc}}{2} \right] \right]}{R_2 \left[1 - \cos \left[\frac{\Delta_{tc}}{2} \right] \right]} \quad [5.21]$$

This will further be used to calculate the radius of vehicle through path around the Central Island R_2 . It was also observed during the fastest path development process that \bar{L}_2 is the function of D_c , which was fixed through Equation [5.22]. R_2 is the function of D_c and Δ_{tc} and calculated by solving the geometry of right-angle triangle ΔBOL in

Figure 5.5, as shown in Equation [5.23]. Equation [5.23a] uses the value of that radius and calculates the vehicle speed at that curve, which should be less than the maximum speed limit.

$$L_2 = 0.4D_c \quad [5.22]$$

$$R_2 = \frac{L_2}{\left[\sin \left(\frac{\Delta_{tc}}{2} \right) \right]} \quad [5.23]$$

$$V_2 = 11.27 \sqrt{[f_s - 0.02]R_2} \quad [5.23a]$$

Through entry path curve

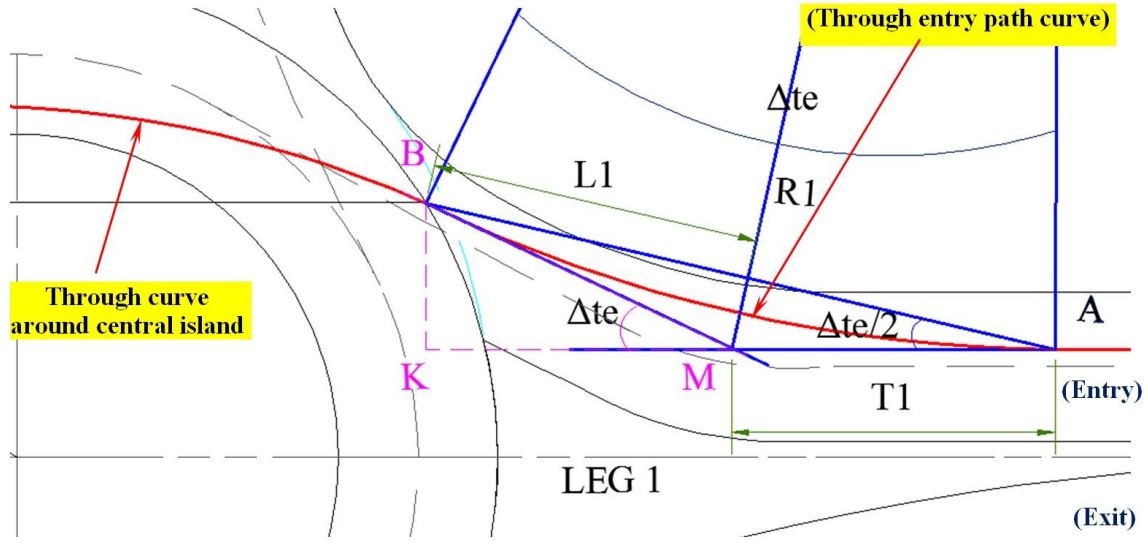


Figure 5.6 Fastest through entry paths curve at right-angle roundabout

Equations [5.24] and [5.25] represent the vertical and horizontal components of the fastest through entry path curve tangent T_{1i} , and it depends on $\theta_{1i}, \theta_{2i}, E_{wi}, \Delta_{tci}$ and D_c . A_{mi} is the mean difference between the entry and exit angles of through curve around Central Island with respect to the center of central island along vertical axis of approach leg i as illustrated in Figure 5.5. It is angular measurement and represented by A_{mi} as indicated in Equation [5.26].

$$\overline{B_i K_i} = [0.5D_c \sin[\theta_{1i}] - 0.5E_{wi} - n] \quad [5.24]$$

$$\overline{K_i M_i} = \frac{\overline{B_i K_i}}{[\tan[\Delta_{tei}]]} \quad [5.25]$$

$$A_{mi} = \left[\frac{\theta_{2i} - \theta_{1i}}{2} \right] \quad [5.26]$$

This is due to different entry and exit geometries at dual-lane roundabouts. The entry curve deflection angle is the sum of the half deflection angle of fastest path through curve around Central Island $\Delta_{tc}/2$ and its mid-point inclination A_{mi} , with the vertical axis of inscribed circle diameter, as shown in Equation [5.27]. The tangent length of fastest through entry path curve T_{1i} as indicated in Equation [5.28] is calculated by solving the geometry of triangle ΔBMK in Figure 5.6; it is used later for calculating half cord length $\overline{L_{1i}}$, as described in Equation [5.29].

$$\Delta_{tei} = \left[\frac{\Delta_{tci}}{2} \right] + A_{mi} \quad [5.27]$$

$$T_{1i} = \sqrt{(B_i K_i)^2 + (K_i M_i)^2} \quad [5.28]$$

$$\overline{L}_{1i} = T_{1i} \cos \left(\frac{\Delta_{tei}}{2} \right) \quad [5.29]$$

Finally, Equation [5.30] gives the radius of entry through path curve R_{1i} . That radius calculates the vehicle speed at that curve which should be less than the maximum speed limit.

$$R_{1i} = \frac{\overline{L}_{1i}}{\sin \left[\frac{\Delta_{tei}}{2} \right]} \quad [5.30]$$

$$V_{1i} = 11.27 \sqrt{(f_s + 0.02) R_{1i}} \quad [5.30a]$$

Through exit path curve;

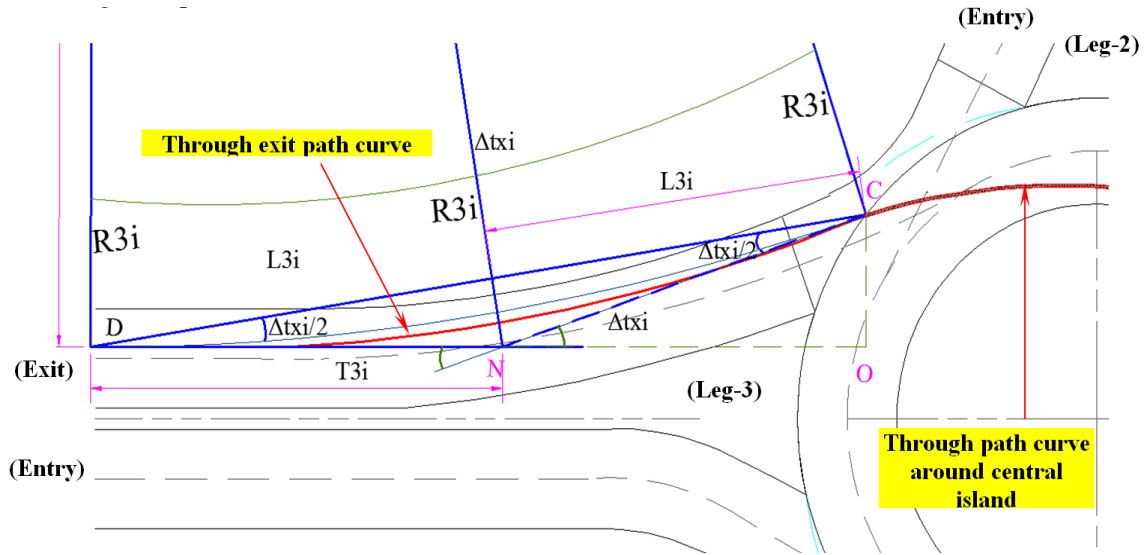


Figure 5.7 Fastest through exit paths curve at right-angle roundabout

Similarly, the exit curve deflection angle $\Delta_{tx[i+2]}$ is the difference between half deflection angle of fastest path through curve around Central Island $\Delta_{tc}/2$ and its mid-point inclination A_{mi} , with the vertical axis of inscribed circle diameter, as shown in Equation [5.31].

$$\Delta_{tx[i+2]} = \frac{\Delta_{tc}}{2} - A_{mi} \quad [5.31]$$

Equations [5.32] and [5.33] represent the vertical and horizontal component of fastest through exit path curve tangent $\bar{T}_{3[i+2]}$, and it depends upon θ_{1i} , θ_{2i} , E_{wi} , Δ_{tci} and D_c .

$$O_{[i+2]}C_{[i+2]} = [0.5D_c\sin[\theta_{2i}] - 0.5E_{wi} - n] + X_{ei} \quad [5.32]$$

$$N_{[i+2]}O_{[i+2]} = \frac{O_{[i+2]}C_{[i+2]}}{\text{Tan}[\Delta_{tx[i+2]}]} \quad [5.33]$$

The tangent length of the fastest through entry path curve $\bar{T}_{3[i+2]}$, as indicated in Equation [5.34], is calculated by solving the geometry of the right-angle triangle ΔCNO as shown in Figure 5.7, which was used later for calculating the half cord length $\bar{L}_{3[i+2]}$, as described in Equation [5.35].

$$\bar{T}_{3[i+2]} = \sqrt{(O_{[i+2]}C_{[i+2]})^2 + (N_{[i+2]}O_{[i+2]})^2} \quad [5.34]$$

$$\bar{L}_{3[i+2]} = \bar{T}_{3[i+2]}\cos\left[\frac{\Delta_{tx[i+2]}}{2}\right] \quad [5.35]$$

Equation [5.36] gives the radius of exit through path curve $\bar{R}_{3[i+2]}$, which further calculates the vehicle speed $V_{3[i+2]}$ at that curve, which should be less than the maximum speed limit.

$$\bar{R}_{3[i+2]} = \frac{\bar{L}_{3[i+2]}}{\sin\left[\frac{\Delta_{tx[i+2]}}{2}\right]} \quad [5.36]$$

$$V_{3[i+2]} = 11.27\sqrt{(f_s + 0.02)\bar{R}_{3[i+2]}} \quad [5.37]$$

$[i+2]$ represents the vehicle exit leg number, whereas i represents the vehicle approach leg number, and its range is $[i = 1, \dots, 4]$ for four legs dual-lane roundabouts. When $(i + 2) > 4$, then subtract 4 from this value to achieve the proper leg number.

The only difference between entry and exit curve geometrics is at the calculation of their deflection angles. For entry curve deflection angle, we need to add the mid-point inclination A_{mi} in the half deflection angle of fastest through path curve around Central Island $\Delta_{tc}/2$. For exit curve deflection angle, however, the mid-point inclination A_{mi} must be subtracted from the half deflection angle of fastest through path curve around Central Island $\Delta_{tc}/2$.

5.5.2 Fastest right turn path radii

The fastest right turn path is a combination of three consecutive curves: right entry curve, right circular curve inside the central island, and the right exit curve with radii of R_4 , R_5 and R_6 , respectively, turning in same direction, as illustrated in Figure 4.18 and Figure 5.8.

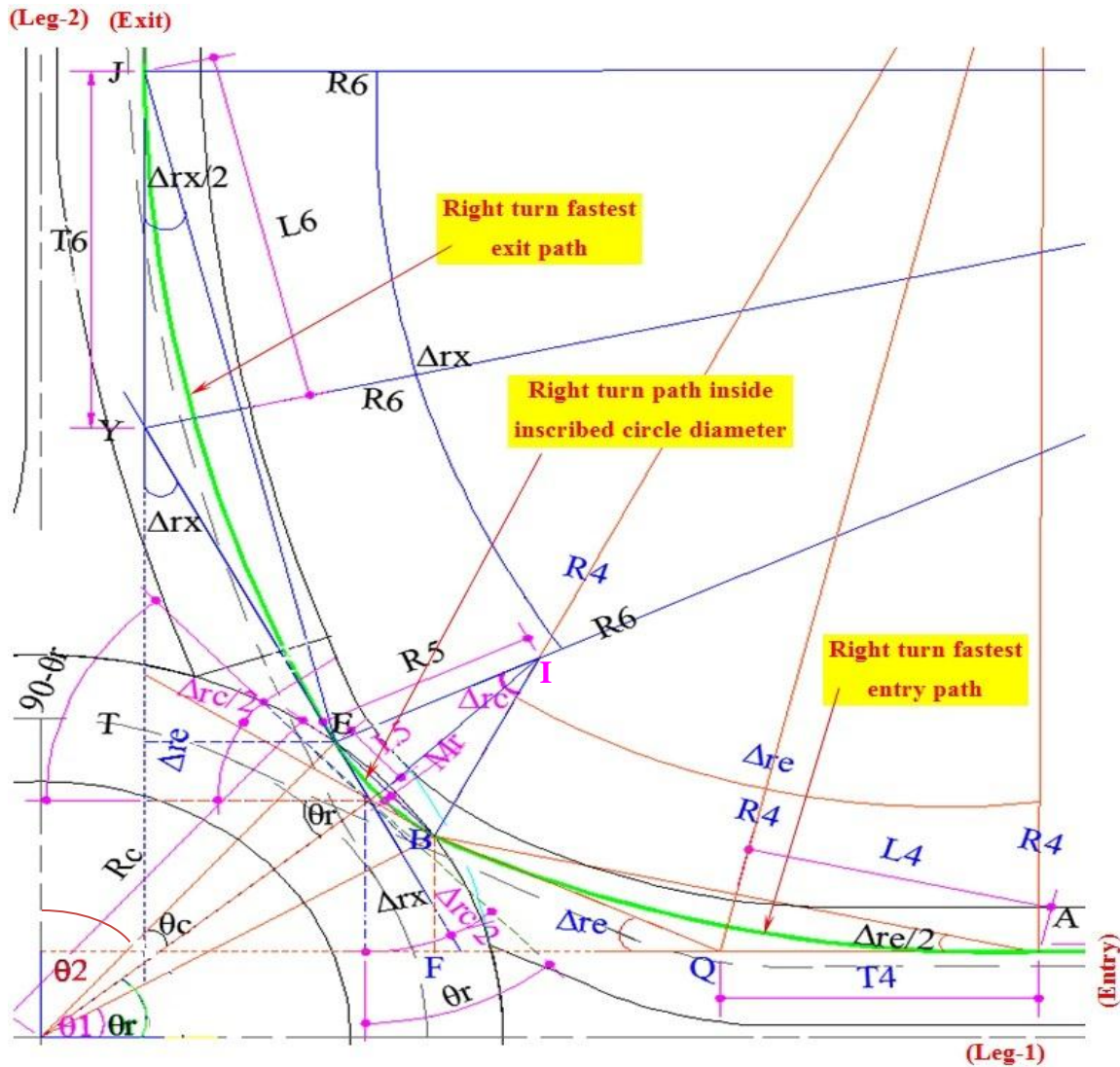


Figure 5.8 Vehicle fastest through path curve at entry, exit and around central island

This is the path created by a vehicle traveling in the outer lane while keeping its sustainable centerline distance of 1 m from the lane marking and 1.5 m from the outer curb line. It also turns in the same direction with different radii at entry and circulatory area, and then takes a safe exit in the next consecutive roundabout approach, as shown in Figure 5.8. The following

section includes details of each right turn curve path at entry, exit, and inside the inscribed circle diameter with the help of modeling drawings and equations.

Right turn path inside inscribed circle diameter

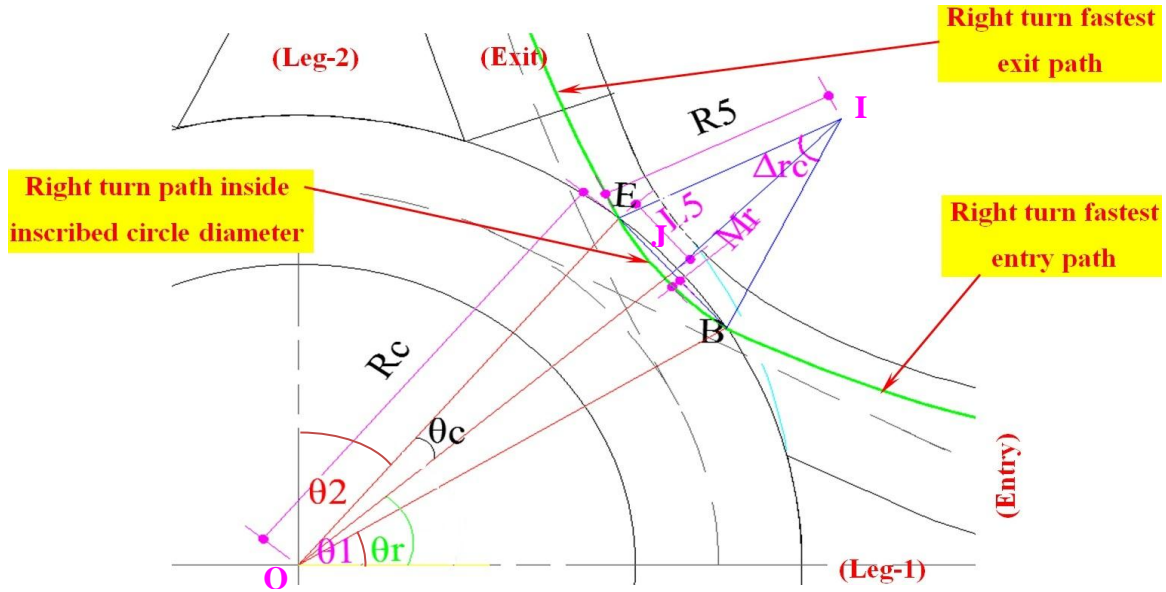


Figure 5.9 Vehicle fastest right turn path curve at inside inscribed circle diameter

The half cord length \bar{L}_{5i} is the function of inscribed circle diameter; therefore a relationship is developed between cord length and inscribed circle diameter, as represented in Equation [5.38].

$$[E_iB_i]^2 - [0.194D_c]^2 = 0 \quad [5.38]$$

$$\bar{L}_{5i} = 0.5E_iB_i \quad [5.39]$$

According to (Mehmood, 2003), the mid-ordinate M_{ri} is quite sensitive to circulatory roadway width. It is also observed when drawing negotiation radii with different combination sets of roundabout geometric data, and an appropriate relation from that drawing is shown in Equation [5.40].

$$M_{ri} = 0.066C_w \quad [5.40]$$

The half cord lengths \bar{L}_{5i} and M_{ri} can be determined by solving the geometry of the right-angle triangle ΔEBI in Figure 5.9. The deflection angle of right turn curve Δ_{rci} is calculated by dividing the half cord length with mid-ordinate, as indicated in Equation [5.41].

$$\frac{L_{5i}}{M_{ri}} = \frac{\sin\left(\frac{\Delta_{rci}}{2}\right)}{1 - \cos\left(\frac{\Delta_{rci}}{2}\right)} \quad [5.41]$$

$$\left[1 - \cos\left(\frac{\Delta_{rci}}{2}\right)\right] \geq 0 \quad [5.42]$$

This will further be used to calculate the radius of right turn vehicle path inside the inscribed circle diameter R_{5i} . This radius further calculates the vehicle speed V_{5i} at that curve, which should be less than the maximum speed limit.

$$R_{5i} = \frac{L_{5i}}{\sin\left(\frac{\Delta_{rci}}{2}\right)} \quad [5.43]$$

$$V_{5i} = 11.27\sqrt{(f_s + 0.02)R_{5i}} \quad [5.44]$$

It is also observed that Δ_{rci} is the function of entry, exit angles with respect to the center of inscribed circle diameter, and right turn entry deflection angle Δ_{rei} . Therefore the length of half cord L_{5i} is the function of D_c and Δ_{rci} . With the increase of D_c , it is observed that there is an increase in Δ_{rci} and similarly, entry and exit yield points of consecutive approaches apart result in an increase of L_{5i} . Equations [5.41] and [5.43] were developed for calculating Δ_{rci} , and R_{5i} , respectively.

Right turn path at entry

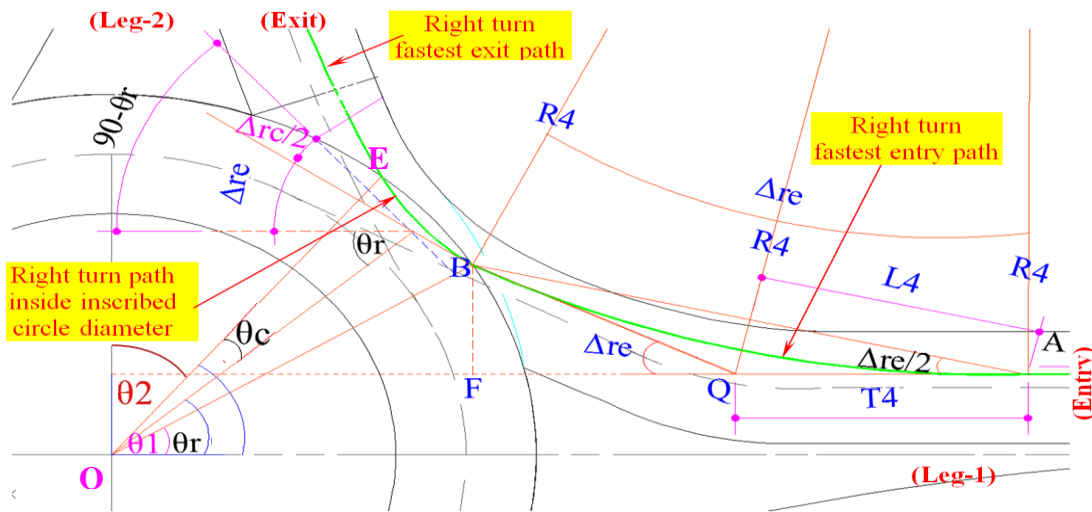


Figure 5.10 Vehicle fastest right turn entry path curve at right-angle roundabout

θ_{ci} is the angle between the mid-point of cord length \overline{EB} and the exit point E of the right- turn curve. It is calculated by solving the geometry of triangle ΔBOE in Figure 5.10.

$$\theta_{ci} = \frac{90 * 0.01745 - [\theta_{2[i+3]} + \theta_{1i}]}{2} \quad [5.45]$$

$$\theta_{ri} = \theta_{ci} + \theta_{1i} \quad [5.46]$$

The deflection angle of the right turn entry curve Δ_{rei} is dependent on the angle θ_{ri} and the half deflection angle of right turn curve in the inscribed circle diameter, as described in Equation [5.47]. Equations, [5.48] and [5.49] represent the vertical and horizontal components of fastest right turn entry curve tangent T_{4i} , and it is dependent on θ_{1i} , E_{wi} , Δ_{rei} and D_c . They are calculated by solving the right-angle triangle ΔBQF in Figure 5.10.

$$\Delta_{rei} = [90 * 0.01745] - \theta_{ri} - \left[\frac{\Delta_{rci}}{2} \right] \quad [5.47]$$

$$B_i F_i = [0.5 D_c \sin[\theta_{1i}] - 0.5 E_{wi} - n] + X_{ci} \quad [5.48]$$

$$F_i Q_i = \frac{B_i F_i}{\left[\tan[\Delta_{rei}] \right]} \quad [5.49]$$

The tangent length of fastest right entry path curve T_{4i} is calculated by the Pythagoras theorem as shown in Equation [5.50]; this further calculates the half cord length L_{4i} and radius of right turn entry curve R_{4i} .

$$T_{4i} = \sqrt{(B_i F_i)^2 + (F_i Q_i)^2} \quad [5.50]$$

$$L_{4i} = T_{4i} \cos \left[\frac{\Delta_{rei}}{2} \right] \quad [5.51]$$

$$R_{4i} = \frac{L_{4i}}{\sin \left[\frac{\Delta_{rei}}{2} \right]} \quad [5.52]$$

This radius R_{4i} further calculates the vehicle speed V_{4i} at that curve, which should be less than the maximum speed limit.

$$V_{4i} = 11.27 \sqrt{[f_s + 0.02] R_{4i}} \quad [5.53]$$

Right turn path at exit

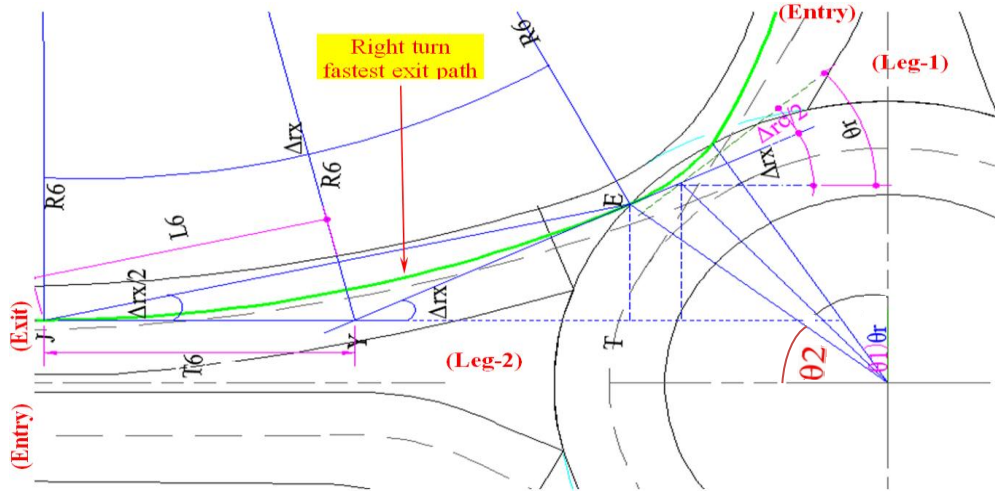


Figure 5.11 Vehicle fastest right turn exit path curve at right-angle roundabout

Equations [5.54] and [5.55] represent the vertical and horizontal components of fastest through exit path curve tangent $\bar{T}_{6[i+1]}$, and depend upon θ_{2i} , E_{wi} , Δ_{rx_i} and D_c .

$$T_{[i+1]}E_{[i+1]} = 0.5D_c \sin(\theta_{2[i+3]}) - 0.5E_{w[i+3]} - n + X_{fi} \quad [5.54]$$

$$T_{[i+1]}Y_{[i+1]} = \frac{T_{[i+1]}E_{[i+1]}}{\tan[\Delta_{rx[i+1]}]} \quad [5.55]$$

The tangent length of fastest right exit path curve $\bar{T}_{6[i+1]}$ as shown in Equation [5.56] is calculated by solving the geometry of the triangle ΔEYT in Figure 5.11. It is used later to calculate the half cord length $\bar{L}_{6[i+1]}$ as described in Equation [5.57].

$$\bar{T}_{6[i+1]} = \sqrt{(T_{[i+1]}E_{[i+1]})^2 + (T_{[i+1]}Y_{[i+1]})^2} \quad [5.56]$$

$$L_{6[i+1]} = \bar{T}_{6[i+1]} \cos\left[\frac{\Delta_{rx[i+1]}}{2}\right] \quad [5.57]$$

Equation [5.58] gives the radius of the fastest right turn exit path curve $R_{6[i+1]}$, and this further calculates the vehicle speed $V_{6[i+1]}$, which should be less than the maximum speed limit.

$$R_{6[i+1]} = \frac{L_{6[i+1]}}{\sin\left[\frac{\Delta_{rx[i+1]}}{2}\right]} \quad [5.58]$$

$$V_{6[i+1]} = 11.27 \sqrt{[f_s + 0.02]R_{6[i+1]}} \quad [5.59]$$

[$i+1$] represents the vehicle exit leg number, whereas i represents the vehicle approach leg number, and its range is [$i = 1, \dots, 4$] for four legs dual-lane roundabouts. When $(i + 1) > 4$, then subtract 4 from this value to achieve the proper leg number.

5.5.3 Fastest left turn path radii

A left turn path contains three turning radii (entry, circulatory and exit). A vehicle enters the inscribed circle diameter parallel to the painted edge of the splitter, while maintaining a centerline distance of 1m from painted edge.

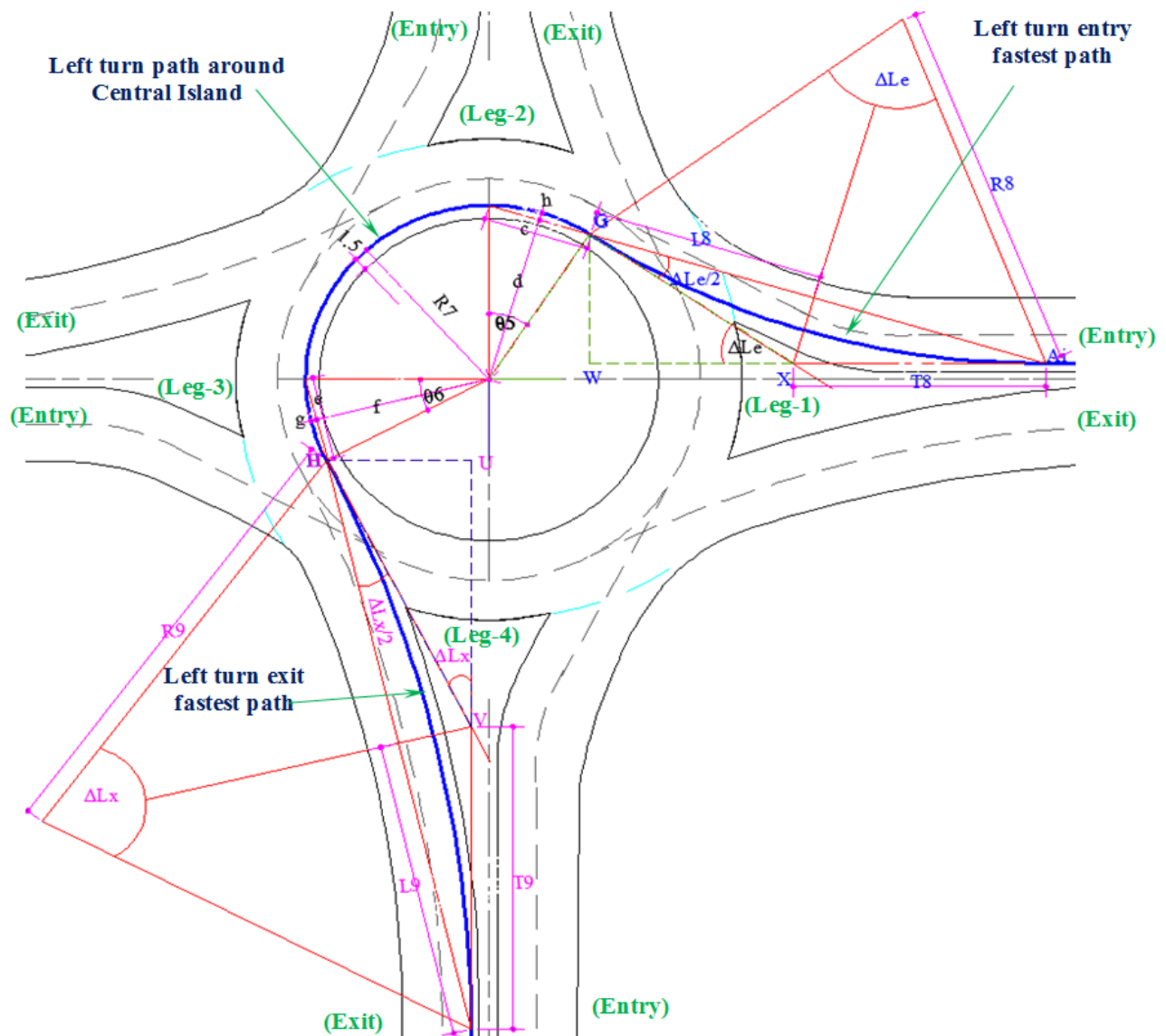


Figure 5.12 Vehicle fastest left turn path curve at right-angle roundabout

It continues its journey in the same direction until it reaches a safe point where it can take a left turn. The geometry of a roundabout is symmetrical, but entry and exit approach designs at a dual-lane roundabout have different criteria; therefore all entry and exit curves will have different radii. The following section includes the details of each left turn curve path at entry, exit, and around the central, with the help of modeling drawings and equations:

Fastest left turn path around central island

The curve *GH* presents the left turn path around Central Island. It depends upon the radius of the Central Island and on the circulatory width.

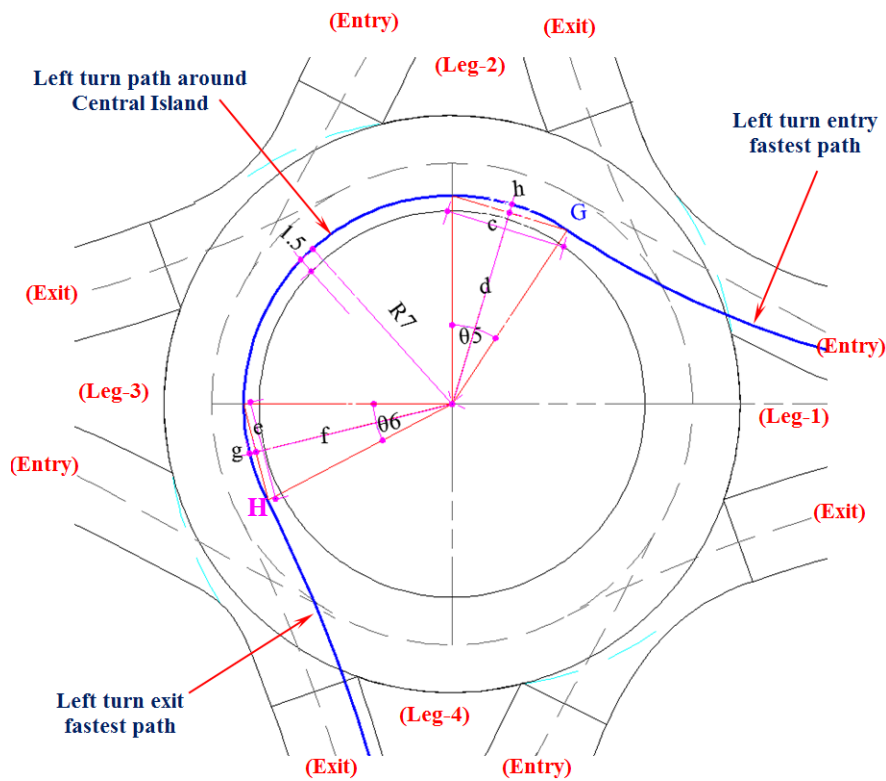


Figure 5.13 Left turn path curve around Central Island at right-angle roundabout

Equation [5.60] calculates the radius of the fastest left turn path around Central Island, while the vehicle maintains 1.5 m of safe centerline distance from the edge of the Central Island, as presented in Figure 5.13. R_{ic} is the radius of the central island and can be influenced by D_C and C_w , as indicated by Equation [5.9].

$$R_7 = R_{ic} + 1.52 \quad [5.60]$$

Fastest left turn entry path

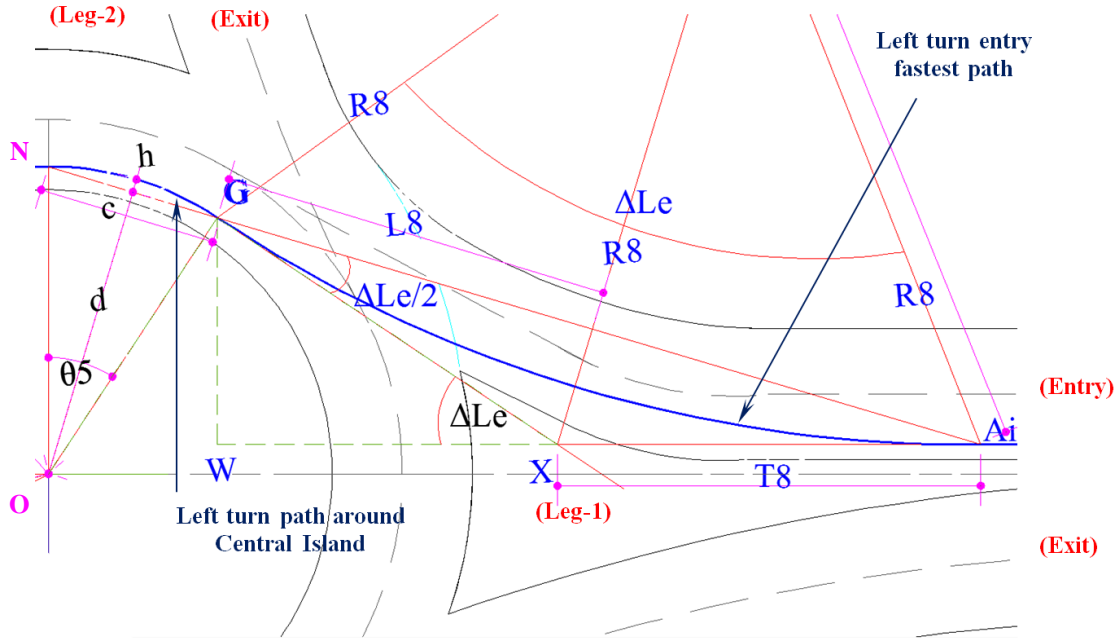


Figure 5.14 Left turn entry path curve at right-angle roundabout

Equations [5.61], [5.62], [5.63] and [5.64] are the result of the geometry of triangle ΔGON through using the Pythagoras theorem as shown in Figure 5.14. θ_{5i} is the function of R_7 , c and d . In fact, as D_c increases there is a perceived reduction in the calculation of cord length c , which results in an increase of length d , as shown in Equation [5.62].

$$c_i = R_7 \left[\sqrt{2 - 2 \cos[\theta_{5i}]} \right] \quad [5.61]$$

$$d_i = \sqrt{(R_7)^2 - \left(\frac{c_i}{2}\right)^2} \quad [5.62]$$

$$h_i = R_7 - d_i \quad [5.63]$$

$$\theta_{5i} = 2 \cos^{-1} \left[\frac{d_i}{R_7} \right] \quad [5.64]$$

Similarly, with the increase of D_c , the value of R_7 also increases. As I described earlier, that increase in D_c results in the reduction of cord length c , but an increase in length d . Therefore an optimization is requisite between R_7 , c and d , which provides us the superlative calculation of θ_{5i} . This θ_{5i} value is later used in Equation [5.65] for calculating the vertical component of the

left entry curve tangent G_iW_i . It depends upon θ_{5i} and the radius of left turn curve around the central island R_7 . Therefore, G_iW_i is calculated by deducting the value of n from the vertical component of radius R_7 , whereas the $[X_{di}]$ is an optimization variable.

$$G_iW_i = R_7 \cos[\theta_{5i}] - n + X_{di} \quad [5.65]$$

It is also noticed that during left turn entry fastest path development process, the left turn entry radius is the function of the central island radius R_{ic} and W_iX_i is the function of R_{ic} . Therefore a relationship is developed between R_{ic} and W_iX_i through Equation [5.66].

$$W_iX_i = 0.836R_{ic} \quad [5.66]$$

It also observed that the horizontal component of the left turn entry path curve W_iX_i is a function of its deflection angle, which is illustrated through triangle ΔGXW , as shown in Figure 5.11 and defined in Equation [5.66a]. The tangent length of fastest left turn entry path curve T_{8i} , as shown in Equations [5.67] and [5.68], is calculated by solving the geometry of triangle ΔGXW , as shown in Figure 5.11.

$$W_iX_i = \frac{G_iW_i}{[\tan[\Delta_{Lei}]]} \quad [5.66a]$$

$$T_{8i} = \sqrt{(G_iW_i)^2 + (W_iX_i)^2} \quad [5.67]$$

$$T_{8i} = \frac{G_iW_i}{\sin[\Delta_{Lei}]} \quad [5.68]$$

It is used later for calculating the half cord length L_{8i} as described in Equation [5.69]. The radius and vehicle speed at the left turn entry path are calculated from Equations [5.70] and [5.71], respectively.

$$L_{8i} = T_{8i} * \cos\left[\frac{\Delta_{Lei}}{2}\right] \quad [5.69]$$

$$R_{8i} = \frac{L_{8i}}{\sin\left[\frac{\Delta_{Lei}}{2}\right]} \quad [5.70]$$

$$V_{8i} = 11.27\sqrt{[f_s + 0.02]R_{8i}} \quad [5.71]$$

Fastest left turn exit path

It is observed that the connection point H between left turn exit and circulatory curve is a function of C_w and D_c , indirectly a function of the central island radius. Therefore, the value of θ_{6i} depends on C_w and D_c .

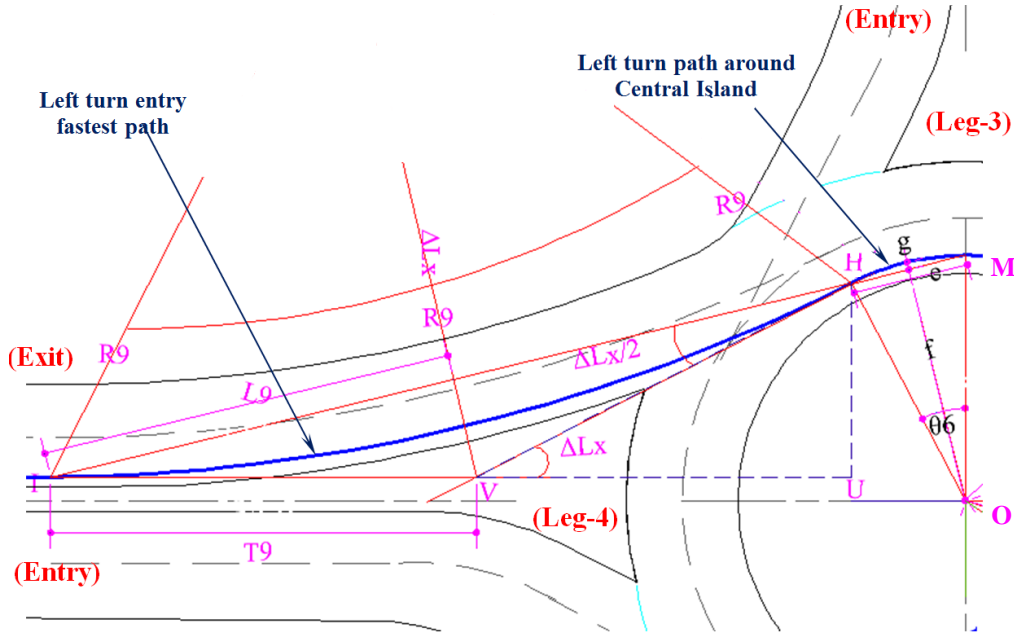


Figure 5.15 Left turn exit path curve at right-angle roundabout

Equations [5.72], [5.73], [5.74] and [5.75] are the result of the geometry of triangle ΔHOM through using the Pythagoras theorem, as shown in Figure 5.15. θ_{6i} is the function of R_7 , e and f . In fact, as D_c increases there is a perceived reduction in the calculation of cord length e , which results in an increase of length f , as shown in Equation [5.73].

$$e_{[i+3]} = R_7 \left[\sqrt{2 - 2 \cos[\theta_{6[i+3]}} \right] \quad [5.72]$$

$$f_{[i+3]} = \sqrt{(R_7)^2 - \left(\frac{e_{[i+3]}}{2}\right)^2} \quad [5.73]$$

$$g_{[i+3]} = R_7 - f_{[i+3]} \quad [5.74]$$

$$\theta_{6[i+3]} = 2\cos^{-1} \left[\frac{f_{[i+3]}}{R_7} \right] \quad [5.75]$$

θ_{6i} is further used in Equation [5.76] for calculating the vertical component $[H_{[i+3]}U_{[i+3]}]$ of the left turn exit curve tangent VH . It is also noticed that during left turn exit fastest path development process, that the horizontal component $[V_{[i+3]}U_{[i+3]}]$ of tangent VH is a function of left turn exit deflection, as shown in Equation [5.77] and R_{ic} , therefore relationships developed with respect to R_{ic} , as illustrated in Equations [5.78].

$$H_{[i+3]}U_{[i+3]} = R_7 \cos[\theta_{6[i+3]}] - n \quad [5.76]$$

$$V_{[i+3]}U_{[i+3]} = \frac{H_{[i+3]}U_{[i+3]}}{\left[\tan[\Delta_{Lx[i+3]}] \right]} \quad [5.77]$$

$$V_{[i+3]}U_{[i+3]} = 0.6R_{ic} \quad [5.78]$$

The tangent length of the fastest left turn exit path curve $[T_{9[i+3]}]$ as shown in Equation [5.79] is calculated by resolving the geometry of triangle ΔHVU , as illustrated in Figure 5.15.

$$T_{9[i+3]} = \sqrt{(V_{[i+3]}U_{[i+3]})^2 + (H_{[i+3]}U_{[i+3]})^2} \quad [5.79]$$

This is used later to calculate the half cord length $L_{9[i+3]}$ as described in Equation [5.80]. The radius and vehicle speed at the left turn entry path are calculated from Equation [5.81] and [5.82] respectively.

$$L_{9[i+3]} = T_{9[i+3]} * \cos \left[\frac{\Delta_{Lx[i+3]}}{2} \right] \quad [5.80]$$

$$R_{9[i+3]} = \frac{L_{9[i+3]}}{\sin \left[\frac{\Delta_{Lx[i+3]}}{2} \right]} \quad [5.81]$$

$$V_{9[i+3]} = 11.27 \sqrt{[f_s + 0.02]R_{9[i+3]}} \quad [5.82]$$

$[i+3]$ represents the vehicle exit leg number, whereas i represents the vehicle approach leg number, and its range is $[i = 1, \dots, 4]$ for four legs dual-lane roundabouts. When $(i + 3) > 4$, then we subtract 4 from this value to achieve the correct exit leg number.

5.6 MODEL DEVELOPMENT PROCESS

5.6.1 Define site constraints

To avoid tight entry and exit radii to support reduction in entry and exit paths overlap, therefore, a design constraint indicated in Equation [5.83] is provided. The constraint is for safe movement of design vehicle (WB-50) provided it ensures the safe movement of design vehicle around the roundabout, as indicated in Equation [5.84]. It is necessary to ensure the slowest speed at entry and improves the safety at the roundabouts; therefore, the constraint is provided as indicated in Equation [5.85], and it satisfies the slowest speed at entry and improves the speed consistency.

$$\{[AER_i, AXR_i] \geq R_2\}, \quad \{AXR_{[i+2]} \geq AER_i\} \quad [5.83]$$

$$[R_2, R_{5_i} \text{ and } R_7] \geq 12.5m \quad [5.84]$$

$$[AXV_{[i+1]} \geq V_{5i}], \quad [AXV_i \geq V_2], \quad [V_{9i} \geq V_7] \quad [5.85]$$

It is assumed that the outer lane carries the traffic of right turn and through movements, at entry and exit, whereas the inner lane carries the left turning traffic at entry and exits of approaches. Therefore, we need the average entry radius at the outer lane for calculation of operational measurements at a roundabout. Equations [5.86] and [5.87] represent the average entry and exit radii at the roundabout outer lane.

$$AER_i = \left[\frac{R_{1i} + R_{4i}}{2} \right] \quad [5.86]$$

$$AXR_{[i+2]} = \left[\frac{R_{6[i+2]} + R_{3[i+2]}}{2} \right] \quad [5.87]$$

Similarly for the calculation of consistency measurements at the outer lane, we need average entry and exit velocity at each approach lane. Equations [5.88] and [5.89] represent the average velocity in the outer lanes at leg i at entry and exit of a roundabout.

$$AEV_i = \left[\frac{V_{1i} + V_{4i}}{2} \right] \quad [5.88]$$

$$AXV_{[i+2]} = \left[\frac{V_{6[i+2]} + V_{3[i+2]}}{2} \right] \quad [5.89]$$

5.6.2 Measurement of speed difference (Consistency measure)

Safe negotiable speed

Equation [5.90] represents the safe negotiating speed $V_{j[i]}$ corresponding to safe negotiating radius $R_{j[i]}$ with j vehicle fastest path at approach leg i of a roundabout. f_s is the side friction factor as described earlier., and e is the value of super elevation [+0.02 for entry and exit path and -0.02 for around central island path].

$$V_{j[i]} = 11.27 \sqrt{[f_s \pm e]R_{j[i]}} \quad [5.90]$$

where $[j = 1,2,3,4,5,6,7,8,9]$ and $[i = 1,2,3,4]$. Therefore, all vehicle path speed must be constrained to less than the desired maximum design speed, as shown in Equation [5.91].

$$[V_{ji}] \leq V_{max} \quad [5.91]$$

Relative speed difference

The most opposing points as illustrated in Figure 5.16 are conflicting – consecutive points. The relative difference at each consecutive point is determined as shown in Equations [5.92] to [5.97]

$$AEV_i - V_{2i} - M_{1i} + M_{2i} = 0 \quad [5.92]$$

$$AXV_{[i+2]} - V_{2i} - M_{3i} + M_{4i} = 0 \quad [5.93]$$

$$AEV_i - V_{5i} - M_{5i} + M_{6i} = 0 \quad [5.94]$$

$$AXV_{[i+1]} - V_{5i} - M_{7i} + M_{8i} = 0 \quad [5.95]$$

$$V_7 - V_{8i} - M_{9i} + M_{10i} = 0 \quad [5.96]$$

$$V_{9i} - V_7 - M_{11} + M_{12i} = 0 \quad [5.97]$$

Equations [5.98] and [5.105] show the relative difference at each conflicting points.

$$V_2 - V_7 - M_{13} + M_{14} = 0 \quad [5.98]$$

$$V_2 - V_{5i} - M_{15i} + M_{16i} = 0 \quad [5.99]$$

$$V_{8i} - V_2 - M_{17i} + M_{18i} = 0 \quad [5.100]$$

$$V_{9i} - V_2 - M_{19i} + M_{20i} = 0 \quad [5.101]$$

$$V_{4i} - V_{5i} - M_{21i} + M_{22i} = 0 \quad [5.102]$$

$$V_{6i} - V_{5i} - M_{23i} + M_{24i} = 0 \quad [5.103]$$

$$V_{8i} - V_{9[i+1]} - M_{25i} + M_{26i} = 0 \quad [5.104]$$

$$V_{4i} - V_2 - M_{27i} + M_{28i} = 0 \quad [5.105]$$

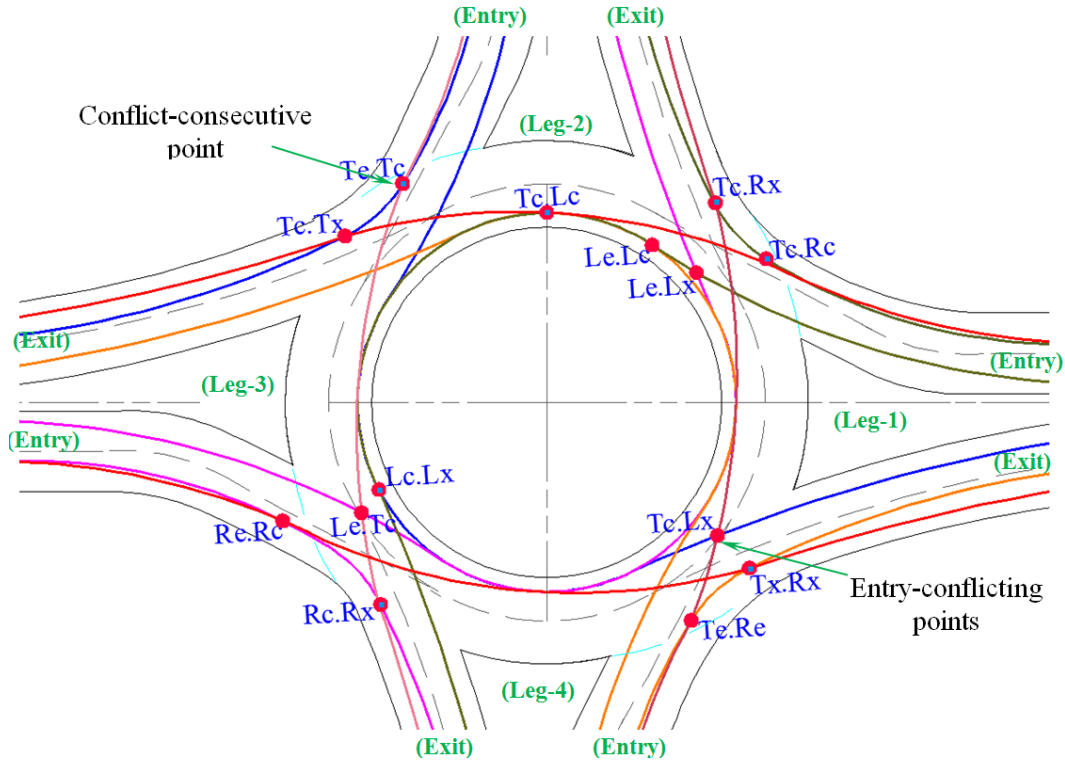


Figure 5.16 Conflicting points at right-angle dual-lane roundabout

where;

- Te.Tc = Through entry- through circular conflict
- Tc.Tx = Through circular- through exit conflict
- Lc.Lx = Left turn circular- left turn exit conflict
- Re.Rc = Right turn entry- right turn circular conflict
- Rc.Rx = Right turn circular – right turn exit conflict
- Le.Tc = Left turn entry – through circular conflict
- Te.Re = Through entry – right turn entry conflict

- Tx.Rx = Through exit- right turn exit conflict
Tc.Lx = Through circular- left turn exit conflict
Le.Lx = Left turn entry-left turn exit conflict
Le.Lc = Left turn entry- left turn circular conflict
Tc.Lc = Through circular- left turn circular conflict
Tc.Rc = Through circular- right turn circular conflict
Tc.Rx = Through circular- right turn exit conflict

where M_{1i} and M_{2i} in eq. [5.92] are additional variables used because the speed difference may be positive or negative (and similarly for M_{3i} , M_{4i} , and so on). The term i , represents the approach leg number at roundabout and it range from 1 to 4 for dual-lane roundabouts. For speed consistency, the objective function of the model will minimize the M_{SD} . Therefore, Equations [5.92] to [5.105] are used to calculate the relative speed difference at all conflicting points.

5.6.3 Measurement of average intersection delay (Operational measures)

The average intersection delay controls the operational measure, and therefore we need an objective function which minimizes the average intersection delay $DATI$. In a dual-lane roundabout, the flow is in both lanes, so a proper lane configuration is required for best operation. In the present case, the outer lane holds through and right turn traffic flow, while the inner lane holds only left turn flow and U-turn flow. This type of configuration reduces the number of crashes at an intersection. Equation [5.106] represents the entry capacity $C_{ei[l,o]}$ of inner and outer lanes at each approach of a dual-lane roundabout, as described in Chapter 3.

$$C_{ei[l,o]} = K_{i[l,o]} [F_{ei} - F_{ci} Q_{ci}] \quad [5.106]$$

The constant F_{ci} is the slope of capacity equation and depends on Dc .

$$F_{ci} = 0.21 \left\{ 1 + \frac{0.5}{1 + \text{Exp} \left[\frac{Dc - 60}{10} \right]} \right\} \left\{ 1 + 0.2 \left[W_i + \frac{E_{wi} - W_i}{1 + 2S_i} \right] \right\} \quad [5.107]$$

F_{ei} is the capacity equation intercept, which holds the effect of sharpness of flare. K_{oi} depends on the entry angle. 30° is the best entry angle, and therefore, for best geometry, a range

of P_i in degree is used as a constraint. All angles including θ_i are used in radian for actual modeling of a roundabout design, but for capacity analysis it should be in degree.

$$F_{ei} = 303 \left\{ 0.5W_i + \frac{0.5[E_{wi} - W_i]}{[1 + 2S_i]} \right\} \quad [5.108]$$

$$S_i = \frac{1.6[E_{wi} - W_i]}{F_i} \quad [5.109]$$

$$K_{oi} = 1.151 - [0.00347P_i] - \left[\frac{0.978}{AER_i} \right] \quad [5.110]$$

$$K_{Ii} = 1.151 - [0.00347P_i] - \left[\frac{0.978}{R_{8i}} \right] \quad [5.111]$$

$$BND(0.9, K_{i_{[l,o]}}, 1.1) \quad [5.112]$$

In the optimization model, the reduction factor P_{ei} is the pedestrian effect on capacity; it is multiply by the entry capacity of each approach to obtain the effective entry capacity $C_{eei_{[l,o]}}$.

$$C_{eei_{[l,o]}} = C_{ei_{[l,o]}} P_{ei} \quad [5.113]$$

The volume to capacity ratio $VC_{i_{[l,o]}}$ of inner and outer lanes at each approach of a dual-lane roundabout is calculated as shown in Equation [5.114].

$$VC_{i_{[l,o]}} = \left[\frac{Qt_{i_{[l,o]}}}{C_{eei_{[l,o]}}} \right] \quad [5.114]$$

QT_{i_o} , QT_{i_I} and Qe_i as shown in Equations [5.115], [5.116] and [5.117] and are the entry flows at outer lane, inner lane, and total entry flow at each approach of a roundabout, respectively.

$$QT_{i_o} = Qt_i + Qr_i \quad [5.115]$$

$$QT_{i_I} = QL_i \quad [5.116]$$

$$Qe_i = QT_{i_o} + QT_{i_I} \quad [5.99]$$

$De_{i_{[l,o]}}$ is the control delay at each approach in each entry lane of roundabout calculated by Equation [5.118].

$$De_{i_{[I,o]}} = \frac{3600}{C_{eei_{[I,o]}}} + 900T_p \left[VC_{i_{[I,o]}} - 1 + \sqrt{\left[VC_{i_{[I,o]}} - 1 \right]^2 + \frac{3600VC_{i_{[I,o]}}}{450T_p C_{eei_{[I,o]}}} \right] \quad [5.118]$$

The total delay $DeT_{[I,o]_i}$ and average intersection delay $[DATI]$ at a roundabout are calculated by using Equations [5.119] and [5.120], respectively. “I” is the inner lane and “o” is the outer lane at approach legs $[i = 1 \dots \dots \dots 4]$ at a dual-lane roundabout.

$$DeT_{[I,o]_i} = De_{[I,o]_i} * QT_{[I,o]_i} \quad [5.100]$$

$$DATI = \frac{\sum_{i=1}^4 [DeT_{[I,o]_i}]}{\sum_{i=1}^4 Qe_i} \quad [5.101]$$

When $(i + 1) > 4$, then subtract 4 from this value to achieve the correct approach leg number.

Average queue length measurement

Queue length is an important performance check because it may block traffic at the intersection. For design purposes, as discussed in Chapter 3, the 95th percentile queue length $Q_{i_{[i,o]}}$ during peak hour time used is shown in Equation [5.121].

$$Q_{i_{[i,o]}} = 900T_p \left[VC_{i_{[i,o]}} - 1 + \sqrt{\left[VC_{i_{[i,o]}} - 1 \right]^2 + \frac{3600VC_{i_{[i,o]}}}{450T_p C_{eei_{[i,o]}}} \right] \left[\frac{3600}{C_{eei_{[i,o]}}} \right] \quad [5.102]$$

A constraint is used to ensure that the 95th percentile queue length should be less than the maximum expected queue length based on site conditions, as shown in Equation [5.122].

$$Q_{i_{[i,o]}} \leq Q_{max_i} \quad [5.103]$$

A constraint is used to limit the degree of saturation to ensure an unsaturated condition for the given roundabout design, as shown in Equation [5.123].

$$VC_i \leq VC_{max} \quad [5.104]$$

Therefore, the Equations from [5.106] to [5.123] are used in optimization models for measurements of the operational performance of dual-lane roundabout intersections.

5.6.4 Define an multi-objective function

Multi-objective optimization (or multi-objective programming or "pareto optimization"), also known as multi-criteria or multi-attribute optimization, is the process of simultaneously optimizing two or more conflicting objectives subject to certain constraints. A single aggregate objective function (AOF) as shown in Equation [5.124] is constructed in this model for finding a solution to a multi-objective optimization problem. This is an intuitive approach to solving the multi-objective problem. The basic idea is to combine all of the objectives into a single objective function, called the AOF, such as the well-known weighted linear sum of the objectives. This objective function is optimized subject to technological constraints specifying how much of one objective must be sacrificed, from any given starting point, in order to gain a certain amount regarding the other objective. Often the aggregate objective function is not linear in the objectives, but rather is non-linear, expressing increasing marginal dissatisfaction with greater incremental sacrifices in the value of either objective. Furthermore, sometimes the aggregate objective function is additively separable, so that it is expressed as a weighted average of a non-linear function of one objective and a non-linear function of another objective. Then the optimal solution obtained will depend on the relative values of the weights specified. The weighted sum method, like any method of selecting a single solution as preferable to all others, is essentially subjective, in that a decision manager needs to supply the weights. Moreover, this approach may prove difficult to implement if the Pareto frontier is not globally convex and/or the objective function to be minimized is not globally concave.

$$Min = \alpha M_{SD} + (1-\alpha)DATI \quad [5.105]$$

The main purpose of consistency limit is to minimize mean speed difference M_{SD} , and to minimize the average intersection delay $[DATI]$ as shown in Equation [5.124]. M_{SD} , represents the mean speed difference ranges from (6-12) mph. $[\alpha]$, is the weighting factor ranges from (0 to

1). At [$\alpha= 0$] objective function minimize the average intersection delay; while at [$\alpha= 1$] the mean speed difference will be minimized.

5.7 SUMMARY

This chapter describes existing design methodology for modeling of dual-lane roundabouts, its feasibility study for design and the requirement of data for designing purpose. This chapter can explain modeling procedures for right-angle roundabouts. It also describes the model development process based on the site constraints, consistency measurements (safe negotiable speed and relative speed difference) and operational measures (average intersection delay and queue length) and an objective function.

CHAPTER 6 : OPTIMIZATION MODEL DEVELOPMENT: DUAL-LANE SKEWED-ANGLE ROUNDABOUTS

6.1 INTRODUCTION

Conventional forms of traffic control are often less efficient than roundabouts at intersections with skewed-angles. In right-angle roundabouts, modeling the fastest path is simpler due to its symmetrical properties. Only the vehicle paths pertaining to one entry approach must be modeled, and then the same model can be applied to the other approaching vehicle paths. For skewed-angle roundabouts, the calculations are more complex. To determine the speed through the roundabout, one needs to model the vehicle's fastest paths (right, through and left), turns pertaining to both consecutive entry and exit (skewing away and skewed toward the driver), and approaches which intersect each other at some angle other than 90° . Skewed-angles ranging from 70° to 110° are selected for modeling standards (TAC , 2007). Generally, through movement is the critical fastest path, but in some circumstances it may be a right turn.

6.2 SKEWED-ANGLE ROUNDABOUTS

Highly skewed intersection angles often require significantly larger inscribed circle diameters to achieve the speed objectives. Designing the approaches at perpendicular or near-perpendicular angles generally results in relatively slow and consistent speeds for all movements. For low speed urban roundabouts where large trucks are not present, it may be acceptable to allow larger intersection angles provided the entry curvature is sufficiently tight to ensure low entry speeds. At skewed-angle roundabouts with consecutive approaches skewed away the driver, the fastest right turn path deals with higher speeds at entry and exit, and larger radii of the inscribed circle. When the approach is skewed towards the driver, the fastest right turn paths have slower speeds at entry and exit, and smaller inscribed circle radii. The design speed of a roundabout is determined using the smallest radius along the fastest path.

This chapter deals with the modeling process of skewed-angle, dual-lane roundabouts. As discussed earlier, skewed-angle intersections are designed using two types of approaches depending on whether the path is skewed away from or towards the driver, as illustrated in Figure 6.1. Therefore, in this chapter two sub-models will be developed.

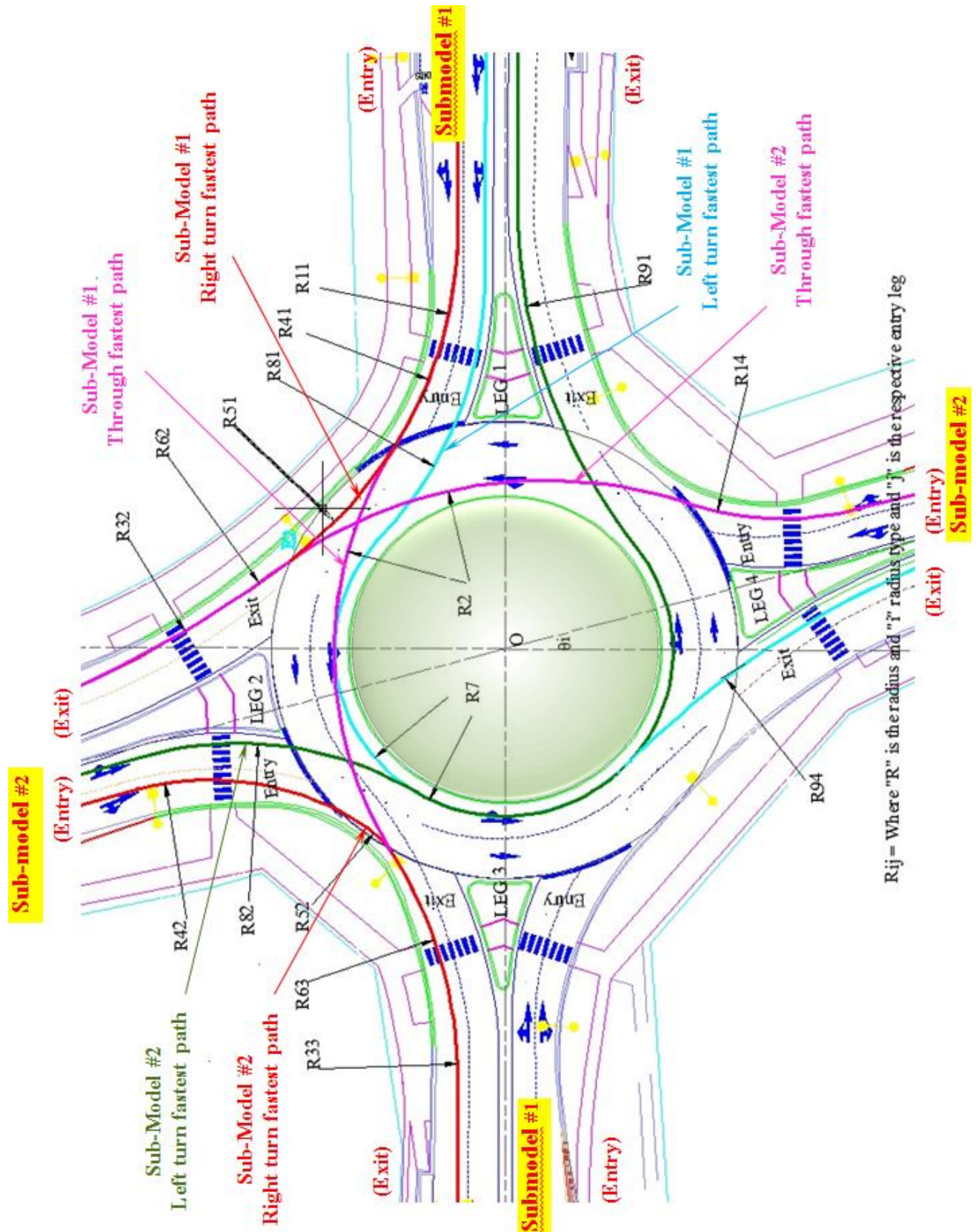


Figure 6.1 Vehicle fastest paths at skewed-angle roundabouts

Sub-model 1 models a vehicle's fastest paths (through, right and left turn) when consecutive approaches are skewed away from the driver. Sub-model 2 models a vehicle's fastest paths (through, right and left turn) when consecutive approaches are skewed towards the driver (Figure 6.1). The development of both sub-models for skewed-angle roundabouts are described as follows with the support of modeling equations and drawings.

6.3 SUB-MODEL 1: VEHICLE ENTERING THROUGH AN APPROACH LEGS (1, 3)

Sub-model 1 models a vehicle's fastest paths (through, right and left turn) relating to entry approach where consecutive approach that is skewed away from driver, as illustrated in Figure 6.1. The following section is about the modeling procedure of entry, exit and around central island curves for fastest through, right turn and left turn paths. In the case of skewed-angle roundabouts sub-model 1, the modeling of the fastest through, entry and exit paths is the same as in right-angle roundabouts; it has the fastest through, entry and exit path modeling. However, in the case of a through circulatory curve path around a central island, it is necessary to model for both approaching consecutive legs separately.

6.3.1 Fastest through path radii

Sub-model 1, is based on the assumption that a vehicle entering with along a horizontal axis approach leg (leg-1) and entry path is similar to a right-angle roundabouts case. Therefore, for skewed-angle roundabouts, modeling of the fastest through, entry and exit paths using sub-model 1 is the same as in right-angle roundabouts, and has the fastest through entry and exit path modeling. The only difference is that we need to model the through entry and exit fastest paths for both consecutive approach legs of the roundabout separately, while in the case of a right-angle we need to model only one approach because the other approach is symmetrical to the first one. The through fastest vehicle path is a combination of three reversal curves: the entry curve, the circular curve around the central island, and the exit curve, with radii of R_{1i} , R_{2i} and R_{3i} respectively Figure 5.4. The central island radius R_{ic} is the function of the inscribed circle diameter and circulatory width, as described in Equation [5.9]. The circulatory width is dependent upon the maximum entry width amongst all the entries at roundabout, as Equation [5.8] indicates.

Fastest through path curve around a central island

The radius R_2 is calculated using the deflection angle between both ends of the through circulatory fastest path arc joined by the yield line at distance of 1.5m from the edge of curve. The midpoint of the arc maintains a space of 1.5m from the edge of the central island, as demonstrated in Figure 6.3.

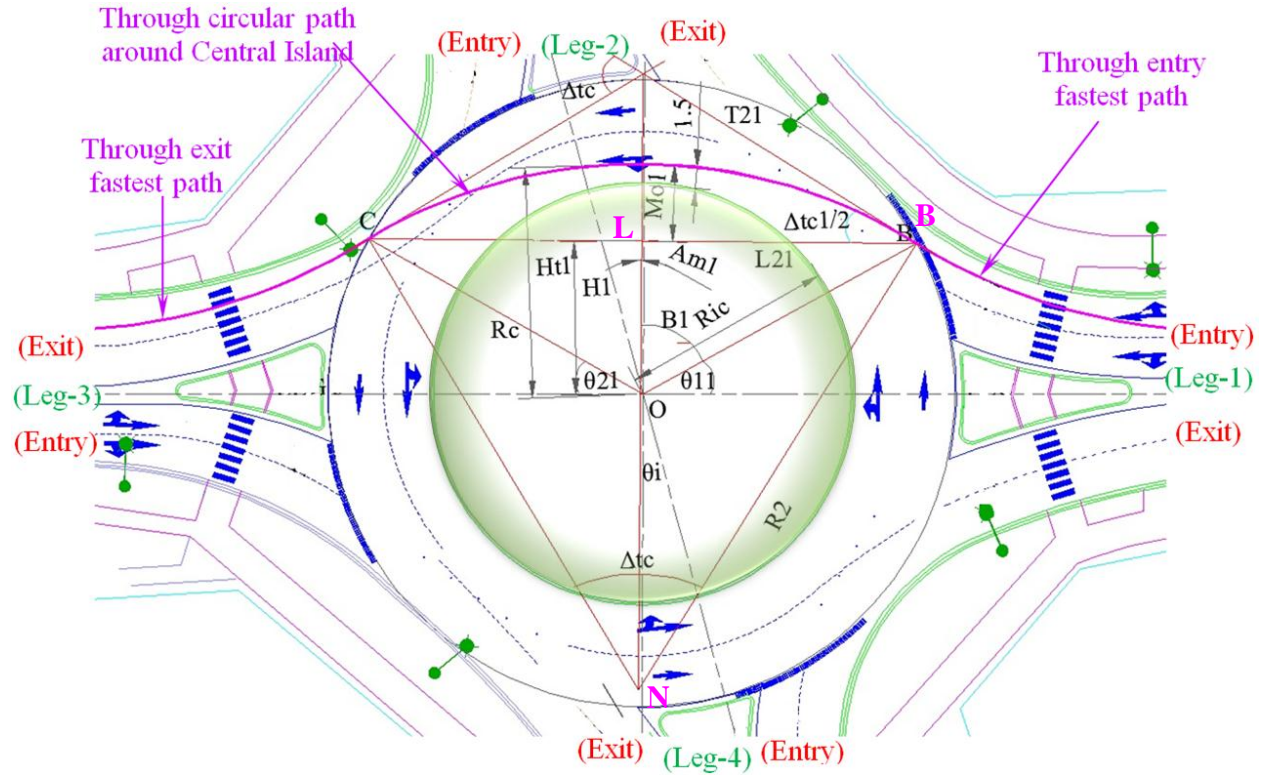


Figure 6.3 Through path around central island at skewed-angle roundabout (Sub-model 1)

\bar{H}_{ti} is depend on the central island radius, whereas \bar{H}_i depends on the inscribed circle diameter. X_{ai} is the optimization factor used in the modeling, with minimum and maximum value ranges. The M_{oi} in Equation [6.3] is the mid-ordinate length, and it is the difference between lengths of \bar{H}_{ti} and \bar{H}_i , which depends on D_c and R_{ic} . The constraint in Equation [6.4] ensures that the mid-ordinate will be in the proper position.

$$\bar{H}_i = 0.19D_c + X_{ai} \quad [6.1]$$

$$\bar{H}_{ti} = R_{ic} + 1.52 \quad [6.2]$$

$$\bar{M}_{oi} = \bar{H}_{ti} - \bar{H}_i \quad [6.3]$$

$$R_{ic} \geq \bar{H}_i \quad [6.4]$$

The half cord length \bar{L}_{2i} and \bar{M}_{oi} can be determined by solving the geometry of the right-angle triangle ΔBNL in Figure 6.3. The deflection angle of the through curve around the central island Δ_{tci} is calculated by dividing the half cord length by the mid-ordinate, as indicated in Equation [6.5].

$$\frac{\bar{L}_{2i}}{\bar{M}_{oi}} = \frac{\left[\sin\left(\frac{\Delta_{tci}}{2}\right) \right]}{\left[1 - \cos\left(\frac{\Delta_{tci}}{2}\right) \right]} \quad [6.5]$$

This will further be used in the calculation of the radius of the path the vehicle will take around the central island R_{2i} . It has been observed during the fastest path development process that \bar{L}_{2i} is the function of D_c , which was fixed through Equation [6.6]. R_{2i} is the function of D_c and Δ_{tci} and calculated by solving the geometry of right-angle triangle ΔBNL in Figure 6.3 as indicated in Equation [6.7].

$$L_{2i} = 0.4D_c \quad [6.6]$$

$$R_{2i} = \frac{L_{2i}}{\left[\sin\left(\frac{\Delta_{tci}}{2}\right) \right]} \quad [6.7]$$

Equation [6.8] utilizes the value of that radius R_{2i} and calculates the vehicle speed at that curve which should be less than the maximum speed limit.

$$V_{2i} = 11.27\sqrt{[f_s - 0.02]R_{2i}} \quad [6.8]$$

In Equation [6.8] i represent the number of approach legs from which the vehicle can enter the roundabout. In the case of a dual-lane roundabout with four legs its value ranges as $[i= 1,2,3,4]$.

Fastest through entry & exit paths

As discussed earlier, the through entry and exit path geometry in the case of a skew angle roundabout (Sub-model 1) is identical as in a right-angle roundabout. Therefore, the same modeling equations developed in Chapter 5, section 5.5.1 are used: Equations [5.24] to [5.30a] are used for modeling the through entry path and Equations [5.31] to [5.37] for the through exit path.

Fastest right turn path inside an inscribed circle diameter

The mid-ordinate M_{ri} is quite sensitive to the circulatory roadway width in the case of a right-angle roundabout intersection (Mehmood, 2003). It has also been observed that in the case of skewed-angle roundabouts, the geometry of a right turn circular curve is also dependent upon θ_i and C_w , as shown in Figure 6.5. C_w is a function of the maximum entry width, so we can say that the mid-ordinate length can be the function E_w . Therefore Equation [5.40] is modified to a new form which takes care of the effect of the skewed-angle, as shown in Equation [6.9].

$$M_{ri} = 0.066C_w + \left[\frac{0.00667\theta_i}{0.01745} \right] \quad [6.9]$$

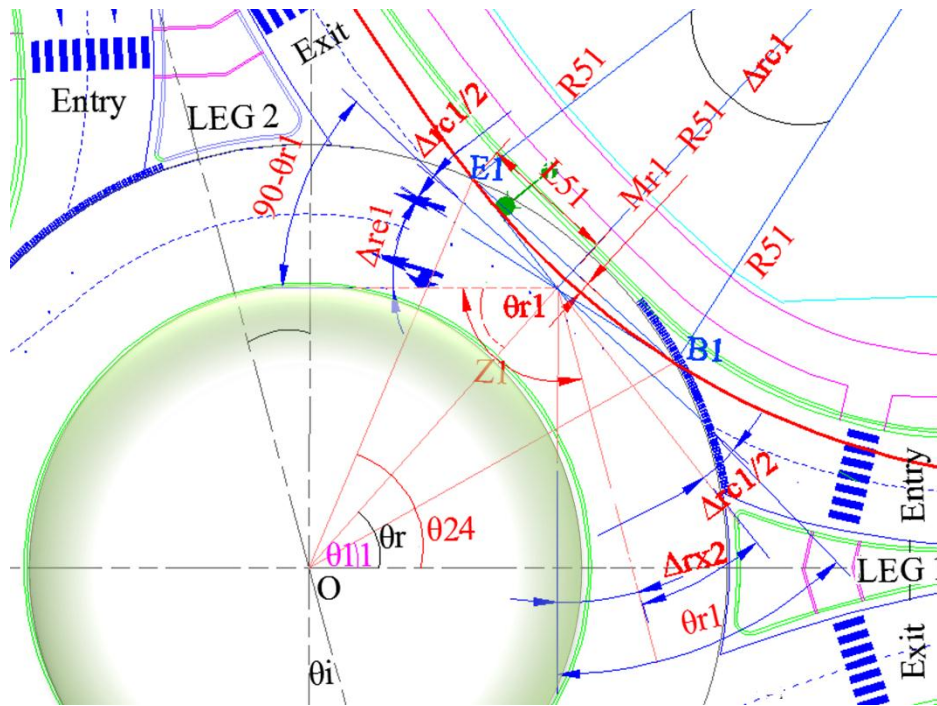


Figure 6.5 Right turn fastest path in ICD at skewed-angle roundabouts (sub-model 1)

It has also been observed that Δ_{rci} is the function of the entry and exit angles with respect to the center of the inscribed circle diameter and right turn entry deflection angle Δ_{rei} . Therefore, the length of the half cord $\overline{L_{5i}}$ is a function of D_c and Δ_{rci} . With an increase of D_c , it is observed that there is an increase in Δ_{rci} which affects the right turn entry radius. Therefore, a modification is done in the model of a right-angle roundabout. When Equation [5.38] is used in

the right-angle roundabout model, it only considers the effects of the inscribed circle diameter. Therefore, after several analyses on the effects of a skewed-angle on the length of a cord of a right turn circular curve, the equation is modified with Equation [6.10], which accounts for the effect of an inscribed circle diameter as well as the skewed-angle at roundabout.

$$[E_i B_i]^2 - \left[0.194 D_c + \left(0.46 \theta_i / 0.01745 \right) \right]^2 = 0 \quad [6.10]$$

Both Equations [6.9] and [6.10] are modified forms of the right turn fastest path model of a right-angle roundabout and consider the effects of θ_i and C_w . The rest of the modeling equations are the same as for right-angle roundabout modeling.

Fastest right turn entry path

It has been observed that in skewed-angle roundabouts, the entry point B as show in Figure 5.10 is not affected by the intersection angle θ_i . However entry point B can be affected by smooth transition curve requirements from entry to the circulating area. The modeling procedure for right turn entry paths is the same as in the right-angle roundabouts case, and Equations [5.45] to [5.52] can also be utilized to calculate the right turn entry radius.

Fastest right exit path

As discussed earlier, the entry and exit points of a right turn circular curve depend upon the roundabout geometry and its alignment. When modeling a skewed-angle roundabout intersection it has been observed that as θ_i moves from 0 to the skewed away angle with respect to the vertical axis, the exit point E also moves away on the yield line of a consecutive intersecting approach, resulting in a higher radius and speed at the exit and a larger inscribed circular diameter, as shown in Figure 6.6.

With slight modifications of the right-angle roundabout model in Equations [5.54], [5.55] and [5.56], a new model can be developed for skewed-angle roundabouts. Instead of Equation [5.54], a new Equation [6.11] is formulated by solving the geometry of the triangle $\Delta E_1 O T_{a2}$ in Figure 6.6.

$$T_{b[i+1]} E_{[i+1]} = 0.5 D_c \sin(\theta_{2[i+3]} + \theta_i) - 0.5 E_{w[i+3]} - n + X_{fi} \quad [6.11]$$

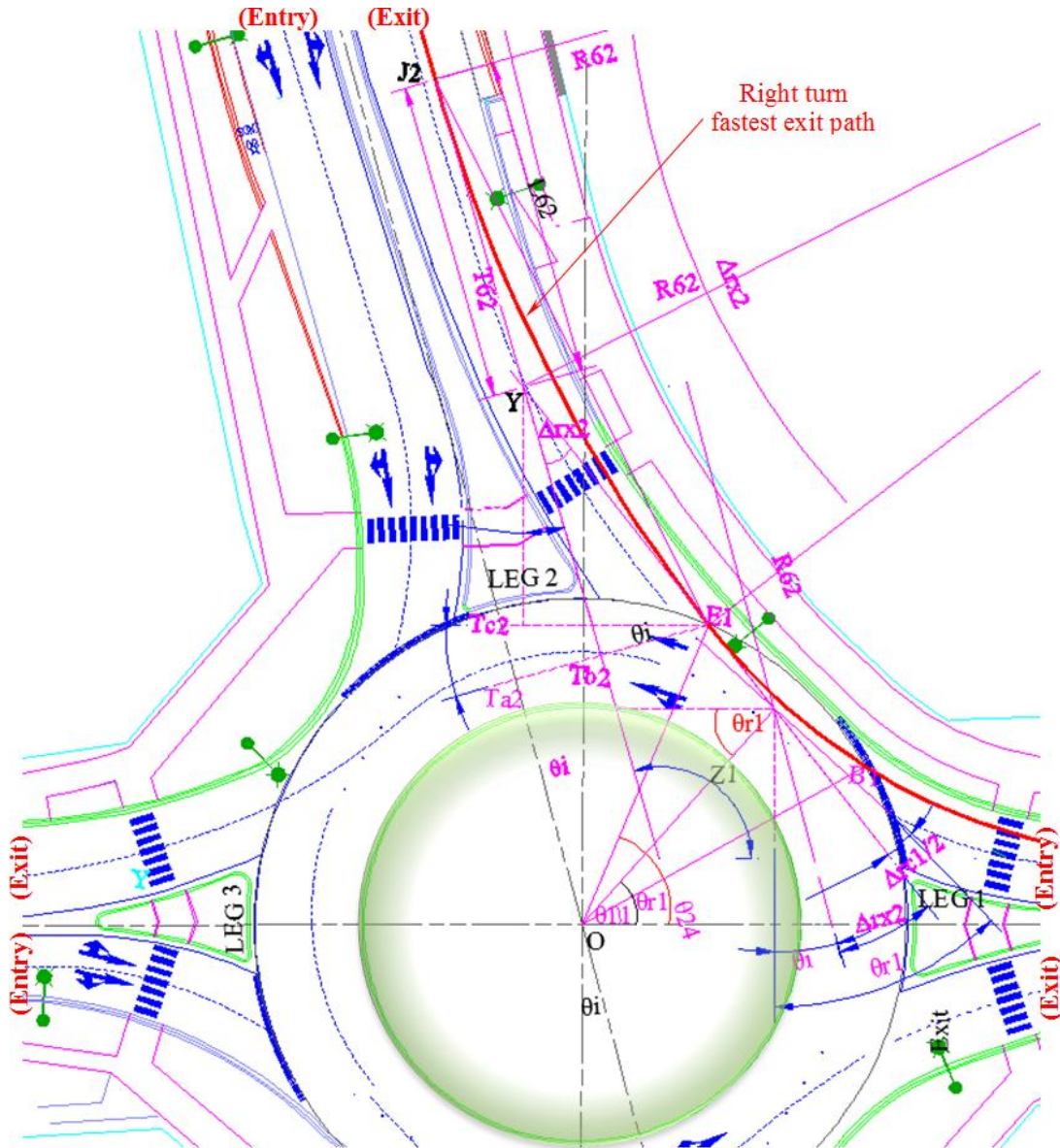


Figure 6.6 Right turn exit path at skewed-angle roundabouts (sub-model 1)

Similarly, Equation [5.55] is modified to [6.12], and [5.56] modified to [6.13] by solving the geometry of the triangle ΔE_1OT_{a2} in Figure 6.6. These new model equations consider the effects of θ_i at exit.

$$T_{b[i+1]}Y_{[i+1]} = \frac{T_{b[i+1]}E_{[i+1]}}{\tan[\Delta_{rx[i+1]}]} \quad [6.12]$$

$$T_{6[i+1]} = \sqrt{(T_{b[i+1]}E_{[i+1]})^2 + (T_{b[i+1]}Y_{[i+1]})^2} \quad [6.13]$$

6.3.3 Fastest left turn path radii

Left turn paths contain three turning radii: entry, circulatory and exit. A vehicle enters in the inscribed circle diameter parallel to the painted edge of the splitter, while maintaining a centerline distance of 1m from the painted edge, as illustrated in Figure 6.7.

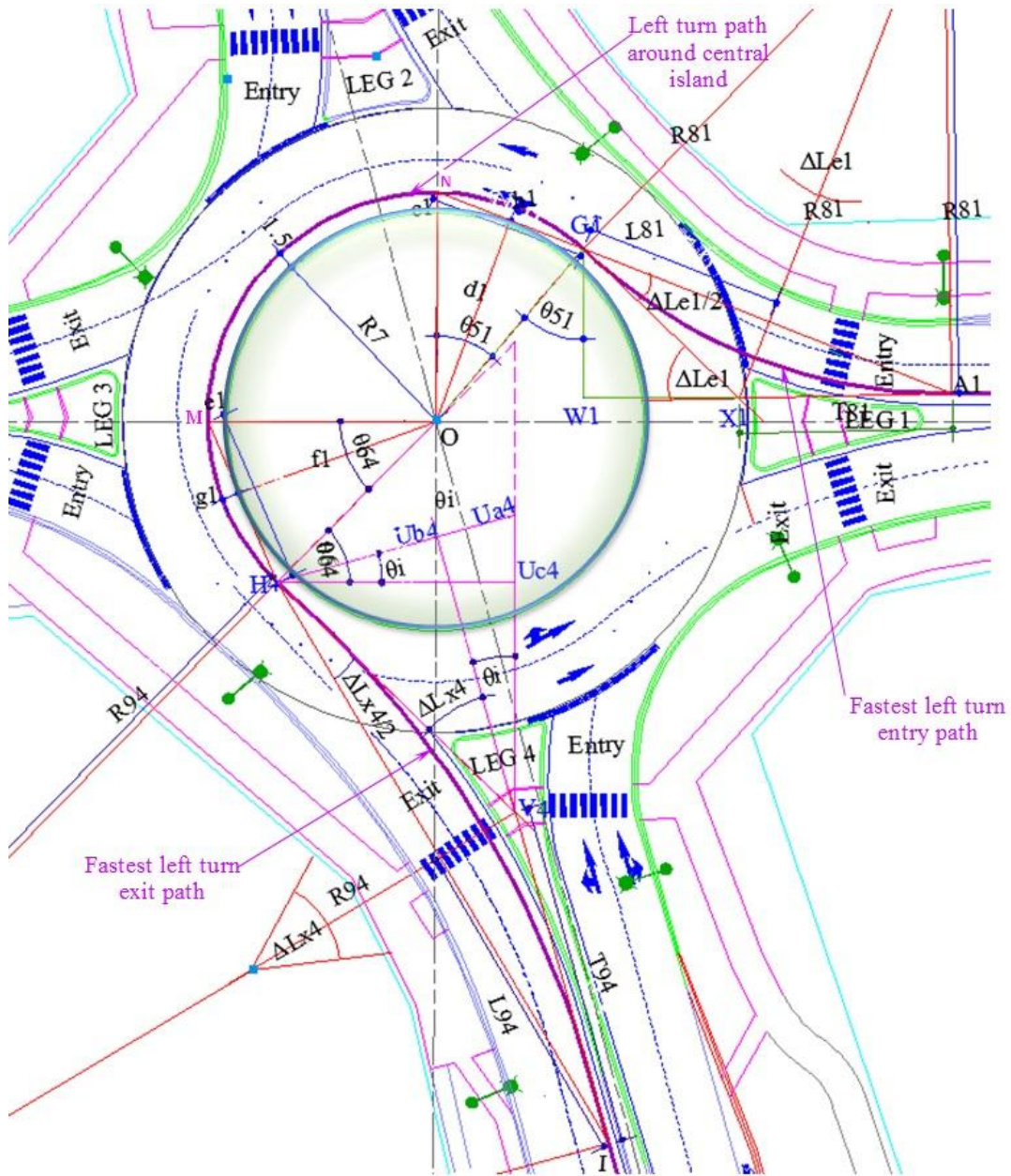


Figure 6.7 Fastest left turn path at skewed-angle roundabout (sub-model 1)

Fastest left turn path inside an inscribed circle diameter

Equation [5.60] calculates the radius of a left turn's fastest path around a central island, while maintaining a 1.5m safe centerline distance from edge of the central island, as shown in Figure 6.7.

Fastest left turn entry path

The skewed-angle roundabouts left turn path modeling process is similar to the right-angle roundabouts left turn path modeling process. There is no effect of θ_i on the left turn entry radius because the approach alignment is analogous to the right-angle approach alignment. θ_i is only effected in the exit left turn path radius when a vehicle approaches from an entry leg, as described in sub-model 1, which is (leg-1). Therefore, the same equation that was used in the modeling of a right-angle roundabouts left turn entry path can be used to model the left turn entry path in skewed-angle roundabouts.

Fastest left exit path

During the exit approach of a left turn path the skewed-angle of the roundabout θ_i , causes a reduction in the vertical component $[H_{[i+3]}U_{b[i+3]}]$ and an increase in the horizontal component $[V_{[i+3]}U_{b[i+3]}]$ of the tangent of an exit left turn fastest path curve. The effects of the vertical and horizontal components on the tangent length of the left turn exit path curve results in a reduction in the left turn exit deflection angle, as indicated in Figure 6.8. Therefore, it is essential to modify the horizontal and vertical component equations of a right-angle roundabout, which is later helpful in the calculation of the tangent length of exit for the left turn path curve of a skewed-angle roundabout. Equation [6.14] is the modified form of Equation [5.76] and is obtained by solving the geometry of triangle ΔH_4OU_{a4} , as described in Figure 6.8.

$$H_{[i+3]}U_{b[i+3]} = R_7 \cos[\theta_{6[i+3]} - \theta_I] - n \quad [6.14]$$

In Equation [6.14], θ_I causes a reduction in the vertical component of a left turn exit path curve. Similarly the horizontal component of the tangent, as described in Equation [6.15], is the modified form of Equation [5.78] and is obtained by solving the geometry of triangle $\Delta H_4V_4U_{b4}$, as described in Figure 6.8. The element $[H_{[i+3]}U_{b[i+3]} \tan \theta_I]$ causes the increase in the horizontal component and decrease in the deflection angle.

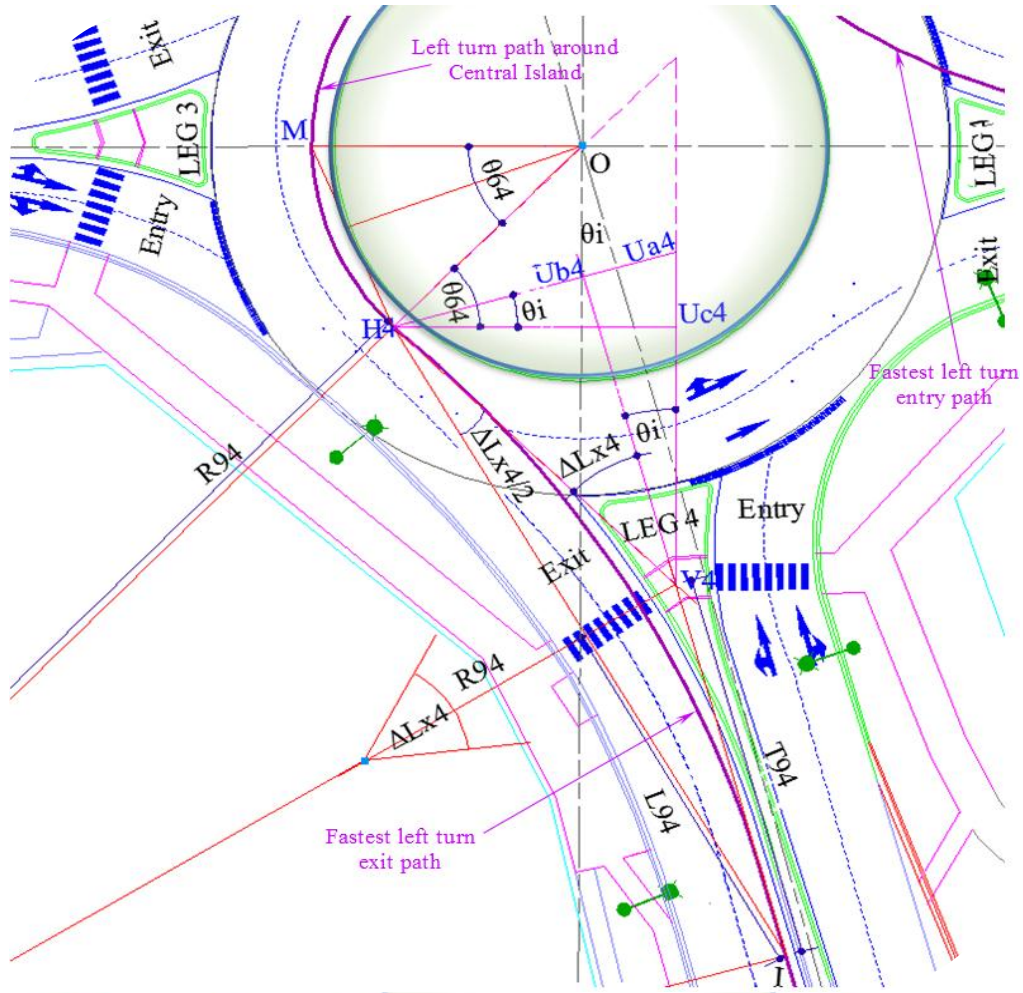


Figure 6.8 Fastest left turn exit path at skewed-angle roundabouts (sub-model 1)

$$V_{[i+3]}U_{b[i+3]} = 0.6R_{ic} + H_{[i+3]}U_{b[i+3]} \tan[\theta_i] \quad [6.15]$$

The horizontal component of the tangent, as described in Equation [6.15] is also dependent on the left turn exit deflection angle, as shown in Equation [6.16], which is the modified form of Equation [5.77].

$$V_{[i+3]}U_{b[i+3]} = \frac{H_{[i+3]}U_{b[i+3]}}{\left[\tan[\Delta L_{x[i+3]}] \right]} \quad [6.16]$$

The equation of the tangent for the left turn exit path curve, as shown in Equation [6.17], is modified to form Equation [5.79].

$$T_{9[i+3]} = \sqrt{(V_{[i+3]}U_{b[i+3]})^2 + (H_{[i+3]}U_{b[i+3]})^2} \quad [6.17]$$

6.4 SUB-MODEL 2: A VEHICLE ENTERING THROUGH APPROACH LEGS (2, 4)

6.4.1 Fastest through path radii

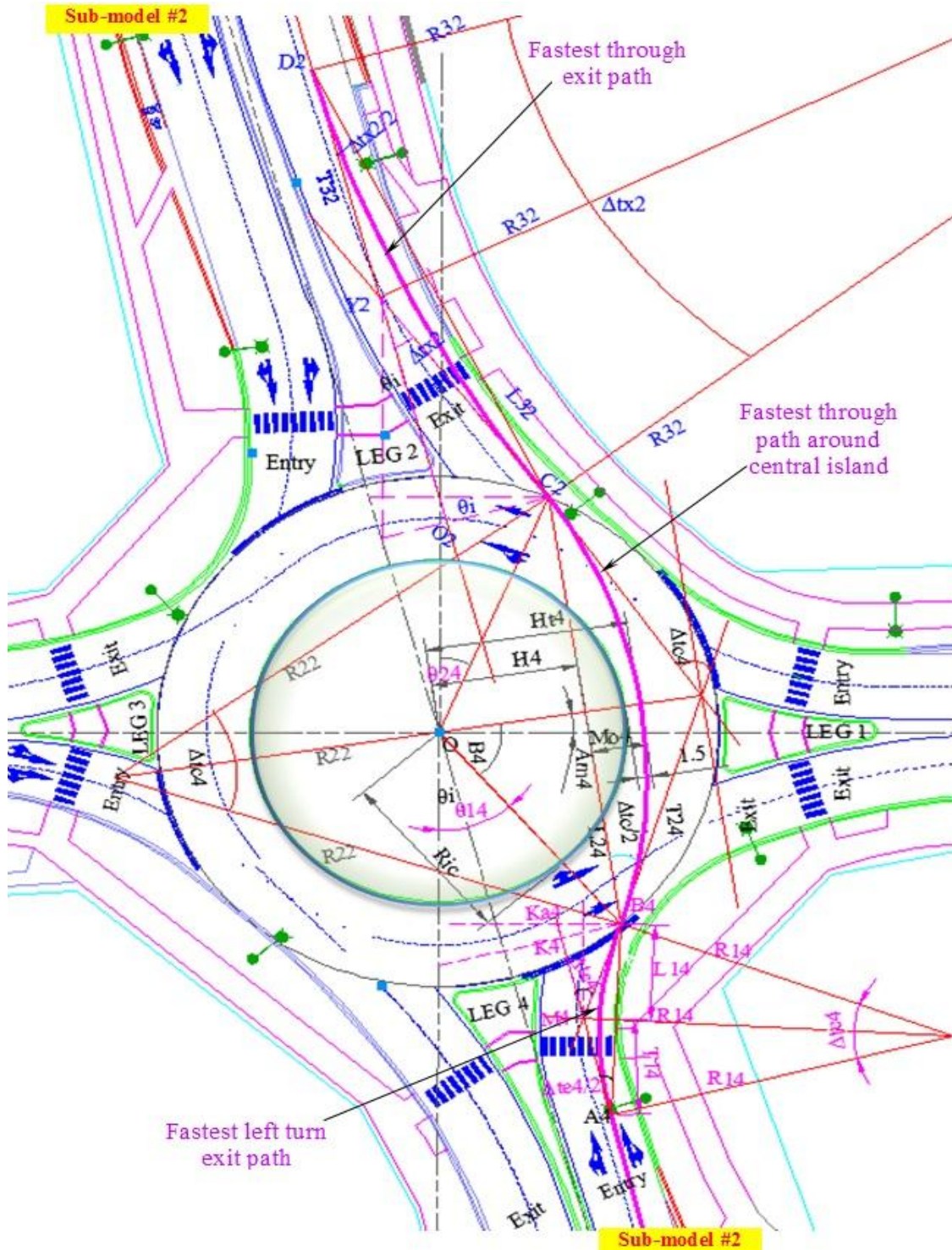


Figure 6.9 Fastest through path modeling at a skewed-angle roundabout (sub-model 2)

Sub-model 2 is based on the assumption that a vehicle entering with approach leg (leg-2) where the consecutive approach is skewed toward the vehicle driver. In this case the fastest entry path modeling is not similar to the right-angle roundabout case. Figure 6.9 represents the complete fastest through path at entry, around a central island and at exit. It results in a tight radius for the right turn path.

Fastest through path curve around a central island

It has been observed when sketching the fastest through path in a circulatory portion that the mid-point inclination of the curve A_{mi} with the vertical axis of inscribed circle diameter, as shown in Figure 6.10, is more than the right-angle roundabout case.

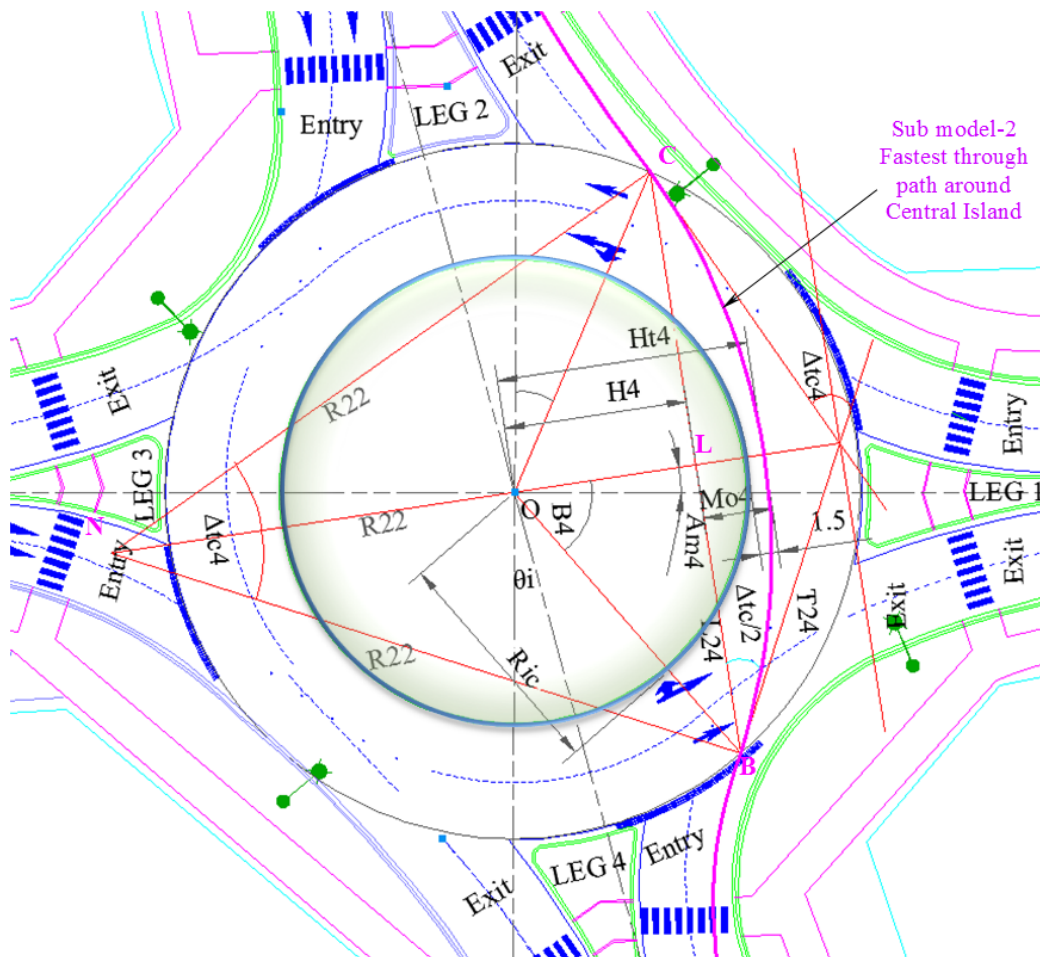


Figure 6.10 Through path around central island at a skewed-angle roundabout (sub-model 2)

This is due to the incline approach with respect to the axis of the inscribed circle diameter. It shows that a vehicle enters and exits the inscribed circle diameter at different angles, but it is not affected in the previous model equation developed in sub-model 1. The modeling equations of a through path around a central island already consider the effect of mid-point inclination A_{mi} with reference to the vertical axis of a roundabout inscribed circle diameter.

Equations from [6.1] to [6.8] are the general forms of the equations used for designing the fastest through circular path around a central island.

Fastest through entry path

The through entry path geometry in the case of a skewed-angle roundabout (sub-model 2) is not identical to the right-angle roundabout's. The entry path curve is affected due to the effects of θ_i . Therefore the same modeling equations as developed in Chapter 5, section 5.5.1 must be modified to consider the effect of θ_i at entry.

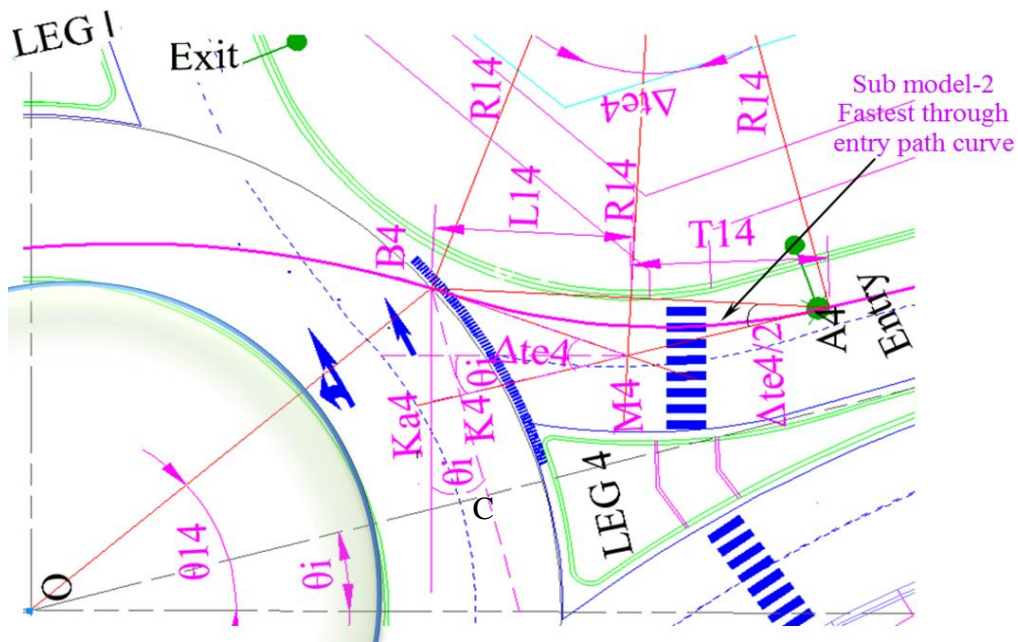


Figure 6.11 Fastest through entry path at a skewed-angle roundabout (Sub-model 2)

The vertical component of a through entry path curve B_4K_4 can be obtain by solving the geometry of triangle ΔB_4OU_{b4} , as shown in Figure 6.11 and indicated by Equation [6.18]. With the increase of θ_i the vertical component of the through entry path curve B_4K_4 decreases. Therefore, it has been observed that the change in equation of the vertical component affects the

whole geometry of entry through path curve in a skewed-angle roundabout. Therefore, only Equation [5.24] from the right-angle roundabout modeling equation needs to be modified to an Equation [6.18], where i is the approach leg number and its range is from 1 to 4.

$$B_i K_i = [0.5D_c \sin[\theta_{1i} - \theta_i] - 0.5E_{wi} - n] \quad [6.18]$$

Fastest through exit path

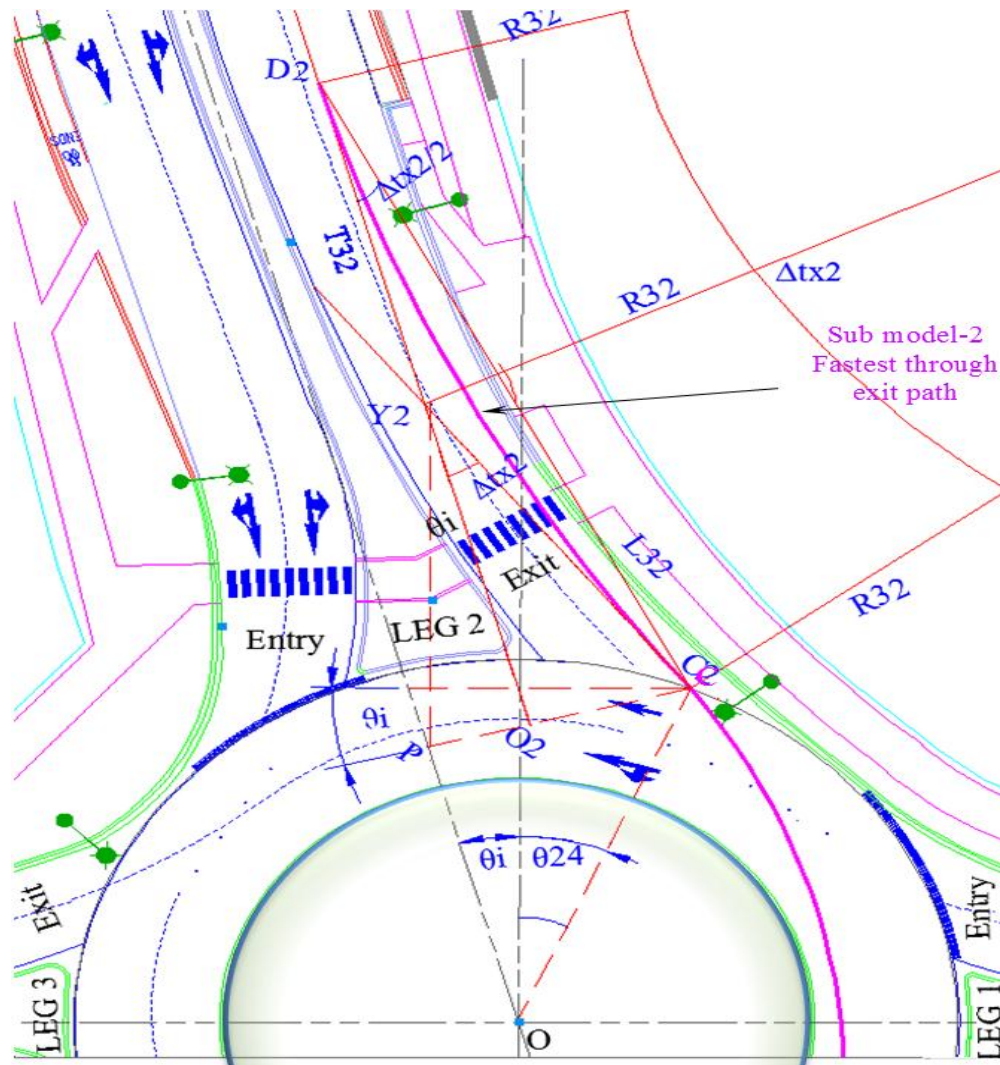


Figure 6.12 Fastest through exit path at a skewed-angle roundabout (sub-model 2)

The through exit path geometry in the case of skewed-angle roundabouts (sub-model 2) is not identical to the right-angle roundabouts. The exit through path curve is affected due to effects of θ_i . Therefore, the same modeling equations as developed in Chapter 5, section 5.5.1 need to

be modified to consider the effect of θ_i at exit. The vertical component of a through exit path curve O_2C_2 , can be obtained by solving the geometry of triangle ΔC_2OP , as shown in Figure 6.12 and indicated by Equation [6.19]. The increase in θ_i , results decrease in vertical component of through exit path curve O_2C_2 . It is observed that change in the equation of the vertical component affects the whole geometry of exit through path curve in a skewed-angle roundabouts. Therefore, only Equation [5.32] from the right-angle roundabout exit through path modeling equation needs to be modified to create Equation [6.19], where i is the approach leg number and its range is from 1 to 4.

$$O_{[i+2]}C_{[i+2]} = [0.5D_c \sin[\theta_{2i} + \theta_i] - 0.5E_{wi} - n] + X_{ei} \quad [6.19]$$

6.4.2 Fastest right turn path radii

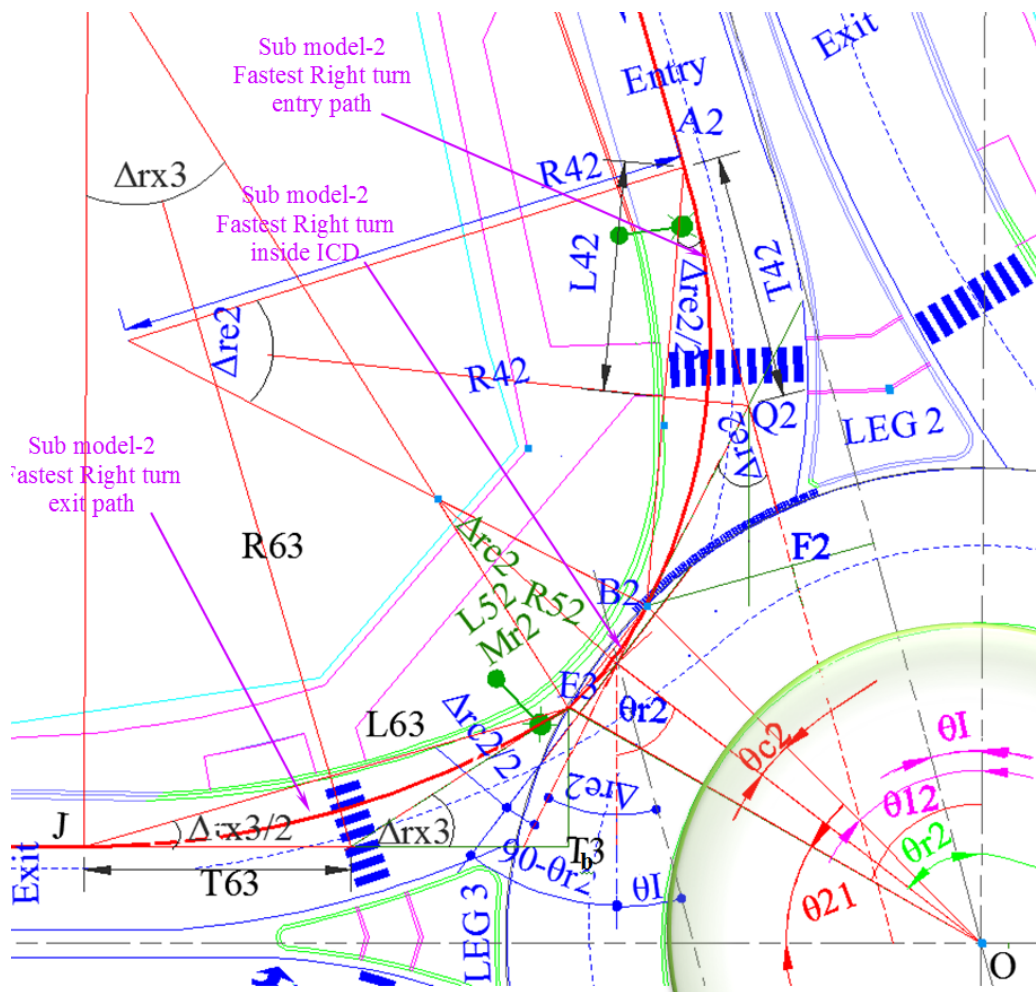


Figure 6.13 Fastest right turn path modeling at skewed-angle roundabout (sub-model 2)

In skewed-angle roundabouts there is a major difference in the radii and speeds at fastest right turn paths at both consecutive approaches. Figure 6.13 illustrates the right turn fastest path for sub-model 2, where the consecutive approach is skewed towards the vehicle driver. Figure 6.13 represents the complete right turn fastest paths (entry, circulatory and exit) that are created by the vehicle in the absence of other traffic. The following section explains each right turn path and its effects in the case of skewed-angle roundabouts when the exit approach is skewed towards the driver.

Fastest right turn entry path

In the case of a right turn entry design when the vehicle is entering from the skewed away approach as (*leg-2, 4*), and exits at an approach which is skewed toward the driver as (*leg 3, 1*), the entry design of approach (*leg-2, 4*) take into account the effect of θ_i as illustrated in Figure 6.14.

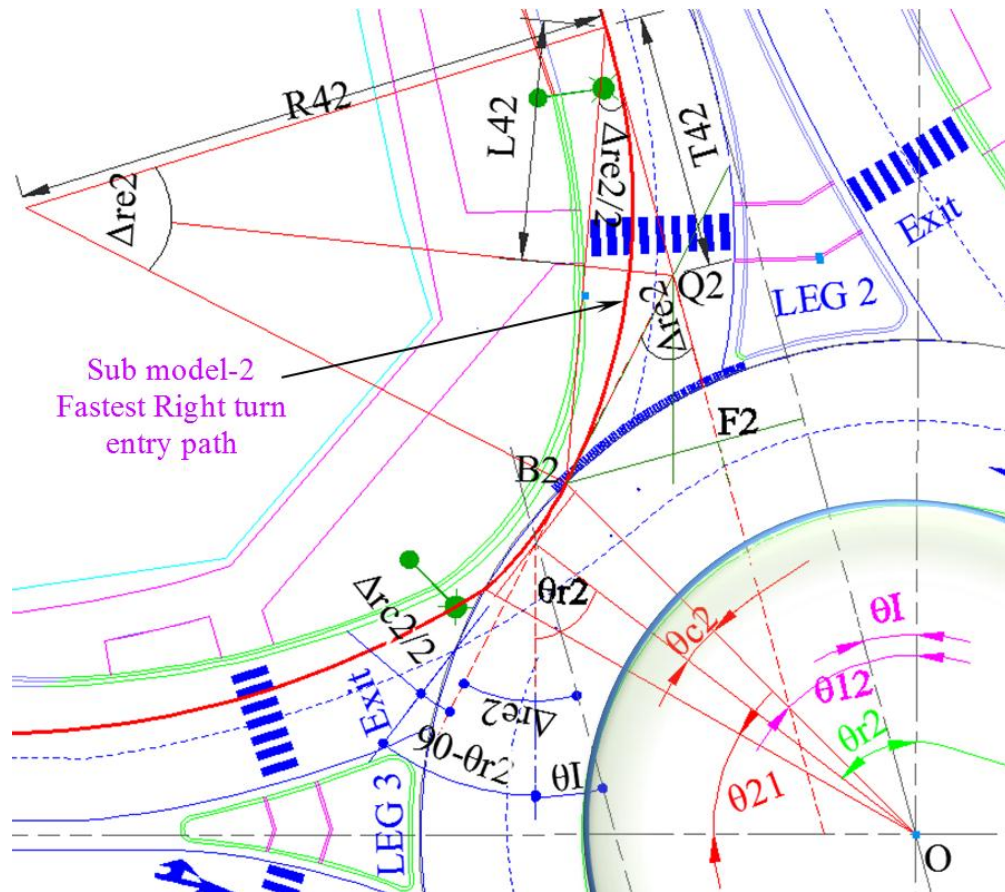


Figure 6.14 Fastest right turn entry path at skewed-angle roundabouts (sub-model 2)

It has also been observed that θ_i mainly affects the vertical component of the fastest vehicle path curve, which later changes the whole geometry of the right turn fastest path curve. The same modeling equations from the right-angle roundabout design can be used in a skewed-angle roundabout design for sub-model 2, with slight modification of the vertical component of right turn entry fastest path curve Equation [5.48]. Therefore, Equation [6.20] is the new modified form of Equation [5.48] and accounts for the effects of a skewed-angle and an inscribed circle diameter.

$$B_i F_i = [0.5D_c \sin[\theta_{1i} - \theta_I] - 0.5E_{wi} - n] + X_{ci} \quad [6.20]$$

Fastest right turn path inside an inscribed circle diameter

Both the entry and exit points come closer because of the acute-angle between consecutive approaches. This results in the tight, circulatory entry and exit radii, as shown in Figure 6.13. The half cord length \bar{L}_{5i} is a function of the inscribed circle diameter as well as the skewed-angle between the approaches, although in the case of right-angle roundabouts it is only a function of the inscribed circle diameter. It has been observed that there is a need to modify the relationship of a right-angle roundabout modeling design for sub-model 2 defined in Equation [5.38] to skewed-angle roundabouts. Therefore, a new relationship is developed between the cord length and inscribed circle diameter with consideration of a skewed-angle at approaches in Equation [6.21].

$$[E_i B_i]^2 - \left[0.2D_c + \left(0.37\theta_I / 0.01745 \right) \right]^2 = 0 \quad [6.21]$$

The mid-ordinate M_{ri} is quite sensitive to the circulatory roadway width in the case of right-angle roundabouts (Mehmood, 2003). It has been observed that in the case of skewed-angle roundabouts the geometry of a right turn circular curve is also dependent upon θ_i and C_w , as shown in Figure 6.13 and Figure 6.14. Because C_w , is a function of the maximum entry width, we can say that the mid-ordinate length can be the function of E_w . Therefore, Equation [5.40] is modified to a new form that considers the effect of a skewed-angle toward the driver, as shown in Equation [6.22].

$$M_{ri} = 0.066C_w - \left[0.00667\theta_i / 0.01745 \right] \quad [6.22]$$

Fastest right exit path

There is no effect of θ_i on exit and the design of fastest right turn exit path curve is the same as in case of right-angle roundabouts.

6.4.3 Fastest left turn path radii

Left turn paths contain three turning radii: entry, circulatory and exit. A vehicle enters in an inscribed circle diameter parallel to the painted edge of a splitter, while maintaining a centerline distance of 1 m from the painted edge, as illustrated in Figure 6.15. Figure 6.15 depicts the left turn path at entry, around the central island, and at exit. The entry path considers the effect of θ_i , while the left turn exit path is free from the effect of a skewed-angle at a roundabout in the case of sub-model 2.

The skewed-angle roundabouts left turn entry path modeling process is similar to the right-angle roundabouts left turn entry path modeling process. There is no effect of θ_i on the left turn exit because the approach alignment is analogous to the right-angle approach alignment. θ_i only affects the entry left turn path radius when the vehicle approaches from entry (leg-2), as described in sub-model 2. Therefore, the same equation that was used in modeling a right-angle roundabouts left turn exit path can be used to model a left turn entry path in skewed-angle roundabouts in sub-model 2.

Equation [5.60] calculates the radius of the left turn fastest path around a central island, while the vehicle maintains a 1.5 m safe centerline distance from the edge of the central island, as shown in Figure 6.15. This radius of the left turn fastest path around a central island is similar for all vehicles regardless of the approach leg at the roundabout.

Therefore, when designing skewed-angle dual-lane roundabouts for the left turn path, consideration of sub-model 2 conditions where a vehicle enters from a skewed away approach from the driver must be included. Only a left turn entry path must be designed, and the modeling process of a left turn circular and left turn exit fastest path is similar to the right-angle roundabouts' geometric design.

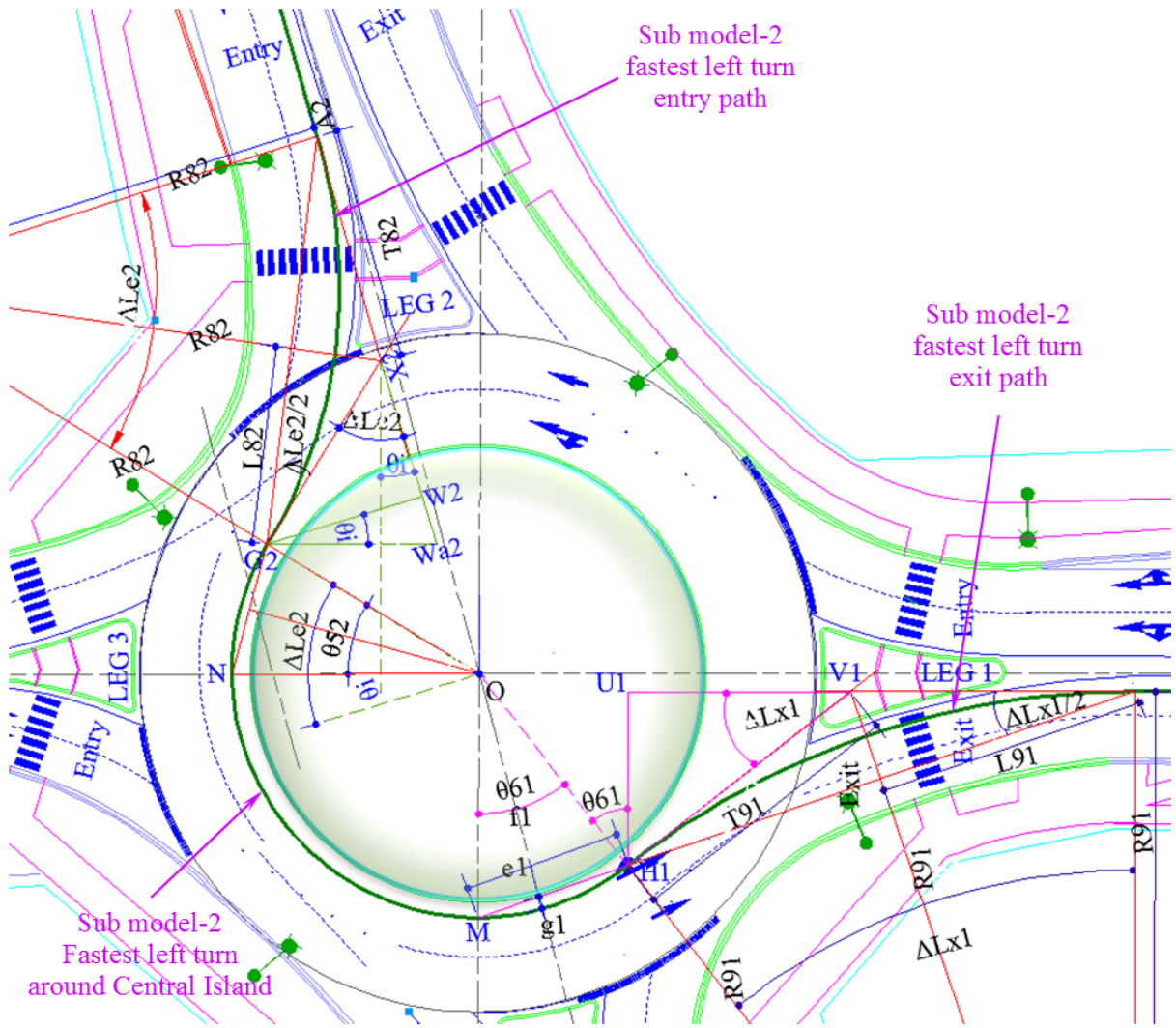


Figure 6.15 Fastest left turn path at a skewed-angle roundabout (sub-model 2)

Fastest left turn entry path;

θ_i in skewed-angle roundabouts affects the left turn entry path at the entry approach: it causes an enhancement of the vertical component $G_i W_i$ and a reduction of the horizontal component $W_i X_i$ of the left turn entry path curve, as shown in Figure 6.16. Due to these effects the point G is shifted up which results in a reduction of the angle θ_{5i} . Therefore, modification of the modeling equations of right-angle roundabout is needed so that it accounts for the effects of θ_i , D_c and R_{ic} . Therefore, $G_i W_i$ in Equation [5.65] needs some modification with respect to the θ_i – axis. This is calculated by deducting the value of n from the vertical component of radius

R_7 with respect to the θ_i – axis instead of the vertical axis of the inscribed circle diameter, and X_{di} is optimized, as described in Equation [6.23].

$$G_i W_i = R_7 \cos[90 * 0.01745 - \theta_i - \theta_{5i}] - n + X_{di} \quad [6.23]$$

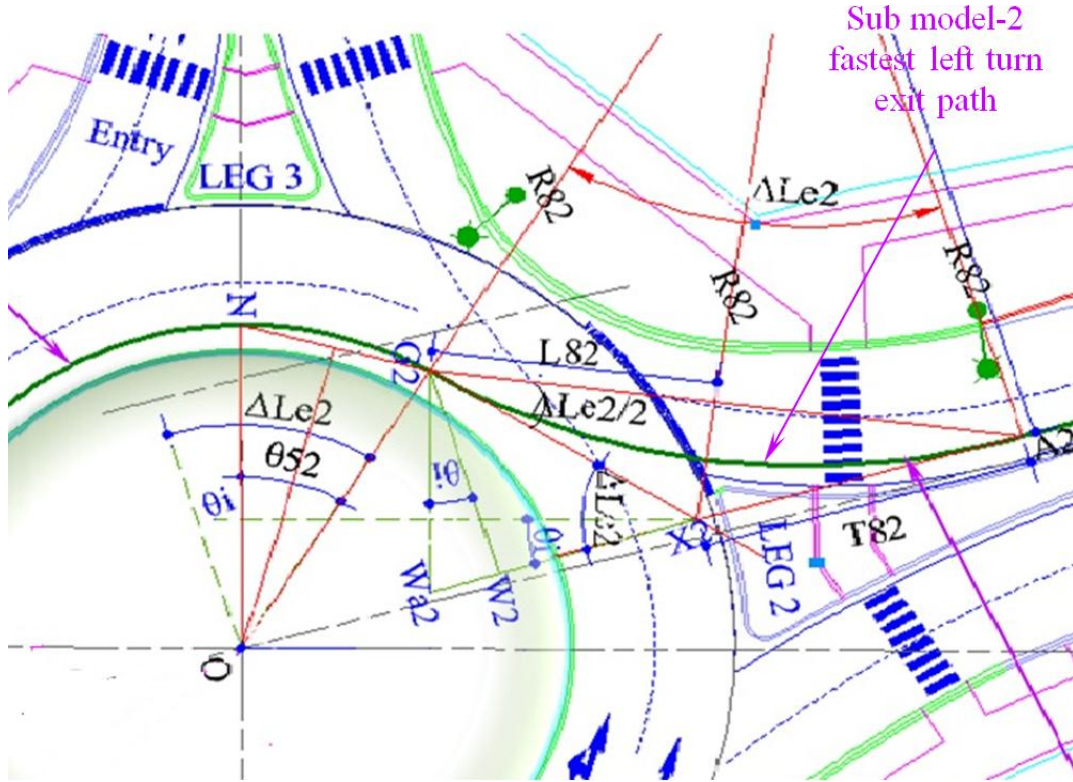


Figure 6.16 Fastest left turn entry path at a skewed-angle roundabout (sub-model 2)

It has been detected during the left turn entry fastest path development process for sub-model 2 that the left turn entry radius is a function of $W_i X_i$, and $W_i X_i$ is a function of θ_i and central island radius R_{ic} . Therefore, a relationship is developed between R_{ic} , $W_i X_i$, and θ_i through Equation [6.23]. Equation [6.23] is the modified form of Equation [5.66], where i represent the vehicle approach leg number. In this case ($i = 2$), whereas generally for a dual-lane roundabout with four approach entries has a range of ($i = 1$ to 4).

$$W_i X_i = 0.836 R_{ic} - 19.8324(\theta_i) \quad [6.24]$$

For the optimization of skewed-angle dual-lane roundabouts, Equations [6.1] to [6.23] that utilized in the dual-lane right-angle roundabout model can be used with the modification of equations, as mentioned in this chapter.

6.5 MODEL DEVELOPMENT PROCESS

The optimization model gives the results of speed consistency, radii of all entry path deflection angles, tangent lengths, etc. It is further used in delay and queue operational modeling. The skewed-angle between approaches has no effect on delay and queue modeling procedure: both right-angle and skewed-angle roundabouts have the same procedure in delay and queue operational modeling. Therefore, the rest of the process is similar to that described in Chapter 5, section 5.6.

CHAPTER 7 : APPLICATION OF MODELS TO ACTUAL ROUNDABOUT

7.1 INTRODUCTION

Based on optimization techniques, an optimization model developed for dual-lane right-angle and skewed-angle roundabouts was designed using Lingo-13 software, as described in Chapter 5 and 6. This chapter will describe the application of these models in the field and their sensitive analyses. The application of a given developed model is limited to dual-lane roundabouts with four legs where entry and consecutive exit legs are separated at a right-angle or at a skewed-angle range of 70° to 110° .

The proposed site for application of the model in the field is located at Ira Needles Boulevard and Erb Street West in Waterloo, Ontario. This intersection already has a dual-lane roundabout. Erb Street has 4 lanes in the vicinity of the development, with adjacent, existing and proposed commercial development on all four corners of the intersection. Further to the south of Ira Needles Boulevard there is a residential development. It is the first dual-lane roundabout on an arterial road in Ontario.

7.2 DATA PREPARATION

After preliminary study of the site the next step is to collect geometric and traffic data for the application of optimization model. The range of design parameter can be defined from an aerial photograph using GIS software such as ArcView. With the help of Google satellite images, the approximate decision variables (entry width, inscribed circle diameter, central island diameter, and approach half width and flare length) can be measured. These ranges include the minimum and maximum measurement values of those specific elements. If the intersection is between the populated areas where right-of-way is a constraint, the maximum inscribed circle diameter $D_{c_{max}}$ is calculated between the available spaces of road curb, as explain in Figure 7.1. On the other hand, the locations that have no problem of right-of-way restriction, designers select the $D_{c_{max}}$ value based on experience, as illustrate in Figure 7.2. The minimum inscribed circle diameter $D_{c_{min}}$ depends on the design vehicle.

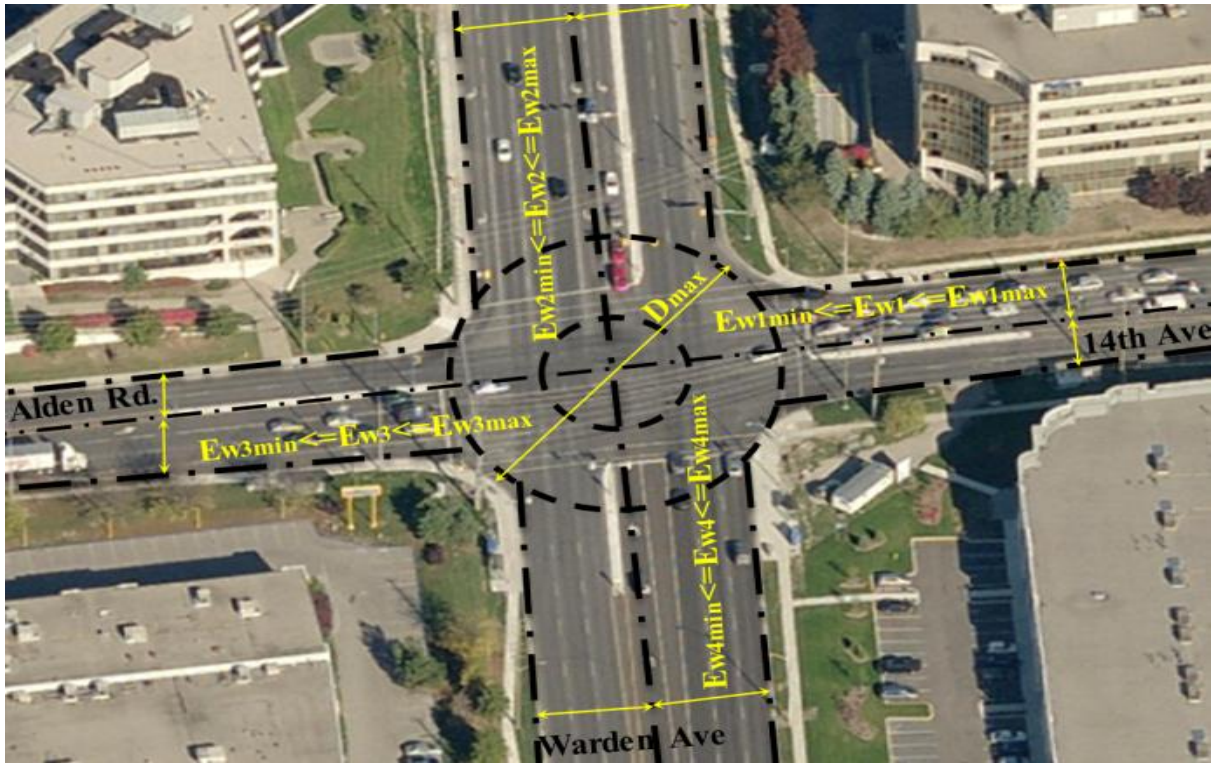


Figure 7.1 The intersection at Warden Avenue @ 14th avenue (Google image).

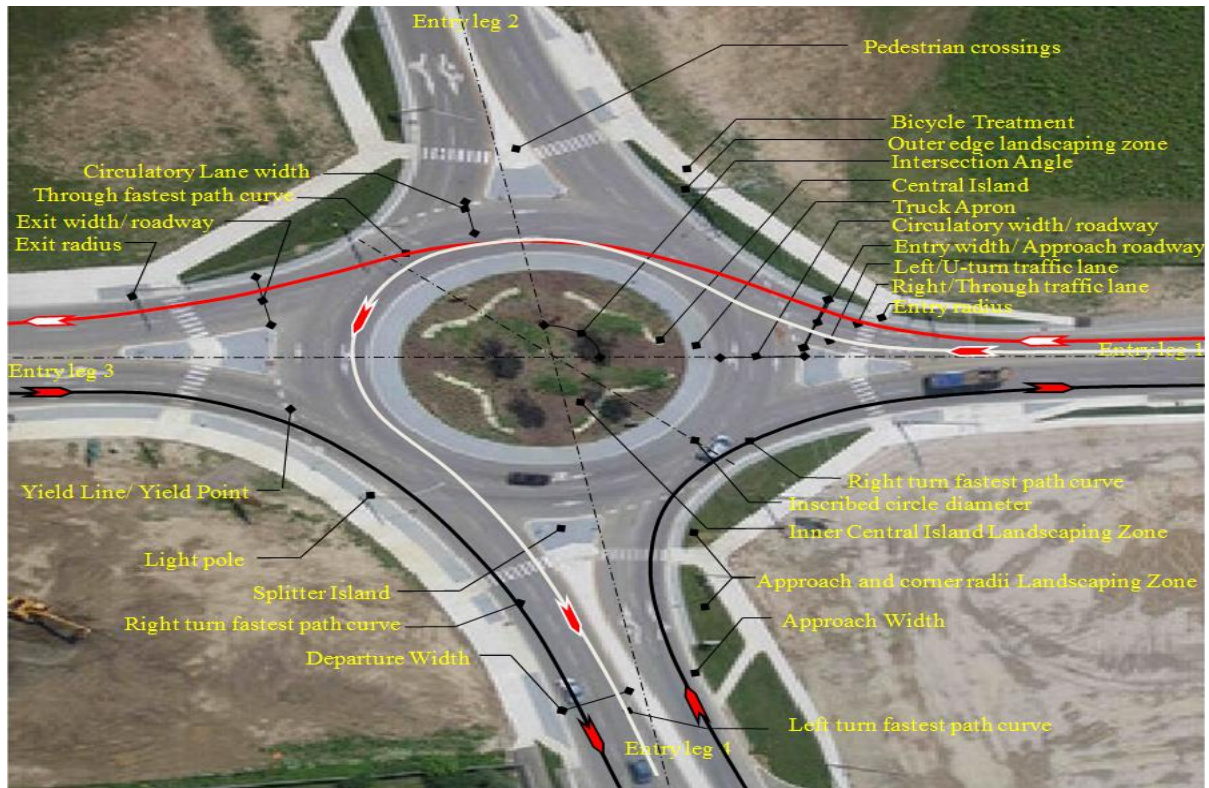


Figure 7.2 Ira Needles Boulevard @ Erb Street intersection (Google image).

Therefore, the inscribed circle diameter D_c should lie between both the minimum and maximum ranges for the best design. Similarly, maximum entry width $E_{wi_{max}}$ and exit width $E_{xwi_{max}}$ can be calculated from the centerline, as explain in Figure 7.1, while the minimum entry width $E_{wi_{min}}$ and exit width $E_{xwi_{min}}$ is dependent upon the minimum dual-lane width of the roundabout.

For this specific site location, the maximum limit of each parameter was selected from data given by Steve van De Keere, Head of the Transportation Expansion Program, Region of Waterloo, and Philip A. Weber, Principal Project Manager at Ourston Roundabout Engineering. The minimum limits were defined based on the minimum requirements of a dual-lane roundabout. Table 7.1 describes the maximum and minimum limits of input geometric parameters that will be used in the optimization model. WB-15 (WB-50) design vehicle is selected because the roundabout is in an urban environment. The minimum inscribed circle diameter value is selected based on the design vehicle.

The minimum entry width for a dual-lane roundabout is 7.3 m, and the minimum circulatory width is 9.8 m whereas the maximum limit for circulatory width is $1.2E_{wmax}$ (FHWA, 2000). Maximum approach half width limits are according to the site limits. The FHWA mention a range of relative speed differences between the conflicting and consecutive point selected. If there is no flaring then the entry width will be equal to the approach half width. The entry angle range is selected based on FHWA guidelines.

Table 7.2 represents the AM, PM and Saturday peak hour traffic volume data for through, right turn, left turn and circulatory traffic for each approach to the roundabout intersection. For modeling purposes the maximum traffic volume was selected for through, right and left turning traffic at each roundabout approach among AM, PM and Saturday peak hour traffic data. The circulatory flow rate at front of each entry can be calculated with Equations [5.13] with those selected maximum AM, PM and Saturday peak hour traffic volume data, which will later be used in the model application process at the actual site.

The inscribed circle diameter D_c range used for the right-angle roundabout case is between 45- 55 m, while for skewed-angle roundabout cases the range used in the model is 45- 65 m.

Table 7.1 Input geometric parameter range for proposed site roundabout.

Geometric parameter of roundabout			Minimum limits (m)	Maximum limits (m)	Used range
Inscribed circle diameter		D_c	45	65	45-55
Design vehicle		WB-15 (WB-50)			
Entry width	Approach leg-1	E_{w1}	7.3	13.5	7.3-13.5
	Approach leg-2	E_{w2}	7.3	14.0	7.3-14.0
	Approach leg-3	E_{w2}	7.3	13.5	7.3-13.5
	Approach leg-4	E_{w4}	7.3	13.5	7.3-13.5
Circulatory width		E_{w4}	9.8	$1.2E_{wmax}$	
Design entry speed (km/hr.)		E_{w4}	40	48	40-48
Approach Flaring Length		F	25	100	25-100
Approach half width	Approach leg-1	W_1	7.3	9.0	7.3-9.0
	Approach leg-2	W_2	7.3	8.5	7.3-8.5
	Approach leg-3	W_3	7.3	8.0	7.3-8.0
	Approach leg-4	W_4	7.3	9.5	7.3-9.5
Queue Length		Q_{max}		90	
Average intersection delay (sec)		DATI	7.0	9.0	7.0-9.0
Relative speed difference (km/hr.)		MSD	10	20	10-20
Entry Angle (i=1, 2, 3, 4) degree		P_i	20	40	20-40
Super elevation		e	± 0.02		
Skewed-angle		θ_i	0°	20°	15°
Average entry radius	Approach leg-1	AER_1	30	85	30-85
	Approach leg-2	AER_2	20	85	20-85
	Approach leg-3	AER_3	30	85	30-85
	Approach leg-4	AER_4	20	85	20-85
Average exit radius	Approach leg-1	AXR_1	35	75	35-75
	Approach leg-2	AXR_2	35	75	35-75
	Approach leg-3	AXR_3	35	75	35-75
	Approach leg-4	AXR_4	35	75	35-75
Left turn entry radius	Approach leg-1	R_{81}	15	80	15-80
	Approach leg-2	R_{82}	20	80	20-80
	Approach leg-3	R_{83}	20	80	20-80
	Approach leg-4	R_{84}	15	80	15-80
Left turn exit radius	Approach leg-1	R_{91}	20	80	20-80
	Approach leg-2	R_{92}	30	80	30-80
	Approach leg-3	R_{93}	20	80	20-80
	Approach leg-4	R_{94}	30	80	30-80

Table 7.2 Input traffic data for proposed site roundabout.

Traffic Volume		Unit	LEG (1)	LEG (2)	LEG (3)	LEG (4)	Remarks
Through traffic volume [Qt_i]	AM	Pec/hr	110	547	269	556	
	PM	Pec/hr	268	610	164	690	
	Sat	Pec/hr	134	176	195	290	
Max. TH. traffic volume		Pec/hr	268	610	269	690	Selected values
Right turn traffic volume [Qr_i]	AM	Pec/hr	148	70	95	194	
	PM	Pec/hr	209	222	109	148	
	Sat	Pec/hr	224	135	148	69	
Max. RT. traffic volume		Pec/hr	224	222	148	194	Selected values
Left turn traffic volume [QL_i]	AM	Pec/hr	92	215	124	61	
	PM	Pec/hr	105	216	127	163	
	Sat	Pec/hr	35	100	140	72	
Max. LT. traffic volume		Pec/hr	105	216	140	163	Selected values
U-turn traffic volume	QU_i	Pec/hr	0	0	0	0	
Circulatory flow rate at front of entry (i) [Qc_i]	AM	Pec/hr	741	536	854	608	
	PM	Pec/hr	980	163	931	507	
	Sat	Pec/hr	502	241	861	345	
Max. Cir. traffic volume		Pec/hr	993	536	931	625	Selected values
$P_{ei} = 0.99, VC_i = 0.85, M_{vLv} = 1400 \text{ Kg}, M_{vHv} = 11000 \text{ Kg}$							

7.3 SENSITIVE ANALYSIS

The results from the optimization model vary because they depend on the design requirements, and geometric and traffic volume conditions. As long as the requirements for design consistency are enhanced, the operation of the roundabout is affected. Therefore, a sensitive analysis is required to find a balanced design. A balanced design is one which contains the effects of both average intersection delay and speed consistency. When the value of the sensitive analysis factor α is equal to 0.5 the weight of the design consistency and the average intersection delay model the same way. The model results are then collected for different values of (α) and compared to determine the best design based on operational performance and safety.

7.3.1 Right-angle roundabout sensitive analysis

Table 7.3 Comparison of the sensitive analyses for a right-angle roundabout.

Analysis serial number		1	2	3	4
Mean speed difference (km/hr.)	MSD	15	16	18	15
Avg. intersection delay (s)	$DATI_{max}$	6.0	5.0	7.0	6.0
Sensitive analysis factor	α	0.5	0.5	0.5	1.0
Resulted Avg. intersection delay (s)	$DATI_{rslt}$	2.78	2.785	2.795	2.79
Resulted mean speed difference (km/hr.)	MSD_{rslt}	10.40	10.30	10.09	10.45
Average delay at each leg (s)	De_1	3.09	3.09	3.10	3.05
	De_2	2.47	2.47	2.445	2.47
	De_3	3.15	3.15	3.16	3.15
	De_4	2.57	2.57	2.57	2.56
Effective entry capacity at each approach	C_{ee1}	1188	1188	1185	1188
	C_{ee2}	1522	1515	1510	1515
	C_{ee3}	1165	1165	1161	1165
	C_{ee4}	1467	1467	1465	1468
Degree of saturation at each approach	VC_1	0.238	0.238	0.239	0.238
	VC_2	0.345	0.345	0.345	0.340
	VC_3	0.241	0.238	0.239	0.238
	VC_4	0.351	0.352	0.355	0.345
Queue length at each approach (m)	Q_1	2.050	2.050	2.060	2.050
	Q_2	3.480	3.480	3.510	3.480
	Q_3	1.630	1.640	1.630	1.630
	Q_4	2.320	2.320	2.320	2.30
Entry width (m)	Ew_1	13.50	13.50	13.50	13.50
	Ew_2	14.00	14.00	14.00	14.00
	Ew_3	13.50	13.50	13.50	13.50
	Ew_4	13.50	13.50	13.50	13.50
Inscribed circle diameter (m)	D_c	48.89	48.89	49.63	49.133
Circulatory width (m)	C_w	9.80	9.80	9.80	9.92
Average entry radius	AER_1	36.76	36.76	35.97	35.623
	AER_2	38.45	38.42	37.61	37.228
	AER_3	35.79	35.79	36.00	35.618
	AER_4	35.73	35.73	38.44	37.97
Average exit radius	AXR_1	35.79	35.79	36.00	37.22
	AXR_2	35.73	35.73	38.44	37.97
	AXR_3	37.23	39.77	37.03	36.08
	AXR_4	39.24	39.28	37.62	39.25
Right turn radius	R_{51}	17.71	17.71	18.23	17.65
	R_{52}	18.81	18.80	19.36	18.76
	R_{53}	17.71	17.71	18.23	17.67
	R_{54}	18.80	19.36	18.76	19.36

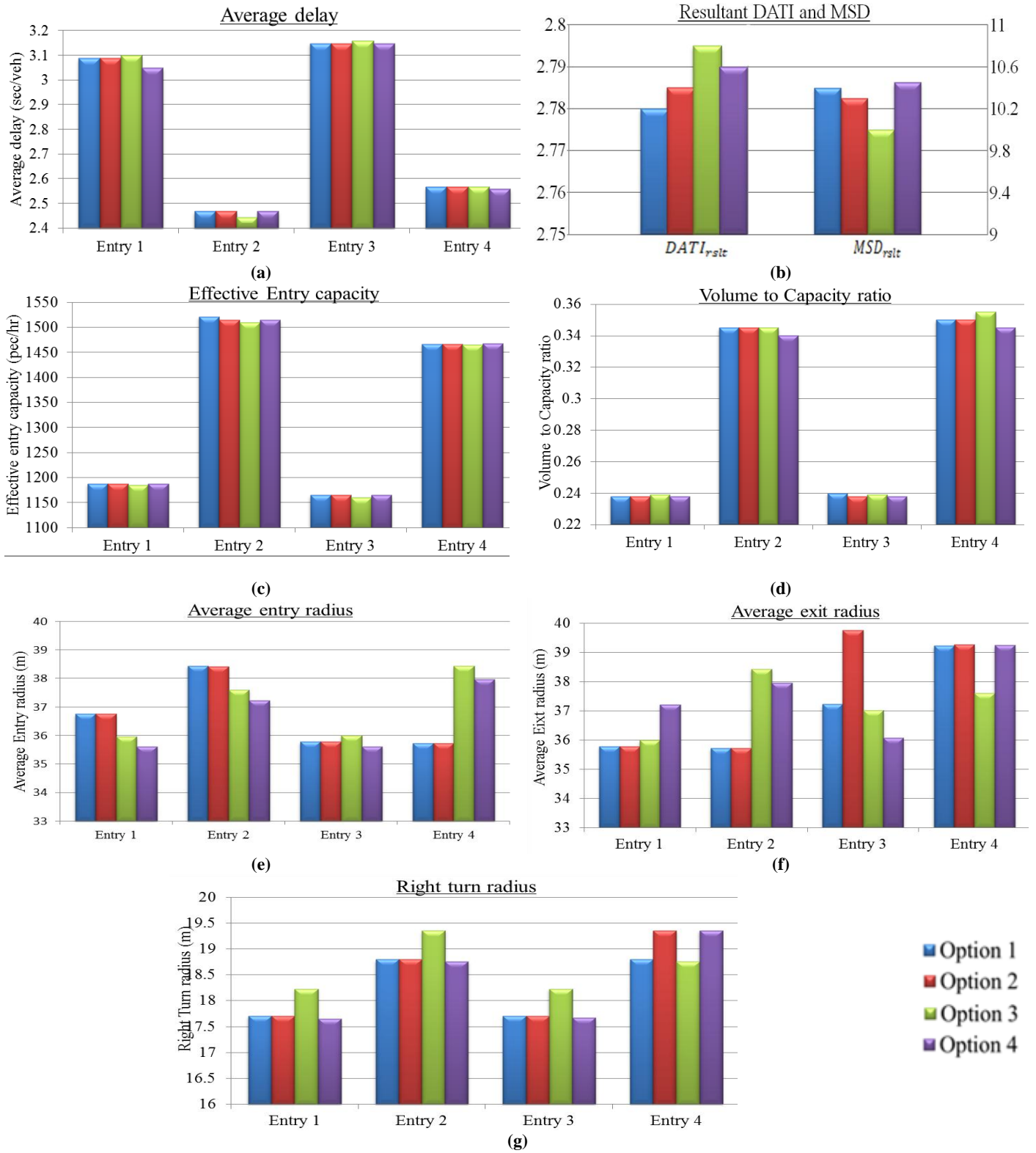


Figure 7.3 Graphical comparison of the sensitive analyses for a right-angle roundabout.

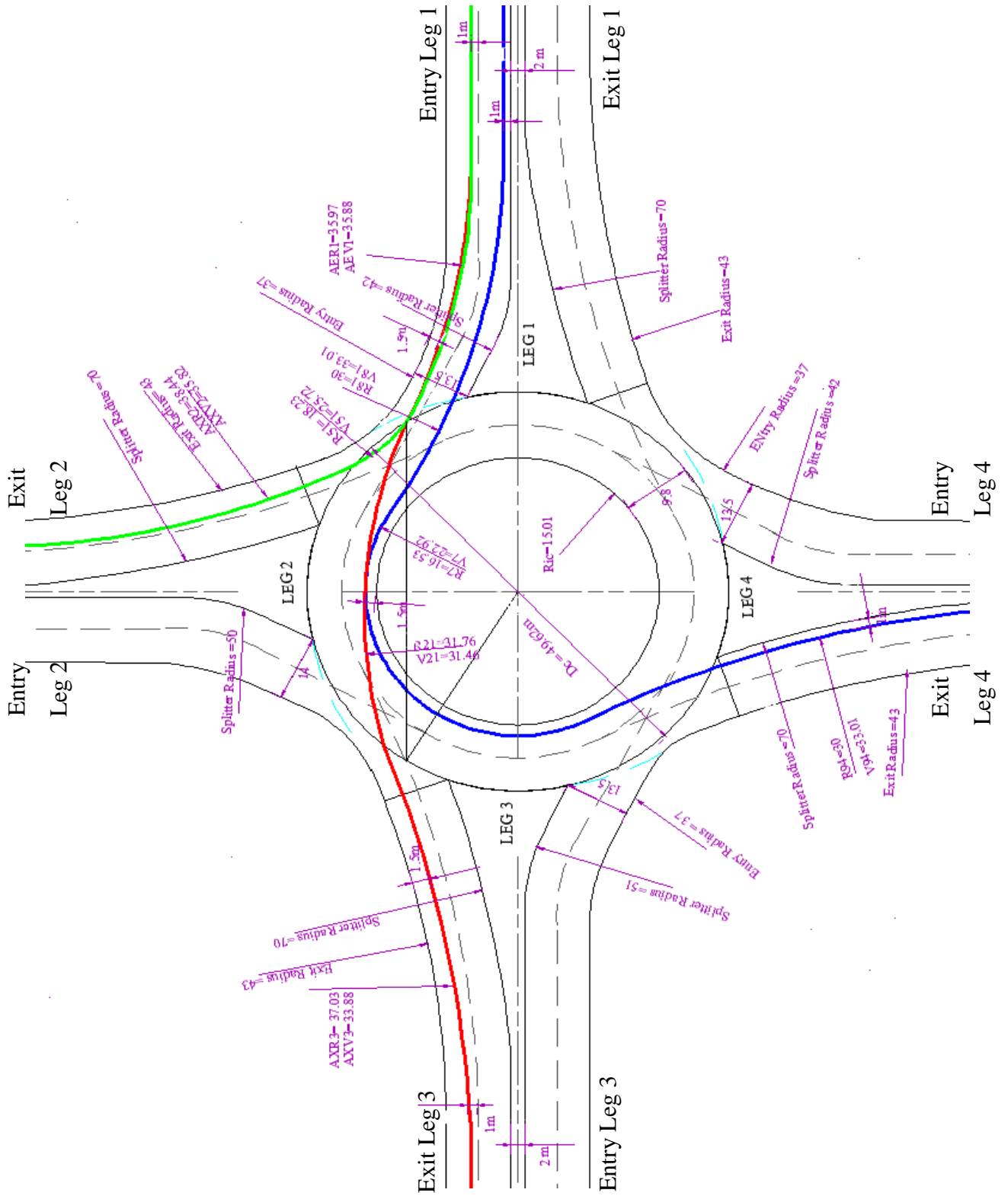


Figure 7.4 Drawing of a right-angle dual-lane roundabout.

In the right-angle roundabout intersection of the purposed location there is a need to perform sensitivity analysis. Table 7.3 represents the sensitive analysis for right-angle dual-lane roundabouts. The first analysis was performed for equal weights of MSD and $DATI_{max}$ at a V_{max} of 48 km/hr. The resultants values of $DATI_{rslt}$ and MSD_{rslt} are acceptable. The second analysis was performed with a larger MSD and smaller $DATI_{max}$ for equal weights of MSD and $DATI_{max}$ at a V_{max} of 48 km/hr. Here, the results shows that $DATI_{rslt}$ and MSD_{rslt} remain unchanged. In a third analysis, an increase in MSD and $DATI_{max}$ values result in a drop in delay and mean speed difference. The fourth analysis, performed for the 100% weights of MSD results in an increase in delay and means speed difference. A graphical comparison is shown in Figure 7.3, where the comparisons of average delay, effective entry width, velocity to capacity ratio, average entry radius, average exit radius and right turn radius are shown for each option of analysis at each approach leg of a right-angle dual-lane roundabout. According to the analyses in Figure 7.3, the third sensitivity analysis gives the best design for the given site data. The third analysis has a lower mean speed difference while the delay is comparably the same. The results are nearly comparable for each because the geometric data is nearly the same for all approaches due to symmetrical behavior of a right-angle dual-lane roundabout. The geometry of analysis three is illustrated in Figure 7.4, which was created with the help of AutoCAD software.

Another sensitivity analysis for a skewed-angle roundabout case was done with the same input geometric data from Table 7.1 and traffic data from Table 7.2. The results are shown in Table 7.4. Here, both the second and fourth analyses are the best options when considering the mean speed difference and average delay for the given site data. The second analysis is based on a speed limit of 50 km/hr, while fourth analysis is based on 55 km/hr. With an increase in speed limit there is an increase in radius and speed between the vehicle path, and a reduction in queue length and delay at each approach. A graphical analysis has been done of all approaches for all options in Figure 7.7. When comparing both the second and fourth analyses, can also be seen that if all other conditions are the same, an increase in maximum entry speed limit results in a reduction in the average delay, mean speed difference, volume to capacity ratio, and queue length, while improving the effective entry capacity, average entry and exit radii, and right turn radius (Figure 7.5).

Similarly a sensitive analysis carried out for weightage factor as shown in Figure 7.5. It also indicates that to achieve the minimum mean speed difference and minimum average delay, the multi-objective optimization model results in larger entry widths, circulating width, entry and exit radii, entry and exit speeds, and effective entry capacity, and a smaller circulatory width, inscribed circular diameter, central island radius, average overall delay, velocity to capacity ratio and individual delay at each entry approach.

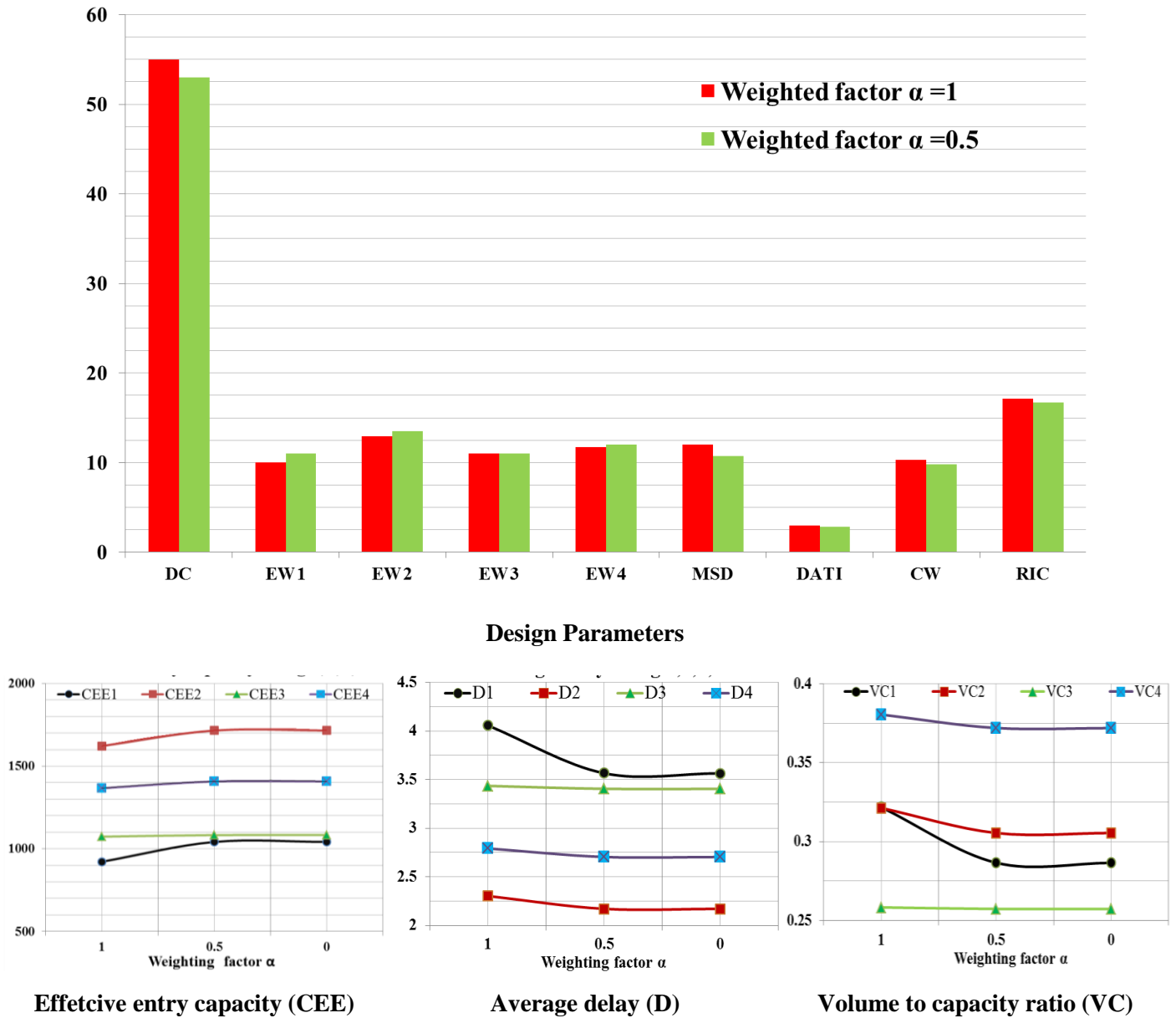


Figure 7.5 Effect of weighted factor α on multi-objective optimization model analysis.

In the case of dual-objective problems, informing the decision maker concerning the Pareto frontier is usually carried out by its visualization: the Pareto frontier, often named the tradeoff curve in this case, can be drawn at the objective plane. Figure 7.6 shows the graphical representation of that's actually what a multi-objective solution obtain. The graphical tradeoff curve is plot between two objectives as in the model one is mean speed difference M_{SD} , and the second objective is average roundabout delay $DATI$, as we change weighted factor α on multi-objective optimization model analysis from 0 to 1.

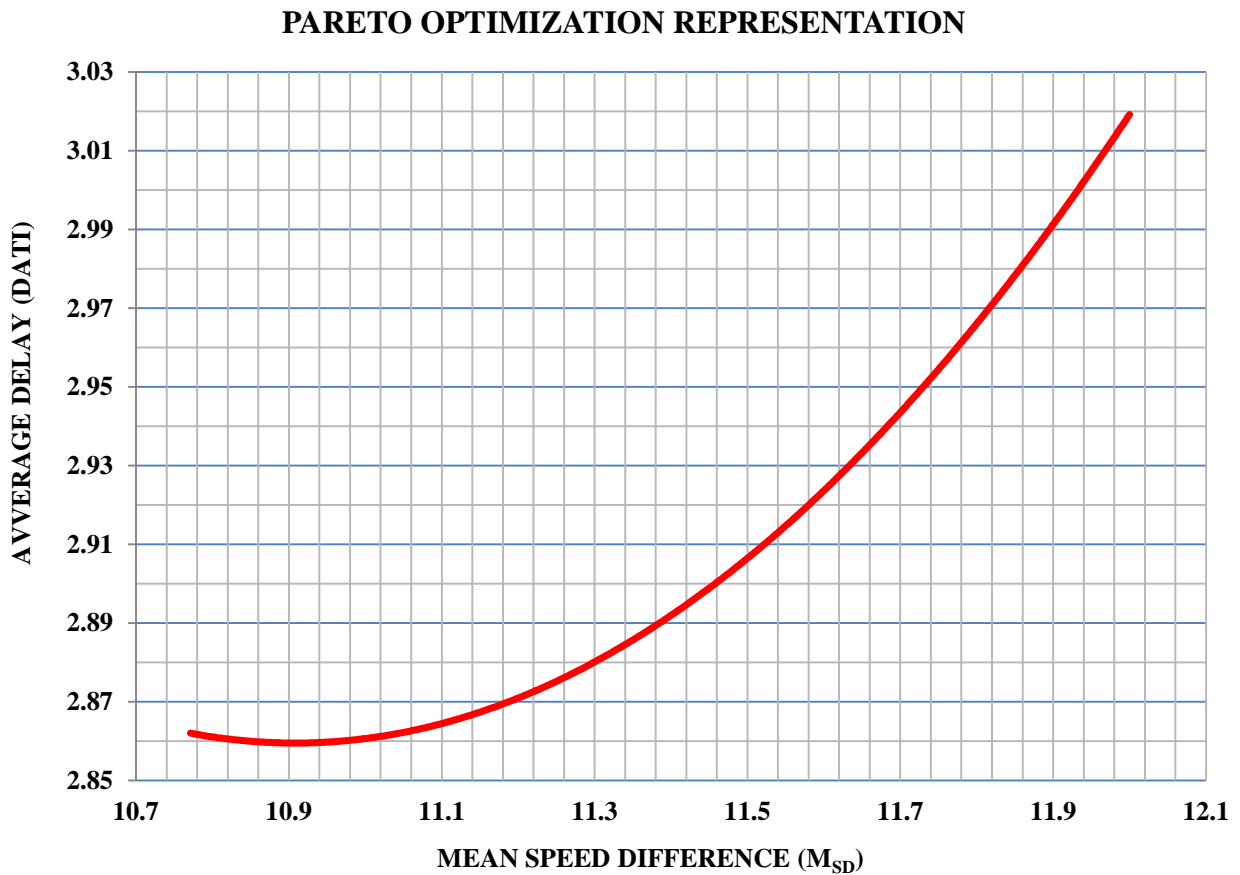


Figure 7.6 Graphical representation of multi-objective optimization function.

The tradeoff curve as shown in Figure 7.6 gives full information on objective values and on objective tradeoffs, which inform how improving one objective is related to deteriorating the second one while moving along the tradeoff curve.

7.3.2 Skewed-angle roundabout sensitive analysis

Table 7.4 Comparison of the sensitive analyses for a skewed-angle roundabout.

Analysis serial number		1	2	3	4
Mean speed difference (km/hr.)	MSD	20	21	21	21
Avg. intersection delay (s)	$DATI_{max}$	6.0	5.0	5.0	5.0
Sensitive analysis factor	α	0.5	0.5	0.3	0.5
Maximum entry speed (km/hr)	V_{max}	50	50	55	55
Result Avg. intersection delay (s)	$DATI_{rslt}$	2.71	2.69	2.34	2.34
Resulted Mean speed difference (km/hr.)	MSD_{rslt}	18.06	18.77	20.99	20.67
Average delay at each leg (s)	De_1	3.00	3.00	2.47	2.47
	De_2	2.42	2.38	2.15	2.15
	De_3	3.04	3.03	2.52	2.52
	De_4	2.52	2.52	2.24	2.24
Effective entry capacity at each leg.	C_{ee1}	1230	1231	1483	1483
	C_{ee2}	1543	1566	1716	1719
	C_{ee3}	1208	1207	1450	1450
	C_{ee4}	1489	1504	1665	1668
Degree of saturation at each leg	VC_1	0.24	0.24	0.21	0.21
	VC_2	0.34	0.33	0.31	0.31
	VC_3	0.24	0.25	0.19	0.19
	VC_4	0.39	0.39	0.31	0.31
Queue Length (m)	Q_1	1.97	1.97	1.48	1.48
	Q_2	3.38	3.28	2.75	2.75
	Q_3	1.55	1.55	1.21	1.21
	Q_4	4.15	4.06	3.28	3.28
Entry width (m)	EW_1	13.5	13.5	13.5	13.5
	EW_2	13.5	13.5	14.0	14.0
	EW_3	13.5	13.5	13.5	13.5
	EW_4	13.5	13.5	13.5	13.5
Inscribed circle diameter (m)	D_c	57.00	56.98	65.00	65.00
Average entry radius	AER_1	41.74	40.80	42.36	42.36
	AER_2	44.76	46.51	56.97	56.97
	AER_3	41.55	40.62	42.36	42.36
	AER_4	44.64	46.39	57.35	57.35
Average exit radius	AXR_1	41.56	40.63	42.36	42.36
	AXR_2	54.60	54.62	64.04	64.04
	AXR_3	41.74	40.80	42.36	42.36
	AXR_4	54.61	54.58	64.15	64.15
Right turn radius	R_{51}	54.33	54.33	64.08	64.08
	R_{52}	12.5	12.5	20.17	20.17
	R_{53}	54.33	54.33	64.08	64.08
	R_{54}	12.5	12.5	20.17	20.17

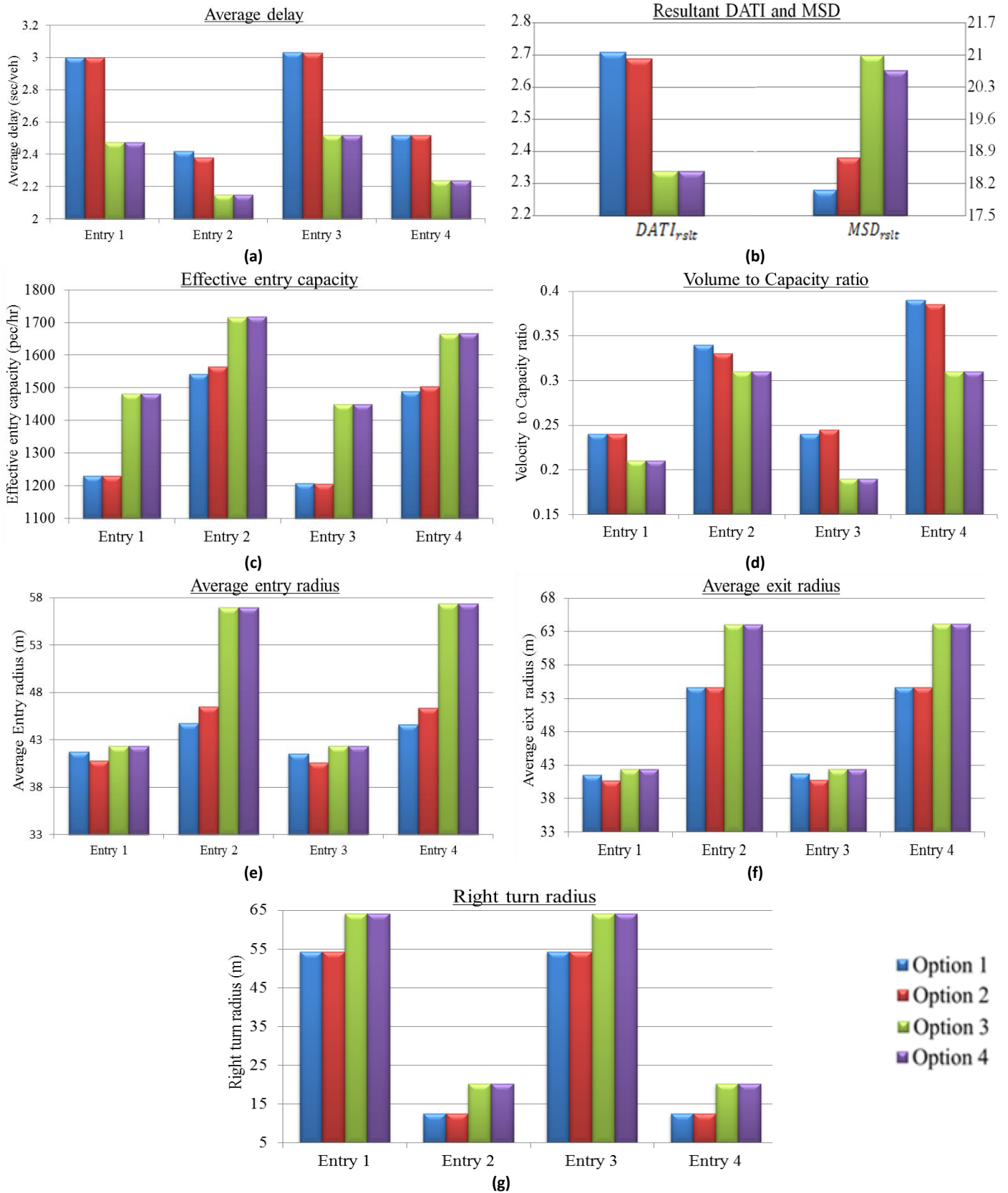


Figure 7.7 Graphical comparison of the sensitive analyses for a skewed-angle roundabout.

According to the graphical analysis of Figure 7.7, the fourth option is the best design for the given site data, if a skewed-angle roundabout is an acceptable approach towards design implementations. The geometry of the fourth option is illustrated in Figure 7.8, which was created with the help of AutoCAD software.

Paradigm Transportation Solutions Limited was retained by Sifton Properties Limited to conduct the Transportation Impact Study in November 2011 in support of the proposed development “Ira Needles Boulevard & Erb Street West Proposed Commercial Development Transportation Impact Study”. The purpose of the study was to determine the impact of the development on the surrounding roadway network. The operation of intersections in the study area was evaluated using the existing turning movement volumes. The results from this study are in Table 7.5.

Comparison	Paradigm Transportation Solutions Limited study in 2011	Right-angle roundabout Optimization model application results with 2011 traffic flow	Skewed-angle roundabout Optimization model application results with 2011 traffic flow
Overall delay (sec)	4.00	2.97	2.34
V/C ratio	0.34	0.30	0.26
Level of service	A	A	A

Table 7.5 Comparison of model results

7.4 RESULTS COMPARISON FOR SKEWED & RIGHT-ANGLE ROUNDABOUTS

Based on both sensitivity analyses of right-angle and skewed-angle roundabouts, a graphical comparison has been performed in Figure 7.9. This comparison is based on the average delay, mean speed difference, effective entry capacity, volume to capacity ratio, average entry and exit radii, right turn radius and inscribed circle diameter. It is observed that the average delay in the skewed-angle approach roundabout is less than in the right-angle approach roundabout, but the mean speed difference in a skewed-angle roundabout is higher than in a right-angle roundabout. As both consecutive approaches move apart there is an increase in effective entry capacity, volume to capacity ratio, average entry radius and average exit radius (Figure 7.9). In a right-angle roundabout the right turn radius is nearly comparable in all approaches, but it is a very sensitive element in skewed-angle roundabouts (Figure 7.9g).

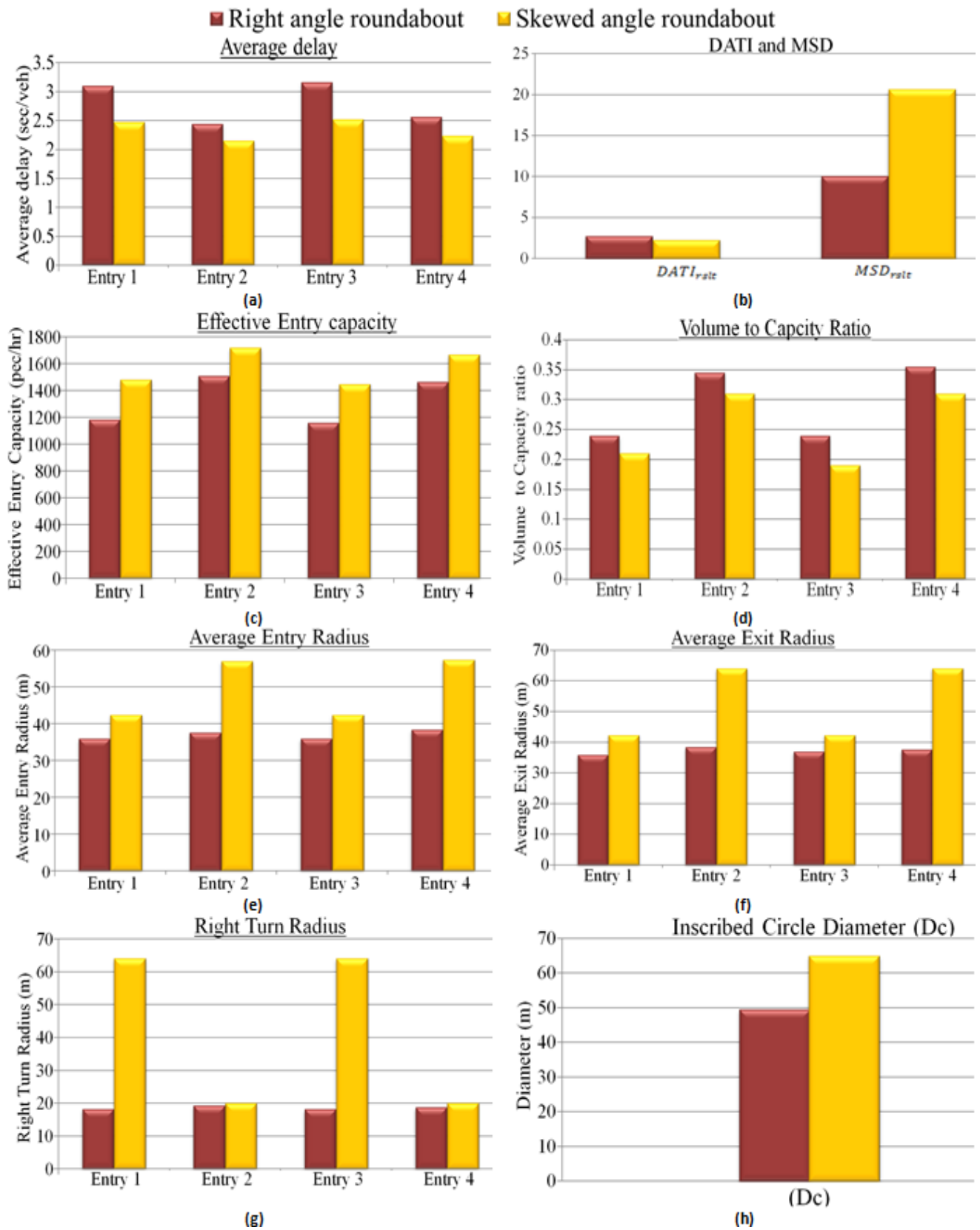


Figure 7.9 Graphical comparison of right-angle and skewed-angle roundabouts.

Figure 7.9g shows that both consecutive roundabout entries have different right turn radii. It is observed that when a vehicle enters a dual-lane skewed-angle roundabout from leg 1 or 3 turning right and exits at leg 2 or 4, respectively, deals with larger right turn entry, circulatory radius and exit radius. On the other hand, when a vehicle enters from leg 2 or 4 turning right and exits at leg 3 or 1, respectively, it deals with a smaller right turn entry, circulatory radius and exit radius. Therefore, the right turn radius needs to be constrained in the design by a vehicle minimum turning radius. Both right turning paths must be accommodated in the presence of other site constraints. Therefore, the inscribed circle diameter must be increased for skewed-angle roundabouts with the same site conditions as right-angle roundabouts (Figure 7.9h). The increase in diameter results in an increase in mean speed difference and a reduction in average delay. It also increases the vehicle path movement distance in an inscribed circle diameter area, which may result in more conflict with the other traffic movements.

CHAPTER 8 : CONCLUSIONS AND FUTURE RESEARCH

8.1 SUMMARY

Dual-lane roundabouts are successful at controlling traffic in high traffic volume intersections because of the slower entry speeds and fewer conflict points compared to an intersection with traffic lights. The all existing design approaches for dual-lane roundabouts use a trial-and-error procedure to choose the design parameters in order to satisfy design standards. An optimization model has been developed for only single-lane roundabouts at right angle approaches. Most desirable alignment for dual-lane roundabout is 90° approaches; however, it is observed that most of the intersections are not at right angle. If it is possible to re-arrange the approaches alignment of an intersection from skewed-angle to right angle then we go for right angle roundabout design otherwise we design the roundabout as skewed-angle roundabout. For a new intersection, it is preferred to construct a right angle roundabout. Currently most of the geometric design software in the field is based upon the trial and error methods. Dual-lane roundabouts designs require large numbers of calculations as compared to single-lane roundabouts; therefore, the design is best performed by an optimization computer program. An optimization technique is one of the modern programming techniques for geometric design of roundabouts, which is used to determine decision variables (entry width, inscribed circle diameter, central island diameter, circulatory width, entry and exit radii), subject to certain constraints (site and geometric design standards) for a given objective function which includes design consistency and average intersection delay to satisfy the design requirements of roundabouts. Therefore, an optimization model for dual-lane roundabouts design has been developed in this research, which gives more accurate results after thousands of trail in short time as compare to other computerized software which is based on trial and error method and time consuming.

The main focus point of this thesis is the development of an optimization model for the geometric design of a dual-lane roundabout in both the right-angle and skewed-angle approaches. Therefore in this thesis two cases will be discussed:

- 1) The optimization model for right-angle dual-lane roundabouts

- 2) The optimization model for skewed-angle dual-lane roundabouts where approaches intersect in the 70° to 110° range.

In the first case the developed optimization model can only be utilized for right-angle dual-lane roundabouts geometric design. As it was observed that most roundabout intersections in the field are not at right-angle, and in fact contain some intersection angle between intersecting approach legs other than 90° , the right-angle optimization model was future extended to include skewed-angle dual-lane roundabout cases. In skewed-angle roundabout cases two sub-models were created. Sub-model 1 is for drivers who enter the roundabout and exit at an intersection leg which is skewing away from the driver. Sub-model 2 was created for drivers who enter the roundabout and exit through leg which is skewing towards the driver. The advantage of a skewed-angle optimization model is that it can also be utilized for right-angle roundabouts design by inputting the value of the intersection angle equal to zero in the model.

Lingo 13 extended, optimization software was used in this thesis to develop an optimization model of dual-lane roundabouts design. It directly provides the optimum design for dual-lane roundabouts subjected to a wide variety of geometric and operational constraints. These models calculate design limits for the utmost design consistency and least average intersection delay for dual-lane roundabouts. The models also calculate the vehicle path radii for through, left, and right turn traffic paths, which can further be used to determine the operating speed along each traffic path at all entry roundabout approaches. The design consistency of an individual path is considered by minimizing the relative difference of speed along each vehicle path at all approaches. The operational analysis gives an estimation of the capacity and level of the performance in terms of queue length and delay. This model inputs site conditions and design vehicles, and provides to the utmost design consistency the least average intersection delay for given traffic and geometric circumstances. It also takes into account the effects of flaring length, entry radius, intersection angle, safety of pedestrians, bicycle safety, geometry, entry width, inscribed circle diameter, central island, exit radius and senior drivers. In addition, it also accommodates vehicles with large turning radii such as trucks, buses, and tractor-trailers.

These optimization models are nonlinear models and they are extremely complex to solve. By definition, all constraints that are not linear are nonlinear constraints. Nonlinear expressions include relationships in which variables are squared, cubed, taken to powers other

than one, or multiplied or divided by each other. Models with nonlinear expressions are much more difficult to solve than linear models. Unlike linear models, nonlinear models may prevent LINGO from finding a solution, though one exists. LINGO may find a solution to a nonlinear model that appears to be the "best", even though a better one may exist. These results are obviously undesirable. In this research model the constraints are non-linear. When LINGO finds a solution to a linear optimization model, it is the definitive best solution-we say it is the global optimum. The ability to obtain a globally optimal solution is attributable to certain properties of linear models. LINGO can automatically linearize a number of nonlinear relationships through the addition of constraints and integer variables so that the transformed linear model is mathematically equivalent to the original nonlinear model. Determining the convexity of a multiple variable problem is not an easy task. However, the model is convex for a minimization problem, Therefore I can ensure that any solution I reach is a global optimum (including nonlinear models).

Multi-objective optimization (or multi-objective programming or "pareto optimization"), also known as multi-criteria or multi-attribute optimization, is the process of simultaneously optimizing two or more conflicting objectives subject to certain constraints. This model has the multi-objective optimization function which comprises two objectives speed consistency and average intersection delay. The model measures speed consistency in terms of the mean speed difference of consecutive and conflicting speeds. The model performs operational analyses to calculate the capacity, queue length, delay and degree of saturation at each approach. The model will decide the best fit values for the design elements of the roundabout which gives the optimum solution. A single aggregate objective function (AOF) is constructed in this model for finding a solution to a multi-objective optimization problem. This is an intuitive approach to solving the multi-objective problem. The basic idea is to combine all of the objectives into a single objective function, called the AOF, such as the well-known weighted linear sum of the objectives. This objective function is optimized subject to technological constraints specifying how much of one objective must be sacrificed, from any given starting point, in order to gain a certain amount regarding the other objective. Often the aggregate objective function is not linear in the objectives, but rather is non-linear, expressing increasing marginal dissatisfaction with greater incremental sacrifices in the value of either objective. Furthermore, sometimes the aggregate objective function is additively separable, so that it is expressed as a weighted average of a non-

linear function of one objective and a non-linear function of another objective. Then the optimal solution obtained will depend on the relative values of the weights specified. The weighted sum method, like any method of selecting a single solution as preferable to all others, is essentially subjective, in that a decision manager needs to supply the weights. Moreover, this approach may prove difficult to implement if the Pareto frontier is not globally convex and/or the objective function to be minimized is not globally concave.

For the field application of these roundabout models, the input traffic and geometric data ranges for a proposed site (IRA NEEDLES at ERB St. Region of Waterloo) were used to design the dual-lane roundabout. The same traffic and geometric data were used for both right-angle and skewed-angle roundabout models. After getting the results from the model, a sensitive analysis was carried out for both models and the best design was selected for the right-angle roundabout and skewed-angle roundabout options. The right-angle and skewed-angle roundabout results chosen by the model were compared with the actual operational study done by Paradigm Transportation Solutions Limited with RODAL software in November 2011. It was observed that the results were comparable.

In a skewed-angle roundabout, when the intersection angle between intersection legs varies from 70° to 110°, there is a need to increase the inscribed circle diameter and speed limits. This is because one leg's right turn circular radius and speed increases, while the other leg's right turn radius in circular radius and speed decreases while the total intersection delay is reduced. The model satisfied all constraints and gave the global optimum results. This model can be used for any kind of dual-lane roundabouts whose approach legs intersect at 70° to 110° angles and both approaches intersect each other at one single point. This point should be the same as the center of the inscribed circle diameter of a roundabout. The results show that the entry speed of a skewed-angle dual-lane roundabout is greater than a right-angle dual-lane roundabout which results in an operational problem at roundabouts. The skewed-angle roundabout design does not encourage traffic to reduce speeds upon entry, can create abrupt or sudden speed changes with higher roadway speeds, and are typically reserved for low speed urban environments with extreme right-of-way constraints. Therefore, most roundabout specialists and roundabout savvy jurisdictions do not allow a skewed-angle roundabout design.

8.2 CONCLUSIONS

Based on this research the following conclusions can be made:

1. The roundabout design, especially the dual-lane roundabout design, is one of the most critical designs because it involves several conflicts that are not present in single-lane roundabouts. The models developed in this thesis can be used to design dual-lane roundabouts with or without right-angle approaches based on safety and operational performance. The model is programmed in such a manner that all design parameters work together to find an optimum design solution. Therefore, each parameter is intertwined with the other; a change in one affects the other parameters. The user just needs to give the geometric parameters a range (entry widths, average entry and exit radii, inscribed circle diameter, flare length, half entry width and consecutive approaches intersection angle) as well as traffic volume details for each approach.
2. These models are able to calculate the best design values for entry and exit widths, flare length, deflection angles of each vehicle path, entry angle for each vehicle path, all vehicle path radii at entry, exit and around a central island, delay, average delay and queue length, entry capacity and effective capacities, entry flow in each lane, conflicting flow at front of each approach, volume to capacity ratios, vehicle speed along each vehicle path radii at each approach of dual-lane roundabout. The models are a valuable achievement in the design of roundabouts because it saves time and effort.
3. The vehicle path radii along each path are modeled in such a way that they depend only on the roundabout geometry of the specially inscribed circle diameter. The model uses radii from the modeled vehicle paths to check the design's consistency with respect to the given constraints values during the optimization process. In this way it eliminates the iterative design process, which is time consuming.
4. The sensitivity analysis helps in selecting the best design option based on the given objective function and established data ranges. The model can help optimize the existing design of dual-lane roundabouts. This model can forecast future requirements with the change of traffic volume condition.
5. It has been observed that an increase in the angle between approach legs causes the relative speed difference between the conflicting radii paths to increase. It has also been observed that as the alignment of a roundabout changes from right-angle to skewed-angle, the

geometry of the roundabout requires a larger inscribed circle diameter and entry width to compensate for the effects of a skewed-angle between the consecutive approaches. In the case of skewed-angle roundabouts, it has also been observed that if all other conditions are the same, an increase in maximum entry speed limit results in a reduction in average delay, mean speed difference, volume to capacity ratio, and queue length, while improving effective entry capacity, average entry and exit radii and right turn radius.

6. From the comparison of skewed and right-angle roundabouts models results, it has been observed that the average delay at the skewed-angle roundabout is less than the right-angle roundabout, but the mean speed difference at the skewed-angle roundabout approach is higher than the right-angle roundabouts. As both consecutive approaches move apart there are increases in the effective entry capacity, volume to capacity ratio, average entry radius and average exit radius.
7. In the right-angle roundabout case the right turn radius is nearly comparable at all approaches, but it is very sensitive in skewed-angle roundabouts. Therefore, we need to accommodate both right turning paths in the presences of other site constraints, for which we need to increase the inscribed circle diameter for a skewed-angle roundabouts case with the same site conditions as a right-angle roundabouts. This increase in diameter results in an increase in mean speed difference and a reduction in average delay. It also increases the vehicle path movement distance in an inscribed circle diameter area when the vehicle starts moving from the entry point and then exits at the next consecutive approach point, which may cause more conflict with the other traffic movements. It has been observed that designing the approaches at perpendicular or near-perpendicular angles generally results in relatively slow and consistent speeds for all movements at all approaches. Highly skewed intersection angles can often require significantly larger inscribed circle diameters to achieve the speed objectives.
8. This model can be used with little modification for the optimization of roundabouts with different lane arrangements at each approach instead of a dual-lane at each approach. This model can be utilized for any kind of design vehicle with a constrained minimum turning radius. Many roundabouts site conditions have definite alignment and grade limitations on the intersection roads. However, it is often possible to modify the alignment and grades to

better suit traffic conditions and reduces hazards. For safety and economic reasons it is desirable that intersecting approaches meet at or near 90°.

8.3 FUTURE RESEARCH DIRECTIONS

1. A future extension of this model can be for multi-lane or turbo roundabouts, and it can be upgraded with the spiral shape design of the roundabout.
2. This model itself is the complete software required for roundabout optimum design with design consistency and operational performance objectives. The effect of roundabouts on pedestrians and cyclists demands remains an open question. This model can be upgraded by optimizing pedestrians' and cyclists' movements at the roundabout.
3. A modification in the model can be helpful in optimization of the roundabout for different types of lane arrangement at their entries.
4. This optimization model considers the safety in terms of design consistency, but safety can also be integrated into the model in additional measures, which requires additional research.
5. Although signing and pavement marking can play a strong role in enhancing driver understanding of multi-lane roundabouts, other traditional methods of educating motorists are also needed. Public education campaigns should be considered, involving brochures, websites, and other print and broadcast media.
6. Further research can be conducted to determine how this modeling formulation compares to other roundabouts designs models. There are currently several design softwares that can be used for modeling. Future research can be carried out to compare the optimization techniques of this software's model with those of other design software.
7. Future research in geometric design will likely involve a number of areas, such as human factors, smart technologies, design consistency, design flexibility, and reliability analysis. In particular, the link between geometric design and human factors (which contributes to 90% of road collisions) will require significant research efforts to improve our understanding of the close link between how roundabouts are built and how people use them. The dynamic nature of geometric design will aid in these developments.

8. Future research should be done to determine how vehicles truly travel in the circulatory roadway based on several factors including circulating volume, different traffic maneuvers, roundabout speed and geometry, and many others.

APPENDIX-A

Optimization model for right-angle dual-lane roundabouts

Consistency Measure

Fastest Through Path Modeling

$$\begin{aligned}H &= 0.19D_c + X_{ai} \\H_t &= R_{ic} + 1.52 \\M_o &= H_t - H \\R_{ic} &\geq H \\ \frac{L_2}{M_o} &= \frac{\sin\left[\frac{\Delta_{tc}}{2}\right]}{1 - \cos\left[\frac{\Delta_{tc}}{2}\right]} \\L_2 &= 0.4D_c \\R_2 &= \frac{L_2}{\left[\sin\left(\frac{\Delta_{tc}}{2}\right)\right]} \\V_2 &= 11.27\sqrt{[f_s - 0.02]R_2} \\B_iK_i &= [0.5D_c\sin[\theta_{1i}] - 0.5E_{wi} - n] \\K_iM_i &= \frac{[B_iK_i]}{[Tan[\Delta_{tei}]]} \\A_{mi} &= \left[\frac{\theta_{2i} - \theta_{1i}}{2}\right] \\\Delta_{tei} &= \left[\frac{\Delta_{tci}}{2}\right] + A_{mi} \\T_{1i} &= \sqrt{(B_iK_i)^2 + (K_iM_i)^2} \\L_{1i} &= T_{1i}\cos\left(\frac{\Delta_{tei}}{2}\right) \\R_{1i} &= \frac{L_{1i}}{\sin\left[\frac{\Delta_{tei}}{2}\right]} \\V_{1i} &= 11.27\sqrt{(f_s + 0.02)R_{1i}} \\\Delta_{tx[i+2]} &= \frac{\Delta_{tc}}{2} - A_{mi} \\O_{[i+2]}C_{[i+2]} &= [0.5D_c\sin[\theta_{2i}] - 0.5E_{wi} - n] + X_{ei} \\N_{[i+2]}O_{[i+2]} &= \frac{O_{[i+2]}C_{[i+2]}}{\tan[\Delta_{tx[i+2]}]} \\T_{3[i+2]} &= \sqrt{(O_{[i+2]}C_{[i+2]})^2 + (N_{[i+2]}O_{[i+2]})^2} \\L_{3[i+2]} &= T_{3[i+2]}\cos\left[\frac{\Delta_{tx[i+2]}}{2}\right] \\R_{3[i+2]} &= \frac{L_{3[i+2]}}{\sin\left[\frac{\Delta_{tx[i+2]}}{2}\right]} \\V_{3[i+2]} &= 11.27\sqrt{(f_s + 0.02)R_{3[i+2]}}\end{aligned}$$

Fastest Right Turn Path Curve Modeling;

$$\begin{aligned}[E_iB_i]^2 - [0.194D_c]^2 &= 0 \\L_{5i} &= 0.5E_iB_i \\M_{ri} &= 0.066C_w\end{aligned}$$

$$\begin{aligned}
\frac{L_{5i}}{M_{ri}} &= \frac{\sin\left(\frac{\Delta_{rci}}{2}\right)}{1 - \cos\left(\frac{\Delta_{rci}}{2}\right)} \\
\left[1 - \cos\left(\frac{\Delta_{rci}}{2}\right)\right] &> 0 \\
R_{5i} &= \frac{L_{5i}}{\sin\left(\frac{\Delta_{rci}}{2}\right)} \\
V_{5i} &= 11.27\sqrt{(f_s + 0.02)R_{5i}} \\
\theta_{ci} &= \frac{90 * 0.01745 - [\theta_{2[i+3]} + \theta_{1i}]}{2} \\
\theta_{ri} &= \theta_{ci} + \theta_{1i} \\
\Delta_{rei} &= [90 * 0.01745] - \theta_{ri} - \left[\frac{\Delta_{rci}}{2}\right] \\
B_i F_i &= [0.5D_c \sin[\theta_{1i}] - 0.5E_{wi} - n] + X_{ci} \\
F_i Q_i &= \frac{B_i F_i}{\left[Tan[\Delta_{rei}]\right]} \\
T_{4i} &= \sqrt{(B_i F_i)^2 + (F_i Q_i)^2} \\
L_{4i} &= T_{4i} \cos\left[\frac{\Delta_{rei}}{2}\right] \\
R_{4i} &= \frac{L_{4i}}{\sin\left[\frac{\Delta_{rei}}{2}\right]} \\
V_{4i} &= 11.27\sqrt{[f_s + 0.02]R_{4i}} \\
T_{[i+1]}E_{[i+1]} &= 0.5D_c \sin(\theta_{2[i+3]}) - 0.5E_{w[i+3]} - n + X_{fi} \\
T_{[i+1]}Y_{[i+1]} &= \frac{T_{[i+1]}E_{[i+1]}}{\left[Tan[\Delta_{rx[i+1]}]\right]} \\
T_{6[i+1]} &= \sqrt{(T_{[i+1]}E_{[i+1]})^2 + (T_{[i+1]}Y_{[i+1]})^2} \\
L_{6[i+1]} &= T_{6[i+1]} \cos\left[\frac{\Delta_{rx[i+1]}}{2}\right] \\
R_{6[i+1]} &= \frac{L_{6[i+1]}}{\sin\left[\frac{\Delta_{rx[i+1]}}{2}\right]} \\
V_{6[i+1]} &= 11.27\sqrt{[f_s + 0.02]R_{6[i+1]}}
\end{aligned}$$

Fastest Left Turn Path Curve;

$$\begin{aligned}
R_7 &= R_{ic} + 1.52 \\
c_i &= R_7 \left[\sqrt{2 - 2 \cos[\theta_{5i}]} \right] \\
d_i &= \sqrt{(R_7)^2 - \left(\frac{c_i}{2}\right)^2} \\
h_i &= R_7 - d_i \\
\theta_{5i} &= 2 \cos^{-1} \left[\frac{d_i}{R_7} \right] \\
G_i W_i &= R_7 \cos[\theta_{5i}] - n + X_{di} \\
W_i X_i &= 0.836R_{ic}
\end{aligned}$$

$$\begin{aligned}
W_i X_i &= \frac{G_i W_i}{\tan[\Delta_{Lei}]} \\
T_{8i} &= \sqrt{(G_i W_i)^2 + (W_i X_i)^2} \\
T_{8i} &= \frac{G_i W_i}{\sin[\Delta_{Lei}]} \\
L_{8i} &= T_{8i} * \cos\left[\frac{\Delta_{Lei}}{2}\right] \\
V_{8i} &= 11.27 \sqrt{[f_s + 0.02] R_{8i}} \\
e_{[i+3]} &= R_7 \left[\sqrt{2 - 2 \cos[\theta_{6[i+3]}} \right] \\
f_{[i+3]} &= \sqrt{(R_7)^2 - \left(\frac{e_{[i+3]}}{2}\right)^2} \\
g_{[i+3]} &= R_7 - f_{[i+3]} \\
\theta_{6[i+3]} &= 2 \cos^{-1} \left[\frac{f_{[i+3]}}{R_7} \right] \\
H_{[i+3]} U_{[i+3]} &= R_7 \cos[\theta_{6[i+3]}] - n \\
V_{[i+3]} U_{[i+3]} &= 0.6 R_{ic} \\
V_{[i+3]} U_{[i+3]} &= \frac{H_{[i+3]} U_{[i+3]}}{\tan[\Delta_{Lx[i+3]}} \\
T_{9[i+3]} &= \sqrt{(V_{[i+3]} U_{[i+3]})^2 + (H_{[i+3]} U_{[i+3]})^2} \\
L_{9[i+3]} &= T_{9[i+3]} * \cos\left[\frac{\Delta_{Lx[i+3]}}{2}\right] \\
R_{9[i+3]} &= \frac{L_{9[i+3]}}{\sin\left[\frac{\Delta_{Lx[i+3]}}{2}\right]} \\
V_{9[i+3]} &= 11.27 \sqrt{[f_s + 0.02] R_{9[i+3]}} \\
AER_i &= \left[\frac{R_{1i} + R_{4i}}{2} \right] \\
AXR_{[i+2]} &= \left[\frac{R_{6[i+2]} + R_{3[i+2]}}{2} \right] \\
AEV_i &= \left[\frac{V_{1i} + V_{4i}}{2} \right] \\
AXV_{[i+2]} &= \left[\frac{V_{6[i+2]} + V_{3[i+2]}}{2} \right] \\
V_{j[i]} &= 11.27 \sqrt{[f_s \pm e] R_{j[i]}} \\
[V_{ji}] &\leq V_{max} \\
AEV_i - V_{2i} - M_{1i} + M_{2i} &= 0 \\
AXV_{[i+2]} - V_{2i} - M_{3i} + M_{4i} &= 0 \\
AEV_i - V_{5i} - M_{5i} + M_{6i} &= 0 \\
AXV_{[i+1]} - V_{5i} - M_{7i} + M_{8i} &= 0 \\
V_7 - V_{8i} - M_{9i} + M_{10i} &= 0 \\
V_{9i} - V_7 - M_{11} + M_{12i} &= 0
\end{aligned}$$

$$\begin{aligned}
V_2 - V_7 - M_{13} + M_{14} &= 0 \\
V_2 - V_{5i} - M_{15i} + M_{16i} &= 0 \\
V_{8i} - V_2 - M_{17i} + M_{18i} &= 0 \\
V_{9i} - V_2 - M_{19i} + M_{20i} &= 0 \\
V_{4i} - V_{5i} - M_{21i} + M_{22i} &= 0 \\
V_{6i} - V_{5i} - M_{23i} + M_{24i} &= 0 \\
V_{8i} - V_{9[i+1]} - M_{25i} + M_{26i} &= 0 \\
V_{4i} - V_2 - M_{27i} + M_{28i} &= 0 \\
[M_{ji}, M_{[j+1]i}] &\leq M_{SD} \\
\{[AER_i, AXR_i] > R_2\}, \quad \{AXR_i > AER_i\} \\
[R_2, R_{5i} \text{ and } R_7] &> 12.5m \\
[AXV_{[i+1]} > V_{5i}], \quad [AXV_i > V_2], \quad [V_{9i} > V_7]
\end{aligned}$$

Operational Measures;

$$\begin{aligned}
C_{ei[l,o]} &= K_{i[l,o]} [F_{ei} - F_{ci} Q_{ci}] \\
&\quad \text{BND}(0.9, K_{i[l,o]}, 1.1) \\
K_{oi} &= 1.151 - [0.00347P_i] - \left[\frac{0.978}{AER_i} \right] \\
K_{Ii} &= 1.151 - [0.00347P_i] - \left[\frac{0.978}{R_{8i}} \right] \\
F_{ei} &= 303 \left\{ 0.5W_i + \frac{0.5[E_{wi} - W_i]}{[1 + 2S_i]} \right\} \\
S_i &= \frac{1.6[E_{wi} - W_i]}{F_i} \\
F_{ci} &= 0.21 \left\{ 1 + \frac{0.5}{1 + \text{Exp} \left[\frac{Dc - 60}{10} \right]} \right\} \left\{ 1 + 0.2 \left[W_i + \frac{E_{wi} - W_i}{1 + 2S_i} \right] \right\} \\
C_{eei[l,o]} &= C_{ei[l,o]} P_{ei} \\
QT_{i_o} &= Qt_i + Qr_i \\
QT_{i_l} &= QL_i \\
Qe_i &= QT_{i_o} + QT_{i_l} \\
VC_{i[l,o]} &= \left[\frac{QT_{i[l,o]}}{C_{eei[l,o]}} \right] \\
De_{i[l,o]} &= \frac{3600}{C_{eei[l,o]}} + 900T_p \left[VC_{i[l,o]} - 1 + \sqrt{[VC_{i[l,o]} - 1]^2 + \frac{3600VC_{i[l,o]}}{450T_p C_{eei[l,o]}}} \right] \\
Q_{i[i,o]} &= 900T_p \left[VC_{i[i,o]} - 1 + \sqrt{[VC_{i[i,o]} - 1]^2 + \frac{3600VC_{i[i,o]}}{450T_p C_{eei[i,o]}}} \right] \left[\frac{3600}{C_{eei[i,o]}} \right] \\
Q_{i[i,o]} &< Q_{max_i} \\
VC_i &< VC_{max} \\
DeT_{[l,o]i} &= De_{[l,o]i} * QT_{[l,o]i}
\end{aligned}$$

Objective function;

$$DATI = \frac{\sum_{i=1}^4 [DeT_{[L,o]_i}]}{\sum_{i=1}^4 Qe_i}$$

$$Min = \alpha M_{SD} + (1-\alpha)DATI$$

APPENDIX-B

Optimization model for skewed-angle dual-lane roundabouts

Consistency Measure

Fastest Through Path Modeling

$$\bar{H}_i = 0.19D_c + X_{ai}$$

$$\bar{H}_{ti} = R_{ic} + 1.52$$

$$\bar{M}_{oi} = \bar{H}_{ti} - \bar{H}_i$$

$$R_{ic} \geq \bar{H}_i$$

$$\frac{\bar{L}_{2i}}{\bar{M}_{oi}} = \frac{\left[\sin\left(\frac{\Delta_{tci}}{2}\right) \right]}{\left[1 - \cos\left(\frac{\Delta_{tci}}{2}\right) \right]}$$

$$L_{2i} = 0.4D_c$$

$$R_{2i} = \frac{L_{2i}}{\left[\sin\left(\frac{\Delta_{tci}}{2}\right) \right]}$$

$$V_{2i} = 11.27\sqrt{[f_s - 0.02]R_{2i}}$$

$$B_iK_i = [0.5D_c \sin[\theta_{1i}] - 0.5E_{wi} - n]$$

$$B_iK_i = [0.5D_c \sin[\theta_{1i} - \theta_l] - 0.5E_{wi} - n]$$

Sub-model 1 “i” = 1 , 3

Sub-model 2 “i” = 2 , 4

$$K_iM_i = \frac{[B_iK_i]}{[Tan[\Delta_{tei}]]}$$

$$A_{mi} = \left[\frac{\theta_{2i} - \theta_{1i}}{2} \right]$$

$$\Delta_{tei} = \left[\frac{\Delta_{tci}}{2} \right] + A_{mi}$$

$$T_{1i} = \sqrt{(B_iK_i)^2 + (K_iM_i)^2}$$

$$L_{1i} = T_{1i} \cos\left(\frac{\Delta_{tei}}{2}\right)$$

$$R_{1i} = \frac{L_{1i}}{\sin\left[\frac{\Delta_{tei}}{2}\right]}$$

$$V_{1i} = 11.27\sqrt{(f_s + 0.02)R_{1i}}$$

$$\Delta_{tx[i+2]} = \frac{\Delta_{tc}}{2} - A_{mi}$$

$$O_{[i+2]}C_{[i+2]} = [0.5D_c \sin[\theta_{2i}] - 0.5E_{wi} - n] + X_{ei}$$

$$O_{[i+2]}C_{[i+2]} = [0.5D_c \sin[\theta_{2i} + \theta_l] - 0.5E_{wi} - n] + X_{ei}$$

Sub-model 1 “i” = 1 , 3

Sub-model 2 “i” = 2 , 4

$$N_{[i+2]}O_{[i+2]} = \frac{O_{[i+2]}C_{[i+2]}}{\tan[\Delta_{tx[i+2]}]}$$

$$T_{3[i+2]} = \sqrt{(O_{[i+2]}C_{[i+2]})^2 + (N_{[i+2]}O_{[i+2]})^2}$$

$$L_{3[i+2]} = T_{3[i+2]} \cos\left[\frac{\Delta_{tx[i+2]}}{2}\right]$$

$$R_{3[i+2]} = \frac{L_{3[i+2]}}{\sin\left[\frac{\Delta_{tx[i+2]}}{2}\right]}$$

$$V_{3[i+2]} = 11.27\sqrt{(f_s + 0.02)R_{3[i+2]}}$$

Fastest Right Turn Path Curve Modeling;

$$[E_iB_i]^2 - \left[0.194D_c + \left(0.46\theta_l / 0.01745\right)\right]^2 = 0$$

Sub-model 1 “i” = 1 , 3

$$[E_i B_i]^2 - [0.2D_c + (0.37\theta_i/0.01745)]^2 = 0$$

$$L_{5i} = 0.5E_i B_i$$

$$M_{ri} = 0.066C_w + [0.00667\theta_i/0.01745]$$

$$M_{ri} = 0.066C_w - [0.00667\theta_i/0.01745]$$

$$\frac{L_{5i}}{M_{ri}} = \frac{\sin\left(\frac{\Delta_{rci}}{2}\right)}{1 - \cos\left(\frac{\Delta_{rci}}{2}\right)}$$

$$\left[1 - \cos\left(\frac{\Delta_{rci}}{2}\right)\right] > 0$$

$$R_{5i} = \frac{L_{5i}}{\sin\left(\frac{\Delta_{rci}}{2}\right)}$$

$$V_{5i} = 11.27\sqrt{(f_s + 0.02)R_{5i}}$$

$$\theta_{ci} = \frac{90 * 0.01745 - [\theta_{2[i+3]} + \theta_{1i}]}{2}$$

$$\theta_{ri} = \theta_{ci} + \theta_{1i}$$

$$\Delta_{rei} = [90 * 0.01745] - \theta_{ri} - \left[\frac{\Delta_{rci}}{2}\right]$$

$$B_i F_i = [0.5D_c \sin[\theta_{1i}] - 0.5E_{wi} - n] + X_{ci}$$

$$B_i F_i = [0.5D_c \sin[\theta_{1i} - \theta_i] - 0.5E_{wi} - n] + X_{ci}$$

$$F_i Q_i = \frac{B_i F_i}{\left[\tan[\Delta_{rei}]\right]}$$

$$T_{4i} = \sqrt{(B_i F_i)^2 + (F_i Q_i)^2}$$

$$L_{4i} = T_{4i} \cos\left[\frac{\Delta_{rei}}{2}\right]$$

$$R_{4i} = \frac{L_{4i}}{\sin\left[\frac{\Delta_{rei}}{2}\right]}$$

$$V_{4i} = 11.27\sqrt{[f_s + 0.02]R_{4i}}$$

$$T_{b[i+1]}E_{[i+1]} = 0.5D_c \sin(\theta_{2[i+3]} + \theta_i) - 0.5E_{w[i+3]} - n + X_{fi}$$

$$T_{b[i+1]}E_{[i+1]} = 0.5D_c \sin(\theta_{2[i+3]}) - 0.5E_{w[i+3]} - n + X_{fi}$$

$$T_{b[i+1]}Y_{[i+1]} = \frac{T_{b[i+1]}E_{[i+1]}}{\left[\tan[\Delta_{rx[i+1]}]\right]}$$

$$T_{6[i+1]} = \sqrt{(T_{b[i+1]}E_{[i+1]})^2 + (T_{b[i+1]}Y_{[i+1]})^2}$$

$$L_{6[i+1]} = T_{6[i+1]} \cos\left[\frac{\Delta_{rx[i+1]}}{2}\right]$$

$$R_{6[i+1]} = \frac{L_{6[i+1]}}{\sin\left[\frac{\Delta_{rx[i+1]}}{2}\right]}$$

$$V_{6[i+1]} = 11.27\sqrt{[f_s + 0.02]R_{6[i+1]}}$$

Sub-model 2 “i” = 2 , 4

Sub-model 1 “i” = 1 , 3

Sub-model 2 “i” = 2 , 4

Sub-model 1 “i” = 1 , 3

Sub-model 2 “i” = 2 , 4

Sub-model 1 “i” = 1 , 3

Sub-model 2 “i” = 2 , 4

Fastest Left Turn Path Curve;

$$R_7 = R_{ic} + 1.52$$

$$c_i = R_7 \left[\sqrt{2 - 2 \cos[\theta_{5i}]} \right]$$

$$d_i = \sqrt{(R_7)^2 - \left(\frac{c_i}{2}\right)^2}$$

$$h_i = R_7 - d_i$$

$$\theta_{5i} = 2\cos^{-1}\left[\frac{d_i}{R_7}\right]$$

$$G_i W_i = R_7 \cos[\theta_{5i}] - n + X_{di}$$

$$G_i W_i = R_7 \cos[90 * 0.01745 - \theta_i - \theta_{5i}] - n + X_{di}$$

$$W_i X_i = 0.836 R_{ic}$$

$$W_i X_i = 0.836 R_{ic} - 19.8324(\theta_i)$$

$$W_i X_i = \frac{G_i W_i}{\left[\tan[\Delta_{Lei}]\right]}$$

$$T_{8i} = \sqrt{(G_i W_i)^2 + (W_i X_i)^2}$$

$$T_{8i} = \frac{G_i W_i}{\sin[\Delta_{Lei}]}$$

$$L_{8i} = T_{8i} * \cos\left[\frac{\Delta_{Lei}}{2}\right]$$

$$V_{8i} = 11.27 \sqrt{[f_s + 0.02] R_{8i}}$$

$$e_{[i+3]} = R_7 \left[\sqrt{2 - 2 \cos[\theta_{6[i+3]}}] \right]$$

$$f_{[i+3]} = \sqrt{(R_7)^2 - \left(\frac{e_{[i+3]}}{2}\right)^2}$$

$$g_{[i+3]} = R_7 - f_{[i+3]}$$

$$\theta_{6[i+3]} = 2\cos^{-1}\left[\frac{f_{[i+3]}}{R_7}\right]$$

$$H_{[i+3]} U_{b[i+3]} = R_7 \cos[\theta_{6[i+3]} - \theta_i] - n$$

$$H_{[i+3]} U_{b[i+3]} = R_7 \cos[\theta_{6[i+3]}] - n$$

$$V_{[i+3]} U_{b[i+3]} = 0.6 R_{ic} + H_{[i+3]} U_{b[i+3]} \tan[\theta_i]$$

$$V_{b[i+3]} U_{[i+3]} = 0.6 R_{ic}$$

$$V_{[i+3]} U_{b[i+3]} = \frac{H_{[i+3]} U_{b[i+3]}}{\left[\tan[\Delta_{Lx[i+3]}]\right]}$$

$$T_{9[i+3]} = \sqrt{(V_{[i+3]} U_{b[i+3]})^2 + (H_{[i+3]} U_{b[i+3]})^2}$$

$$L_{9[i+3]} = T_{9[i+3]} * \cos\left[\frac{\Delta_{Lx[i+3]}}{2}\right]$$

$$R_{9[i+3]} = \frac{L_{9[i+3]}}{\sin\left[\frac{\Delta_{Lx[i+3]}}{2}\right]}$$

$$V_{9[i+3]} = 11.27 \sqrt{[f_s + 0.02] R_{9[i+3]}}$$

$$AER_i = \left[\frac{R_{1i} + R_{4i}}{2}\right]$$

$$AXR_{[i+2]} = \left[\frac{R_{6[i+2]} + R_{3[i+2]}}{2}\right]$$

$$AEV_i = \left[\frac{V_{1i} + V_{4i}}{2}\right]$$

Sub-model 1 “i”=1 , 3

Sub-model 2 “i”=2 , 4

Sub-model 1 “i”=1 , 3

Sub-model 2 “i”=2 , 4

Sub-model 1 “i”=1 , 3

Sub-model 2 “i”=2 , 4

Sub-model 1 “i”=1 , 3

Sub-model 2 “i”=2 , 4

$$\begin{aligned}
AXV_{[i+2]} &= \left[\frac{V_{6[i+2]} + V_{3[i+2]}}{2} \right] \\
V_{j[i]} &= 11.27 \sqrt{[f_s \pm e]R_{j[i]}} \\
[V_{ji}] &\leq V_{max} \\
AEV_i - V_{2i} - M_{1i} + M_{2i} &= 0 \\
AXV_{[i+2]} - V_{2i} - M_{3i} + M_{4i} &= 0 \\
AEV_i - V_{5i} - M_{5i} + M_{6i} &= 0 \\
AXV_{[i+1]} - V_{5i} - M_{7i} + M_{8i} &= 0 \\
V_7 - V_{8i} - M_{9i} + M_{10i} &= 0 \\
V_{9i} - V_7 - M_{11i} + M_{12i} &= 0 \\
V_2 - V_7 - M_{13i} + M_{14i} &= 0 \\
V_2 - V_{5i} - M_{15i} + M_{16i} &= 0 \\
V_{8i} - V_2 - M_{17i} + M_{18i} &= 0 \\
V_{9i} - V_2 - M_{19i} + M_{20i} &= 0 \\
V_{4i} - V_{5i} - M_{21i} + M_{22i} &= 0 \\
V_{6i} - V_{5i} - M_{23i} + M_{24i} &= 0 \\
V_{8i} - V_{9[i+1]} - M_{25i} + M_{26i} &= 0 \\
V_{4i} - V_2 - M_{27i} + M_{28i} &= 0 \\
[M_{ji}, M_{[j+1i]}] &\leq M_{SD} \\
V_{9i} - V_2 - M_{19i} + M_{20i} &= 0 \\
V_{4i} - V_{5i} - M_{21i} + M_{22i} &= 0 \\
V_{6i} - V_{5i} - M_{23i} + M_{24i} &= 0 \\
V_{8i} - V_{9[i+1]} - M_{25i} + M_{26i} &= 0 \\
V_{4i} - V_2 - M_{27i} + M_{28i} &= 0 \\
[M_{ji}, M_{[j+1i]}] &\leq M_{SD} \\
\{[AER_i, AXR_i] > R_2\}, \quad \{AXR_i > AER_i\} \\
[R_2, R_{5i} \text{ and } R_7] &> 12.5m \\
[AXV_{[i+1]} > V_{5i}], \quad [AXV_i > V_2], \quad [V_{9i} > V_7]
\end{aligned}$$

Operational Measures;

$$\begin{aligned}
C_{ei[l,o]} &= K_{i[l,o]} [F_{ei} - F_{ci} Q_{ci}] \\
&\quad \text{BND}(0.9, K_{i[l,o]}, 1.1) \\
K_{oi} &= 1.151 - [0.00347P_i] - \left[\frac{0.978}{AER_i} \right] \\
K_{li} &= 1.151 - [0.00347P_i] - \left[\frac{0.978}{R_{8i}} \right] \\
F_{ei} &= 303 \left\{ 0.5W_i + \frac{0.5[E_{wi} - W_i]}{[1 + 2S_i]} \right\} \\
S_i &= \frac{1.6[E_{wi} - W_i]}{F_i} \\
F_{ci} &= 0.21 \left\{ 1 + \frac{0.5}{1 + \text{Exp} \left[\frac{Dc - 60}{10} \right]} \right\} \left\{ 1 + 0.2 \left[W_i + \frac{E_{wi} - W_i}{1 + 2S_i} \right] \right\} \\
C_{eei[l,o]} &= C_{ei[l,o]} P_{ei} \\
QT_{io} &= Qt_i + Qr_i
\end{aligned}$$

$$\begin{aligned}
QT_{i_f} &= QL_i \\
Qe_i &= QT_{i_o} + QT_{i_f} \\
VC_{i_{[l,o]}} &= \left[\frac{QT_{i_{[l,o]}}}{C_{eei_{[l,o]}}} \right]
\end{aligned}$$

$$De_{i_{[l,o]}} = \frac{3600}{C_{eei_{[l,o]}}} + 900T_p \left[VC_{i_{[l,o]}} - 1 + \sqrt{\left[VC_{i_{[l,o]}} - 1 \right]^2 + \frac{3600VC_{i_{[l,o]}}}{450T_p C_{eei_{[l,o]}}}} \right]$$

$$Q_{i_{[l,o]}} = 900T_p \left[VC_{i_{[l,o]}} - 1 + \sqrt{\left[VC_{i_{[l,o]}} - 1 \right]^2 + \frac{3600VC_{i_{[l,o]}}}{450T_p C_{eei_{[l,o]}}}} \right] \left[\frac{3600}{C_{eei_{[l,o]}}} \right]$$

$$\begin{aligned}
Q_{i_{[l,o]}} &< Q_{max_i} \\
VC_i &< VC_{max} \\
DeT_{[l,o]i} &= De_{[l,o]i} * QT_{[l,o]i} \\
DATI &= \frac{\sum_{i=1}^4 [DeT_{[l,o]i}]}{\sum_{i=1}^4 Qe_i}
\end{aligned}$$

Objective function;

$$Min = \alpha M_{SD} + (1-\alpha)DATI$$

APPENDIX-C

Lingo-13 software coding for dual-lane right- angle and skewed-
angle roundabouts

**(A) MULTI OBJECTIVE MODEL FOR
DUAL-LANE ROUNDABOUT AT 90
DEGREE INTERSECTIONS;**

```
! Design Vehicle (WB-50(WB-15))
@BND(45,Dc,55);
!Max Speed limit at each vehicle path;
Vmax=48;
X100=0.5;
! INPUT DATA;
! LEG 1;
@BND(7.3,Ew1,13.5);
@BND(30,AER1,85);
@BND(35,AXR1,75);
@BND(15,R81,80);
@BND(20,R91,80);
! LEG 2;
@BND(7.3,Ew2,14);
@BND(20,AER2,85);
@BND(35,AXR2,75);
@BND(20,R82,80);
@BND(30,R92,80);
! LEG 3;
@BND(7,Ew3,13.5);
@BND(30,AER3,85);
@BND(35,AXR3,75);
@BND(20,R83,80);
@BND(20,R93,80);
! LEG 4;
@BND(7.3,Ew4,13.5);
@BND(20,AER4,85);
@BND(35,AXR4,75);
@BND(15,R84,80);
@BND(30,R94,80);
!DELAY INPUT;
TP=0.25;
! LEG 1;
@BND(20,P1,40);
@BND(7.3,W1,9);
Qt1=268;
Qr1=224;
QL1=105;
Pe1=0.99;
Qc1=993;
QLmax1=20;
! LEG 2;
@BND(20,P2,40);
@BND(7.3,W2,8.5);
Pe2=0.99;
Qt2=610;
Qr2=222;
QL2=216;
Qc2=536;
QLmax2=20;
! LEG 3;
@BND(20,P3,40);
@BND(7.3,W3,8);
Pe3=0.99;
Qt3=269;
Qr3=148;
QL3=140;
Qc3=931;
```

```
QLmax3=20;
! LEG 4;
@BND(25,P4,35);
@BND(7.3,W4,9.5);
Pe4=0.99;
Qt4=690;
Qr4=194;
QL4=163;
Qc4=625;
QLmax4=20;


---


! SPEED CONSISTENCY MODEL;
! Circulatory width limits;
Cw>9.8;
Cw<1.2*Emax;
!OFFSET FROM CENTER LINE;
n=1.9;
MSD<18;
DATI<7;
!FOR FLARING;
Ew1>W1;
Ew2>W2;
Ew3>W3;
Ew4>W4;


---


! MAXIMUM ENTRY WIDTH;
Emax=@SMAX (Ew1,Ew2,Ew3,Ew4);


---


! SIDE FRICTION FACTOR FOR LIGHT AND HEAVY VEHICLE;
fsLV=0.3-0.00084*MvLV^0.5;
MvLV=1400;
fsHV=0.3-0.00084*MvHV^0.5;
MvHV=11000;
fs=(1-pHV)*fsLV+pHV*fsHV;
pHV=0.05;


---


! ENTRY FROM LEG 1;
! CENTRAL THROUGH PATH CURVE;
H=0.19*Dc+X19;
@BND(0.01,X19,0.4);
Ht=Ric+1.52;
Ric=(Dc-2*Cw)/2;
Mo=Ht-H;
Ric>H;
L2/Mo=@SIN(STC/2)/(1-@COS(STC/2));
L2=0.4*Dc;
R2=L2/@SIN(STC/2);
V2=11.27*((fs-0.02)*R2)^0.5;
DSTC=57.2957795*STC;
V2<Vmax;
! CENTRAL RIGHT TURN PATH CURVE;
(E1B1)^2-(0.194*Dc)^2=0;
L51=0.5*E1B1;
Mr1=0.066*Cw;
L51/Mr1=@sin(SRC1/2)/(1-@cos(SRC1/2));
(1-@cos(SRC1/2))>=0;
R51=L51/@sin(SRC1/2);
DSRC1=57.2957795*SRC1;
V51=11.27*((fs+0.02)*R51)^0.5;
V51<Vmax;
! CENTRAL LEFT TURN PATH CURVE;
R7=Ht;
V7=11.27*((fs-0.02)*R7)^0.5+X10;
@BND(0.01,X10,0.3);
V7<Vmax;
```

```

! THROUGH CURVE ENTRY FROM LEG 1;
B1K1=(0.5*Dc*@SIN(A11)-0.5*EW1-n);
K1M1=(B1K1)/(@TAN(STE1));
B1=@ABS((90*0.01745)-Aml-A11);
Am1=(A21-A11)/2;
STE1=(STC/2)+Am1;
T11=((B1K1)^2+(K1M1)^2)^0.5;
L11=T11*@COS(0.5*STE1);
R11=L11/@SIN(0.5*STE1);
DSTE1=57.2957795*STE1;
V11=11.27*((fs+0.02)*R11)^0.5;
V11<Vmax;
! RIGHT TURN ENTRY CURVE AT LEG 1;
Ac1=(90*0.01745-(A24+A11))/2;
Ar1=Ac1+A11;
SRE1=(90*0.01745)-Ar1-(SRC1/2);
B1F1=(0.5*Dc*@SIN(A11)-0.5*EW1-n)+X1;
@BND(0.01,X1,0.2);
F1Q1=B1F1/(@TAN(SRE1));
T41=((B1F1)^2+(F1Q1)^2)^0.5;
L41=T41*@COS(0.5*SRE1);
R41=L41/(@SIN(0.5*SRE1));
DSRE1=57.2957795*SRE1;
V41=3.6*(9.81*(fs+0.02)*R41)^0.5;
V41<Vmax;
! LEFT TURN ENTRY CURVE AT LEG 1;
c1=R7*(2-2*@COS(A51))^0.5;
d1=((R7)^2-((c1)^2)/4)^0.5;
h1=R7-d1;
A51=2*@ACOS((d1)/R7);
G1W1=R7*@COS(A51)-n+X2;
@BND(0.01,X2,0.3);
W1X1=0.836*Ric;
W1X1=(G1W1)/(@TAN(SLE1));
T81=((G1W1)^2+(W1X1)^2)^0.5;
T81=G1W1/@SIN(SLE1);
L81=T81*@COS(0.5*SLE1);
DSLE1=57.2957795*SLE1;
V81=3.6*(9.81*(fs+0.02)*R81)^0.5;
V81<Vmax;
!THROUGH EXIT AT LEG 3;
STX3=0.5*STC-Am1;
O3C3=0.5*Dc*@SIN(A21)-0.5*EW1-n+X3;
@BND(0.01,X3,0.2);
N3O3=O3C3/(@TAN(STX3));
T33=((O3C3)^2+(N3O3)^2)^0.5;
L33=T33*@COS(0.5*STX3);
R33=L33/@SIN(0.5*STX3);
DSTX3=57.2957795*STX3;
V33=11.27*((fs+0.02)*R33)^0.5;
V33<Vmax;
! RIGHT TURN EXIT AT LEG 2;
T2E2=0.5*Dc*@SIN(A24)-0.5*EW4-n+X14;
@BND(0.01,X14,0.2);
T2Y2=T2E2/(@TAN(SRX2));
T62=((T2E2)^2+(T2Y2)^2)^0.5;
L62=T62*@COS(0.5*SRX2);
R62=L62/(@SIN(0.5*SRX2));
DSRX2=57.2957795*SRX2;
V62=3.6*(9.81*(fs+0.02)*R62)^0.5;
V62<Vmax;
! LEFT TURN EXIT AT LEG 4;
e4=R7*(2-2*@COS(A64))^0.5;
f4=((R7)^2-((e4)^2)/4)^0.5;
g4=R7-f4;
A64=2*@ACOS((f4)/R7);
H4U4=R7*@COS(A64)-n;
V4U4=0.60*Ric;
V4U4=(H4U4)/(@TAN(SLX4));
T94=((H4U4)^2+(V4U4)^2)^0.5;
L94=T94*@COS(0.5*SLX4);
R94=L94/(@SIN(0.5*SLX4));
DSLX4=57.2957795*SLX4;
V94=3.6*(9.81*(fs+0.02)*R94)^0.5;
V94<Vmax;
! ENTRY FROM LEG 2;
!CENTRAL RIGHT TURN PATH CURVE;
(E2B2)^2-(0.2*Dc)^2=0;
L52=0.5*E2B2;
Mr2=0.066*Cw;
L52/Mr2=@sin(SRC2/2)/(1-@cos(SRC2/2));
R52=L52/@sin(SRC2/2);
DSRC2=57.2957795*SRC2;
V52=11.27*((fs+0.02)*R52)^0.5;
V52<Vmax;
! THROUGH CURVE ENTRY FROM LEG 2;
B2K2=(0.5*Dc*@SIN(A12)-0.5*EW2-n);
K2M2=(B2K2)/(@TAN(STE2));
B2=@ABS((90*0.01745)-A12);
Am2=(A22-A12)/2;
STE2=(STC/2)+Am2;
T12=((B2K2)^2+(K2M2)^2)^0.5;
L12=T12*@COS(0.5*STE2);
R12=L12/@SIN(0.5*STE2);
DSTE2=57.2957795*STE2;
V12=11.27*((fs+0.02)*R12)^0.5;
V12<Vmax;
! RIGHT TURN ENTRY CURVE AT LEG 2;
Ac2=(90*0.01745-(A24+A12))/2;
Ar2=Ac2+A12;
SRE2=(90*0.01745)-Ar2-(SRC2/2);
B2F2=(0.5*Dc*@SIN(A12)-0.5*EW2-n)+X4;
@BND(0.01,X4,0.3);
F2Q2=B2F2/(@TAN(SRE2));
T42=((B2F2)^2+(F2Q2)^2)^0.5;
L42=T42*@COS(0.5*SRE2);
R42=L42/(@SIN(0.5*SRE2));
DSRE2=57.2957795*SRE2;
V42=3.6*(9.81*(fs+0.02)*R42)^0.5;
V42<Vmax;
! LEFT TURN ENTRY CURVE AT LEG 2;
c2=R7*(2-2*@COS(A52))^0.5;
d2=((R7)^2-((c2)^2)/4)^0.5;
h2=R7-d2;
A52=2*@ACOS((d2)/R7);
G2W2=R7*@COS(90*0.01745-A51)-n+X5;
@BND(0.01,X5,0.3);
W2X2=0.836*Ric;
W2X2=(G2W2)/(@TAN(SLE2));
T82=((G2W2)^2+(W2X2)^2)^0.5;
T82=G2W2/@SIN(SLE2);
L82=T82*@COS(0.5*SLE2);
DSLE2=57.2957795*SLE2;
V82=3.6*(9.81*(fs+0.02)*R82)^0.5;
V82<Vmax;
!EXIT;

```

```

!THROUGH EXIT AT LEG 4;
STX4=0.5*STC-Am2;
O4C4=0.5*Dc*@SIN(A22)-0.5*EW2-n+X15;
@BND(0.01,X15,0.2);
N4O4=O4C4/(@TAN(STX4));
T34=((O4C4)^2+(N4O4)^2)^0.5;
L34=T34*@COS(0.5*STX4);
R34=L34/@SIN(0.5*STX4);
DSTX4=57.2957795*STX4;
V34=11.27*((fs+0.02)*R34)^0.5;
V34<Vmax;
! RIGHT TURN EXIT AT LEG 3;
T3E3=0.5*Dc*@SIN(A21)-0.5*EW3-n+X6;
@BND(0.01,X6,0.2);
T3Y3=T3E3/(@TAN(SRX3));
T63=((T3E3)^2+(T3Y3)^2)^0.5;
L63=T63*@COS(0.5*SRX3);
R63=L63/(@SIN(0.5*SRX3));
DSRX3=57.2957795*SRX3;
V63=3.6*(9.81*(fs+0.02)*R63)^0.5;
V63<Vmax;
! LEFT TURN EXIT AT LEG 1;
e1=R7*(2-2*@COS(A61))^0.5;
f1=((R7)^2-((e1)^2)/4)^0.5;
g1=R7-f1;
A61=2*@ACOS((f1)/R7);
H1U1=R7*@COS(A61)-n;
V1U1=0.60*Ric;
V1U1=(H1U1)/(@TAN(SLX1));
T91=((H1U1)^2+(V1U1)^2)^0.5;
L91=T91*@COS(0.5*SLX1);
R91=L91/(@SIN(0.5*SLX1));
DSLX1=57.2957795*SLX1;
V91=3.6*(9.81*(fs+0.02)*R91)^0.5;
V91<Vmax;


---


! ENTRY FROM LEG 3;
!CENTRAL RIGHT TURN PATH CURVE;
(E3B3)^2-(0.194*Dc)^2=0;
L53=0.5*E3B3;
Mr3=0.066*Cw;
L53/Mr3=@sin(SRC3/2)/(1-@cos(SRC3/2));
R53=L53/@sin(SRC3/2);
DSRC3=57.2957795*SRC3;
V53=11.27*((fs+0.02)*R53)^0.5;
V53<Vmax;
! THROUGH CURVE ENTRY FROM LEG 3;
B3K3=(0.5*Dc*@SIN(A13)-0.5*EW3-n);
K3M3=(B3K3)/(@TAN(STE3));
B3=@ABS((90*0.01745)-Am3-A13);
Am3=(A23-A13)/2;
STE3=(STC/2)+Am3;
T13=((B3K3)^2+(K3M3)^2)^0.5;
L13=T13*@COS(0.5*STE3);
R13=L13/@SIN(0.5*STE3);
DSTE3=57.2957795*STE3;
V13=11.27*((fs+0.02)*R13)^0.5;
V13<Vmax;
! RIGHT TURN ENTRY CURVE AT LEG 3;
Ac3=(90*0.01745-(A23+A13))/2;
Ar3=Ac3+A13;
SRE3=(90*0.01745)-Ar3-(SRC3/2);
B3F3=(0.5*Dc*@SIN(A13)-0.5*EW3-n)+X7;
@BND(0.01,X7,0.2);
F3Q3=B3F3/(@TAN(SRE3));
T43=((B3F3)^2+(F3Q3)^2)^0.5;
L43=T43*@COS(0.5*SRE3);
R43=L43/(@SIN(0.5*SRE3));
DSRE3=57.2957795*SRE3;
V43=3.6*(9.81*(fs+0.02)*R43)^0.5;
V43<Vmax;
! LEFT TURN ENTRY CURVE AT LEG 3;
c3=R7*(2-2*@COS(A53))^0.5;
d3=((R7)^2-((c3)^2)/4)^0.5;
h3=R7-d3;
A53=2*@ACOS((d3)/R7);
G3W3=R7*@COS(A53)-n+X8;
@BND(0.01,X8,.9);
W3X3=0.836*Ric+X17;
@BND(0.01,X17,0.4);
W3X3=(G3W3)/(@TAN(SLE3));
T83=((G3W3)^2+(W3X3)^2)^0.5;
T83=G3W3/@SIN(SLE3);
L83=T83*@COS(0.5*SLE3);
DSLE3=57.2957795*SLE3;
V83=3.6*(9.81*(fs+0.02)*R83)^0.5;
V83<Vmax;
! EIXT;
!THROUGH EXIT AT LEG 1;
STX1=0.5*STC-Am3;
O1C1=0.5*Dc*@SIN(A23)-0.5*EW3-n+X16;
@BND(0.01,X16,0.2);
N1O1=O1C1/(@TAN(STX1));
T31=((O1C1)^2+(N1O1)^2)^0.5;
L31=T31*@COS(0.5*STX1);
R31=L31/@SIN(0.5*STX1);
DSTX1=57.2957795*STX1;
V31=11.27*((fs+0.02)*R31)^0.5;
V31<Vmax;
! RIGHT TURN EXIT AT LEG 4;
T4E4=0.5*Dc*@SIN(A22)-0.5*EW4-n+X13;
@BND(0.01,X13,0.2);
T4Y4=T4E4/(@TAN(SRX4));
T64=((T4E4)^2+(T4Y4)^2)^0.5;
L64=T64*@COS(0.5*SRX4);
R64=L64/(@SIN(0.5*SRX4));
DSRX4=57.2957795*SRX4;
V64=3.6*(9.81*(fs+0.02)*R64)^0.5;
V64<Vmax;
! LEFT TURN EXIT AT LEG 2;
e2=R7*(2-2*@COS(A62))^0.5;
f2=((R7)^2-((e2)^2)/4)^0.5;
g2=R7-f2;
A62=2*@ACOS((f2)/R7);
H2U2=R7*@COS(A62)-n;
V2U2=0.60*Ric;
V2U2=(H2U2)/(@TAN(SLX2));
T92=((H2U2)^2+(V2U2)^2)^0.5;
L92=T92*@COS(0.5*SLX2);
R92=L92/(@SIN(0.5*SLX2));
DSLX2=57.2957795*SLX2;
V92=3.6*(9.81*(fs+0.02)*R92)^0.5;
V92<Vmax;


---


! ENTRY FROM LEG 4;
!CENTRAL RIGHT TURN PATH CURVE;
(E4B4)^2-(0.2*Dc)^2=0;
L54=0.5*E4B4;

```

```

Mr4=0.066*Cw;
L54/Mr4=@sin(SRC4/2)/(1-@cos(SRC4/2));
R54=L54/@sin(SRC4/2);
DSRC4=57.2957795*SRC4;
V54=11.27*((fs+0.02)*R54)^0.5;
V54<Vmax;

! THROUGH CURVE ENTRY FROM LEG 4;
B4K4=(0.5*Dc*@sin(A14)-0.5*EW4-n);
K4M4=(B4K4)/(@tan(STE4));
B4=@abs((90*0.01745)-A14);
Am4=(A24-A14)/2;
STE4=(STC/2)+Am4;
T14=((B4K4)^2+(K4M4)^2)^0.5;
L14=T14*@cos(0.5*STE4);
R14=L14/@sin(0.5*STE4);
DSTE4=57.2957795*STE4;
V14=11.27*((fs+0.02)*R14)^0.5;
V14<Vmax;
! RIGHT TURN ENTRY CURVE AT LEG 4;
Ac4=(90*0.01745-(A23+A14))/2;
Ar4=Ac4+A14;
SRE4=(90*0.01745)-Ar4-(SRC4/2);
B4F4=(0.5*Dc*@sin(A14)-0.5*EW4-n)+X9;
@BND(0.01,X9,0.2);
F4Q4=B4F4/(@tan(SRE4));
T44=((B4F4)^2+(F4Q4)^2)^0.5;
L44=T44*@cos(0.5*SRE4);
R44=L44/@sin(0.5*SRE4);
DSRE4=57.2957795*SRE4;
V44=3.6*(9.81*(fs+0.02)*R44)^0.5;
V44<Vmax;
! LEFT TURN ENTRY CURVE AT LEG 4;
c4=R7*(2-2*@cos(A54))^0.5;
d4=((R7)^2-((c4)^2)/4)^0.5;
h4=R7-d4;
A54=2*@acos((d4)/R7);
G4W4=R7*@cos(90*0.01745-A54)-n+X10;
@BND(0.01,X10,0.2);
W4X4=0.836*Ric-19.8324*Ai+X18;
@BND(0.01,X18,0.4);
W4X4=(G4W4)/(@tan(SLE4));
T84=((G4W4)^2+(W4X4)^2)^0.5;
T84=G4W4/@sin(SLE4);
L84=T84*@cos(0.5*SLE4);
DSLE4=57.2957795*SLE4;
V84=3.6*(9.81*(fs+0.02)*R84)^0.5;
V84<Vmax;
!EXIT;
!THROUGH EXIT AT LEG 2;
STX2=0.5*STC-Am4;
O2C2=0.5*Dc*@sin(A24)-0.5*EW4-n;
N2O2=O2C2/(@tan(STX2));
T32=((O2C2)^2+(N2O2)^2)^0.5;
L32=T32*@cos(0.5*STX2);
R32=L32/@sin(0.5*STX2);
DSTX2=57.2957795*STX2;
V32=11.27*((fs+0.02)*R32)^0.5;
V32<Vmax;
! RIGHT TURN EXIT AT LEG 1;
T1E1=0.5*Dc*@sin(A23)-0.5*EW1-n+X12;
@BND(0.01,X12,0.2);
T1Y1=T1E1/(@tan(SRX1));

T611=((T1E1)^2+(T1Y1)^2)^0.5;
L61=T61*@cos(0.5*SRX1);
R61=L61/(@sin(0.5*SRX1));
DSRX1=57.2957795*SRX1;
V61=3.6*(9.81*(fs+0.02)*R61)^0.5;
V61<Vmax;
! LEFT TURN EXIT AT LEG 3;
e3=R7*(2-2*@cos(A63))^0.5;
f3=((R7)^2-((e3)^2)/4)^0.5;
g3=R7-f3;
A63=2*@acos((f3)/R7);
H3U3=R7*@cos(A63)-n;
V3U3=0.60*Ric;
V3U3=(H3U3)/(@tan(SLX3));
T93=((H3U3)^2+(V3U3)^2)^0.5;
L93=T93*@cos(0.5*SLX3);
R93=L93/(@sin(0.5*SLX3));
DSLX3=57.2957795*SLX3;
V93=3.6*(9.81*(fs+0.02)*R93)^0.5;
V93<Vmax;

! AVERAGE ENTRY RADIUS AT EACH LEG;
AER1=(R11+R41)/2;
AER2=(R12+R42)/2;
AER3=(R13+R43)/2;
AER4=(R14+R44)/2;
! AVERAGE EXIT RADIUS AT EACH LEG;
AXR1=(R61+R31)/2;
AXR2=(R62+R32)/2;
AXR3=(R63+R33)/2;
AXR4=(R64+R34)/2;
! AVERAGE ENTRY VELOCITY AT EACH LEG;
AEV1=(V11+V41)/2;
AEV2=(V12+V42)/2;
AEV3=(V13+V43)/2;
AEV4=(V14+V44)/2;
! AVERAGE EXIT VELOCITY AT EACH LEG;
AXV1=(V61+V31)/2;
AXV2=(V62+V32)/2;
AXV3=(V63+V33)/2;
AXV4=(V64+V34)/2;

! CONSTRAINTS;
AER1>R2;
AXR3>R2;
AXR3>AER1;
AER2>R2;
AXR4>R2;
AXR4>AER2;
AER3>R2;
AXR1>R2;
AXR1>AER3;
AER4>R2;
AXR2>R2;
AXR2>AER4;
! CONSTRAINT FOR MINIMUM TURNING WIDTH
FOR WB-50 DESIGN VEHICLE;
R2>12.5;
R51>12.5;
R52>12.5;
R53>12.5;
R54>12.5;
R7>12.5;

!RIGHT TURN PATHS;
AEV1-V51-M94+M95=0;

```

```

M94<MSD;
M95<MSD;
AXV2-V51-M96=0;
M96<MSD;
AXV2>V51;
AEV2-V52-M97+M98=0;
M97<MSD;
M98<MSD;
AXV3-V52-M99=0;
M99<MSD;
AXV3>V52;
AEV3-V53-M100+M101=0;
M100<MSD;
M101<MSD;
AXV4-V53-M102=0;
M102<MSD;
AXV4>V53;
AEV4-V54-M103+M104=0;
M103<MSD;
M104<MSD;
AXV1-V54-M105=0;
M105<MSD;
AXV1>V54;
!THROUGH PATHS;
V2-AEV1-M106+M107=0;
M106<MSD;
M107<MSD;
AXV3-V2-M108=0;
M108<MSD;
AXV3>V2;
V2-AEV3-M109+M110=0;
M109<MSD;
M110<MSD;
AXV1-V2-M111=0;
M111<MSD;
AXV1>V2;
V2-AEV4-M112+M113=0;
M112<MSD;
M113<MSD;
AXV4-V2-M114=0;
M114<MSD;
AXV4>V2;
V2-AEV2-M115+M116=0;
M115<MSD;
M116<MSD;
AXV2-V2-M117=0;
M117<MSD;
AXV2>V2;
!LEFT TURN PATHS;
V7-V81-M120+M121=0;
M120<MSD;
M121<MSD;
V91-V7-M122=0;
M122<MSD;
V91>V7;
V7-V82-M123+M124=0;
M123<MSD;
M124<MSD;
V92-V7-M125=0;
M125<MSD;
V92>V7;
V7-V83-M126+M127=0;
M126<MSD;
M127<MSD;
V93-V7-M128=0;
M128<MSD;
V93>V7;
V7-V84-M129+M130=0;
M129<MSD;
M130<MSD;
V94-V7-M131=0;
M131<MSD;
V94>V7;
!THROUGH AND LEFT TURN CONFLICT;
V2-V7-M132+M133=0;
M132<MSD;
M133<MSD;
!THROUGH AND RIGHT TURN CONFLICT;
V2-V51-M140+M141=0;
M140<MSD;
M141<MSD;
V2-V52-M142+M143=0;
M142<MSD;
M143<MSD;
V2-V53-M144+M145=0;
M144<MSD;
M145<MSD;
V2-V54-M146+M147=0;
M146<MSD;
M147<MSD;
!THROUGH AND RIGHT TURN CONFLICT;
V41-V51-M148+M149=0;
M148<MSD;
M149<MSD;
V62-V51-M150+M151=0;
M150<MSD;
M151<MSD;
V42-V52-M152+M153=0;
M152<MSD;
M153<MSD;
V63-V52-M154+M155=0;
M154<MSD;
M155<MSD;
V43-V53-M156+M157=0;
M156<MSD;
M157<MSD;
V64-V53-M158+M159=0;
M158<MSD;
M159<MSD;
V44-V54-M160+M161=0;
M160<MSD;
M161<MSD;
V61-V54-M162+M163=0;
M162<MSD;
M163<MSD;
! CAPACITY DELAY MODEL;
! LEG 1;
! OUTER LANE;
Ceo1=Ko1*(Fe1-Fc1*Qc1);
@BND(0.9,Ko1,1.1);
Ko1=1.151-(0.00347*P1)-(0.978/AER1);
Fe1=303*((0.5*W1)+0.5*(Ew1-
W1)/(1+2*S1));
S1=1.6*0.5*(Ew1-W1)/F1;

```

```

Fc1=(0.21)*(1+(0.5/(1+@EXP(Dc-
60)/10)))*(1+0.2*0.5*(W1+(Ew1-
W1)/(1+2*S1)));
Ceeo1=Ceo1*Pe1;
VCo1=(Qt1+Qr1)/Ceeo1;
Deo1=(3600/Ceeo1)+900*TP*(VCo1-
1+(VCo1-
1)^2+(3600*VCo1/Ceeo1)/450*TP)^0.5);
DeTo1=Deo1*(Qt1+Qr1);
Qo1=(Ceeo1/3600)*(900*TP)*(VCo1-1+((1-
VCo1)^2+(3600*VCo1/Ceeo1)/(150*TP))^0.5);
! INNER LANE;
Ceil=Ki1*(Fe1-Fc1*Qc1);
@BND(0.9,Ki1,1.1);
Ki1=1.151-(0.00347*P1)-(0.978/R81);
Ceei1=Ceil*Pe1;
VCi1=(QL1)/Ceei1;
Dei1=(3600/Ceei1)+900*TP*(VCi1-1+((VCi1-
1)^2+(3600*VCi1/Ceei1)/450*TP)^0.5);
DeTi1=Dei1*(QL1);
Qi1=(Ceei1/3600)*(900*TP)*(VCi1-1+((1-
VCi1)^2+(3600*VCi1/Ceei1)/(150*TP))^0.5);
! Constraints;
Qo1<Qmax1;
VCo1<=0.85;
Qi1<Qmax1;
VCi1<=0.85;


---


! LEG 2;
! OUTER LANE;
Ceo2=Ko2*(Fe2-Fc2*Qc2);
@BND(0.9,Ko2,1.1);
Ko2=1.151-(0.00347*P2)-(0.978/AER2);
Fe2=303*((0.5*W2)+0.5*(Ew2-
W2)/(1+2*S2));
S2=1.6*0.5*(Ew2-W2)/F2;
Fc2=(0.21)*(1+(0.5/(1+@EXP(Dc-
60)/10)))*(1+0.2*0.5*(W2+(Ew2-
W2)/(1+2*S2)));
Ceeo2=Ceo2*Pe2;
VCo2=(Qt2+Qr2)/Ceeo2;
Deo2=(3600/Ceeo2)+900*TP*(VCo2-
1+(VCo2-
1)^2+(3600*VCo2/Ceeo2)/450*TP)^0.5);
DeTo2=Deo2*(Qt2+Qr2);
Qo2=(Ceeo2/3600)*(900*TP)*(VCo2-1+((1-
VCo2)^2+(3600*VCo2/Ceeo2)/(150*TP))^0.5);
! INNER LANE;
Ce2=Ki2*(Fe2-Fc2*Qc2);
@BND(0.9,Ki2,1.1);
Ki2=1.151-(0.00347*P2)-(0.978/R82);
Ceei2=Ce2*Pe2;
VCi2=(QL2)/Ceei2;
Dei2=(3600/Ceei2)+900*TP*(VCi2-
1+(VCi2-
1)^2+(3600*VCi2/Ceei2)/450*TP)^0.5);
DeTi2=Dei2*(QL2);
Qi2=(Ceei2/3600)*(900*TP)*(VCi2-1+((1-
VCi2)^2+(3600*VCi2/Ceei2)/(150*TP))^0.5);
! Constraints;
Qo2<Qmax2;
VCo2<=0.85;
Qi2<Qmax2;
VCi2<=0.85;


---



```

```

! LEG 3;
! OUTER LANE;
Ceo3=Ko3*(Fe3-Fc3*Qc3);
@BND(0.9,Ko3,1.1);
Ko3=1.151-(0.00347*P3)-(0.978/AER3);
Fe3=303*((0.5*W3)+0.5*(Ew3-
W3)/(1+2*S3));
S3=1.6*0.5*(Ew3-W3)/F3;
Fc3=(0.21)*(1+(0.5/(1+@EXP(Dc-
60)/10)))*(1+0.2*0.5*(W3+(Ew3-
W3)/(1+2*S3)));
Ceeo3=Ceo3*Pe3;
VCo3=(Qt3+Qr3)/Ceeo3;
Deo3=(3600/Ceeo3)+900*TP*(VCo3-
1+(VCo3-
1)^2+(3600*VCo3/Ceeo3)/450*TP)^0.5);
DeTo3=Deo3*(Qt3+Qr3);
Qo3=(Ceeo3/3600)*(900*TP)*(VCo3-1+((1-
VCo3)^2+(3600*VCo3/Ceeo3)/(150*TP))^0.5);
! INNER LANE;
Ce3=Ki3*(Fe3-Fc3*Qc3);
@BND(0.9,Ki3,1.1);
Ki3=1.151-(0.00347*P3)-(0.978/R83);
Ceei3=Ce3*Pe3;
VCi3=(QL3)/Ceei3;
Dei3=(3600/Ceei3)+900*TP*(VCi3-
1+(VCi3-
1)^2+(3600*VCi3/Ceei3)/450*TP)^0.5);
DeTi3=Dei3*(QL3);
Qi3=(Ceei3/3600)*(900*TP)*(VCi3-1+((1-
VCi3)^2+(3600*VCi3/Ceei3)/(150*TP))^0.5);
! Constraints;
Qo3<Qmax3;
VCo3<=0.85;
Qi3<Qmax3;
VCi3<=0.85;


---


! LEG 4;
! OUTER LANE;
Ceo4=Ko4*(Fe4-Fc4*Qc4);
@BND(0.9,Ko4,1.1);
Ko4=1.151-(0.00347*P4)-(0.978/AER4);
Fe4=303*((0.5*W4)+0.5*(Ew4-
W4)/(1+2*S4));
S4=1.6*0.5*(Ew4-W4)/F4;
Fc4=(0.21)*(1+(0.5/(1+@EXP(Dc-
60)/10)))*(1+0.2*0.5*(W4+(Ew4-
W4)/(1+2*S4)));
Ceeo4=Ceo4*Pe4;
VCo4=(Qt4+Qr4)/Ceeo4;
Deo4=(3600/Ceeo4)+900*TP*(VCo4-
1+(VCo4-
1)^2+(3600*VCo4/Ceeo4)/450*TP)^0.5);
DeTo4=Deo4*(Qt4+Qr4);
Qo4=(Ceeo4/3600)*(900*TP)*(VCo4-1+((1-
VCo4)^2+(3600*VCo4/Ceeo4)/(150*TP))^0.5);
! INNER LANE;
Ce4=Ki4*(Fe4-Fc4*Qc4);
@BND(0.9,Ki4,1.1);
Ki4=1.151-(0.00347*P4)-(0.978/R84);
Ceei4=Ce4*Pe4;
VCi4=(QL4)/Ceei4;

```

```

Dei4=(3600/Ceei4)+900*TP*(VCi4-
1+(VCi4-
1)^2+(3600*VCi4/Ceei4)/450*TP)^0.5);
DeTi4=Dei4*(QL4);
Qi4=(Ceei4/3600)*(900*TP)*(VCi4-1+((1-
VCi4)^2+(3600*VCi4/Ceei4)/(150*TP))^0.5);
! Constraints;
Qo4<Qmax4;
VCo4<=0.85;
Qi4<Qmax4;
VCi4<=0.85;
-----
! TOTAL ENTRY VOLUME;
Qe1=Qt1+Qr1+QL1;
Qe2=Qt2+Qr2+QL2;
Qe3=Qt3+Qr3+QL3;
Qe4=Qt4+Qr4+QL4;

! AVERAGE INTERSECTION DELAY;
DATI=(DeTi1+DeTo1+DeTi2+DeTo2+DeTi3+DeT
o3+DeTi4+DeTo4)/(Qe1+Qe2+Qe3+Qe4);
-----
! OBJECTIVE FUNCTION FOR MULTI
OBJECTIVE MODEL;
MIN=(x100)*MSD+(1-x100)*DATI;
END

```

**(B) MULTI OBJECTIVE MODEL FOR
DUAL-LANE ROUNDABOUT AT
SKEWED-ANGLE INTERSECTIONS;**

Design vehicle WB-50(WB-15)

@BND(45,Dc,65);

! ANGLE OF INCLINATION WITH THE Y-AXIS;

Ai=15*0.01745;

!Max Speed limit at each vehicle path;

Vmax=55;

X₁₀₀=0.5;

! INPUT DATA;

! LEG 1;

@BND(7.3,Ew1,13.5);

@BND(30,AER1,85);

@BND(35,AXR1,75);

@BND(15,R81,80);

@BND(20,R91,80);

! LEG 2;

@BND(7.3,Ew2,14);

@BND(20,AER2,85);

@BND(35,AXR2,75);

@BND(20,R82,80);

@BND(30,R92,80);

! LEG 3;

@BND(7,Ew3,13.5);

@BND(30,AER3,85);

@BND(35,AXR3,75);

@BND(20,R83,80);

@BND(20,R93,80);

! LEG 4;

@BND(7.3,Ew4,13.5);

@BND(20,AER4,85);

@BND(35,AXR4,75);

@BND(15,R84,80);

@BND(30,R94,80);

! DELAY INPUT;

TP=0.25;

! LEG 1;

@BND(20,P1,40);

@BND(7.3,W1,9);

Qt1=268;

Qr1=224;

QL1=105;

Pe1=0.99;

Qc1=993;

QLmax1=20;

! LEG 2;

@BND(20,P2,40);

@BND(7.3,W2,8.5);

Pe2=0.99;

Qt2=610;

Qr2=222;

QL2=216;

Qc2=536;

QLmax2=20;

! LEG 3;

@BND(20,P3,40);

@BND(7.3,W3,8);

Pe3=0.99;

Qt3=269;

Qr3=148;

QL3=140;

Qc3=931;

QLmax3=20;

! LEG 4;

@BND(25,P4,35);

@BND(7.3,W4,9.5);

Pe4=0.99;

Qt4=690;

Qr4=194;

QL4=163;

Qc4=625;

QLmax4=20;

SPEED CONSISTENCY MODEL;

! Circulatory width limits;

Cw>9.8;

Cw<1.2*Emax;

! OFFSET FROM CENTER LINE;

n=1.9;

MSD<21;

DATI<5;

! FOR FLARING;

Ew1>W1;

Ew2>W2;

Ew3>W3;

Ew4>W4;

! MAXIMUM ENTRY WIDTH;

Emax=@SMAX (Ew1,Ew2,Ew3,Ew4);

! SIDE FRICTION FACTOR FOR LIGHT AND HEAVY VEHICLE;

fsLV=0.3-0.00084*MvLV^0.5;

MvLV=1400;

fsHV=0.3-0.00084*MvHV^0.5;

MvHV=11000;

fs=(1-pHV)*fsLV+pHV*fsHV;

pHV=0.05;

! ENTRY FROM LEG 1;

! CENTRAL THROUGH PATH CURVE;

H=0.19*Dc+X19;

@BND(0.01,X19,0.4);

Ht=Ric+1.52;

Ric=(Dc-2*Cw)/2;

Mo=Ht-H;

Ric>H;

L2/Mo=@SIN(STC/2)/(1-@COS(STC/2));

L2=0.4*Dc;

R2=L2/@SIN(STC/2);

V2=11.27*((fs-0.02)*R2)^0.5;

V2<Vmax;

! CENTRAL RIGHT TURN PATH CURVE;

(E1B1)^2-

0.194*Dc+0.46*(Ai/0.01745))^2=0;

L51=0.5*E1B1;

Mr1=0.066*Cw+0.00667*(Ai/0.01745);

L51/Mr1=@sin(SRC1/2)/(1-@cos(SRC1/2));

(1-@cos(SRC1/2))>0;

R51=L51/@sin(SRC1/2);

V51=11.27*((fs+0.02)*R51)^0.5;

V51<Vmax;

! CENTRAL LEFT TURN PATH CURVE;

R7=Ht;

V7=11.27*((fs-0.02)*R7)^0.5+X10;

@BND(0.01,X10,0.3);

V7<Vmax;

```

! THROUGH CURVE ENTRY FROM LEG 1;
B1K1=(0.5*Dc*@SIN(A11)-0.5*EW1-n);
K1M1=(B1K1)/(@TAN(STE1));
B1=@ABS((90*0.01745)-Aml-A11);
Aml=(A21-A11)/2;
STE1=(STC/2)+Aml;
T11=((B1K1)^2+(K1M1)^2)^0.5;
L11=T11*@COS(0.5*STE1);
R11=L11/@SIN(0.5*STE1);
V11=11.27*((fs+0.02)*R11)^0.5;
V11<Vmax;
! RIGHT TURN ENTRY CURVE AT LEG 1;
Ac1=(90*0.01745-(A24+A11))/2;
Ar1=Ac1+A11;
SRE1=(90*0.01745)-Ar1-(SRC1/2);
B1F1=(0.5*Dc*@SIN(A11)-0.5*EW1-n)+X1;
@BND(0.01,X1,0.2);
F1Q1=B1F1/(@TAN(SRE1));
T41=((B1F1)^2+(F1Q1)^2)^0.5;
L41=T41*@COS(0.5*SRE1);
R41=L41/(@SIN(0.5*SRE1));
V41=3.6*(9.81*(fs+0.02)*R41)^0.5;
V41<Vmax;
! LEFT TURN ENTRY CURVE AT LEG 1;
c1=R7*(2-2*@COS(A51))^0.5;
d1=((R7)^2-((c1)^2)/4)^0.5;
h1=R7-d1;
A51=2*@ACOS((d1)/R7);
G1W1=R7*@COS(A51)-n+X2;
@BND(0.01,X2,0.3);
W1X1=0.836*Ric;
W1X1=(G1W1)/(@TAN(SLE1));
T81=((G1W1)^2+(W1X1)^2)^0.5;
T81=G1W1/@SIN(SLE1);
L81=T81*@COS(0.5*SLE1);
V81=3.6*(9.81*(fs+0.02)*R81)^0.5;
V81<Vmax;
! THROUGH EXIT AT LEG 3;
STX3=0.5*STC-Aml;
O3C3=0.5*Dc*@SIN(A21)-0.5*EW1-n+X3;
@BND(0.01,X3,0.2);
N3O3=O3C3/(@TAN(STX3));
T33=((O3C3)^2+(N3O3)^2)^0.5;
L33=T33*@COS(0.5*STX3);
R33=L33/@SIN(0.5*STX3);
V33=11.27*((fs+0.02)*R33)^0.5;
V33<Vmax;
! RIGHT TURN EXIT AT LEG 2;
Tb2E2=0.5*Dc*@SIN(A24+Ai)-0.5*EW4-n+X14;
@BND(0.01,X14,0.2);
Tb2Y2=Tb2E2/(@TAN(SRX2));
T62=((Tb2E2)^2+(Tb2Y2)^2)^0.5;
L62=T62*@COS(0.5*SRX2);
R62=L62/(@SIN(0.5*SRX2));
V62=3.6*(9.81*(fs+0.02)*R62)^0.5;
V62<Vmax;
! LEFT TURN EXIT AT LEG 4;
e4=R7*(2-2*@COS(A64))^0.5;
f4=((R7)^2-((e4)^2)/4)^0.5;
g4=R7-f4;
A64=2*@ACOS((f4)/R7);
H4Ub4=R7*@COS(A64-Ai)-n;
V4Ub4=0.60*Ric+H4Ub4*@TAN(Ai);
V4Ub4=(H4Ub4)/(@TAN(SLX4));
T94=((H4Ub4)^2+(V4Ub4)^2)^0.5;
L94=T94*@COS(0.5*SLX4);
R94=L94/(@SIN(0.5*SLX4));
V94=3.6*(9.81*(fs+0.02)*R94)^0.5;
V94<Vmax;
! ENTRY FROM LEG 2;
! CENTRAL RIGHT TURN PATH CURVE;
(E2B2)^2-(0.2*Dc-0.37*(Ai/0.01745))^2=0; L52=0.5*E2B2;
Mr2=0.066*Cw-0.02*(Ai/0.01745);
L52/Mr2=@sin(SRC2/2)/(1-@cos(SRC2/2));
R52=L52/@sin(SRC2/2);
V52=11.27*((fs+0.02)*R52)^0.5;
V52<Vmax;
! THROUGH CURVE ENTRY FROM LEG 2;
B2K2=(0.5*Dc*@SIN(A12-Ai)-0.5*EW2-n);
K2M2=(B2K2)/(@TAN(STE2));
B2=@ABS((90*0.01745)-Ai-A12);
Am2=(A22-A12)/2;
STE2=(STC/2)+Am2;
T12=((B2K2)^2+(K2M2)^2)^0.5;
L12=T12*@COS(0.5*STE2);
R12=L12/@SIN(0.5*STE2);
V12=11.27*((fs+0.02)*R12)^0.5;
V12<Vmax;
! RIGHT TURN ENTRY CURVE AT LEG 2;
Ac2=(90*0.01745-(A21+A12))/2;
Ar2=Ac2+A12;
SRE2=(90*0.01745)-Ar2-(SRC2/2);
B2F2=(0.5*Dc*@SIN(A12-Ai)-0.5*EW2-n)+X4;
@BND(0.01,X4,0.3);
F2Q2=B2F2/(@TAN(SRE2));
T42=((B2F2)^2+(F2Q2)^2)^0.5;
L42=T42*@COS(0.5*SRE2);
R42=L42/(@SIN(0.5*SRE2));
V42=3.6*(9.81*(fs+0.02)*R42)^0.5;
V42<Vmax;
! LEFT TURN ENTRY CURVE AT LEG 2;
c2=R7*(2-2*@COS(A52))^0.5;
d2=((R7)^2-((c2)^2)/4)^0.5;
h2=R7-d2;
A52=2*@ACOS((d2)/R7);
G2W2=R7*@COS(90*0.01745-A51-Ai)-n+X5;
@BND(0.01,X5,0.3);
W2X2=0.836*Ric-19.8324*Ai;
W2X2=(G2W2)/(@TAN(SLE2));
T82=((G2W2)^2+(W2X2)^2)^0.5;
T82=G2W2/@SIN(SLE2);
L82=T82*@COS(0.5*SLE2);
V82=3.6*(9.81*(fs+0.02)*R82)^0.5;
V82<Vmax;
! EXIT;
! THROUGH EXIT AT LEG 4;
STX4=0.5*STC-Am2;
O4C4=0.5*Dc*@SIN(A22+Ai)-0.5*EW2-n+X15;
@BND(0.01,X15,0.2);
N4O4=O4C4/(@TAN(STX4));
T34=((O4C4)^2+(N4O4)^2)^0.5;
L34=T34*@COS(0.5*STX4);

```

```

R34=L34/@SIN(0.5*STX4);
V34=11.27*((fs+0.02)*R34)^0.5;
V34<Vmax;
! RIGHT TURN EXIT AT LEG 3;
Tb3E3=0.5*Dc*@SIN(A21)-0.5*EW3-n+X6;
@BND(0.01,X6,0.2);
Tb3Y3=Tb3E3/(@TAN(SRX3));
T63=((Tb3E3)^2+(Tb3Y3)^2)^0.5;
L63=T63*@COS(0.5*SRX3);
R63=L63/(@SIN(0.5*SRX3));
V63=3.6*(9.81*(fs+0.02)*R63)^0.5;
V63<Vmax;
! LEFT TURN EXIT AT LEG 1;
e1=R7*(2-2*@COS(A61))^0.5;
f1=((R7)^2-((e1)^2)/4)^0.5;
g1=R7-f1;
A61=2*@ACOS((f1)/R7);
H1Ub1=R7*@COS(A61)-n;
V1Ub1=0.60*Ric;
V1Ub1=(H1Ub1)/(@TAN(SLX1));
T91=((H1Ub1)^2+(V1Ub1)^2)^0.5;
L91=T91*@COS(0.5*SLX1);
R91=L91/(@SIN(0.5*SLX1));
V91=3.6*(9.81*(fs+0.02)*R91)^0.5;
V91<Vmax;


---


! ENTRY FROM LEG 3;
! CENTRAL RIGHT TURN PATH CURVE;
(E3B3)^2-
0.194*Dc+0.46*(Ai/0.01745))^2=0;
L53=0.5*E3B3;
Mr3=0.066*Cw+0.00667*(Ai/0.01745);
L53/Mr3=@sin(SRC3/2)/(1-@cos(SRC3/2));
R53=L53/@sin(SRC3/2);
V53=11.27*((fs+0.02)*R53)^0.5;
V53<Vmax;
! THROUGH CURVE ENTRY FROM LEG 3;
B3K3=(0.5*Dc*@SIN(A13)-0.5*EW3-n);
K3M3=(B3K3)/(@TAN(STE3));
B3=@ABS((90*0.01745)-Am3-A13);
Am3=(A23-A13)/2;
STE3=(STC/2)+Am3;
T13=((B3K3)^2+(K3M3)^2)^0.5;
L13=T13*@COS(0.5*STE3);
R13=L13/(@SIN(0.5*STE3));
V13=11.27*((fs+0.02)*R13)^0.5;
V13<Vmax;
! RIGHT TURN ENTRY CURVE AT LEG 3;
Ac3=(90*0.01745-(A22+A13))/2;
Ar3=Ac3+A13;
SRE3=(90*0.01745)-Ar3-(SRC3/2);
B3F3=(0.5*Dc*@SIN(A13)-0.5*EW3-n)+X7;
@BND(0.01,X7,0.2);
F3Q3=B3F3/(@TAN(SRE3));
T43=((B3F3)^2+(F3Q3)^2)^0.5;
L43=T43*@COS(0.5*SRE3);
R43=L43/(@SIN(0.5*SRE3));
V43=3.6*(9.81*(fs+0.02)*R43)^0.5;
V43<Vmax;
! LEFT TURN ENTRY CURVE AT LEG 3;
c3=R7*(2-2*@COS(A53))^0.5;
d3=((R7)^2-((c3)^2)/4)^0.5;
h3=R7-d3;
A53=2*@ACOS((d3)/R7);
G3W3=R7*@COS(A53)-n+X8;
@BND(0.01,X8,-.9);
W3X3=0.836*Ric+X17;
@BND(0.01,X17,0.4);
W3X3=(G3W3)/(@TAN(SLE3));
T83=((G3W3)^2+(W3X3)^2)^0.5;
T83=G3W3/(@SIN(SLE3));
L83=T83*@COS(0.5*SLE3);
V83=3.6*(9.81*(fs+0.02)*R83)^0.5;
V83<Vmax;
! EIXT;
! THROUGH EXIT AT LEG 1;
STX1=0.5*STC-Am3;
O1C1=0.5*Dc*@SIN(A23)-0.5*EW3-n+X16;
@BND(0.01,X16,0.2);
N1O1=O1C1/(@TAN(STX1));
T31=((O1C1)^2+(N1O1)^2)^0.5;
L31=T31*@COS(0.5*STX1);
R31=L31/(@SIN(0.5*STX1));
V31=11.27*((fs+0.02)*R31)^0.5;
V31<Vmax;
! RIGHT TURN EXIT AT LEG 4;
Tb4E4=0.5*Dc*@SIN(A22+Ai)-0.5*EW4-
n+X13;
@BND(0.01,X13,0.2);
Tb4Y4=Tb4E4/(@TAN(SRX4));
T64=((Tb4E4)^2+(Tb4Y4)^2)^0.5;
L64=T64*@COS(0.5*SRX4);
R64=L64/(@SIN(0.5*SRX4));
V64=3.6*(9.81*(fs+0.02)*R64)^0.5;
V64<Vmax;
! LEFT TURN EXIT AT LEG 2;
e2=R7*(2-2*@COS(A62))^0.5;
f2=((R7)^2-((e2)^2)/4)^0.5;
g2=R7-f2;
A62=2*@ACOS((f2)/R7);
H2Ub2=R7*@COS(A62-Ai)-n;
V2Ub2=0.60*Ric+H2Ub2*@TAN(Ai);
V2Ub2=(H2Ub2)/(@TAN(SLX2));
T92=((H2Ub2)^2+(V2Ub2)^2)^0.5;
L92=T92*@COS(0.5*SLX2);
R92=L92/(@SIN(0.5*SLX2));
V92=3.6*(9.81*(fs+0.02)*R92)^0.5;
V92<Vmax;


---


! ENTRY FROM LEG 4;
! CENTRAL RIGHT TURN PATH CURVE;
(E4B4)^2-(0.2*Dc-
0.37*(Ai/0.01745))^2=0;
L54=0.5*E4B4;
Mr4=0.066*Cw-0.02*(Ai/0.01745);
L54/Mr4=@sin(SRC4/2)/(1-@cos(SRC4/2));
R54=L54/@sin(SRC4/2);
V54=11.27*((fs+0.02)*R54)^0.5;
V54<Vmax;
! THROUGH CURVE ENTRY FROM LEG 4;
B4K4=(0.5*Dc*@SIN(A14-Ai)-0.5*EW4-n);
K4M4=(B4K4)/(@TAN(STE4));
B4=@ABS((90*0.01745)-Ai-A14);
Am4=(A24-A14)/2;
STE4=(STC/2)+Am4;
T14=((B4K4)^2+(K4M4)^2)^0.5;
L14=T14*@COS(0.5*STE4);

```

```

R14=L14/@SIN(0.5*STE4);
V14=11.27*((fs+0.02)*R14)^0.5;
V14<Vmax;
! RIGHT TURN ENTRY CURVE AT LEG 4;
Ac4=(90*0.01745-(A23+A14))/2;
Ar4=Ac4+A14;
SRE4=(90*0.01745)-Ar4-(SRC4/2);
B4F4=(0.5*Dc*@SIN(A14-Ai)-0.5*EW4-n)+X9;
@BND (0.01,X9,0.2);
F4Q4=B4F4/(@TAN(SRE4));
T44=((B4F4)^2+(F4Q4)^2)^0.5;
L44=T44*@COS(0.5*SRE4);
R44=L44/(@SIN(0.5*SRE4));
V44=3.6*(9.81*(fs+0.02)*R44)^0.5;
V44<Vmax;
! LEFT TURN ENTRY CURVE AT LEG 4;
c4=R7*(2-2*@COS(A54))^0.5;
d4=((R7)^2-((c4)^2)/4)^0.5;
h4=R7-d4;
A54=2*@ACOS((d4)/R7);
G4W4=R7*@COS(90*0.01745-A54-Ai)-n+X10;
@BND (0.01,X10,0.2);
W4X4=0.836*Ric-19.8324*Ai+X18;
@BND (0.01,X18,0.4);
W4X4=(G4W4)/(@TAN(SLE4));
T84=((G4W4)^2+(W4X4)^2)^0.5;
T84=G4W4/@SIN(SLE4);
L84=T84*@COS(0.5*SLE4);
V84=3.6*(9.81*(fs+0.02)*R84)^0.5;
V84<Vmax;

! EXIT;
! THROUGH EXIT AT LEG 2;
STX2=0.5*STC-Am4;
O2C2=0.5*Dc*@SIN(A24+Ai)-0.5*EW4-n;
N2O2=O2C2/(@TAN(STX2));
T32=((O2C2)^2+(N2O2)^2)^0.5;
L32=T32*@COS(0.5*STX2);
R32=L32/@SIN(0.5*STX2);
V32=11.27*((fs+0.02)*R32)^0.5;
V32<Vmax;
! RIGHT TURN EXIT AT LEG 1;
Tb1E1=0.5*Dc*@SIN(A23)-0.5*EW1-n+X12;
@BND (0.01,X12,0.2);
Tb1Y1=Tb1E1/(@TAN(SRX1));
T611=((Tb1E1)^2+(Tb1Y1)^2)^0.5;
L61=T611*@COS(0.5*SRX1);
R61=L61/(@SIN(0.5*SRX1));
V61=3.6*(9.81*(fs+0.02)*R61)^0.5;
V61<Vmax;
! LEFT TURN EXIT AT LEG 3;
e3=R7*(2-2*@COS(A63))^0.5;
f3=((R7)^2-((e3)^2)/4)^0.5;
g3=R7-f3;
A63=2*@ACOS((f3)/R7);
H3Ub3=R7*@COS(A63)-n;
V3Ub3=0.60*Ric;
V3Ub3=(H3Ub3)/(@TAN(SLX3));
T93=((H3Ub3)^2+(V3Ub3)^2)^0.5;
L93=T93*@COS(0.5*SLX3);
R93=L93/(@SIN(0.5*SLX3));
V93=3.6*(9.81*(fs+0.02)*R93)^0.5;

V93<Vmax;
! AVERAGE ENTRY RADIUS AT EACH LEG;
AER1=(R11+R41)/2;
AER2=(R12+R42)/2;
AER3=(R13+R43)/2;
AER4=(R14+R44)/2;
! AVERAGE EXIT RADIUS AT EACH LEG;
AXR1=(R61+R31)/2;
AXR2=(R62+R32)/2;
AXR3=(R63+R33)/2;
AXR4=(R64+R34)/2;
! AVERAGE ENTRY VELOCITY AT EACH LEG;
AEV1=(V11+V41)/2;
AEV2=(V12+V42)/2;
AEV3=(V13+V43)/2;
AEV4=(V14+V44)/2;
! AVERAGE EXIT VELOCITY AT EACH LEG;
AXV1=(V61+V31)/2;
AXV2=(V62+V32)/2;
AXV3=(V63+V33)/2;
AXV4=(V64+V34)/2;

! CONSTRAINTS;
AER1>R2;
AXR3>R2;
AXR3>AER1;
AER2>R2;
AXR4>R2;
AXR4>AER2;
AER3>R2;
AXR1>R2;
AXR1>AER3;
AER4>R2;
AXR2>R2;
AXR2>AER4;
! CONSTRAINT FOR MINIMUM TURNING WIDTH
FOR WB-50 DESIGN VEHICLE;
R2>12.5;
R51>12.5;
R52>12.5;
R53>12.5;
R54>12.5;
R7>12.5;
! CIRCULATORY WIDTH LIMITS;
! RIGHT TURN PATHS;
AEV1-V51-M94+M95=0;
M94<MSD;
M95<MSD;
AXV2-V51-M96=0;
M96<MSD;
AXV2>V51;
AEV2-V52-M97+M98=0;
M97<MSD;
M98<MSD;
AXV3-V52-M99=0;
M99<MSD;
AXV3>V52;
AEV3-V53-M100+M101=0;
M100<MSD;
M101<MSD;
AXV4-V53-M102=0;
M102<MSD;
AXV4>V53;
AEV4-V54-M103+M104=0;

```

```

M103<MSD;
M104<MSD;
AXV1-V54-M105=0;
M105<MSD;
AXV1>V54;
! THROUGH PATHS;
V2-AEV1-M106+M107=0;
M106<MSD;
M107<MSD;
AXV3-V2-M108=0;
M108<MSD;
AXV3>V2;
V2-AEV3-M109+M110=0;
M109<MSD;
M110<MSD;
AXV1-V2-M111=0;
M111<MD;
AXV1>V2;
V2-AEV4-M112+M113=0;
M112<MSD;
M113<MSD;
AXV4-V2-M114=0;
M114<MSD;
AXV4>V2;
V2-AEV2-M115+M116=0;
M115<MSD;
M116<MSD;
AXV2-V2-M117=0;
M117<MSD;
AXV2>V2;
! LEFT TURN PATHS;
V7-V81-M120+M121=0;
M120<MSD;
M121<MSD;
V91-V7-M122=0;
M122<MSD;
V91>V7;
V7-V82-M123+M124=0;
M123<MSD;
M124<MSD;
V92-V7-M125=0;
M125<MSD;
V92>V7;
V7-V83-M126+M127=0;
M126<MSD;
M127<MSD;
V93-V7-M128=0;
M128<MSD;
V93>V7;
V7-V84-M129+M130=0;
M129<MSD;
M130<MSD;
V94-V7-M131=0;
M131<MSD;
V94>V7;
! THROUGH AND LEFT TURN CONFILICT;
V2-V7-M132+M133=0;
M132<MSD;
M133<MSD;
! THROUGH AND RIGHT TURN CONFILICT;
V2-V51-M140+M141=0;
M140<MSD;
M141<MSD;

V2-V52-M142+M143=0;
M142<MSD;
M143<MSD;
V2-V53-M144+M145=0;
M144<MSD;
M145<MSD;
V2-V54-M146+M147=0;
M146<MSD;
M147<MSD;


---


! CAPACITY DELAY MODEL;
! LEG 1;
! OUTER LANE;
Ceo1=Ko1*(Fe1-Fc1*Qc1);
@BND (0.9,Ko1,1.1);
Ko1=1.151-(0.00347*P1)-(0.978/AER1);
Fe1=303*((0.5*W1)+0.5*(Ew1-
W1)/(1+2*S1));
S1=1.6*0.5*(Ew1-W1)/F1;
Fc1=(0.21)*(1+(0.5/(1+@EXP(Dc-
60)/10)))*(1+0.2*0.5*(W1+(Ew1-
W1)/(1+2*S1)));
Ceeo1=Ceo1*Pe1;
VCo1=(Qt1+Qr1)/Ceeo1;
Deo1=(3600/Ceeo1)+900*TP*(VCo1-
1+((VCo1-
1)^2+(3600*VCo1/Ceeo1)/450*TP)^0.5);
DeTo1=Deo1*(Qt1+Qr1);
Qo1=(Ceeo1/3600)*(900*TP)*(VCo1-1+((1-
VCo1)^2+(3600*VCo1/Ceeo1)/(150*TP))^0.5
);
! INNER LANE;
Ceil=Ki1*(Fe1-Fc1*Qc1);
@BND (0.9,Ki1,1.1);
Ki1=1.151-(0.00347*P1)-(0.978/R81);
Ceei1=Ceil*Pe1;
VCi1=(QL1)/Ceei1;
Dei1=(3600/Ceei1)+900*TP*(VCi1-
1+((VCi1-
1)^2+(3600*VCi1/Ceei1)/450*TP)^0.5);
DeTi1=Dei1*(QL1);
Qi1=(Ceei1/3600)*(900*TP)*(VCi1-1+((1-
VCi1)^2+(3600*VCi1/Ceei1)/(150*TP))^0.5
);
! Constraints;
Qo1<Qmax1;
VCo1<=0.85;
Qi1<Qmax1;
VCi1<=0.85;


---


! LEG 2;
! OUTER LANE;
Ceo2=Ko2*(Fe2-Fc2*Qc2);
@BND (0.9,Ko2,1.1);
Ko2=1.151-(0.00347*P2)-(0.978/AER2);
Fe2=303*((0.5*W2)+0.5*(Ew2-
W2)/(1+2*S2));
S2=1.6*0.5*(Ew2-W2)/F2;
Fc2=(0.21)*(1+(0.5/(1+@EXP(Dc-
60)/10)))*(1+0.2*0.5*(W2+(Ew2-
W2)/(1+2*S2)));
Ceeo2=Ceo2*Pe2;
VCo2=(Qt2+Qr2)/Ceeo2;

```

```

Deo2=(3600/Ceeo2)+900*TP*(VCo2-
1+(VCo2-
1)^2+(3600*VCo2/Ceeo2)/450*TP)^0.5);
DeTo2=Deo2*(Qt2+Qr2);
Qo2=(Ceeo2/3600)*(900*TP)*(VCo2-1+((1-
VCo2)^2+(3600*VCo2/Ceeo2)/(150*TP))^0.5
);
! INNER LANE;
Cei2=Ki2*(Fe2-Fc2*Qc2);
@BND (0.9,Ki2,1.1);
Ki2=1.151-(0.00347*P2)-(0.978/R82);
Ceei2=Cei2*Pe2;
VCi2=(QL2)/Ceei2;
Dei2=(3600/Ceei2)+900*TP*(VCi2-
1+(VCi2-
1)^2+(3600*VCi2/Ceei2)/450*TP)^0.5);
DeTi2=Dei2*(QL2);
Qi2=(Ceei2/3600)*(900*TP)*(VCi2-1+((1-
VCi2)^2+(3600*VCi2/Ceei2)/(150*TP))^0.5
);
! Constraints;
Qo2<Qmax2;
VCo2<=0.85;
Qi2<Qmax2;
VCi2<=0.85;

```

```

! LEG 3;
! OUTER LANE;
Ceo3=Ko3*(Fe3-Fc3*Qc3);
@BND (0.9,Ko3,1.1);
Ko3=1.151-(0.00347*P3)-(0.978/AER3);
Fe3=303*((0.5*W3)+0.5*(Ew3-
W3)/(1+2*S3));
S3=1.6*0.5*(Ew3-W3)/F3;
Fc3=(0.21)*(1+(0.5/(1+@EXP(Dc-
60)/10)))*(1+0.2*0.5*(W3+(Ew3-
W3)/(1+2*S3)));
Ceeo3=Ceo3*Pe3;
VCo3=(Qt3+Qr3)/Ceeo3;
Deo3=(3600/Ceeo3)+900*TP*(VCo3-
1+(VCo3-
1)^2+(3600*VCo3/Ceeo3)/450*TP)^0.5);
DeTo3=Deo3*(Qt3+Qr3);
Qo3=(Ceeo3/3600)*(900*TP)*(VCo3-1+((1-
VCo3)^2+(3600*VCo3/Ceeo3)/(150*TP))^0.5
);
! INNER LANE;
Cei3=Ki3*(Fe3-Fc3*Qc3);
@BND (0.9,Ki3,1.1);
Ki3=1.151-(0.00347*P3)-(0.978/R83);
Ceei3=Cei3*Pe3;
VCi3=(QL3)/Ceei3;
Dei3=(3600/Ceei3)+900*TP*(VCi3-
1+(VCi3-
1)^2+(3600*VCi3/Ceei3)/450*TP)^0.5);
DeTi3=Dei3*(QL3);
Qi3=(Ceei3/3600)*(900*TP)*(VCi3-1+((1-
VCi3)^2+(3600*VCi3/Ceei3)/(150*TP))^0.5
);
! Constraints;
Qo3<Qmax3;
VCo3<=0.85;
Qi3<Qmax3;
VCi3<=0.85;

```

```

! LEG 4;
! OUTER LANE;
Ceo4=Ko4*(Fe4-Fc4*Qc4);
@BND (0.9, Ko4,1.1);
Ko4=1.151-(0.00347*P4)-(0.978/AER4);
Fe4=303*((0.5*W4)+0.5*(Ew4-
W4)/(1+2*S4));
S4=1.6*0.5*(Ew4-W4)/F4;
Fc4=(0.21)*(1+(0.5/(1+@EXP(Dc-
60)/10)))*(1+0.2*0.5*(W4+(Ew4-
W4)/(1+2*S4)));
Ceeo4=Ceo4*Pe4;
VCo4=(Qt4+Qr4)/Ceeo4;
Deo4=(3600/Ceeo4)+900*TP*(VCo4-
1+(VCo4-
1)^2+(3600*VCo4/Ceeo4)/450*TP)^0.5);
DeTo4=Deo4*(Qt4+Qr4);
Qo4=(Ceeo4/3600)*(900*TP)*(VCo4-1+((1-
VCo4)^2+(3600*VCo4/Ceeo4)/(150*TP))^0.5
);
! INNER LANE;
Cei4=Ki4*(Fe4-Fc4*Qc4);
@BND (0.9,Ki4,1.1);
Ki4=1.151-(0.00347*P4)-(0.978/R84);
Ceei4=Cei4*Pe4;
VCi4=(QL4)/Ceei4;
Dei4=(3600/Ceei4)+900*TP*(VCi4-
1+(VCi4-
1)^2+(3600*VCi4/Ceei4)/450*TP)^0.5);
DeTi4=Dei4*(QL4);
Qi4=(Ceei4/3600)*(900*TP)*(VCi4-1+((1-
VCi4)^2+(3600*VCi4/Ceei4)/(150*TP))^0.5
);
! Constraints;
Qo4<Qmax4;
VCo4<=0.85;
Qi4<Qmax4;
VCi4<=0.85;

```

```

! TOTAL ENTRY VOLUME;
Qe1=Qt1+Qr1+QL1;
Qe2=Qt2+Qr2+QL2;
Qe3=Qt3+Qr3+QL3;
Qe4=Qt4+Qr4+QL4;

```

```

! AVERAGE INTERSECTION DELAY;
DATI=(DeTi1+DeTo1+DeTi2+DeTo2+DeTi3+DeT
o3+DeTi4+DeTo4)/(Qe1+Qe2+Qe3+Qe4);

```

```

! OBJECTIVE FUNCTION FOR MULTI
OBJECTIVE MODEL;
MIN=( X100)*MSD+(1- X100)*DATI;
END

```

APPENDIX-D

Glossary of terms

C_w	=	Circulatory width (m)
D_c	=	Inscribed circle diameter (m)
$D_{c_{min}}$	=	Minimum inscribed circle diameter (m)
$D_{c_{max}}$	=	Maximum inscribed circle diameter (m)
E_{wi}	=	Entry width (m)
$E_{wi_{min}}$	=	Minimum entry width for leg i (m)
$E_{wi_{max}}$	=	Maximum entry width for leg i (m)
E_{max}	=	Maximum entry width (m)
f_{sLV}	=	Side friction factor for light vehicle
f_{sHV}	=	Side friction factor for heavy vehicle
f_s	=	Average side friction factor
M_{vLV}	=	Average vehicle masses for light vehicles (kilograms)
M_{vHV}	=	Average vehicle masses for heavy vehicles (kilograms)
P_{HV}	=	Percentage of heavy vehicles at roundabout (decimal)
F_i	=	Effective flare length (m)
F_{imax}	=	Maximum effective flare length for leg i (m)
F_{imin}	=	Minimum effective flare length for leg i (m)
W_i	=	Approach half width for leg i (m)
M_o	=	Mid ordinate of through curve
R_{ic}	=	Central island radius (m)
Δ_{tci}	=	Through circular path curve deflection angle while vehicle entering from leg “ i ” (radian)
Δ_{rci}	=	Right turn circular path curve deflection angle while vehicle entering from leg i (radian)
Δ_{tei}	=	Through entry path curve deflection angle while vehicle entering from leg i (radian)

- Δ_{Lei} = Left turn entry path curve deflection angle while vehicle entering from leg i (radian)
- Δ_{rei} = Right turn entry path curve deflection angle while vehicle entering from leg i (radian)
- $\Delta_{tx[i+2]}$ = Through exit path curve deflection angle while vehicle entering from leg i (radian)
- $\Delta_{rx[i+1]}$ = Right exit path curve deflection angle while vehicle entering from leg i (radian)
- $\Delta_{Lx[i+3]}$ = Left exit path curve deflection angle while vehicle entering from leg i (radian)
- θ_{1i} = Through curve entry angle with respect to center of ICD at yield line while vehicle entering the roundabout at leg i (radian)
- θ_{2i} = Through curve exit angle with respect to center of ICD at yield line while vehicle entering from leg i at the roundabout (radian)
- $B_i K_i$ = Vertical component of through path entry curve at leg i (m)
- $K_i M_i$ = Horizontal component of through path entry curve at leg i (m)
- $O_{[i+2]} C_{[i+2]}$ = Vertical component of through path exit curve while vehicle entering from leg i (m)
- $N_{[i+2]} O_{[i+2]}$ = Horizontal component of through path exit curve while vehicle entering from leg “ i ” (m)
- $T_{[i+1]} E_{[i+1]}$ = Vertical component of right turn exit path curve while vehicle entering from leg i (m)
- $T_{[i+1]} Y_{[i+1]}$ = Horizontal component of right turn exit path curve while vehicle entering from leg i (m)
- $B_i F_i$ = Vertical component of right turn entry path curve while vehicle entering from leg i (m)
- $F_i Q_i$ = Horizontal component of right turn entry path curve while vehicle entering from leg i (m)
- $E_i B_i$ = Horizontal half cord length of right turn circular path while vehicle entering from leg i (m)

- M_{ri} = Right turn circular curve mid ordinates when vehicle enter from leg i (m)
 AER_i = Average entry radius at leg i (m)
 AXR_i = Average exit radius at leg i (m)
 AEV_i = Average entry speed at leg i (km/hr.)
 AXV_i = Average exit speed at leg i (km/hr.)
 V_{ji} = Vehicle speed at “j” movement path curve when entering from leg i (km/hr.)
 R_{ji} = Fastest path radius at “j” movement path curve when entering from leg i (m)
 L_{ji} = Horizontal cord length of “j” movement path curve when vehicle entering from leg i (m)
 T_{ji} = Entry curve tangent length of “j” movement when vehicle entering from leg i (m)
 $T_{6[i+1]}$ = Right turn exit curve tangent length when vehicle entering from leg i (m)
 $T_{9[i+3]}$ = Left turn exit curve tangent length when vehicle entering from leg i (m)
 $T_{3[i+2]}$ = Through exit curve tangent length when vehicle entering from leg i (m)
 L_{ji} = Entry curve half cord length of “j” movement when vehicle entering from leg i (m)
 $L_{6[i+1]}$ = Right turn exit curve half cord length when vehicle entering from leg i (m)
 $L_{9[i+3]}$ = Left turn exit curve half cord length when vehicle entering from leg i (m)
 $L_{3[i+2]}$ = Through exit curve half cord length when vehicle entering from leg i (m)
 R_{ji} = Curve radius for “j” movement when vehicle entering from leg i (m)
 $R_{6[i+1]}$ = Right turn exit radius when vehicle entering from leg i (m)
 $R_{9[i+3]}$ = Left turn exit radius when vehicle entering from leg i (m)
 $R_{3[i+2]}$ = Through curve exit radius when vehicle entering from leg i (m)
 V_{ji} = Vehicle speed for “j” movement when vehicle entering from leg i (km/hr.)
 $V_{6[i+1]}$ = Right turn exit vehicle speed while vehicle entering from leg i (km/hr.)
 $V_{9[i+3]}$ = Left turn exit vehicle speed while vehicle entering from leg i (km/hr.)

$V_{3[i+2]}$	= Through curve exit vehicle speed when vehicle entering from leg i (km/hr.)
$C_{ei[l,o]}$	= Entry capacity at leg i in inner and outer lanes (pec/hr.)
$C_{eei[l,o]}$	= Effective entry capacity at leg i in inner and outer lanes (pec/hr.)
$VC_{i[l,o]}$	= Volume to capacity ratio at leg i in inner and outer lane (decimal)
$De_{i[l,o]}$	= Delay at leg i in inner and outer lanes (s)
DeT	= Total delay at roundabout(s)
$DATI$	= Total average delay at roundabout (s)
M_{SD}	= Mean speed difference (km/hr.) Or mph
X_{ji}	= Variable for optimization
S_i	= Sharpness of flare (m/m)
\propto	= Objective function for minimizing or maximizing
Q_{c_i}	= Circulatory flow rate at front of entry leg i (pec/hr)
Qt_i	= Through entry flow for each leg i (pec/hr)
Qr_i	= Right turn entry flow for each leg i (pec/hr)
Qe_{o_i}	= Entry flow for outer lane for each leg i (pec/hr)
QL_i	= Left-turn entry flow for each leg i (pec/hr)
QU_i	= U-turn entry flow for each leg i (pec/hr)
Qe_{l_i}	= Entry flow for inner lane for each leg i (pec/hr)
$Q_{i[l,o]}$	= Queue length for each leg i in inner and outer lane (m)
Q_{max_i}	= Maximum queue length for each leg i (m)
$VC_{i[l]}$	= Ratio of entry capacity / entry flow for inner lane
$VC_{i[o]}$	= Ratio of entry capacity / entry flow for outer lane

REFERENCE

- Highway Capacity Manual. (2000). Transportation Research Board, National Academy of Sciences, Washington, D.C.
- Maryland DOT. (1995). Maryland Department of Transportation, Roundabout Design Guidelines, State Highway Administration, Hanover. Maryland.
- Paradigm Transportation Solutions Limited. (2011). *"Ira Needles Boulevard & Erb Street West Proposed Commercial Development Transportation Impact Study" Sifton Properties Limited. Paradigm Transportation Solutions Limited 43 Forest Road Cambridge ON.*
- Rahmi Akcelik. (2007, December). "A Review of Gap-acceptance capacity models",. *Paper presented at 29th conference of Australian Institutes of Transport Research (CAITR 2007), University of South Australia, Adelaide, Australia.*
- Roundabout Design Standards. (2005). "A Section of the Traffic Engineering Policy & Design Standards", City of Colorado Springs – Transportation Engineering.
- Kansas Roundabout Guide.* (2005). Kansas: Kansas Department of Transportation.
- Facilities Development Manual.* (2009). Wisconsin Department of Transportation,.
- AASHTO. (1994). American Association of State Highway and Transportation Officials (AASHTO). A Policy on Geometric Design of Highways and Streets. Washington, D.C.
- AASHTO. (2004). *American Association of State Highway and Transportation Officials (AASHTO). A Policy on Geometric Design of Highways and Streets. Washington, DC.*
- AASHTO. (2006). *"Roadside Design Guide"*. Washington, D.C.
- Akcelik, R. (1997). "Lane-by-Lane Modeling of Unequal lane Use and Flares at Roundabouts and Signalized Intersections: the SIDRA Solution." *Traffic Engineering & Control*, Vol. 38, No. 7/8.

- Akçelik, R. (2003, July). "A Roundabout Case Study Comparing Capacity Estimates from Alternative Analytical Models",. *Paper for presentation at the 2nd Urban Street Symposium, Anaheim, California, USA.*
- Arndt, O. (1998, August). "Road Design Incorporating Three Fundamental Safety Parameters." Technology Transfer Forum 5 & 6, Transport Technology Division, Main Roads Department.
- Ashmead, D. e. (2005, November). "Street Crossing by Sighted and Blind Pedestrians at a Modern Roundabout". *Journal of Transportation Engineering, Volume 131, Issue 11,* 812-821.
- Associates, K. a. (2002). *On-Line Roundabout database.* Retrieved from URL; <http://roundabouts.kittelson.com/dbase/invmain.html>.
- AUSTROADS. (1993). "Guide to Traffic Engineering Practice", Part 6 - Roundabouts, Sydney, Australia.
- Avent, A. a. (1979). "Roundabouts-Aspects of their Design and Operations,". *Queensland Division Technical Papers, Vol. 20, No. 17,* pp. 1-10.
- Bared, J. G. and K. Kennedy. (1999). "Safety Impacts of Modern Roundabouts." In ITE Safety Toolbox . *Institute of Transportation Engineers.*
- Bared, J.G., and K. Kennedy. (2000). "Safety Impacts of Modern Roundabouts;" Chapter 28, *The Traffic Safety Toolbox: A Primer on Traffic Safety, Institute of Transportation Engineers.*
- BC MOT. (2007). *SUPPLEMENT TO TAC GEOMETRIC DESIGN GUIDE 2007, Ministry of Transportation British Columbia.*
- Bramwell, F. (1982). 20 Years of Roundabout Construction in Buckinghamshire. . *The Highway Engineer.*

- Brilon, W. M. (1991). "Toward a New German Guideline for Capacity of Un-signalized Intersections",. *Proceeding of the Third International Symposium on Intersections Without Traffic Signals*, 61-70.
- Brilon, W., and Wu, N. (2006). Merkblatt für die Anlage von Kreisverkehren [Guideline for the design of roundabouts], FGSV Verlag GmbH, Cologne, Germany.
- Brilon, Werner, Ning Wu, and Lothar Bondzio. (1997). "Un-signalized intersection in Germany; A State of the Art 1997",. *Proceeding of the Third International Symposium on Intersections Without Traffic Signals*, 61-70.
- Bureau of Local Roads & Streets. (2007). "BUREAU OF LOCAL ROADS & STREETS" , Chapter 34 INTERSECTIONS.
- Carl C., Chuan K., Brice S. (2004). "Roundabouts in Edmonton - A Comparison to the State-of-the-Art", Paper Prepared for Presentation at the Innovative Intersection and Interchange Designs Session of the 2004 Annual Conference of the Transportation Association of Canada, Quebec.
- CDOT. (2006). *California Department of Transportation. Highway Design Manual. Sacramento, California: California Department of Transportation.*
- CETUR. (1988). Conception des Carrefours a sens Giratoire Implantes en Milieu Urbain,. *Centre d'Etudes des Transports Urbains (CETUR), Ministere de l'Equipement, du Logement, del'Amenagement du Territoire et des Transports.*
- CETUR. (1992). "Safety of Roundabouts in Urban and Suburban Areas." .
- Colorado DOT. (2005). Roundabout Design Standards, A Section of the Traffic Engineering Policy & Design Standards. City of Colorado Springs – Transportation Engineering.
- CROW. (1993). "Signup for the bike; Design manual for a cycle- friendly infrastructure", *Center for standardization in Civil Engineering (CROW)* . The Netherlands.

- Cunningham, R. B. (March 2007). Maryland's Roundabouts: *Accident Experience and Economic Evaluation*. Traffic Development & Support Division, Office of Traffic and Safety, State Highway Administration, Maryland Department of Transportation.
- Fambro, D.B., et al. (1997). NCHRP Report 400: "Determination of Stopping Sight Distances", National Cooperative Highway Research Program, Transportation Research Board, National Research Council. Washington, D.C.: National Academy Press.
- FDOT. (1995). *"Florida roundabout design guide"*, Florida Department of Transportation. Tallahassee, Florida.
- FHWA. (2000). *United States Federal Highway Administration's "Roundabouts: An informational Guide*.
- Flannery. (1998). "Safety, Delay, and Capacity of Single-Lane Roundabouts in the United States". Transportation Research Record 1646.
- Glauz, W., and Migletz, D. (1980). "Application of Traffic Conflict Analysis at Intersections, National Cooperative Highway Research Program Report 219", Washington, D.C., Transportation Research Board, National Research Council.
- GMT Toronto. (2008). " Feasibility and Benefits of Roundabouts in Toronto", General Manager, Transportation Services City of Toronto.
- Harder. J. (1989). "Mediterranean Carrousal-Ginde Caacite dun' Carrefour Giratoire, Guide de l' Utilisateur" CETE, France.
- HCM. (2010). "Highway Capacity Manual(HCM 2010)", Transportation Research Board, National Research Council. Washington, DC, USA.
- Heidemann, D. (1991). "Queue lengths and waiting-time distributions at priority intersections." In Transportation Research B, Vol 25B, (4) . pp. 163–174.

- Huddart, K.W. (1983). "Signalling of Hyde Park Corner, Elephant and Castle and other roundabouts". PTRC 11th Summer Annual Meeting, Proceedings of Seminar K, . pp 193-208.
- Jacquemart, G. (1998). "Modern Roundabout Practice in the United States". Synthesis of Highway Practice 264. Transportation Research Board, Washington, D.C., U.S.A.
- KDOT. (2003). Chapter 6, "Geometric design". In *"Kansas Roundabout Guide, A supplement to FHWA's Roundabouts: An Informational Guide"* (p. 68).
- Kimber, R. (1980). *TRRL Laboratory Report 942; The traffic capacity of roundabouts*. Crowthorne: TRRL.
- Kimber, R. (n.d.). *Gap-Acceptance and Empiricism in Capacity Prediction*. TRRL.
- Kimber, R.M. (1978). Peak-period traffic delays at road junctions and other bottlenecks, *Traffic Engineering and Control*.
- Kimber, R.M. and Maycock, G. (1980). Roundabout Capacity; "Proceedings of Seminar on Design Standards", PTRC Summer Annual Meeting. *Planning and Transport Research and Computation (International) Co., Ltd.* London.
- Kimber, R.M., E.M. Hollis. (1978). "Peak period traffic delays at road junctions and other bottlenecks", *Traffic Engineering and Control*, No.10. pp.442-446.
- Kimber, R.M., Marlow, M., and Hollis, Erica M. (1977). "Flow/delay relationships for major/minor priority junctions",. *Traffic Engineering and Control*.
- Kimber, RM & Hollis EM. (1979). *"Traffic Queues and Delays at Road Junctions"*,. TRRL Report LR 909.
- Kittelsohn & Associates, I. a. (2003). *"Kansas Roundabout Guide: A supplement to FHWA's Roundabouts: An Informational Guide"*, Topeka, Kansas. Kansas Department of Transportation.

- Kittelson & Associates, Inc. NCHRP 3-65. (2006). *"Applying Roundabouts in the United States", Final Report, Kittelson & Associates, Inc.*
- Kittelson and Associates. (2002). *on-line roundabout database, URL: <http://roundabouts.kittelson.com/dbase/invmain.html>.*
- Kottegoda, N., Rosso, R. (1997). "Statistic Probability and Reliability for Civil and Environmental Engineers",. *MacGraw-Hill, New York.*
- Kyte, M. (1997). "Capacity and Level of Service of Un-signalized Intersections: New Practices in the United States," Proceeding of the Third International Symposium on Intersections Without Traffic Signals., (pp. pp. 171-177.).
- Lee Engineering and Kittelson & Associates, I. (2003). *" Roundabouts: An Arizona Case Study and Design Guideline", Final Report 545. Phoenix. Arizona Department of Transportation.*
- Mandavilli, S., A. McCartt, and R. Retting. (May, 2008). "Crash Patterns and Potential Engineering Countermeasures at Maryland Roundabouts". *Insurance Institute for Highway Safety, Arlington, Virginia.,*
- Maycock, G and Hall, RD. (1984). *Accidents At 4-Arm Roundabouts., TRRL Report LR 1120.*
- Maycock, G. a. (1984). *Crashes at Four-Arm Roundabouts TRRL Laboratory Report LR 1120.* Transport and Road Research Laboratory, Crowthorne, England.
- MDOT. (1995). *"Roundabout design guidelines", Maryland Department of Transportation.* Hanover, Maryland.
- Mehmood, A. (2003). "Geometric design of Single lane roundabouts for optimum consistency and operation",. *A thesis Master of applied Science in Civil Engineering to Ryerson University.*
- Myers, E. J. (1994). "Modern Roundabouts for Maryland". *ITE Journal.*

- NCHRP Report 572. (2007). *"Roundabouts in the United States"*, Transportation Research Board, National Research Council. Washington, DC, USA.
- NCHRP Report 672. (2010). *"National Cooperative Highway Research Program Report 672", Roundabouts: An Informational Guide", Second Edition*. TRANSPORTATION RESEARCH BOARD WASHINGTON, D.C.
- Oursten, Leif, and Joe G. Bared. (1995). "Roundabouts; A Direct Way to Safer Traffic". *Public Road*.
- Pein, W. (1996). "Trail Intersection Design Guidelines", Prepared for State Bicycle/Pedestrian Program, State Safety Office, Florida Department of Transportation. Highway Safety Research Center, University of North Carolina.
- Persaud, B. N.; R. A. Retting; P. E. Garder; and D. Lord. (March 2000). *Crash reduction Following Installation of Roundabouts in United States*. Insurance Institute for Highway Safety, Arlington, Virginia.
- Raffaele Mauro. (2010). *"Calculation of Roundabouts Capacity, Waiting Phenomena and Reliability"*, Università Trento Dip.to Ingegneria Meccanica eStrutturale (DIMS), latest edition, Trento Italy edition.
- Rahmi Akcelik. (1997). "Lane-by-Lane Modeling of Unequal lane Use and Flares at Roundabouts and Signalized Intersections: the SIDRA Solution.". *Traffic Engineering & Control, Vol. 38, No. 7/8*.
- Rahmi Akcelik. (2002). "Estimating negotiation radius, distance and speed for vehicles using roundabouts". *Paper presented at 24th conference of Australian Institutes of Transport Research (CAITR 2002)*. University of New South Wales, Sydney, Australia.
- Rahmi Akcelik. (2011). "An assessment of the Highway Capacity Manual 2010 Roundabout capacity model", Paper presented at the International Roundabout Conference, Transportation Research Board, Carmel, Indiana, USA.

- Robinson, B. et al. (2000). *"Roundabout an information guide, 2000"*, Report No. FHWA-RD-00-67. Washington, D.C: Federal Highway Administration,.
- Robinson, B. W. (2000). "Capacity and Performance of Roundabouts: A Summary of Recommendations in the FHWA Roundabouts Guide". *Transportation Research E-Circular Number E-C018*.
- Rodegerdts, L. M., & D. Carter, R. M. (2007). Roundabouts in the United States. National Cooperative Highway Research Program Report 572. Transportation Research Board, National Academies of Science, Washington, D.C.
- Rodegerdts, L., M. Blogg, E. Wemple, E. Myers, M. Kyte, M. Dixon, G. List, A. Flannery, R. Troutbeck, W. Brilon, N. Wu, B. Persaud, C. Lyon, D. Harkey and D. Carter. (2007). *NCHRP Report 572: Roundabouts in the United States*. Washington, D.C.: Transportation Research Board of the National Academies.
- Rodegerdtz, L. (2005). "Stat-of-the-Art in U.S. Roundabout Practice", Kittelson & Associates, Inc .
- Rozental, Julian . (2003). "Planning and Design of Modern Roundabouts", British Columbia Ministry of Transportation and Highways, Draft Technical Bulletin.
- Seiberlich, E. L. (2001). " A Formulation To Evaluate Capacity And Delay Of Multilane Roundabouts In The United States For Implementation Into A Travel Forecasting Model". In *Master of Science thesis In Engineering The University of Wisconsin-Milwaukee*.
- SETRA. (1988,1997). Carrefours Giratoires:" Evolution des Caracteristiques Geometriques, Ministere de l'Equipement, du Logement, de l'Amenagement du Territoire et des Transports", Documentation Technique 44.
- Steve van de Keere and Phil Weber. (2008). "Roundabout experience in region of waterloo",. *Paper for the Transportation Research Board National Roundabout Conference Kansas City, Missouri*.

- Swiss Roundabout Guid. (1991). Guide Suisse des Giratoires, Fonds de Securite Routiere, Institut des Transports et de Planification, Ecole Polytechnique Federale de Lausanne, Switzerland.
- TAC . (2007). *"Geometric Design Guide for Canadian Roads"*, September 1999, Updated December 2007. Transportation Association of Canada.
- Taekratok, T. (1998). *"MODERN ROUNDABOUTS FOR OREGON"*, Oregon Department of Transportation Research Unit. Hawthorne Oregon.
- Tanner, J. (1962). "A theoretical analysis of delay At An Uncontrolled Intersections", *Biometrika* 49 (1 and 2). pp, 163-70.
- TD 16/93 DMRB 6.2.3. (2007). Geometric Design of Roundabouts, "DESIGN MANUAL FOR ROADS AND BRIDGES", TD 16/07 Volume 6, Section 2, Part 3.
- Troutbeck, R. (1984). "Capacity and Delays at Roundabouts-A Literature Review," Australian Road Research Board, 14(4). pp. 205-216.
- Troutbeck, R.J. (1989). *"Evaluating the Performance of a Roundabout," Australian Road Research Report SR 45.*
- Troutbeck, R.J. (1991). "Recent Australian Un-signalised Intersection Research and Practices," Intersection without Traffic Signals II, Springer-Verlag, Werner Brilon (Ed.). pp. 238-257.
- Virginia P. Sisiopiku and Heung-Un Oh. (2001, April). Evaluation of Roundabout Performance using SIDRA. *Journal of Transportation Engineering.*
- Wallwork. (1996). *"Modern Roundabouts"*, For the Roundabout Design Workshop. Montpelier, VT.
- WisDOT. (2011). Roundabout Designs , Chapter 11, section 26, Facilities Development Manual, Wisconsin Department of Transportation.

Wu, N. (1994). "An Approximation for the Distribution of Queue Lengths at Unsignalised Intersections", In Akcelik, R. (ed.), Proceeding of the second International Symposium on Highway Capacity, Sydney, Volume 2. pp. 717-736.

Xu, F. (2007). "Driver Behavior And Gap Acceptance Studies At Roundabouts", A thesis submitted in partial fulfillment of the requirements for the degree of Master of Science in Civil Engineering, University of Nevada Reno.

Zong Z. Tian, F. X. (2007). "*Roundabout Geometric Design Guidance California Department of Transportation Division of Research & Innovation*", Federal Report # F/CA/RI-2006/13 .